Mono and Bi-Alkyne Functionalised Polyethylene Glycols: Polymeric Substrates in Palladium Catalysed Oscillatory Carbonylation Reactions

By

Chinyelumndu Jennifer Nwosu

for the degree of

Doctor of Philosophy

Chemistry, Chemical Engineering and Advanced Materials

School of Engineering

Newcastle University, UK

June 2019

Abstract

In this work, the family of oscillatory carbonylation reactions was expanded to include mono and bi-functionalised polymeric substrates. As research around intelligent / stimuli responsive materials progress, it is increasingly important to expand capabilities of chemical oscillators, with a view of merging these two areas to achieve fully pulsatile polymeric materials, capable of autonomous volume changes over longer (i.e. weeks, months) periods of time. This study focused on mono alkyne functionalised polyethylene glycols (A-PEG_{2000}) and bi-alkyne functionalised polyethylene glycols (A-PEG_{2000}-A) as polymeric substrates in oscillatory carbonylation reactions. The work presented here systematically evaluates oscillatory and non-oscillatory reaction profiles recorded in experimental studies. The studies were designed to grasp the reaction processes and elucidate reaction mechanisms responsible for observed trends. Extensive studies were undertaken at different polymeric substrate, PdI_2 and KI (originally added to aid PdI_2 dissolution) concentrations. Across all studies, the concentration of the catalytic mixture consisting of PdI_2 and KI in methanol ranged from 3 - 9 mM for KI and 15.1 - 60.4 µM for PdI_2. Mono alkyne substrate concentrations ranged from 0.508 - 3.55 mM while the bi-alkyne substrate concentration ranged from 0.254 - 3.04 mM. The influence of methanol perturbation during the reaction and varying KI addition times was also investigated. Comparison of pH profiles for both substrates at the same molecular concentrations or same alkyne group concentrations was likewise assessed. At constant catalyst concentration (KI/PdI_2), as the substrate concentration increased, the amplitudes and period of the pH oscillations increased in reactions with mono alkyne substrates. On increasing the bi-alkyne polymeric substrate concentrations, the size and amplitudes of pH oscillations varied, and was significantly dependent on the catalyst / substrate concentration. Increasing PdI_2 concentration at constant KI and substrate concentrations increased [H^+] generated via autocatalytic conversions of both alkyne functionalised polymer substrates. More [H^+] was formed in reactions employing bi-alkyne substrates due to increased concentrations of alkyne groups (two alkyne ends per chain). Delaying KI addition times at constant PdI_2 and mono alkyne substrate concentration shifted the reactions from oscillatory to non-oscillatory modes. Furthermore, increasing KI concentrations induced occurrence of oscillations in both substrates. Simple, complex, Canard and mixed mode oscillations, as well as other complex non-oscillatory features and pH transitions / offsets, were observed in some reactions as the mono alkyne and bi-alkyne polymer substrates and catalytic concentrations were altered. This work confirms the feasibility of pH oscillations with mono and bi-alkyne substrates in Pd-catalysed oxidative carboxylation reaction and opens new avenues in nonlinear chemical

dynamics and intelligent polymeric materials. A merger of intelligent soft materials and this pH oscillator which exhibits extended oscillation duration in batch mode could potentially create self-oscillating regulatory devices for a range of applications including drug delivery and soft robotics.

Dedication

To

Muriel me D'Nonyes Nnem nja

Acknowledgement

I would like to express sincere gratitude to my supervisors, Dr Katarina Novakovic, Dr Julian Knight and Dr Simon Doherty for their valuable suggestions, continuous support, and enthusiasm throughout this research. I am especially thankful to Dr Katarina; your encouragement and feedback has helped me immensely throughout this period.

I must thank Dr Lynn Donlon, (Centre for Process Innovation) for providing some initial support, Dr Corinne Wills for her NMR expertise, and Dr Julie Parker for those informal discussions and technical support with reactor setup.

I am grateful for the financial support from SAgE DTA Newcastle, without which, I would not have had the opportunity to conduct the research.

Special words of gratitude go to my friends Franklin, Jamila, Chris, Onyeka, Chinyem, and Chioma for lending me your ears, you have always been a major source of support when things are a bit discouraging.

Finally, I would like to extend my deepest gratitude to my family: Ejima-me, Mlaa, Toch, Nino and Darriel. Your enormous support and encouragement during my time spent working on this research is immeasurable. Thank you for listening, you have been my biggest motivation.

Table of Contents

List of Figures

List of Tables

Nomenclature

List of Abbreviations and Symbols

A-PEG$_{2000}$	Mono alkyne functionalised methoxy polyethylene glycol
A-PEG$_{2000}$-A	Bi-alkyne functionalised polyethylene glycol
BZ	Belousov–Zhabotinsky reaction
CSTR	Continuous Stirred Tank Reactor (flow reactor)
CORMs	Carbon Monoxide-Releasing Molecules
E-isomer	Dimethyl (2E)-2-phenyl-2-butenedioate
FKN	Field Körös Noyes
GC-MS	Gas Chromatography – Mass Spectroscopy
HPLC	High-performance liquid chromatography
MMO	Mixed-mode Oscillations
MMbO	Mixed-mode bursting Oscillations
NaOAc	Sodium acetate
NMR	Nuclear Magnetic Resonance
OCR	Oxidative Carbonylation Reaction
OOCR	Oscillatory Oxidative Carbonylation Reactions
pH	pH measured as methanol (apparent pH)
PEG	Polyethylene Glycol
P-PEG$_{2000}$	Products from carbonylation of mono alkyne functionalised methoxy PEG
P-PEG$_{2000}$-P	Products from carbonylation of bi-alkyne functionalised PEG
Slow H^+	Region of pH profiles where H^+ concentration increases slowly

TGM	Transition Group Metals
TMS	Tetramethylsilane
Z-isomer	Dimethyl (2Z)-2-phenyl-2-butenedioate

Å	Angstrom, unit of length equal to 10^{-10} m
Da	Unified atomic mass unit, unit of mass that quantifies mass on an atomic or molecular scale (molecular weight)
k_i	Rate constant, $mol^{(1-n)}dm^{-3(n-1)}min^{-1}$ where n = reaction order and i = 1, 2, 3, …(rate constant for individual reactions)
$[KI]_{additional}$	Extra potassium iodide introduced at some point during the reaction
$[KI]_{initial}$	Original concentration of potassium iodide from onset of reaction
R_i	Reaction rate, concentration per unit time, where i = 1, 2, 3, …(Reaction rates for individual reactions)
R_{eff}	Effective reaction rate for a series of reactions with various rates
mM	milli Molarity (unit of molar concentration, 10^{-3})
µM	Micro Molarity (unit of molar concentration, 10^{-6})
m/v	Mass per unit volume (unit of mass concentration)
Ø	Diameter (unit length)
V_{Total}	Total volume of methanol in the reactor.

Chapter 1. Introduction

1.1 Background and Motivation

The significance of transition metal catalysed reactions cannot be overstressed as it continues to play key roles in recent discoveries in several aspects of organic chemistry. Palladium catalysed carbonylation reactions is one of such reactions with growing interest due to its suitability for the production of different materials and substrates (e.g. ketones, aldehydes, carboxylic acids, polycarbonates, esters, urea etc.) for use in various industries [1-5]. Currently, palladium catalysed carbonylation reactions applications focus on producing these materials and substrates for industrial uses hence, foremost interest for most researchers' lies in synthesis routes for desired products.

An alternate use of palladium catalysed carbonylation reactions focuses on nonlinear chemical dynamics behaviours [6-11] that occur during the carbonylation reaction, when substrates with alkyne groups are used. Nonlinear chemical dynamics [12-14] is an acknowledged aspect of physical chemistry and Belousov–Zhabotinsky reactions are the most investigated nonlinear chemical system [15-23]. Nonlinear dynamics in chemical systems continues to generate interest as more reactions with the ability to show these phenomena are identified. Amongst these nonlinear chemical systems, pH oscillators [22, 24-28] are notable because of the possibility of combining them with stimuli responsive materials. Nonlinear chemical dynamic phenomena arising from palladium catalysed oxidative carbonylation reactions are driven by autocatalytic changes in species concentration such as H^+ and hence, comprise pH oscillations [6, 8, 9, 29-33]. They could therefore be integrated with stimuli responsive materials such as pH responsive hydrogel [34-37]. pH responsive materials are materials consisting of interlinks (ionic, covalent crosslinks etc.) of functional polymers that swell and/or contract as pH of their environment changes. Coupling these materials with pH oscillators such as the oxidative carbonylation reactions is aimed at eliminating the need for external stimuli to generate response in responsive materials. It may also resolve diffusion induced delays in response to stimuli associated with bulky pH sensitive materials. This integration with oscillatory chemistry would provide stimuli (arising from the pH oscillations) within the pH responsive material thereby producing soft materials with autonomous motion.

Nonlinear chemical dynamics in palladium catalysed oxidative carbonylation reaction was originally discovered by Malashkevich and co-workers [11], when they observed oscillations in pH (H^+ concentration), redox potential and gas uptake in the carbonylation of phenyl acetylene. Following this discovery, oscillatory modes of palladium catalysed carbonylation

reactions using other small molecule alkynes substrates e.g. non-1-ynes [33] and methyl acetylene [38] were reported. Based on these studies employing small molecule substrates, oscillatory modes were recently identified using mono-alkyne-functionalised polyethylene glycols (A-PEG_{2000}) (approximately 2000 Da and 5000 Da) as substrate [29] and a PdI_2−KI−CH_3OH catalytic system. Considering this advancement, the prospects of applications geared towards autonomous soft materials now appears more realistic. In this instance, the oscillatory dynamics in pH, arising from carbonylation reactions of alkyne functionalised polyethylene glycols can be incorporated into the soft materials, causing it to respond autonomously (independent of any environmental influence) via chemical energy [39]. In order to accomplish this goal, where the above-mentioned application becomes practicable, extensive analysis geared towards understanding the reaction mechanisms and nonlinear chemical dynamic behaviours in the oscillatory carbonylation of alkyne functionalised polymers is vital. Thus, the work presented throughout this thesis aims to elucidate reaction mechanisms, oscillatory and non-oscillatory behaviours in palladium catalysed oscillatory carbonylation reactions employing alkyne functionalised polymers

1.2 Aims and Objectives

This research aims to understand reaction mechanisms and nonlinear behaviours that arise when alkyne functionalised polyethylene glycols are employed as substrates in palladium catalysed oxidative carbonylation reaction. This aim will be achieved by assessing the influence of mono alkyne (A-PEG_{2000}) and bi-alkyne (A-PEG_{2000}-A) functionalised polyethylene glycols as reaction substrates in palladium catalysed oscillatory carbonylation reaction. The initial study with mono alkyne functionalised methoxy polyethylene glycol (A-PEG_{2000}) at a single concentration [29] will be extended to include carefully designed arrays of experimental studies. These studies will assess oscillatory and non-oscillatory modes arising from varying the concentrations of mono alkyne functionalised methoxy polyethylene glycol at constant and variable catalytic concentrations. The aim will equally be accomplished by evaluating the influence of changing KI and/or PdI_2 concentrations in the catalyst makeup and, altering extra KI addition times at constant A-PEG_{2000} concentrations. The influence of different substrate concentrations on the initial behaviour of the reactions and the modes of oscillations will also be investigated.

Studies on palladium catalysed oscillatory carbonylation reactions with bi-alkyne functionalised polyethylene glycol is an original addition to the family of oscillatory polymers. Hence, experimental studies considering the influence of catalytic concentration and bi-alkyne

polymeric substrate concentrations are also incorporated as part of achieving the research aims (oscillatory modes and mechanism elucidation). The results obtained from studying both polymeric substrates will be combined to clarify and deduce the reaction networks responsible for the presence or absence of oscillations, with the goal of understanding the observed behaviour of these reaction when polymeric substrates are present. The knowledge gained may then be transferred to developing autonomous soft materials and possibly in developing new multi-functional polymeric oscillating systems.

Summary of research objectives

1. Extend the preliminary study by Donlon and Novakovic [29] on mono alkyne functionalised polyethylene glycol methoxy ether to include a wider range of PdI_2, KI and mono alkyne substrate concentrations.
2. Assess the effects of maintaining constant reaction volumes to counter evaporative losses by introducing additional methanol as the reactions progress.
3. Establish the possibility of oscillations with bi-alkyne functionalised polyethylene glycol as the reaction substrate by assessing the system at different substrate concentrations.
4. Investigate the effects of a range of KI and PdI_2 concentrations on the system when bi-alkyne functionalised polyethylene glycol is used as substrate in the carbonylation reaction.
5. Examine the effects of KI on oscillatory and non-oscillatory behaviours during the carbonylation reaction with both substrates.
6. Assess the impact of doubling the alkyne groups (bi-alkyne effect) by comparing reactions employing mono alkyne and bi-alkyne polyethylene glycol substrates at constant catalytic concentrations.
7. Identify different forms of nonlinear behaviour achievable with mono and bi-alkyne functionalised polyethylene glycol polymeric substrates.
8. Enhance understanding of reaction networks postulated for nonlinear behaviour from experimental observations in the system when mono alkyne and bi-alkyne polyethylene glycols serve as substrate.

1.3 Thesis Structure

Chapter 2 reviews the literature pertinent to this work. Oscillating chemical reactions and carbonylation reactions with a focus on palladium catalysed carbonylation reactions are

discussed before palladium catalysed oscillatory carbonylation reactions is reviewed. Oscillatory and non-oscillatory modes reported so far in oxidative carbonylation reactions are discussed. Also, an overview of oxidative carbonylation with mono-alkyne functionalised polyethylene glycol with proposed reaction mechanism based on the single study and complementing modelling studies are given. Finally, potential applications of oscillatory carbonylations reactions and oscillatory reactions in general is discussed before the chapter concludes with reiterating the research justification.

In Chapter 3, the experimental methods employed throughout the thesis is described in detail. A systematic description of the steps involved in achieving oscillations with polymeric substrates is discussed. The chapter begins with methods for functionalisation and characterisation of polyethylene glycols such that the final products following functionalisation have terminal alkyne. Then details of carbonylation reactions are discussed and finally, the final products formed after the carbonylation reaction with functionalised polymer, is given. The equipment required for polymer synthesis and functionalisation, catalyst preparation and the in-house designed set of six parallel reacting system with automated online pH and temperature measurements are likewise discussed. Overviews of individual studies designed to assess the influence of varying substrate and catalytic concentrations, additional methanol and KI addition times, are given. In this section, the actual concentrations and designs of experiments are not included, since extensive work was completed using both substrates and catalyst. Rather, they have been included in the respective result chapters so that clarity is kept, and the reader appreciates the purpose of each study.

Chapter 4 focuses on the results obtained from the range of studies performed with mono alkyne functionalised polyethylene glycol as reaction substrate, while Chapter 5 discusses the results obtained when bi-alkyne functionalised polyethylene glycol is employed as the reaction substrate in the palladium catalysed oxidative carbonylation reaction.

Results from studies designed to compare the influence of number of alkyne functional groups present via assessing and comparing the reaction profile when mono alkyne and bi-alkyne functionalised polyethylene glycol are employed as reaction substrates at the same alkyne concentration, or substrate concentration is presented in Chapter 6 and finally, conclusions from the results chapters and recommendations for future work are presented in Chapter 7.

Chapter 2. Literature Review

2.1 Oscillations

Oscillating motion is one of the four basic motions in physical nature. Other basic motions found in nature include random motions, translational motions, and rotational motions. Oscillatory motions are time dependent like other types of motions and are recognised as a motivating force behind many sophisticated and beautiful patterns and phenomena observed, naturally. The significance of oscillatory motion in nature is exemplified in a variety of scientific disciplines [12]. Examples of subjects with prominent presence of oscillations include mechanics; electrical; optics; chemical, biochemical, and biological systems; ecology; economics; mathematics; social science; astronomy; earth and geological sciences and computing. The influence of oscillations are also notable in applied arts with several examples of oscillation themed art pieces such as the 2016 "*Oscillations – Axon and Homeostase*" sculpted pieces by the Dutch artist Joris Strijbos [40]. In systems exhibiting oscillating motions, their characteristic features of time/space dependent repetitions in amplitudes, periods and frequency are preserved, as long the entropy of the system is maintained by ensuring that matter/energy flows through [12]. The likelihood of oscillations to occur in any system is governed by two essential requirements: - the systems involved ought to be nonlinear (dynamic systems) and should possess positive and/or negative feedback mechanisms. The presence of feedback mechanisms is essential for maintaining the periodicity of such motions.

Oscillatory reactions in chemical, biological and biochemical systems are a very remarkable division of oscillating systems because these reactions are the foundations for vast numbers of cyclic processes in living things. Exploring oscillating reactions in biological systems has helped the processes of understanding distinct oscillations that occur as part of life, which in turn, has encouraged the development of other form of chemical and biochemical oscillatory reactions that mimic real life processes. The first known proposition of cyclical chemical reactions was in 1910 by Hirniak [41, 42]. Based on the hypothesis he presented, his system was considered thermodynamically implausible. Although this was the first known system with a mechanistic description, the circadian rhythm/oscillator was already a known subject in life sciences with accessible articles reaching as far back as 1729 [43]. One common fact in biological/biochemical/chemical oscillating systems is the existence of groups of chemical reactions with oscillating intermediate species. Nonetheless, the type, nature, autonomy, and interdependence of the chemical reactions present differ in biological, chemical, and biochemical systems.

In biological and biochemical systems, oscillating reactions are typified by enzymes, proteins, gene, and metabolites based chemical reactions. Oscillations in biological systems are also termed rhythms or cycles and these repetitive cycles occur over a range of periods. Some periods are as small as a fraction of a second, while other could take up to several years [44, 45]. These cycles are observed in single cells, interactions in tissues and between tissues and organs, in whole organisms and in populations of living things [46]. Examples of these rhythms include cardiac rhythms, neural rhythms, circadian rhythms, and hormonal cycles [43, 44, 46-49]. The aforementioned biological rhythms exist naturally and function as regulators for various processes in living things. In addition to these naturally occurring biological systems, synthetic biological oscillators developed via intersection of protein and genetic engineering are also known [50].

In biochemical systems, known oscillations are usually centred on molecular level interactions in subcellular and cellular systems with homogeneity [51]. The origin of biochemical oscillations can be traced back to the Lotka and Lotka–Volterra models, wherein, Lotka proposed schemes of oscillating chemical reactions with an autocatalytic step in 1910 [52]. He extended his scheme to biological systems in 1920 [53] and 1925 [54] and, Volterra the mathematical biologist, extended the Lotka model in 1926 [55] to describe ecological events. Although these discoveries are the foundation of biochemical oscillators, definite oscillations in biochemical systems were evidently identified in nicotinamide adenine dinucleotide in its reduced state (NADH) from pyridine nucleotide cells [56, 57], ionic motions in the mitochondria [51, 58, 59] and glycolytic oscillating reactions of yeast cells reactions between 1957 and 1968 [51, 60]. Other examples of oscillations in biochemical systems are enzymatic oscillations [44, 51, 60-62], metabolite oscillations [44, 47, 60, 63, 64] and epigenetic oscillations [51, 65-67]. Biochemical and biological oscillators are interconnected since oscillations in biochemical systems deal with molecular oscillations in living beings. Like biological oscillators, a range of synthetic biochemical oscillators are also known and a broad classification of biological and/or biochemical oscillators as either natural or synthetic oscillators [50] is given in Figure 2.1.

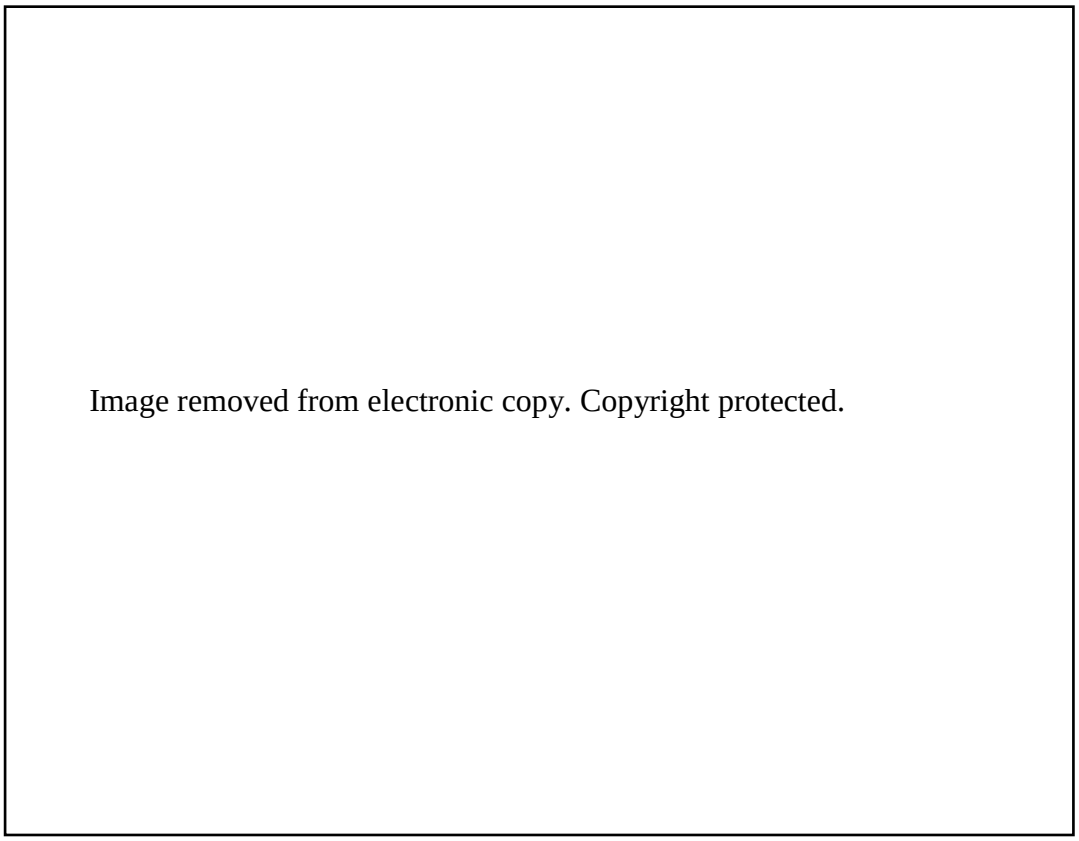

Figure 2.1. Natural and synthetic biological / biochemical oscillators [50]*.

2.2 Chemical Oscillations

Chemical oscillations arise when nonlinear systems are far from thermodynamic equilibrium. In essence, they do not occur around or across equilibrium [12, 68, 69]. In chemical oscillators, the nonlinear dynamic state required for oscillation to occur is the presence of autocatalytic reactions, while the feedback criteria is attained by the catalytic and inhibitory reactions steps present [12, 69]. Chemical oscillators are known to occur in forms of waves, localised physical movements, concentration/pH changes and colour changes as the specie ions are recycled continually due to reduction-oxidation steps [12, 30, 68, 69]. Several factors influence the dynamics of chemical oscillation produced irrespective of the form the oscillations take. These factors include temperature [24, 70-72], stirring speed / mixing (single and multiphase reactions) [73, 74], reactant flow rates [24, 70, 72-74], impurities [75], reaction type (batch/CSTR), diffusion (gas evolved or introduced as reactant), solubility for liquid-gas systems and reactant concentration [24, 70-73]. Since a broad of range of factor could potentially alter the oscillatory dynamics, it is important to ensure that experimental setups are appropriately controlled to limit undesirable interference and thus, improve reproducibility.

For chemical oscillators, the Bray oscillator discovered in 1921 [76] could be considered as the foremost chemical oscillator and subsequent efforts by Liebhafsky solidified Bray's findings. Although it was not easily accepted by chemists upon discovery, this oscillator is now one of the simplest known chemical oscillators [69, 76-79]. Bray-Liebhafsky oscillator as originally developed consisted of potassium iodate and hydrogen peroxide in acidified water [69, 76, 79, 80]. Oscillations in this system are generated from reduction of iodate to iodine and the oxidation of accumulated iodine back to iodate as shown in equations 2.1 to 2.10 [69, 78, 80, 81].

$6H_2O_2 \xrightarrow{KIO_3} 6H_2O + 3O_2$ (Overall chemical change) Eq. 2.1

$5H_2O_2 + 2IO_3^- + 2H^+ \rightarrow I_2 + 6H_2O + 5O_2$ (Autocatalytic, cycle 1) Eq. 2.2

$5H_2O_2 + I_2 \rightarrow 2IO_3^- + 2H^+ + 4H_2O$ (Autocatalytic, cycle 2) Eq. 2.3

Step mechanisms

$IO_3^- + 2H^+ + I^- \leftrightarrow HIO_2 + HOI$ Eq. 2.4

$H^+ + I^- + HIO_2 \rightarrow I_2O + H_2O$ Eq. 2.5

$I_2O + H_2O \leftrightarrow 2HIO$ Eq. 2.6

$HOI + H^+ + I^- \leftrightarrow I_2 + H_2O$ Eq. 2.7

$HOI + H_2O_2 \rightarrow I^- + H^+ + O_2 + H_2O$ Eq. 2.8

$I_2O + H_2O_2 \rightarrow HIO_2 + HIO$ Eq. 2.9

$HIO_2 + H_2O_2 \rightarrow IO_3^- + H_2O + H^+$ Eq. 2.10

After the discovery of the Bray-Liebhafsky chemical oscillator, research efforts on Krebs cycle by Belousov [23] led to the discovery of another chemical oscillator. This experimentally captured oscillating systems was similarly not recognised immediately and faced the same misgivings as Bray's system. In the interim, Prigogine proceeded to show exactly how the existence of oscillation was possible via modelling studies, and why it did not alter the laws of thermodynamics [82]. The work done by Prigogine marked the beginning of a new era for chemical oscillators. Following the acceptance of the possibility of oscillatory phenomena in chemical systems, in 1961, Zhabotinsky [19] improved on the work by Belousov and a comprehensive reaction mechanism for his oscillatory system was then established by Field, Koros and Noyes (FKN model) [83]. This oscillating chemical system now known as the

Belousov-Zabotinsky (BZ) reaction refers to chemical reactions where an organic substrate e.g. malonic acid is oxidized by bromate ions in the presence of transition metal ions e.g. ruthenium, manganese, iron and cerium [19-21, 75]. When malonic acid is involved in the reaction, the product is bromide, carbon dioxide and water. For BZ reaction, the autocatalytic step is the production of $HBrO_2$ [84-86] and Eq. 2.11 to 2.22 provides a detailed scheme of BZ oscillatory chemical reaction mechanism [83, 87].

$$3BrO_3^- + 5CH_2(COOH)_2 + 3H^+ \rightarrow 3BrCH(COOH)_2 + 5H_2O + 2HCOOH + 4CO_2 \quad \text{Eq. 2.11}$$

$$BrO_3^- + Br^- + 2H^+ \rightarrow HBrO_2 + HOBr \quad \text{Eq. 2.12}$$

$$BrO_3^- + HBrO_2 + 2Ce^{3+} + 3H^+ \rightarrow 2HBrO_2 + 2Ce^{4+} + H_2O \quad \text{(Autocatalysis)} \quad \text{Eq. 2.13}$$

$$2HBrO_2 \rightarrow BrO_3^- + HOBr + H^+ \quad \text{Eq. 2.14}$$

Step mechanisms

$$HOBr + Br^- + H^+ \leftrightarrow Br_2 + H_2O \quad \text{Eq. 2.15}$$

$$HBrO_2 + Br^- + H^+ \rightarrow 2HOBr \quad \text{Eq. 2.16}$$

$$BrO_3^- + Br^- + 2H^+ \rightarrow HBrO_2 + HOBr \quad \text{Eq. 2.17}$$

$$HBrO_2 \rightarrow BrO_3^- + HOBr + H^+ \quad \text{Eq. 2.18}$$

$$BrO_2 + Ce^{4+} + H_2O \rightarrow BrO_3^- + Ce^{3+} + 2H^+ \quad \text{Eq. 2.19}$$

$$Br_2 + CH_2(COOH)_2 \rightarrow BrCH(COOH)_2 + H_2O \quad \text{Eq. 2.20}$$

$$6Ce^{4+} + CH_2(COOH)_2 + 2H_2O \rightarrow 6Ce^{3+} + HCOOH + 2CO_2 + 6H^+ \quad \text{Eq. 2.21}$$

$$4Ce^{4+} + BrCH(COOH)_2 + 2H_2O \rightarrow 4Ce^{3+} + HCOOH + 2CO_2 + 5H^+ \quad \text{Eq. 2.22}$$

The last of the earliest set of oscillating chemical reactions discovered was the Brigg-Rauscher oscillators discovered in 1973 [88] hence, succeeding the BZ reaction. This oscillatory reaction consist of a mixture of iodate, hydrogen peroxide, malonic acid, and manganese (II) in acidic solution [89]. In the presence of starch indicator, characteristic colour changes from colourless to golden and finally to blue with a tinge of purple [14, 89] occur in this oscillator. Principally, Brigg-Rauscher oscillator is an adaptation of the BZ and Bray-Liebhafsky oscillators. The iodate and hydrogen peroxide mentioned are components of the Bray-Liebhafsky reaction, while the malonic acid and manganese ion originate from the BZ reaction. The oscillation in this system arises from the changing concentration of iodine and iodide ions and evolution of

O_2 and CO_2. A mechanistic demonstration with malonic acid as organic substrate [90, 91] is given in Eq. 2.23 to 2.36

$$5IO_3^- + 5H_2O_2 + 5CH_2(COOH)_2 \rightarrow 5ICH(COOH)_2 + 10O_2 + 5H_2O \quad \text{Eq. 2.23}$$

key autocatalytic steps

$$2IO_3^- + 5H_2O_2 + 2H^+ (+ Mn^{2+}) \rightarrow I_2 + 5O_2 + 6H_2O(+ Mn^{2+}) * \quad \text{Eq. 2.24}$$

$$5CH_2(COOH)_2 + IO_3^- + H^+ + 2I_2 \rightarrow 5ICH(COOH)_2 + 3H_2O ** \quad \text{Eq. 2.25}$$

Step mechanism for $*$

$$IO_3^- + H^+ + I^- \rightarrow HIO_2 + HOI \quad \text{Eq. 2.26}$$

$$H^+ + I^- + HIO_2 \rightarrow 2HOI \quad \text{Eq. 2.27}$$

$$HOI + H_2O_2 \rightarrow I^- + H^+ + O_2 + H_2O \quad \text{Eq. 2.28}$$

$$IO_3^- + HIO_2 + H^+ \leftrightarrow 2IO_2' + H_2O \quad \text{Eq. 2.29}$$

$$IO_2' + Mn^{2+} + H_2O \rightarrow HIO_2 + Mn(OH)^{2+} \quad \text{Eq. 2.30}$$

$$Mn(OH)^{2+} + H_2O_2 \rightarrow Mn^{2+} + H_2O + HOO' \quad \text{Eq. 2.31}$$

$$2HOO' \rightarrow H_2O_2 + O_2 \quad \text{Eq. 2.32}$$

$$2HIO_2 \rightarrow IO_3^- + HOI + H^+ \quad \text{Eq. 2.33}$$

Step mechanism for $**$

$$HOI + H^+ + I^- \leftrightarrow I_2 + H_2O \quad \text{Eq. 2.34}$$

$$CH_2(COOH)_2 \leftrightarrow ENOL \quad \text{Eq. 2.35}$$

$$I_2 + ENOL \rightarrow ICH(COOH)_2 + H^+ + I^- \quad \text{Eq. 2.36}$$

Consequential to the discovery of the BZ and Bray-Liebhafsky oscillators, and the successful combination of both as the Brigg-Rauscher oscillator, the ability to systematically design chemical oscillators, commenced. The inception of methodical design of chemical oscillators saw an increase in the number of new oscillators based on chlorite, iodate, bromate, periodate, sulphite etc. and a taxonomy of major oscillators as proffered by Epstein [12] is given in Figure 2.2.

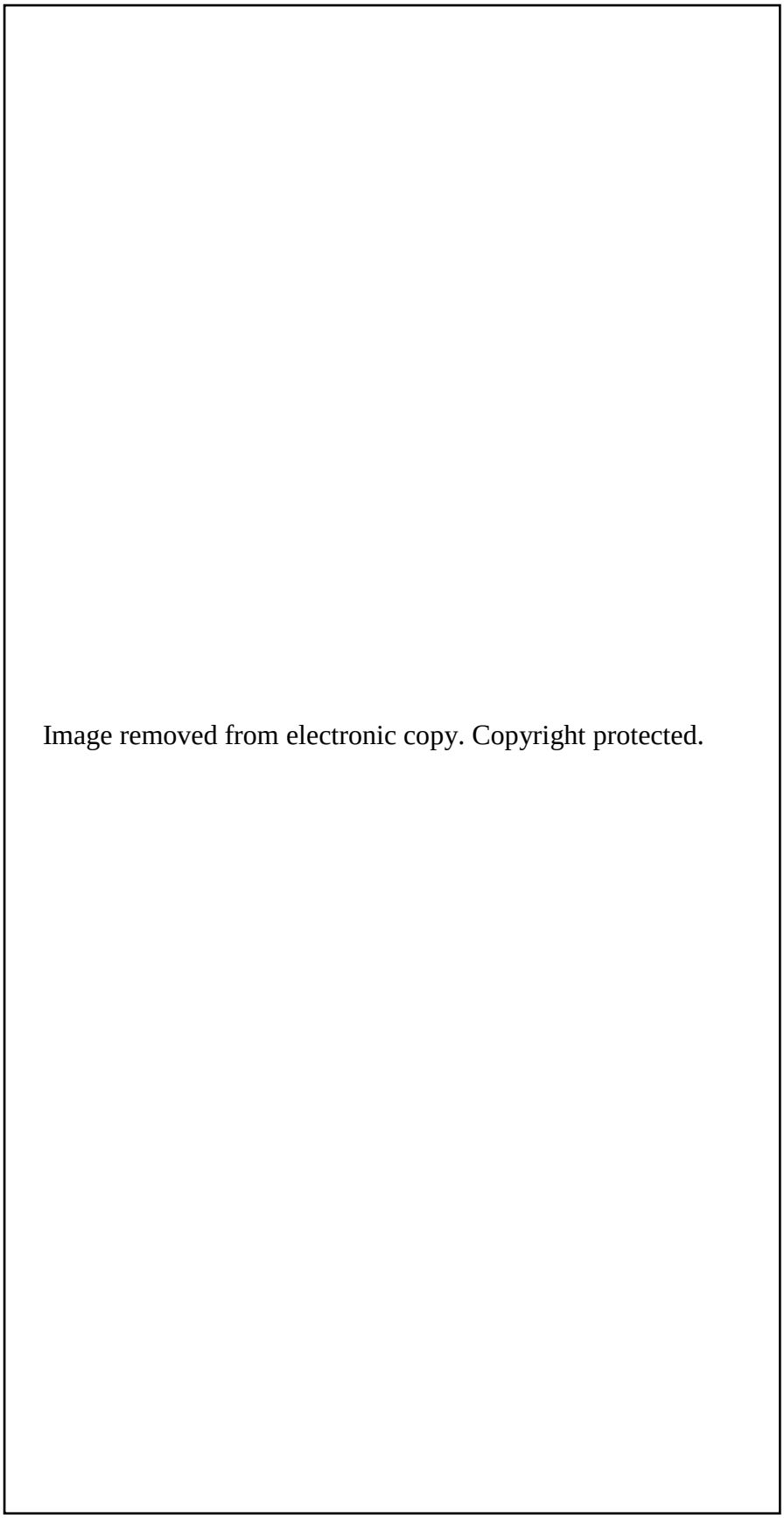

Figure 2.2. Epstein's taxonomy of chemical oscillators [12] *

The theory behind coupling of oscillators was originally designed [92] and first implemented with an iodate-iodide-arsenite system. With some modification to the iodate-iodide-arsenite system, the chlorite-arsenite-iodate system [93, 94], which displays bi-stability and autocatalysis via the reaction between arsenite and iodate (autocatalytic in I^-) was designed as a coupled oscillator. Following extensive research by chemists, the steps listed below were found to be vital to methodical design of chemical oscillators [14, 89, 93, 94]. These steps include

- making educated assumption to decide reactions with autocatalytic species
- determining the of regions of bi-stability
- adding new intermediate to serve as feedback source
- and altering the amount of intermediate generating the feedback such that, bi-stability is decreased and oscillatory region surfaces.

The chlorite-arsenite-iodate system fulfilled these conditions, since it is autocatalytic, shows bi-stability and the chlorite completes the feedback cycle. Bi-stability which is the co-existence of two steady (stationary) states is important as it defines the region within which oscillations may occur [16, 92, 95-100]. It is also possible for coupled oscillating systems to show multi-stability (more than two steady states (tri-stability)) [100] and, the types/modes of oscillations displayed in oscillating systems are linked to the presence of (bi) multi-stability. A variety of oscillations ranging from simple oscillations to compound / complex oscillations; mixed mode oscillations; bursting / intermittent oscillations; multi-rhythmicity; hard excitation and chaotic oscillatory modes are attainable from oscillatory reactions in either continuous or batch modes. However, the variations in modes of oscillations attainable surges when the reacting system is studied under continuous or flow conditions. This increase in forms of oscillations in CSTRs is more likely because, studies under flow conditions allow for improved control and calculated alterations of elements (temperature flowrate etc.) in the reactor which are necessary for occurrence of various oscillatory modes.

Simple oscillations are the most common form of oscillations and they arise from stable limit cycles, formed by substrate and product concentrations in the complex reaction sequence [9, 29, 32, 33, 92, 96, 98, 101-106]. The stable limit cycle is a characteristic feature of nonlinear systems, which is defined as a closed path attracting all adjacent pathways to itself. The ability to attract neighbouring trajectories to itself gives rise to the periodic sustained oscillations, described as simple oscillations here. Compound oscillations are formed when two oscillatory modes become superimposed [18, 95-98, 100, 107, 108] while complex oscillations occur when multiple peaks are present per oscillatory cycle [17, 26, 95-100, 108]. Discerning

compound and complex oscillations is challenging in batch systems as the transition period to superimposed (compound) oscillations may not be distinct, and multi-peaks in complex oscillations may be dampened. In mixed mode oscillations, two or more oscillating modes generate different oscillations in an alternating sequence of small and large amplitude oscillations [31, 109-115]. These are different from compound and complex oscillations as each oscillatory mode is visible (not superimposed) and are usually not multi-peaked.

Bursting and intermittent oscillations [112, 114-117] are quite similar modes of oscillations where each set of oscillations is separated by periods of "quiescent" states. The stationary / inactive states present in these modes of oscillations are more obvious for intermittent oscillations since they last a little longer. It is also possible to observe spiking oscillations [17, 108, 117, 118] in bursting and intermittent oscillatory modes due to the sudden spurts of high frequency oscillations distinctive to them. Oscillating systems exhibit multi-rhythmicity [95, 96, 100, 116, 119, 120] when two or more oscillatory states exist and, one oscillatory state continues until a change in species concentration causes a "jump" in state to the next oscillatory state (either at a higher or lower state). Hard excitation arises if a steady state and an oscillatory state are present [95, 102]. The oscillatory modes formed in systems showing hard excitation are initiated following a transition ("jump") from the steady state. When oscillations become irregular or aperiodic, they are referred to as chaotic oscillations [14, 44, 109, 116, 119, 121-123]. Representations of these forms (types/modes) of oscillations are given in Figures 2.3 to 2.6.

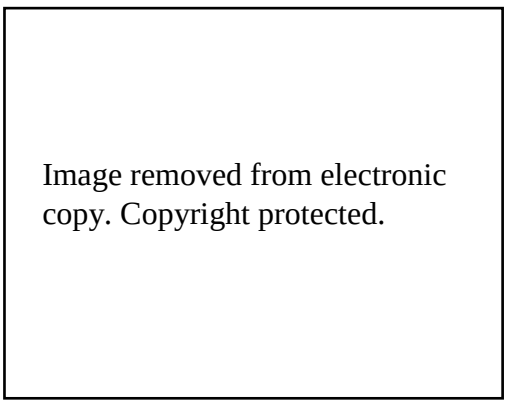

a)

b)

Figure 2.3. Illustration of bi-stability and simple oscillations in pH. Adapted from [32, 124] *. a) Bi-stability showing two steady states (SSI and SS II) and region of oscillations (OSC). b) Simple pH oscillations with time

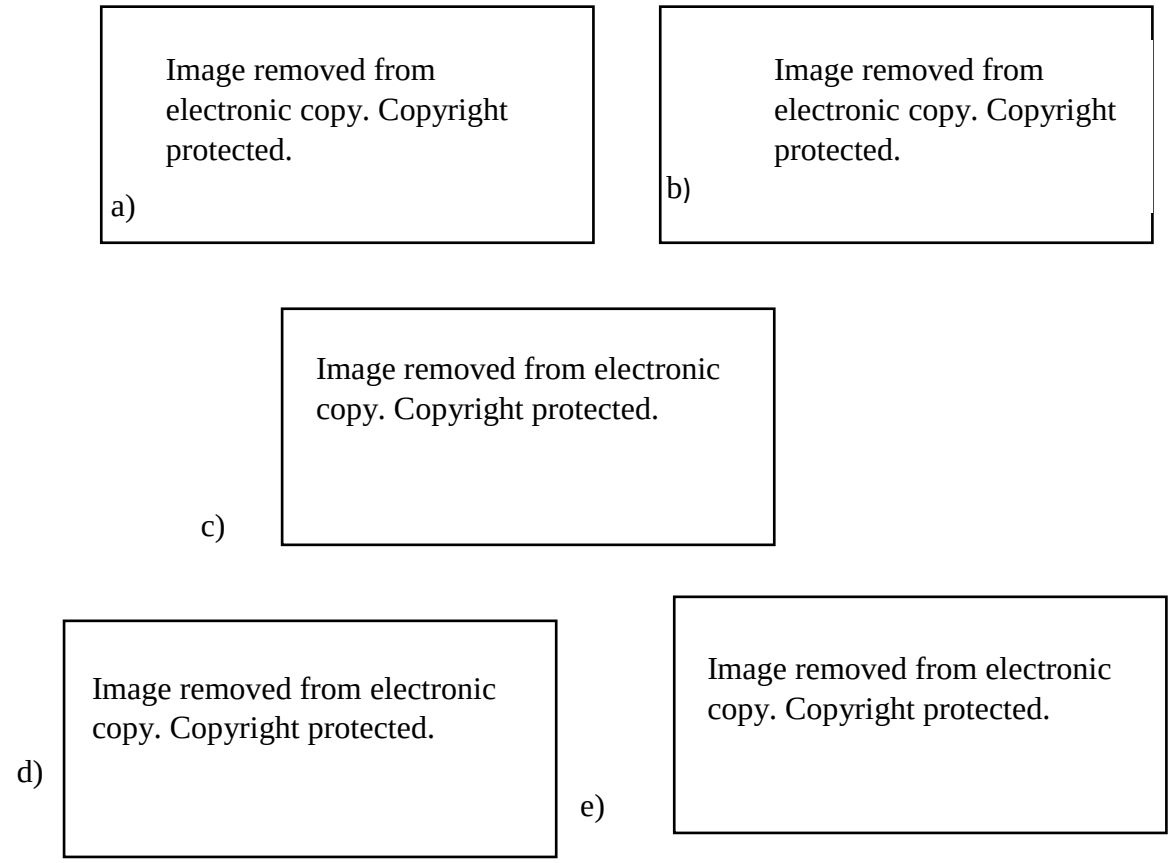

Figure 2.4. Illustrations of complex, compound and mixed mode oscillations. Adapted from [17, 31, 95, 112] *. (a) and (b) complex oscillations; (c) compound oscillation; (d) and (e) mixed mode oscillations

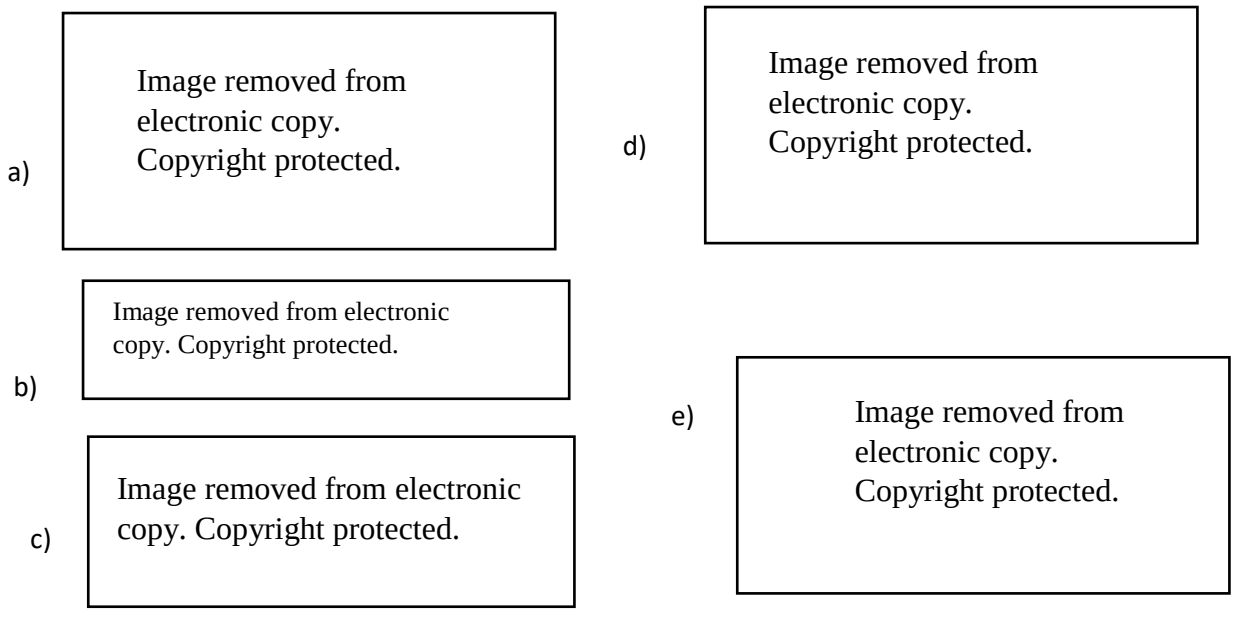

Figure 2.5. Bursts, intermittent and spiked oscillations. Adapted from [8, 104, 117, 118]. (a) intermittent oscillations; (b) and (c) spiked oscillations; (d) and (e) oscillations bursts

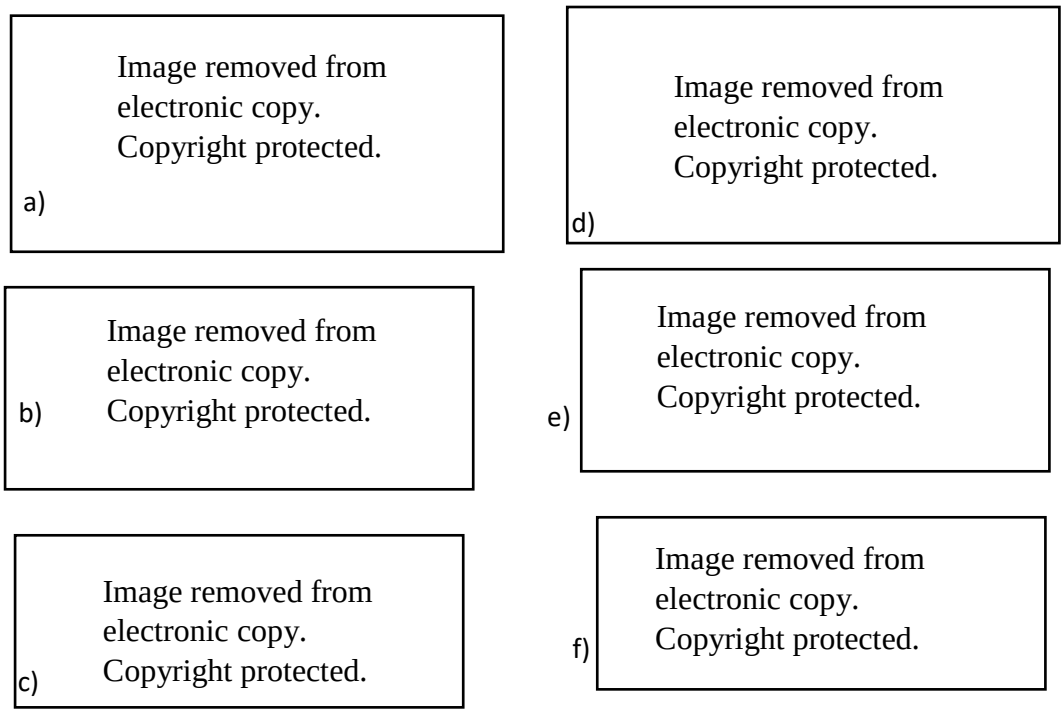

Figure 2.6. Adapted illustrations of bi-rhythmicity, hard excitation and chaos in nonlinear chemical reactions [44, 97, 119, 120] *. Bi-rhythmicity (a, b, d and e); hard excitation (c) and chaos (f)

Due to the diversity of oscillatory modes attainable in one oscillatory system as the process parameters change, these systems are usually represented using bifurcation and phase diagrams. These diagrams are quite useful as they provide comprehensive visual information with respect to regions where different nonlinear phenomena are attainable in a particular system. Bifurcation diagrams show interactions between maximum/minimum of a parameter versus a third changing parameter and indicate various features of nonlinear system, while phase diagrams are used to show regions of oscillations and different types of oscillations attainable. These definitions do not hold strictly as researchers use them interchangeably. Nonetheless, they aim to provide overall pictures of the states in a nonlinear system. Bifurcation and phase diagrams are more common in open systems as changing flowrates makes it easier to study these systems in detail and produce characteristic diagrams. These visual indicators are possible in batch system, with phase diagrams being more common, however, the data provided is usually limited due to constraints that arise in batch systems. Examples of both diagrams in some oscillating systems are given in Figures 2.7 to 2.10 [125-127].

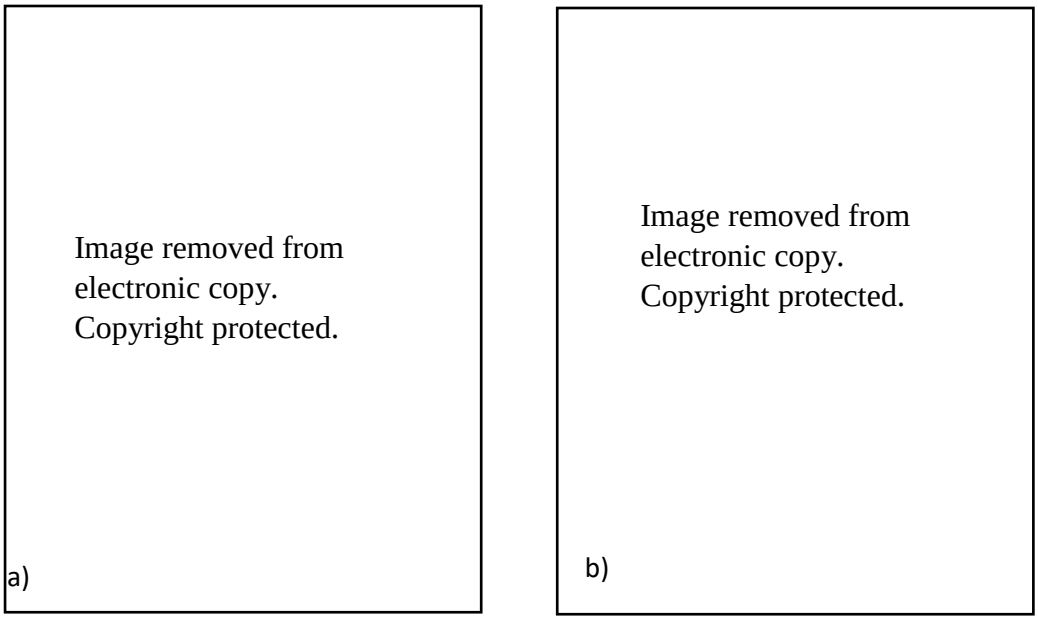

Figure 2.7. Schematic bifurcation diagram giving the minimum and maximum of the oscillatory or stationary current as a function of the (a) applied cell potential V (b) applied current I. (adapted from [125])*

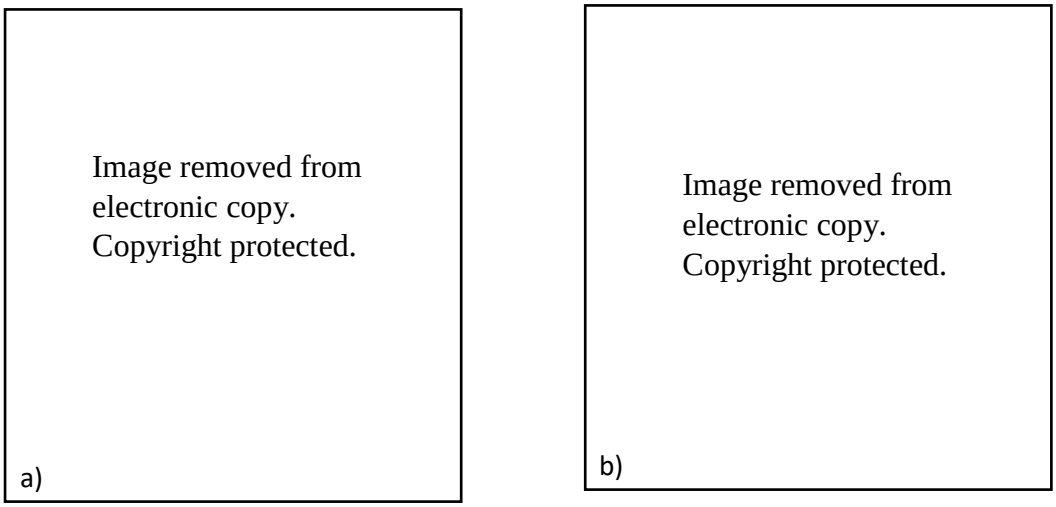

Figure 2.8. Experimental bifurcation and phase diagrams of open systems as a function of specie concentrations. (a) Symbols: (●) weakly basic SS I; (*) weakly acidic SS II; (triangle) oscillations, OSC, oscillations; SS I + SS II, bistability between SS I and SS II; SS I + OSC, bistability between SS I and oscillations [126] *. (b) Symbols: (circle), oscillations, (shaded triangle) SSI; (clear triangle) SSII, (diamond) bistability [128] *.

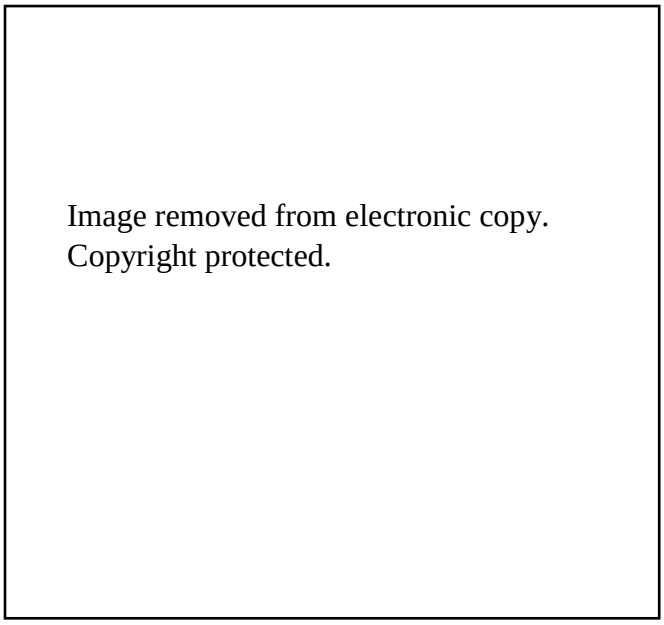

Figure 2.9. Ternary phase diagram for the BZ-reaction-induced mechanical oscillation of poly (NIPAM-*co*-Ru-(vmbipy)(bipy)2) gel particles with variation of substrate concentrations [127].* The dashed line shows the borderline of the oscillatory-steady-state regimes for a control study using non-polymerized catalyst.

Several new oscillators have been developed over time since the first oscillators were discovered and/or coupled. An exhaustive analysis of other oscillatory systems will not be covered in this review, however, other coupled oscillators of interest which fall under the class of pH oscillators [22, 24, 26, 27, 129] will be reviewed before the core chemical oscillator behind this research is then discussed. This group of coupled chemical oscillators (pH oscillators) are important because they are based on an attempt to recreate what is attainable in living organisms, as oscillations in living organisms are usually coupled [22, 129]. Although it is possible to have oscillations in pH in other oscillatory systems, the distinction for pH oscillators lies in their ability to display pH oscillations between large ranges of pH units (up to 4 pH units) in un-buffered solutions [24, 25]. For such oscillators, if the reactions are performed in a buffered solution, oscillations are absent.

In some coupled pH oscillators, precipitation or complexation equilibrium (ligand complexes with metal ions) [129] arising from elements with one stable oxidation state e.g. Al^{3+}, F^{-}, Ca^{2+} is used to achieve oscillations by attaching the elements to a pH oscillator [129]. This type of oscillator is promising because calcium, sodium and potassium can be connected by an artificial synapse to neurons such that, the responses generated are studied and used for biological predictions [49]. The bromate–sulphite–ferrocyanide oscillators are also known for

their ability to oscillate in pH [25, 128, 130]. In these systems, two major reaction sequences (Eq. 2.37 and 2.38) periodically switch between producing hydrogen ions auto-catalytically and, slowly consuming the hydrogen ions produced, giving rise to pH changes which can be as large as 4 pH units [130].

$$BrO_3^- + 3H_2SO_3 \rightarrow Br^- + 3SO_4^{2-} + 6H^+ \quad \text{(Autocatalytic, fast } H^+\text{)} \qquad \text{Eq. 2.37}$$

$$BrO_3^- + 6Fe(CN)_6^{4-} + 6H^+ \rightarrow Br^- + 6Fe(CN)_6^{3-} + 3H_2O \quad (H^+ \text{ consumption}) \qquad \text{Eq. 2.38}$$

The pH oscillators discussed above take place in aqueous media, but oscillations in pH are also possible in non-aqueous and semi aqueous condition. The oscillatory carbonylation reaction is an example of a non-aqueous pH oscillator and is the basis of studies completed in future chapters. This particular pH oscillator is unique since it does not involve the decomposition of complex substrates to facilitate oscillations, rather, it involves the formation of complex substrates [11]. Details of oscillatory carbonylation reaction will be incomplete without an evaluation of carbonylation reactions and the type of carbonylation reaction where these oscillations are attainable as such, carbonylation reaction is reviewed in the next section.

2.3 Carbonylation Reactions

Carbonylation reactions are reactions characterised by the incorporation of carbon monoxide (CO) into substrates with existing bonds or degrees of unsaturation, in the presence of metal catalysts [4, 131]. Carbon monoxide used in carbonylation reactions may be introduced to these substrates as CO gas or in the form of carbon monoxide releasing molecules (CORMs). Examples of CORMs include chromium and molybdenum hexacarbonyls and formic acid (decomposes to release CO on heating) [2, 132-135]. Substrates typically used as starting materials in carbonylation reaction includes alcohols, amines and other nitro compounds, organic halides (carbonylation process using this is usually by insertion instead of addition), aldehydes, ketones, esters and alkynes [5, 136, 137]. Since the initial works on carbonylation reactions by Reppe, other industrial processes such as the Monsanto process (catalytic carbonylation of methanol to produce acetic acid) have followed on and carbonylation reactions are now amongst the most essential reactions in industrial processes [1, 138]. The importance of carbonylation reaction at the industrial scale is exemplified by the vast amount of carbonylation products, which are key starting materials for other industrial applications, especially in the fine chemical sector of the industry. Examples of such key products from carbonylation reactions include ketones, aldehydes, carboxylic acids, polycarbonates, esters,

urea, carbamates, and isocyanates amongst others [1-5]. Figure 2.10 provides a range of substrates employed in carbonylation reactions and some of their corresponding products.

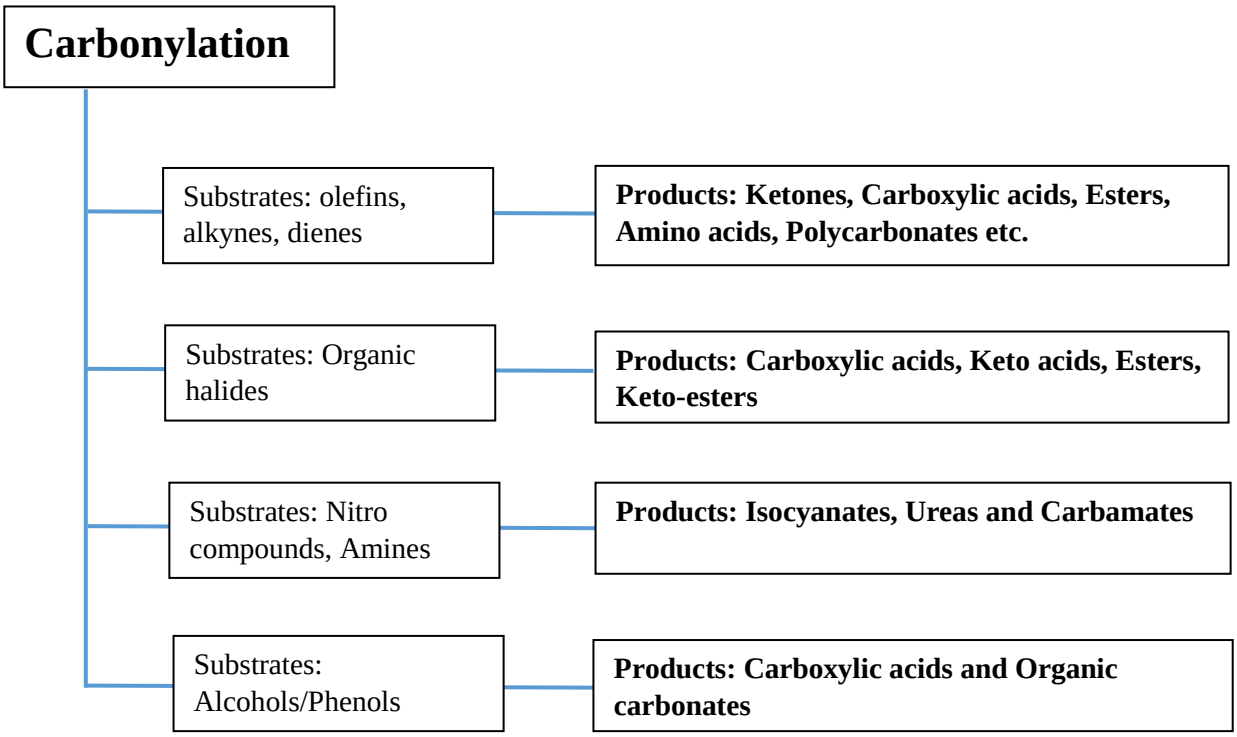

Figure 2.10. Simplified scope of carbonylation reactions as a function of substrates and products

Catalysts employed in carbonylation reactions are based on transition metals, with nickel as the transition group metal (TGM) catalyst originally used by Reppe for carbonylation reaction [1, 2, 4]. Other TGM catalysts including cobalt, iron, palladium, ruthenium, rhodium, platinum and iridium have also been used successfully in carbonylation reactions of alcohols, olefins, alkynes, styrene under a variety of reacting conditions and reaction mechanisms [1, 2, 4].

Several pathways are available to accomplish the carbonylation process. These routes are dependent on the mechanism of CO inclusion and the nature of the substrate employed during the carbonylation reaction. Typical examples of these approaches include hydroxyl [139-141] and alkoxy-carbonylation [2, 4, 142-144], amino-carbonylation [144-146], reductive carbonylation [137, 147, 148], hydroformylation [2, 4, 149], and oxidative carbonylation [3, 148, 150-155] processes. These routes can be summarised as four key carbonylation methods [156]. These routes to carbonylation are:

1. Reduction carbonylation: These reactions are typified as shown in Eq. 2.39 below

$$Su + CO + 2H^{+} \xrightarrow{catalyst} (CO)H_2Su \qquad \text{Eq. 2.39}$$

Su = organic substrate; $H_2Su(CO)$ is the reduced product of carbonylation [156].

2. Addition carbonylation: In addition, carbonylation reactions the degree of substrate unsaturation decreases after carbonylation. Equation 2.40 exemplifies the reaction pathway [156].

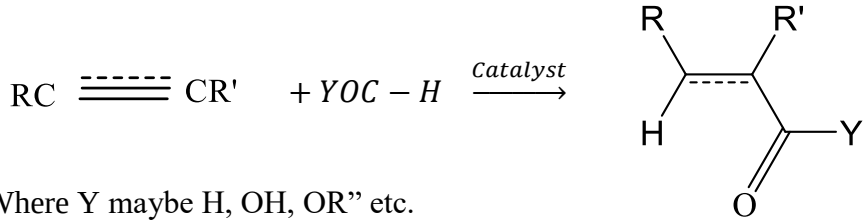

Eq. 2.40

Where Y maybe H, OH, OR" etc.

3. Substitution carbonylation: schematic representation of this reaction is presented in equation 2.41

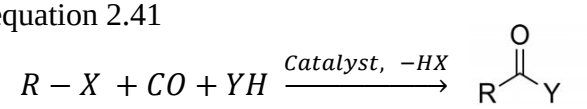

Eq. 2.41

Where YH can be H_2O, R'OH, R^1NHR^2 etc. and X = I, Br, Cl, OSO_2R' etc. [156].

4. Oxidation carbonylation: this reaction is facilitated by the presence of an oxidizing agent and a general scheme is given below [156].

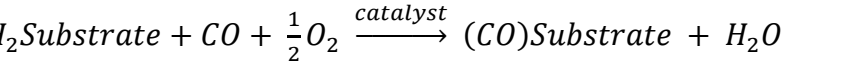

Eq. 2.42

For this review the focus will be on the oxidative carbonylation reaction as this is the mechanism on which known oscillatory carbonylation reactions are centred.

2.3.1 Oxidative Carbonylation Reactions

Oxidative carbonylation reactions OCR refer to chemical processes where carbon monoxide is introduced into organic and inorganic compounds in the presence of an oxidant typically oxygen and a transition metal catalyst e.g. palladium [157]. For OCR to occur, the metal catalyst in its ionic form undergoes reduction while, the oxidant present facilitates catalyst regeneration back to a charged state and the catalytic cycles continues as the reaction proceeds [3]. For example, when a transition metals such as palladium is used in OCR, the palladium starts off with an initial activation state of Pd^{2+} before it is reduced to Pd^0 during substrate conversion and is then recycled back to Pd^{2+} again via oxidation [3, 4]. Another example requiring an inorganic palladium complex and oxygen as oxidizing agent is seen when the iodide ligand complex, PdI_4^{2-}, is the source of palladium. For PdI_4^{2-}, conversions between Pd^{2+} and Pd^0 states are known to be very effective and this has been attributed to the presence of excess iodide ions during the reaction [4]. Thus, iodine may also serve as an oxidizing agent

for reactions of this nature [3, 4, 30]. Although the use of palladium as catalyst in OCRs is the most widely explored option due to its reactivity and increased amounts of reactant conversion other transition metals which have been successfully applied in OCR include Ir (IV), Pt (IV, II), Rh (III) [3].

Substrates and products of oxidative carbonylation reactions

The OCR reaction, like other carbonylation reactions, is employed vastly in the industry for the synthesis of many starting materials [158]. Oxidative carbonylation is achievable using several organic substrates including small organic molecules or larger polymers with certain functionalities attached to them [3, 4]. Examples of products formed from OCR includes carbonates [151] and urea derivate via oxidative carbonylation of alcohols and amines [151, 153]. Similarly, oxamates, ketones, carbamates and oxamides which are necessary intermediates in dyes, agrochemicals and pharmaceutics manufacture amongst others are products of OCRs [158]. Alkenes and alkynes form another important group of substrates and, the application of OCR yields structurally diverse acyclic and heterocyclic carbonyl products such as esters, amides etc. [3, 148, 156, 157]. OCR routes associated with alkenes, alkynes and other substrates include addition, cyclization and displacement reactions mechanisms. These OCR routes are driven by carbon monoxide partial pressure (concentration) [4, 155]. OCR reactions occur by nucleophilic attacks on OH, amines, acids, carbanions, alkyne etc. of the organic substrates followed by the insertion of carbon atoms [3, 4, 150, 152, 155].

2.3.2 Palladium Catalysed Oxidative Carbonylation Reactions of Alkynes Substrates

The use of palladium with different ligands as catalytic source in oxidative carbonylation dominates industries and academia as more efficient palladium catalyst with faster and easier recycling times and mechanisms are developed for carbon-carbon coupling [159, 160]. The initial examples of oxidative carbonylation reaction with alkyne in the form of ethylene occurred in 1958, where ethylene was used to produce acetaldehyde in the now known Wacker process [161]. Following, Tsuji and co-workers [162] demonstrated the carbonylation of acetylene based on Wacker's process. Their choice of catalyst was palladium chloride with the reaction occurring at high temperatures to produce muconyl, fumaryl and maleic acid chlorides [159, 160, 163]. They further expanded their studies by using other alkynes including diphenyl acetylene [164] and terminal alkynes under more suitable reacting conditions [159, 160]. Subsequently, vast forms of palladium catalyst were successfully employed in the carbonylation of alkynes. Summaries on the diversity of palladium-ligands bound catalysts used in these reactions are available in literature [150, 152, 155, 158, 165-169]. Some examples

includes palladium acetate [155, 158, 165, 170], $Pd(MeCN)_2Cl_2$ [155, 158, 165, 170], palladium phosphine [171], palladium bis(diphenylphosphino)ethane [159], palladium 2-pyridyldiphenylphosphine [142, 167] and palladium iodide [148].

A palladium-based catalyst OCR of special interest to this study is the PdI_2-KI-alkynes oxidative carbonylation system, which was introduced about 25 years ago by Bartolo Gabriele's research group [3, 148]. This system is significant because it is the catalytic-substrate system majorly employed in known oscillatory carbonylation reactions. This system has been very effective in OCRs of alkynes, amines, amino alcohols, and diols. When alkynes are used as substrate, carbonylation may occur via a cyclocarbonylation or a cyclization carbonylation pathway [2]. Cyclocarbonylation occurs by the oxidative addition of certain bonds e.g. O-H by Pd species, while cyclization carbonylation occurs when non-bonded electron pair on donor oxygen atom reacts with palladium specie to initiate cyclization. Examples of oxidative carbonylation reactions of alkynes and Pd based catalyst are the oxidative and reductive carbonylation of terminal alkynes e.g. phenyl acetylene, hex-1-yne, acetylenes, di-phenyl acetylenes with palladium iodide as catalyst [137, 148, 159, 160, 172].

In summary, the importance of carbonylation reactions cannot be over emphasised particularly when it involves organic synthesis because C-C bond formation is crucial for key product formation in synthetic organic chemistry. Following this concise review of carbonylation reactions, oscillatory behaviour arising from carbonylation reactions is discussed in the next section.

2.4 Oscillations in Oxidative Carbonylation Reaction

Oscillatory oxidative carbonylation reactions (OOCRs) are batch or semi-batch like pH chemical oscillators, and oscillations have so far been reported only when alkyne substrates were used. OOCRs are termed pH oscillators because like other pH oscillators, the presence of hydrogen ions in these reactions is a criterion for oscillations to occur [24, 25, 29, 130]. This oscillatory carbonylation system was first reported by Temkin and co-workers in the late nineties. Their initial system consisted of phenylacatylene-PdI_2−KI−O_2−NaOAc-CO in methanol and complex organic molecules such as phenyl fumarate and maleate were produced [11]. In OOCR systems, oxygen and iodine are the oxidants while alkyne substrate, CO, methanol, and iodide ion act as reductants. Known OOCRs have been carried out using small molecules substrates such as phenyl acetylene [8-10, 30, 32, 38, 103, 173-176], methyl acetylene [38], non-1-yne [6, 33], dimethylethynyl carbinol [6] and 2-methyl-3-butyn-2-ol

alcohol [7] and a macromolecular substrate; mono alkyne functionalised polyethylene glycol [29].

Amongst the small molecule substrates for OOCR, phenyl acetylene is the most studied and a range of products have been identified when phenyl acetylene is employed as substrate in oxidative carbonylation reactions. The nature of products obtained was found to be dependent on the route by which the oxidative carbonylation occurs [173, 175, 177]. When the OCR occurs in an oscillatory mode, one main product and four minor products were obtained. *Z*-2-phenylbut-2-enedioic acid dimethyl ester was the main product while dimethoxy-3-phenyl-furan-2(5)-one, 3-phenylfuran-2,5-dione, Z-2-phenyl-2-butenedioic acid and E-3-phenylacrylic acid dimethyl ester were the minor products formed [173]. When the carbonylation reaction occurred without oscillations, E-3-phenylacrylic acid methyl ester, 2-phenylacrylic acid methyl ester and 3-phenyl-5H-furan-2-one in addition to products that occur during oscillation were confirmed via GC-MS analysis [8, 173, 175]. Product formation and product selectivity were also found to depend on reaction temperature [8] and phenyl acetylene conversion was higher when pH oscillations were reported. An adaptation portraying the interlink between product formation and pH oscillations recorded in the carbonylation of phenyl acetylene at two different temperatures is given in Figure 2.11 [8]. Figure 2.11 also exemplifies typical features of this reaction including bursts in oscillation at 10^{o}C from onset till termination.

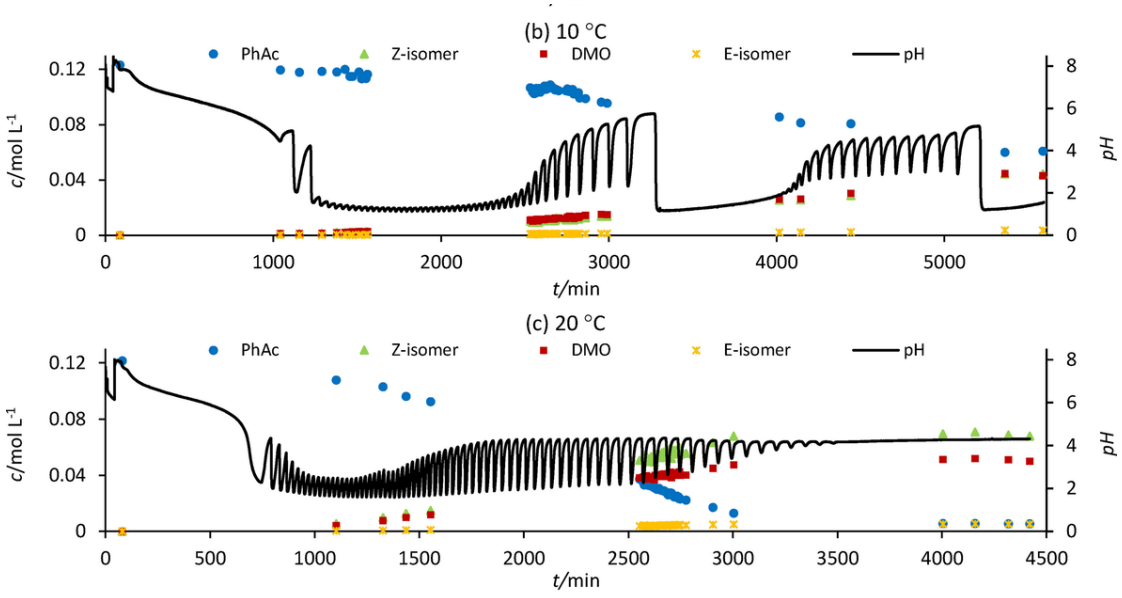

Figure 2.11. Product selectivity at different temperatures and features of reaction profiles recorded when oxidative carbonylation of phenyl acetylene occurs in oscillatory mode (adapted from [8]).

Following on from extensive studies on phenyl acetylene as substrate for OOCRs, oscillations were recently reported when a macromolecular substrate, mono alkyne functionalised polyethylene glycol methyl ether, was employed in oxidative carbonylation reaction [29]. Mono alkyne functionalised polyethylene glycol of two different chain lengths (2000 g/mol and 5000 g/mol) were used to prove the viability of achieving oscillations with larger molecules [29]. From the preliminary results for this system at a specific reaction condition, several advantages were already noted, and they include:

- The use of much lower concentration of catalysts, KI and substrate (two orders of magnitude less than previously required amount in OOCR systems) enabling visual changes (catalyst recycling colour changes) to be fully observed [29].
- Use of functionalised neutral polymers instead of small molecules thereby moving towards biocompatibility and increasing the likelihood for applications.
- Lowered costs with respect to the concentration of catalyst used at developmental stages.

The reaction network given in Eq. 2.43 to 2.48 and corresponding rate expressions in Eq. 2.49 to 2.54 were proposed for OOCR with the mono alkyne functionalised polyethylene glycol substrate based on this initial experimental and complementing computational study [29].

$$A - PEG + 2CO + 2CH_3OH + PdI_2 \overset{HI}{\rightarrow} Pd + P - PEG + 2HI \quad \text{Eq. 2.43}$$

Where $P - PEG$ represents products from the oxidative carbonylation.

$$2HI + \frac{1}{2}O_2 \rightarrow I_2 + H_2O \quad \text{Eq. 2.44}$$

$$Pd + I_2 \rightarrow PdI_2 \quad \text{Eq. 2.45}$$

$$Pd + I_2 \overset{PdI_2}{\longrightarrow} PdI_2 \quad \text{Eq. 2.46}$$

$$PdI_2 + CH_3OH + CO \rightarrow IPdCOOCH_3 + HI \quad \text{Eq. 2.47}$$

$$IPdCOOCH_3 + HI \rightarrow PdI_2 + CH_3OH + CO \quad \text{Eq. 2.48}$$

Respective rate expressions for reactions above

$$R_1 = k_1[A - PEG][HI]^2\,[PdI_2] \quad \text{Eq. 2.49}$$

$$R_2 = k_2[HI]^2 \quad \text{Eq. 2.50}$$

$$R_3 = k_3[Pd][I_2] \quad \text{Eq. 2.51}$$

$$R_4 = k_4[Pd][I_2][PdI_2] \quad \text{Eq. 2.52}$$

$$R_5 = k_5[PdI_2] \quad \text{Eq. 2.53}$$

$$R_6 = k_6[IPdCOOCH_3][HI] \quad \text{Eq. 2.54}$$

These rate expressions are based on the assumptions that the concentrations of methanol, carbon monoxide and oxygen were in excess in comparison to other reactants (and therefore can be considered constant). The assumptions are in line with previous findings from other studies performed with similar or same systems (phenyl acetylene as substrate) involving excess amounts of methanol, CO and oxygen [174, 175, 178, 179]. Rate constants that fit the proposed model were obtained by modelling the reaction mechanism using a BatchCAD software and comparing simulations with experimental findings.

2.5 Computational Analysis in Oscillatory Chemical Reactions

Chemical reactions occur broadly as either simple/elementary reactions or as complex reactions. Simple reactions occur in a single step with the absence of side reactions, and final products are formed directly in this single step. Due to the nature of these reactions, it is easier to determine their rate constants as this can be calculated directly and compared with experimental rates. For complex reactions which are composed of several elementary reactions, the presence of side reactions and intermediates, the complexity of the reaction order and the absence of direct route to product formation makes it difficult to determine the value of the rate constants. Oscillatory chemical reactions are usually complex chemical reaction systems with large numbers of elementary reactions thus, lending themselves to the challenges associated with complex reactions. Determination of governing reaction mechanisms and rate constants for these reactions are as such tedious and typically based on certain assumptions derived from experimental observations and prior knowledge of typical behaviours in similar systems. In oscillatory chemical reactions, this complexity is further heightened because of its nonlinear dynamics and stochastic nature [180]. Stochastic nature used here describes the ability of the complex reactions involved to proceed via different pathways or exhibit different behaviours in different experimental/simulation runs for identical inputs (input include reactant concentrations and reaction conditions). These attributes of oscillatory chemical reactions makes it necessary to use alternate methods to obtain/compare mechanism and rate data to complement experimental results. The use of alternate methods may provide detailed representation that promotes greater understanding of the oscillating system.

Computational chemistry offers this alternate route that supplements experimental data. It could also be used to propose and design new experiments that may not have been exploited but are necessary for mechanism determination. Computational methods are not only useful in mechanism elucidation, they could also be used in other aspects of chemistry such as determining structure and characteristic features of chemicals [181, 182]. The application of computational chemistry to oscillating chemical reactions goes as far back as their discovery as discussed in Section 2.2. Computational chemistry has been applied in the forms of statistics, numerical modelling, and simulations by means of a range of software [183, 184]. Russian STEP program package [38], XPPAUT package [26], MatLab [185, 186], BatchCAD [10, 29, 174] and COMSOL Multiphysics [186] are some examples of software used in modelling oscillatory reactions. It has proved useful in mechanism elucidation especially in the case of BZ oscillatory reactions, where it has been applied beyond fundamental reaction mechanism elucidation. It is also now a useful technique in material development applications incorporating the BZ oscillating reactions [187]. This tool is especially useful when it has predictive properties instead of fitting models to experimental data to show consistency [12, 182-184, 188, 189]. The use of computational techniques is not only limited to BZ reactions, they have also been applied in determining key species and expanding the reaction mechanisms for Bray-Liebhafsky oscillating reactions [80, 121, 185, 190-192], Briggs-Rauscher oscillating reactions [89, 193, 194] and a range of pH oscillators [105, 184, 195-197] including oscillatory carbonylation reactions [7, 10, 29, 38, 103, 173-175, 198].

Known computational methods in oscillatory carbonylation reactions are based on mathematical models and numerical modelling and simulations. They are very useful in interpretation and expansion of mechanism, have predominantly been applied in elucidating the mechanisms of small molecule oscillatory carbonylation reactions. Following the initial findings in 1997 [11], Temkin and co-workers focused on computationally deciphering the elementary steps comprising the mechanism of oscillatory reactions when phenyl acetylene and methyl acetylene were used as reaction substrates. They achieved this by generating a library of elementary reactions using computational tools and then studying potential key reactions from the library experimentally [198]. They also applied this tool in determining possible states of palladium catalyst used [38]. This was extended by Novakovic and co-workers, who investigated the initial steps of catalysis in oscillatory carbonylation reaction [174]. These advancements with small molecule facilitated by both experimental and computational studies ultimately led to macromolecular substrate oscillatory carbonylation reactions [29]. Thus, the importance of a balanced combination of experimental and

computational methods cannot be disregarded. The use of suitable computational methods based on reasonable assumptions allows for exploratory modelling and simulation, saving cost, and increasing the chances of development of predictive models, designs and condition optimization for potential applications of oscillatory chemical systems. As this thesis focuses purely on experimental analysis, the complementing reaction model, and simulation study in the oscillatory carbonylation of mono-alkyne functionalised polyethylene glycol reported by Donlon and Novakovic (2014) [29] has provided some foundation for assumptions and reaction mechanisms postulated in this thesis.

2.6 Applications of Oscillatory Chemical Reactions

Since the discovery and acceptance of oscillating chemical reactions [52], most emphasis have been channelled towards research work aimed at elucidating intricate mechanisms and physio-chemical properties of these reactions. As more information became readily available on the fundamental attributes of these oscillating systems, researchers expanded their focus to include discovery and development of applications of oscillating chemical reactions [20, 199, 200] and consequently, potential applications for oscillating chemical reactions were identified. Their findings suggested and demonstrated several ways through which oscillating chemical reactions could be applied via coupling with soft materials such as gels. Further applications of oscillating chemical reactions were also identified in fields of analytical chemistry, periodic polymerisation (e.g. acrylonitrile in BZ reaction) [15, 201], possible drug delivery (e.g. using a glucose enzymatic oscillatory system) [202, 203], time-lapse processes (e.g. thiol-acrylate polymerisation where base catalyst for reaction is first generated in situ via a pH clock) [204], quorum sensing simulation [205] (similar to biological system) etc.

Belousov-Zhabotinsky, Bray-Liebhafsky, Briggs-Rauscher and Orban-Epstein oscillating chemical reactions are the most sought after approaches for proposed applications due to the availability of comprehensive information on the workings of these systems. For application focused on coupling oscillatory reactions with soft materials, the Belousov-Zhabotinsky reaction and its variants are the most employed systems, while for analytical chemistry applications, all the above mentioned oscillating systems and more have been applied [206-209]. The application of oscillating chemical reaction in soft materials was initially demonstrated in the late nineties by the Yoshida group [20, 210]. They illustrated this application by assessing the behaviour of BZ reaction coupled with ruthenium functionalised poly(*N*-isopropyl acrylamide) gel [20 210] and it was termed “self-oscillating gel”. Since this discovery, other alternatives of self-oscillating polymers driven by variants of BZ reactions

have been illustrated at microscopic and macroscopic levels. In applications where oscillatory chemical reactions are coupled to soft materials, the important constituents include:- presence of polymer bound catalyst in redox states, availability of BZ reactants either within a second appended polymer [211] or externally supplied and stimuli responsive polymers

Examples of soft material applications of oscillating chemical reactions include $Ru(bpy)_3$) based chemical transducer [34], oscillating linear copolymers, branched polymers and block copolymers, one-directional ciliary motion of polymer brushes [212], autonomous vesicles formations for controlled release [213], self-walking gels, self-propelled gels, self-reciprocating gels, intestine-like tubular gels [214], molecular robots, mass transferrable gels, and multi-deformable cross-linked polymersomes and colloidosomes. These examples are not exhaustive and comprehensive literature reviews of these applications are available [20, 85, 213, 215-219].

The original example of an application of oscillating chemical reaction in analytical chemistry was by Tikhonova et al in 1978 [200], and it was promoted when Jimenez-Prieto et al [199] used an oscillating chemical reaction for similar studies. Other examples of these types of applications have been noted using a range of chemical and biochemical oscillators [206, 208]. The use of oscillating chemical reaction in determining the nature, type and concentration of analytes is based on perturbation studies on these oscillating chemical systems [200, 206, 207]. In principle, standard samples of compounds or substances that need to be analysed are passed through the oscillating chemical reactions as pulse perturbations and the characteristic features of these pulses on the oscillating chemical reaction profiles are recorded and analysed. Following, unknown sample mixtures suspected to contain previously analysed standards are passed through the same oscillatory reaction and are then identified quantitatively and qualitatively by comparing with the standard perturbation studies. Other analytical application include isomer differentiation [220], identification of gases and a host of others available in literature [207-209, 221-227].

Range of applications and possibilities of oscillatory systems is vast and as new systems are developed, more applications are envisaged. As more oscillating systems are discovered and comprehensive studies are carried out on already known systems, the chances of applying this aspect of science that cuts across various subjects and disciplines to problems requiring real solutions continues to increase. These endless possibilities have been the driving force where oscillatory chemical reactions are concerned and this, is also applicable to oscillatory carbonylation reactions. Hence, future chapters of this thesis will extend existing knowledge

on the fundamentals of oscillatory carbonylation reactions by exploring different approaches with macromolecular substrates, presenting novel results and discussing findings.

2.7 Summary and Research Justification

General principles of oscillating systems, types, characteristic features, and applications were discussed in preceding sections of this chapter. Oscillatory carbonylation reaction was also reviewed and acknowledged as the oscillatory chemical reaction of interest for this thesis. It offers an alternate route for development of applications, since it focuses on both substrate and catalyst suitability rather than mostly catalyst. Available information on the oscillatory reaction of choice centres mostly on reactions with small molecule substrates. Published communication of research on macromolecular substrate based oscillatory carbonylation reaction is presently limited to two [28, 29]. Observing that most material-based applications discussed in Section 2.6 required macromolecules of some sort, it is conceivable to propose that the likelihood of developing such application with oscillatory carbonylation reactions would likewise involve macromolecules.

Therefore, this thesis aims to contribute to the possibility of developing applications by expansively examining the pH kinetic profiles from macromolecular substrate based oscillatory carbonylation reactions. By examining the reaction profiles, the aim is to identify key features of the reaction and, possible mechanisms occurring during the oscillatory and non-oscillatory modes of the macromolecular substrate based oscillatory carbonylation reaction that may drive this research towards prospective applications. This aim will be achieved by conducting a range of experimental studies and, analyses of various aspects of the reaction profiles gotten from the OOCRs. The experimental studies consider parameters ranging from the catalytic system to the choice of macromolecular substrate concentrations and other reaction conditions.

Chapter 3. Experimental Methods

3.1 Introduction

The justification aims and objectives of this project were defined in Chapter 1 and Section 2.7, Chapter 2. This chapter provides details of the materials, equipment and methods employed in achieving these goals.

3.2 Synthesis of Alkyne Terminated Polyethylene Glycol

The first step towards achieving the aims of this project is the synthesis of alkyne functionalised polyethylene glycol, which serves as the reaction substrate for the oxidative carbonylation reaction. The alkyne functionalised polyethylene glycol was prepared by end group transformation of the hydroxyl group/s (–OH) on polyethylene glycol mono-methyl ether (methoxy polyethylene glycol) and polyethylene glycol (two hydroxyl groups) with alkyne moieties. The functionalisation occurs via a Steglich esterification reaction [228-230] with an alkyne donating molecule, in this case, 4-pentynoic acid was used. The reaction occurs in the presence of an activating agent, 1-ethyl-3-(3-dimethylaminopropyl) carbodiimide (EDCI) and an acylation catalyst, 4-dimethylaminopyridine (DMAP). An overall reaction scheme for the functionalisation of polyethylene glycol mono-methyl ether is given in Figure 3.1.

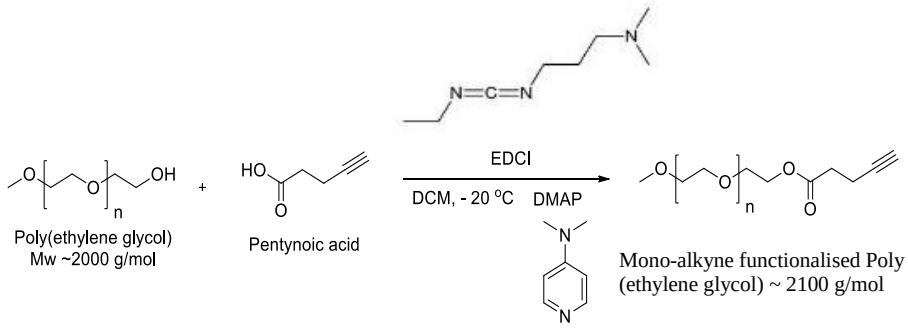

Figure 3.1. Mono alkyne functionalisation of polyethylene glycol via Steglich esterification reaction (DCM: Dichloromethane as reaction solvent)

In a Steglich esterification reaction, EDCI and 4-pentynoic acid react to form an acylisourea intermediate. Following, the urea intermediate specie reacts with DMAP, which is a resilient nucleophile, [228, 231, 232] to form responsive amides. These active amides subsequently react easily with the "OH" on the polymer, and polyethylene glycol esters with alkyne terminal ends are formed.

Reagents:

Polyethylene glycol mono methyl ether (methoxy polyethylene glycol) (for mono-alkyne functionalisation) (~ M_w: 2000 g/mol); polyethylene glycol (for bi-alkyne functionalisation) (~ M_w: 2000 g/mol); 4-pentynoic acid (M_w. 98.10 g/mol); 1-ethyl-3-(3-dimethylaminopropyl) carbodiimide (EDCI); 4-dimethylaminopyridine (DMAP); dichloromethane (DCM) anhydrous, ≥ 99.8%; sodium hydroxide (1M); anhydrous magnesium sulphate; diethyl ether anhydrous, ≥ 99.7%; deionized water; argon gas. All reagents excluding deionized water and argon were purchased from Sigma-Aldrich and used as received. Argon was purchased from BOC.

Equipment:

Equipment used for the synthesis of functionalised polyethylene glycols include vacuum manifold (Schlenk line) in a fume hood; vacuum rotary evaporator (BUCHI R-215); vacuum filtration assembly consisting of a 300 mL funnel top, fritted glass funnel stem/filter paper support, aluminium clamp, tapered rubber stopper and 1 L filtration flask (Sigma Aldrich); Whatman® cellulose filter paper, Ø 42.5 mm (used with the filtration assembly); glassware; glove box (Saffron UK) with moisture level at ~ 5 ppm and oxygen between 0.4-0.5 ppm.

Method:

Procedure for a typical batch synthesis is described. The quantities employed can be adjusted in proportion to size of the batch being produced and the number of functional groups per polymer chain. The method subsequently described is for mono alkyne functionalisation. 4-dimethylaminopyridine (183 mg, 1.49 mmol) and 4-pentynoic acid (1.24 g, 6.46 mmol) were measured into a Schlenk flask holding pre-weighed and vacuum degassed polyethylene glycol (12 g, 6 mmol). 1-ethyl-3-(3-dimethylaminopropyl) carbodiimide (2.4 g, 12.5 mmol) was measured into a different flask. These measurements excluding polyethylene glycol were carried out in a controlled environment using the Saffron UK glove box. A solution of 1-ethyl-3-(3-dimethylaminopropyl)carbodiimide, (2.4 g, 12.5 mmol) in dichloromethane (12 mL) was added drop-wise with a leur lock syringe, to the solution of poly(ethylene glycol) methyl ether, 4-pentynoic acid (1.24 g, 6.46 mmol) and 4-dimethylaminopyridine (183 mg, 1.49 mmol) in dichloromethane (20 mL) at ~ -20 °C. This temperature was achieved using an ice bath consisting of dry ice in methanol. The drop-wise addition was done under argon to keep the atmosphere in the Schlenk vessels inert. Upon complete addition, the mixture was continuously stirring for 36 to 72 hours at ambient temperature. The reaction mixture was subsequently washed with 40 mL of cold 1 M NaOH three times to neutralize the reaction and then with ~ 40 mL of cold distilled water three times. The organic layer obtained after washing and

extraction was dried over anhydrous $MgSO_4$ for 45 to 90 min depending on the batch size. The solution containing $MgSO_4$ was filtered and the solvent (DCM) with dissolved product was collected. The excess solvent was removed *in vacuuo* using a Buchi rotary evaporator until a very concentrated viscous liquid was achieved. The concentrated liquid obtained was precipitated twice into excess diethyl ether. The final product following precipitation was filtered and dried *in vacuuo* with the Sigma Aldrich vacuum filtration unit and Buchi rotary evaporator before a white powdery solid was obtained.

3.2.1 Product Analysis

Yields following alkyne functionalisation ranged from 55% to 92%, with more recovery being achieved in batches with starting polyethylene glycol mass ≥ 4 g. With larger amounts of polyethylene glycol (≥ 25 g), reaction time was increased up to 72 hours with continuous stirring for higher products yields. The recovered product was stored in a fridge at 3±1^{o}C using clear glass vials. No degradation was observed in samples stored for extended periods of time (34 months) in this manner as spectral analysis remained the same.

Nuclear Magnetic Resonance Analysis:

Nuclear magnetic resonance (NMR) spectroscopy is one of the major analytical methods used for structure elucidation, purity confirmation and content determination in complex mixture analysis [233-235]. NMR spectroscopy is a non-destructive technique, which works by detecting the arrangement of elements such as hydrogen (^{1}H), carbon (^{13}C), and phosphorus (^{31}P) present in test samples. NMR analysis of samples with these elements are possible because their nuclei have odd mass or atomic numbers. This odd number gives them a “spin” property that can be detected by the application of external magnetic fields [233-237]. When an external magnetic field is employed, the nuclei with spin property aligns at different energy levels, such that when the electromagnetic waves cease, a free inductive decay is obtained as the nuclei relaxes. The NMR spectra of the sample showing peaks at different frequencies is then obtained by Fourier transformation of the free inductive decay.

Samples obtained from the synthesis of alkyne functionalised polyethylene glycol were analysed for purity and presence of the alkyne end functionality with proton (^{1}H) NMR. A Bruker Avance III HD 500 MHz spectrometer from Brucker BioSpin GmbH was used to acquire the spectra. The analysis was done using deuterated chloroform as solvent and referenced to an internal tetramethylsilane (TMS) standard, in ppm.

NMR Spectra

Sample NMR spectra obtained from the functionalisation of methoxy polyethylene glycol and polyethylene glycol is given in Figures 3.2 to 3.6.

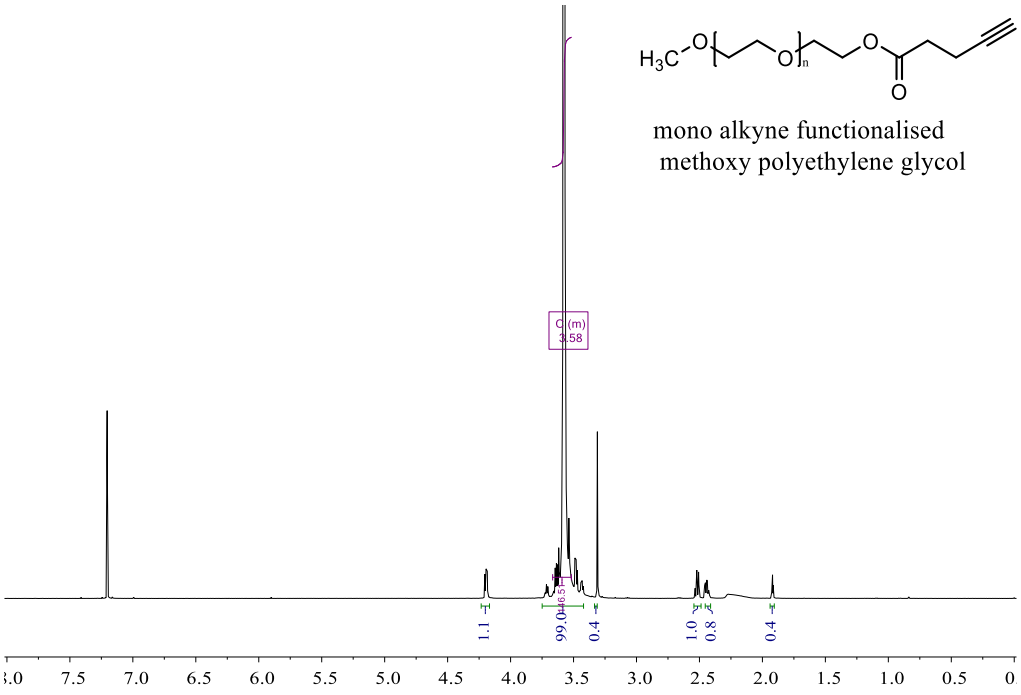

Figure 3.2. Proton (^{1}H) NMR spectrum of mono alkyne functionalised methoxy polyethylene glycol

The spectrum in Figure 3.2 was obtained from NMR analysis following alkyne end functionalisation of methoxy polyethylene glycol. The spectrum was acquired at 500 MHz with chloroform as solvent, identifiable on the spectrum at ≈ 7.26 ppm. The triple peak at 4.18 ppm resonates from protons (CH_2) around the alpha –OC (=O)-C and beta –O-C bonds following attachment of the pentynoic group (provides the alkyne end). The broad base peak between 3.42 ppm and 3.72 ppm consisting of single and triple peaks are protons from the methylene repeating units of the polymer backbone while the single peak at 3.31 ppm is from protons on the methyl (CH_3) end from the methoxy group (O-CH_3) on the polymer chain. The protons resonating at 2.45 ppm and 2.50 ppm arise from the CH_2 groups just before the triple bond and finally, protons from the terminal alkyne resonate at 1.92 ppm. The peaks obtained were consistently very similar to data available in literature for similar alkyne functionalisation [238]. A comparison of the mono functionalised methoxy polyethylene glycol and starting material (methoxy polyethylene glycol) is given in Figure 3.3.

A comparison of spectra from both methoxy polyethylene glycol and alkyne functionalised methoxy polyethylene glycol confirms that the alkyne functionality was successfully incorporated at the OH end of methoxy polyethylene glycol. The functionalised methoxy

polyethylene glycol (Figure 3.3, top) show proton resonances absent in the un-functionalised version (Figure 3.3, bottom). The broad base peak at 1.76 ppm is from residual water impurity in the methoxy polyethylene glycol flakes (Figure 3.3, bottom) that may have occurred due to moisture in glass vial, spatula (rinsed and air dried), or NMR tube during sample transfer and preparation for NMR analysis.

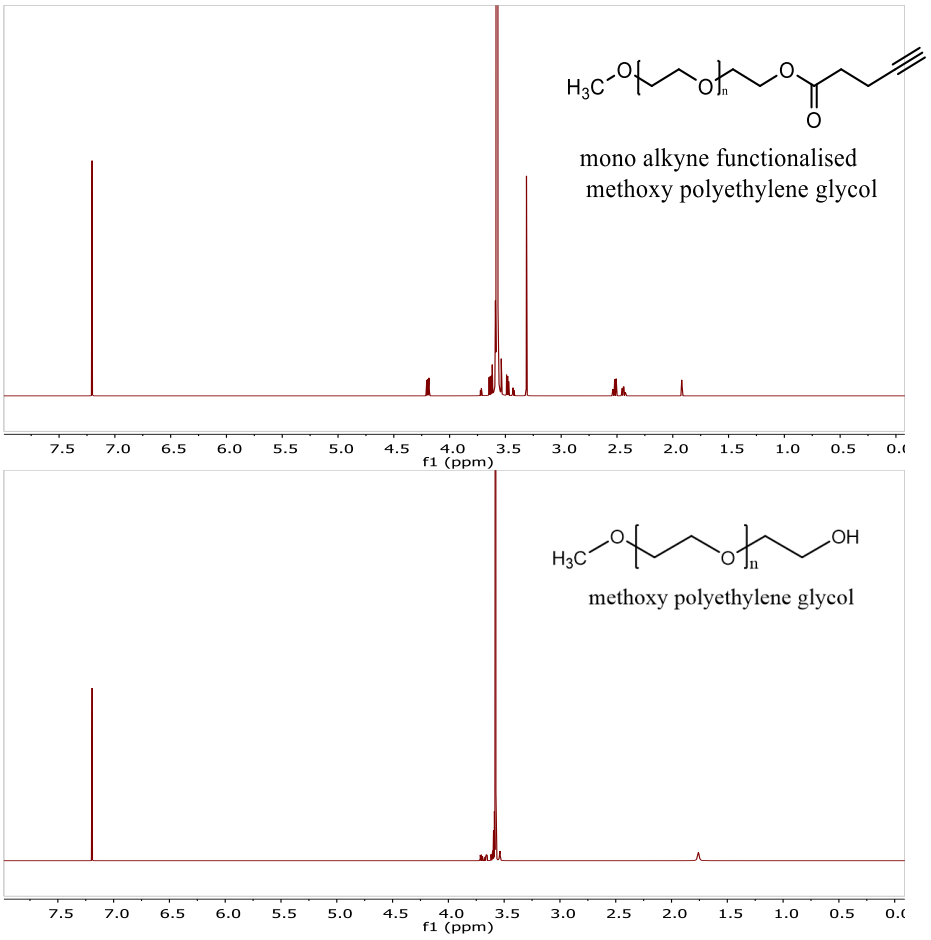

Figure 3.3. Proton (^{1}H) NMR spectra of mono alkyne functionalised methoxy polyethylene glycol (top) and methoxy polyethylene glycol (bottom)

Figure 3.4 shows the NMR spectrum obtained from bi-functionalised polyethylene glycol. Spectrum was also collected at 500 MHz with chloroform as solvent with a chemical shift at 7.26 ppm. The triple peak at 4.25 ppm resonates from the protons on the methylene (CH_2) group in O-CH_2-$C\underline{H_2}$-CO_2 following successful attachment of pentynoic acid. Likewise, the broad-based peak between 3.39 ppm and 3.78 ppm is from interactions between methylene protons within the bulky polymer backbone. The chemical shifts from 2.48 ppm to 2.57 ppm are multiplets from protons in the CH_2 groups just before the alkyne end (O_2C–($C\underline{H_2}$)$_2$–≡), while the last triple peak at 1.98 ppm is from the terminal alkyne proton.

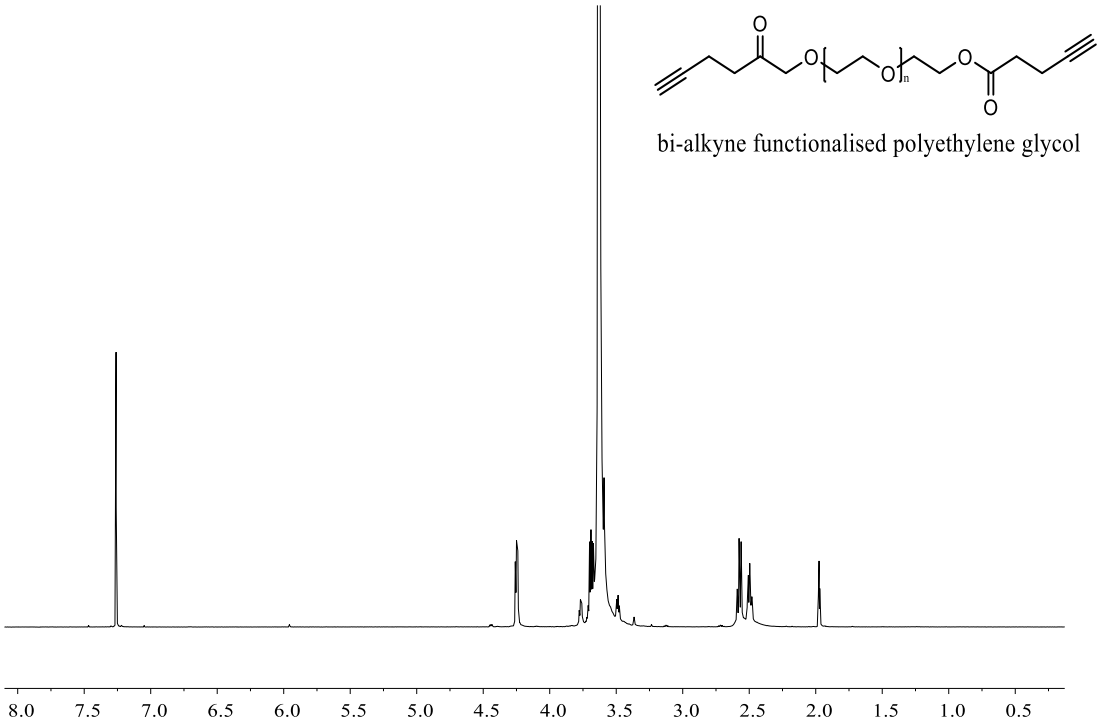

Figure 3.4. Proton (^{1}H) NMR spectrum of bi-alkyne functionalised polyethylene glycol

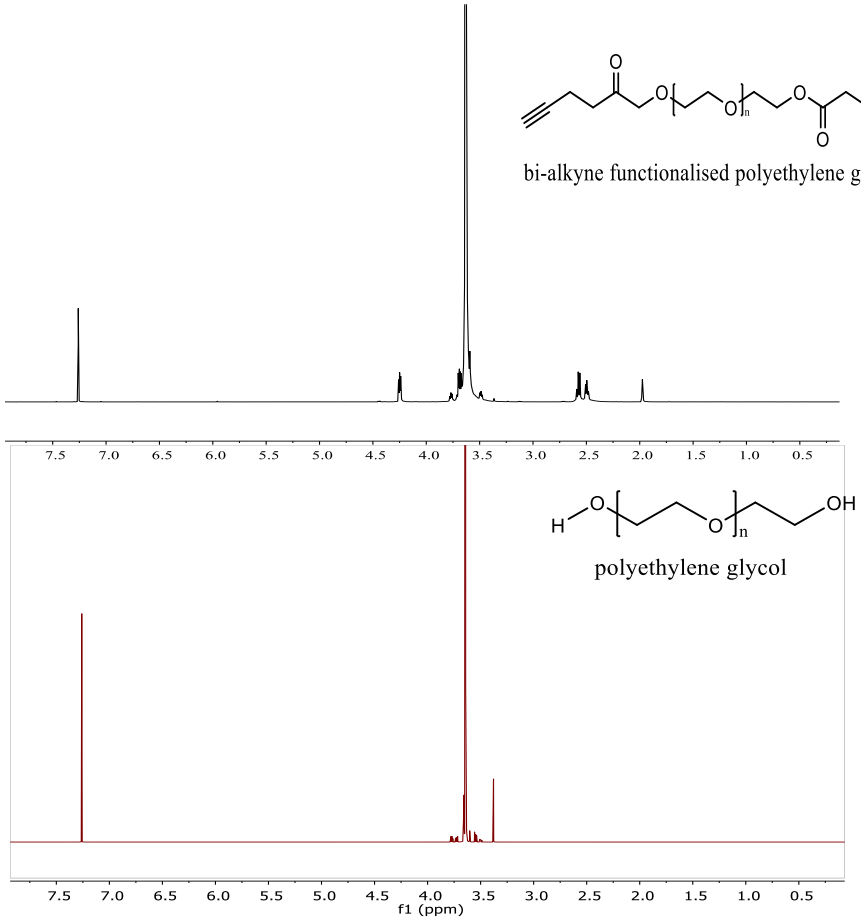

Figure 3.5. Proton (^{1}H) NMR spectra of bi-alkyne functionalised polyethylene glycol (top) and polyethylene glycol (bottom)

A comparison of bi-alkyne functionalised polyethylene glycol and polyethylene glycol starting material is given in Figure 3.5. The absence of peaks associated with alkyne functionality in the polyethylene glycol (Figure 3.5, bottom) spectrum confirms the incorporation of alkyne moieties at both ends of the polymer (Figure 3.5, top). The disappearance of the peak at 3.37 ppm (Figure 3.5, bottom spectrum) arising from the protons associated with the OH groups in polyethylene glycol following functionalisation also serves as confirmation.

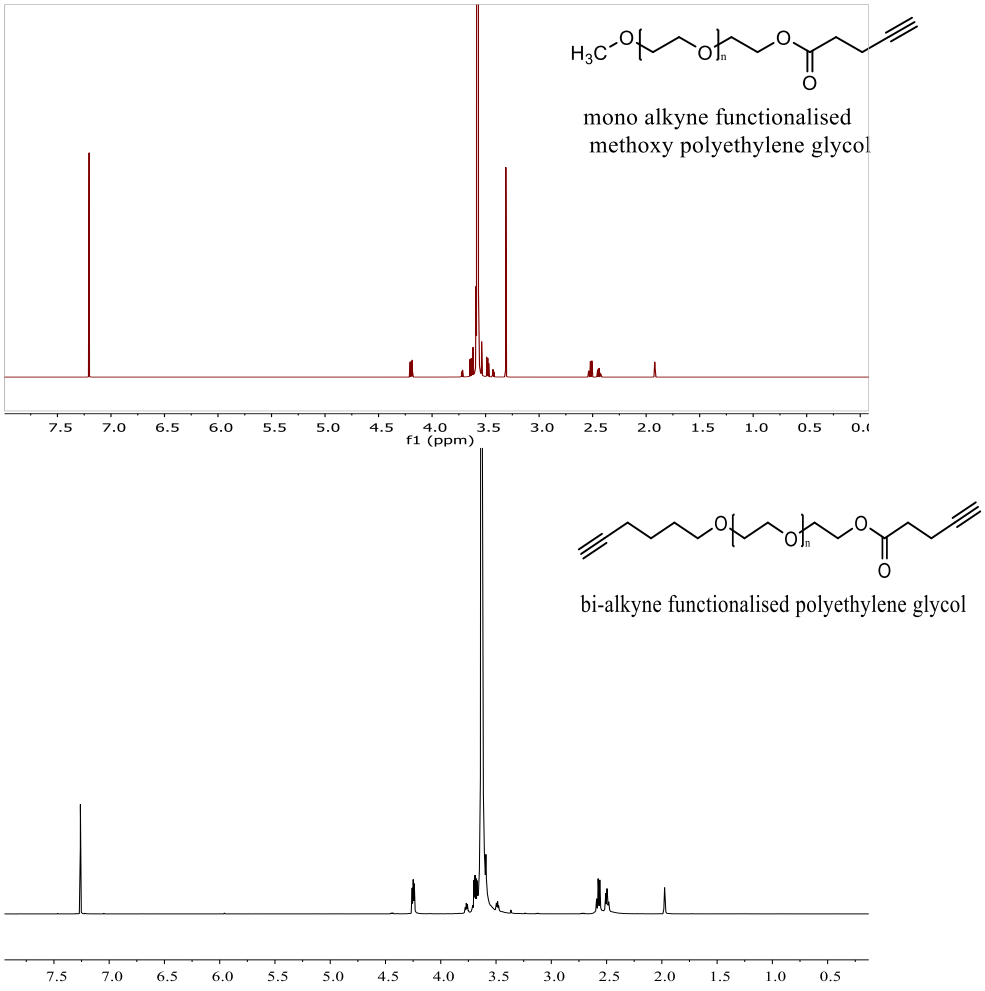

Figure 3.6. Proton (^{1}H) NMR spectra of mono alkyne functionalised methoxy polyethylene glycol (top) and bi-alkyne functionalised polyethylene glycol (bottom)

Figure 3.6 shows spectra of mono and bi alkyne functionalised polyethylene glycols. Peaks following terminal alkyne functionalisation are present in each spectrum and the main difference in the shifts is from the methoxy end group cap placed on one end of the mono alkyne functionalised methoxy polyethylene glycol to allow for single alkyne functionalisation. The minimal differences in ppm between corresponding shift in both mono and bi-alkyne functionalised polyethylene glycol are possibly from errors during NMR analysis. It could also be from the slight difference in molecular weight following

functionalization, as bi-alkyne functionalised polyethylene glycol has a slightly larger molecular weight than mono alkyne functionalised methoxy polyethylene glycol. This difference in molecular weight may have moved the NMR peaks observed (ppm), downward of the spectrum.

3.3 Catalyst Preparation

Catalyst solution consisting of palladium iodide and potassium iodide in methanol was used for all carbonylation experimental studies reported here and were pre-made and stored before use.

Reagents:

Palladium iodide (PdI_2), Chromasolv® HPLC grade (99.9%, <0.03% H_2O content) methanol, potassium iodide and 3 Å molecular sieves were purchased from Sigma-Aldrich.

Equipment:

Buchi R-215 vacuum rotary evaporator; Sigma Aldrich vacuum filtration assembly consisting of 300 mL funnel top, fritted glass funnel stem/membrane support, aluminium clamp, tapered rubber stopper and 1 L filtration flask. A 47 mm (diameter) Millipore membrane filter with 0.2 μM pore size was used with the filtration assembly. The clamp seals the filter membrane between projections on the funnel top and on the funnel stem.

Method:

A concentrated 'stock' solution of catalyst was prepared by dissolving PdI_2 (200.5 mg, 0.5 mmol) and potassium iodide (12.465 g, 75 mmol) in HPLC grade methanol (150 mL). The mixture was stirred in a closed bottle at ambient temperature for 72 hours. The resulting solution was filtered using the vacuum filtration assembly attached to the Buchi rotary evaporator to remove residual PdI_2. 5% m/v 3 Å molecular sieve was added to the resulting catalytic solution to remove residual water. The stock catalyst concentration was calculated based on palladium iodide left in the solution after filtering (PdI_2 concentration = 2.037 mM), and it was stored in a dark cupboard until required.

3.4 Carbonylation of Alkyne Terminated Polyethylene Glycols

Reagents, equipment, and method of experimental studies for the oxidative carbonylation of functionalised (mono and bi functional) polyethylene glycol is discussed here. Several studies covering reactant concentrations and reaction conditions were designed to achieve the objectives of this study. Unless otherwise stated, the method covered in this subsection was generally applied in experimental studies. Exceptions to general method described herein are covered elsewhere in this chapter. Since extensive numbers of studies were carried out using the same procedure, the exact concentrations of reactants with corresponding reaction conditions are listed within the results section for each study to facilitate easier understanding by linking them to the results and discussions.

Reagents

Stock catalyst solution (Section 3.3); mono-alkyne functionalised polyethylene glycol monomethyl ether ~ 2080 g/mole (Section 3.2); bi-alkyne functionalised polyethylene glycol ~ 2160 g/mole (Section 3.2); air and pure carbon monoxide (CO) (BOC); pH 2 (glycine buffer), pH 7 (phosphate buffer) and pH 10 (borate buffer) (Fisher Scientific); Chromasolv® HPLC grade methanol (99.9%, < 0.03% H_2O content) and potassium iodide (Sigma Aldrich), de-ionized water.

Equipment:

A parallel reaction setup was designed in-house to enable pH and temperature monitoring in up to 6 reactors simultaneously (Figure 3.7) and was then used for studies reported in this thesis. The parallel setup consists of an EA Instruments 6-channel pH and temperature monitoring multiport unit connected to a laptop for data logging. Six Hanna Instruments HI-1331B glass combination pH electrodes and six Pt100 temperature probes were connected to the multiport unit for this purpose. Twelve calibrated Omega FMA-2600 series mass flow controllers were fixed on the panel (Figure 3.7) to deliver gases, where six of the mass flow controllers deliver CO and the other 6 deliver air. The mass flow controllers were set at 15 mL/min each for all reactions reported here, though they offer flow rates of up to 100 mL/min. Tubing of 1.58 mm internal diameter and 3.18 mm outer diameter connected to the mass flow controllers were used to deliver the gases to the reaction vessel. Conical flasks (100 mL each) externally fitted with lead rings (to prevent buoyancy) were used as the reaction vessels. The temperature of the flasks was maintained using a Clifton NE4-22HT circulating water bath fitted with a Nickel-Electro DC2-300 immersion dip cooler. The contents of the flasks were

stirred (350 rpm) with the aid of a 2mag MIXdrive 15 HT multi-position stirrer submerged in the water bath. The stirring rate was kept constant at 350 rpm for all studies reported here.

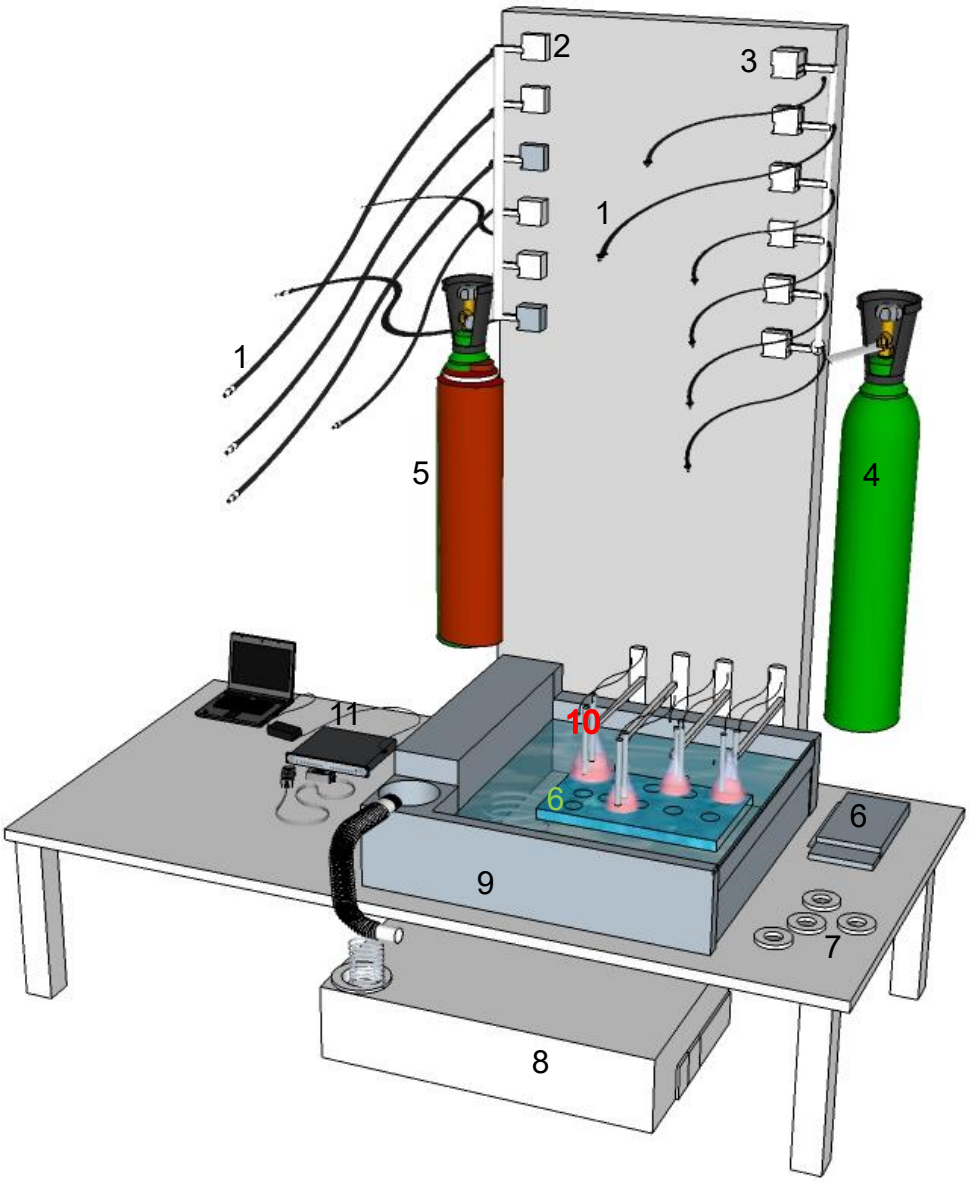

Component Parts

1. Gas pipes (inside flasks during reaction)
2. Mass flow controllers (CO)
3. Mass flow controllers (air)
4. Air cylinder
5. CO cylinder
6. Immersion magnetic stirrer (2mag MIXdrive)
7. Lead rings for flask stability
8. Nickel-Electro Immersion cooler
9. Water bath
10. six pH and six temperature probes
11. Multiport (6) pH and (6) temperature logging unit (EA instruments)

Figure 3.7. Illustrative sketch of the in-house designed parallel reactors setup for parallel carbonylation reaction.

Method:

pH calibration for carbonylation reaction

The pH electrodes for the parallel carbonylation reactions were calibrated before each set of experiments with pH 2 (glycine), pH 7 (phosphate) and pH 10 (borate) aqueous pH buffers. The pH electrodes attached to the multiport unit were washed with deionized water and placed in a buffer solution with corresponding temperature probes. The measured buffer value was recorded against its known pH value once it reached a stable value and slope obtained. This was repeated with each buffer solution and the electrodes were washed after each buffer measurement. The final calibration line during the reaction was automatically generated by the software accompanying the E.A. multiport unit, after the pH and temperature readings were obtained in all buffer solutions.

pH electrode limitations

In recent times, most pH measurements are performed with combination type electrodes. In these electrodes, both the reference and glass membrane electrodes are held in a single vessel. The combination type electrode with silver-silver chloride for internal and external reference was employed for all studies reported here. These electrodes have good stability and reproducibility in pure methanol [239] though several limitations are observed in other circumstances. When methanol has traces of moisture and other cations other than H^+, the pH electrodes become prone to small errors [240]. The deviations in pH recorded in the presence of univalent ions such as potassium is also higher than bivalent ions and, the components of the glass material (e.g. alumina) used in manufacturing the pH electrode similarly influences the interferences of alkali metal ions. Likewise, silver chloride electrodes are quite susceptible to bromide and iodide ions. An increase in the concentration of halide ions increase the interference thus generating potentials with increased negativity and changes in offset, leading to small errors in measurement. Silver is also known to precipitate in hexagonal form in the presence of excess iodide ions [241]. For this study, HI is produced, and KI is present in excess to facilitate Palladium recycling. In view of the excess KI present and the extended duration of these experiments, the possibility of some silver precipitating (electrode poisoning) and influencing the measured pH should be noted. These limitations mentioned above may have contributed to the measurements recorded in some manner, hence, some degree of error may be present. The electrodes were tested occasionally and some deviation ($1/100^{th}$ to lower end of $1/10^{th}$) were observed.

Parallel Oscillatory Carbonylation Reaction Set-up

For each study using the parallel system, 6 runs are possible at once since the multiport logger has provision for 6 sets of pH and temperature probes (Figure 3.7). This allowed for repeat runs to be conducted at the same time in some studies. For each experimental study employing the parallel carbonylation reaction set-up, data logging commenced after the electrodes had been calibrated and placed in bulk methanol (solvent). Other compounds for the reaction were then added subsequently.

General procedure across runs

Desired concentration of PdI_2/KI/methanol stock catalyst solution was diluted in 80±3 mL of methanol in the conical flasks, placed in the bath and fitted with pH and temperature probes. A baseline pH value was obtained over an average duration of 15±5 min and the solutions were then continuously purged with CO and air (15 mL/min each) using the tubes connected to the mass flow controllers. Before purging, the solutions had varying shades of brown/orange colour depending on catalyst/KI concentration. Higher catalyst concentrations (PdI_2/KI) gave rise to deeper shades of brown, and lighter shades or orange colour in less concentrated solutions. After purging for an average of 20±6 min, amber, light yellow (buff) or colourless solutions were obtained. The colour of the solutions after purging also showed similar dependence on catalyst concentration. Required amounts of (bi) alkyne functionalised polyethylene glycol dissolved in methanol (2 mL) was added to each flask. A further defined volume of methanol was used to rinse the vial containing residual functionalised polymer solution and the washings were added to the reaction mixture, giving a total initial reaction volume of 90 mL of methanol. The reaction vessels were carefully sealed off with parafilm to limit evaporative losses. The initial volume of methanol was maintained constant in all studies unless otherwise stated, while the initial concentrations of catalyst / catalytic mixture and polymer substrates varied. Reactions were allowed to run for 4 to 7.1 days. Stirring and temperature within the vessels were maintained using the immersed multi-position Mag stirrer plate in the water bath set at 20±2^{o}C.

3.4.1 Procedure for Experimental Studies with Additional Methanol

Methanol used as solvent in the carbonylation reactions is volatile, hence, some reaction solvent is lost due to evaporation (around the gas tubing and probes) over the course of the reaction, even though layers of parafilm were used as sealant. To account for evaporative loses and assess its impact on the reaction, additional methanol was introduced in one of the

experimental studies as detailed in specific result sections (Section 4.2, Chapter 4). Since methanol and/or residual water in it (from manufacturer) may influence the modes of oscillation [175, 176, 242, 243], a separate study where methanol addition was compared against the initial study (same conditions) without additional methanol was similarly conducted (Section 4.2.1, Chapter 4).

Method

The carbonylation reaction was set up according to the general procedure with a total initial volume of 90 mL. As the reaction progressed, defined volumes of methanol were added over the duration of the experiment. An approximate total volume of 25±5 mL of additional methanol was required for the reactions. This volume was generally enough to maintain the volume in the reactor at approximately 90 mL, however, the final total volume of methanol introduced depended on how long the reaction was run. The methanol was introduced into the reacting vessel with a 5 mL automatic pipette or a leur lock syringe. The vessels were resealed with fresh parafilm each time more methanol was added.

3.4.2 Procedure for Analysing the Effects of Potassium Iodide Concentration

The procedure for setting up reactions for experiments where the effects of KI concentration was investigated, is given below.

Method

A stock catalyst solution wherein the amount of potassium iodide used to facilitate dissolution of palladium iodide was kept constant (0.169 M) was made according to Section 3.3. The pH probes were calibrated, and methanol was added to the reaction vessels. Following, extra potassium iodide was added to each reaction vessels such that the total initial concentration of KI in 90 mL of methanol, including any KI introduced with catalytic mixture was either 3 mM, 6 mM or 9 mM. The fresh KI was allowed to dissolve in methanol before the catalytic solution, gases and substrates were added (see general procedure above, Section 3.4).

3.4.3 Procedure for Studies of the Effect of Potassium Iodide Addition Times

The influence of concentration of KI present was also assessed by changing the times when extra KI was added. Additional KI was introduced either at the start of the reaction (0 hr), 24 hours into the reaction or at 48 hours from onset of the reaction.

Method

A stock catalyst solution wherein the amount of potassium iodide used to facilitate dissolution of palladium iodide was kept constant (36 mmol in 213 mL methanol) was made according to Section 3.3. The pH probes were calibrated, and methanol was added to the reaction vessels. Following, extra potassium iodide was added to reaction vessels such that the total initial moles of KI in 90 mL of methanol (including KI from catalyst mixture) was either 0.54 mmol or 0.81 mmol. The extra KI dissolved before the rest of the general procedure was continued. For the reactions with extra KI addition time set at 24 and 48 hours, the general reaction procedure using the same stock catalyst solution was carried out and the initial amount of KI was 0.237 mmol (introduced with the catalyst solution). Then, for these reactions assessing influence of KI addition times 24 or 48 hours into the reaction, additional KI equating to 0.303 mmol and 0.573 mmol were introduced to each reaction vessels such that the total moles of KI added was kept constant (0.54 mmol or 0.81 mmol) in all flasks irrespective of when it was added (at either 24 hr or 48 hr from onset of reaction).

3.5 Analysis of Mixture of Products from the Carbonylation of (Bi) Alkyne-Terminated Polyethylene Glycol

Products arising from oscillatory carbonylation reactions with phenyl acetylene are known [8, 10, 30, 177]. As phenyl acetylene is a small molecule, it is possible to identify the products and measure reactant conversion using a variety of analytical techniques such as gas chromatography - mass spectrometry (GC-MS) [8, 175]. The use of polymer substrates such as alkyne functionalised polyethylene glycol substrate (Mw: ~ 2000 g/mole) in oscillatory carbonylation presents additional challenges in product identification and quantification, as techniques regularly applied in analysing phenyl acetylene products were not suitable for the polymer substrate. However, GC-MS analysis was used to confirm the absence of small molecule products in polymeric oscillatory carbonylation, indicating that products formed are macromolecular. Thus, determination of suitable analytical techniques for product identification and quantification in oscillatory carbonylation of alkyne functionalised polyethylene glycol would need extensive investigation. Since product identification and quantification is not an objective of this thesis, only NMR spectrometry was used to analyse the mixture of products from oscillatory carbonylation of (bi) alkyne functionalised polyethylene glycol. The spectrum obtained was analysed by associating possible products

formed during the polymer substrate carbonylation using known phenyl acetylene products [8, 30, 173, 175, 177] as a guide.

Reagent:

Chromasolv® HPLC grade (99.9%, <0.03% H_2O content) methanol, purchased from Sigma-Aldrich.

Equipment:

Buchi R-215 vacuum rotary evaporator with Buchi fitted neck flasks, Buchi water bath and flask stands.

Procedure:

The product recovery was initiated on terminating the reactions. The reaction solution was transferred to Buchi fitted neck flasks and attached to the Buchi vacuum rotary evaporator. The height of the evaporator was adjusted such that the part of the flask with residual reaction solution sits in a water bath set at 30^{o}C. A rotation speed of 110 rpm was set and the pressure gradually reduced as more methanol was evaporated under vacuum, until a very viscous oil, with dark brown to orange colour was obtained. The colouring is attributed to the palladium iodide and/or iodine (from excess KI) in the product mixture with shades of brown deepening as the amount of palladium iodide and KI present increased. The product mixture was stored briefly in a fridge before analysing with NMR spectrophotometer.

NMR Analysis

A Bruker Avance III HD 500 MHz spectrometer was used to acquire the spectra. The analysis was done using Deuterated chloroform as solvent at 298 K and referenced to an internal tetramethylsilane (TMS) standard, in ppm. Both proton and ^{13}C spectra were obtained from sample.

NMR Spectra

In Section 2.4 of Chapter 2, products obtained from the carbonylation of phenyl acetylene were discussed. The nature of products as well as percentage conversions of phenyl acetylene was different for carbonylation reactions in oscillatory and non-oscillatory modes [8, 30, 31, 173]. Key products from the oscillatory carbonylation of phenyl acetylene are given in Figure 3.8. In oscillatory modes, products numbered 1 to 5 have been consistently found in various ratios,

following conversion of phenyl acetylene [8, 10, 31] while the product numbered 6 is known to occur in non-oscillatory carbonylation of phenyl acetylene [10, 30, 177].

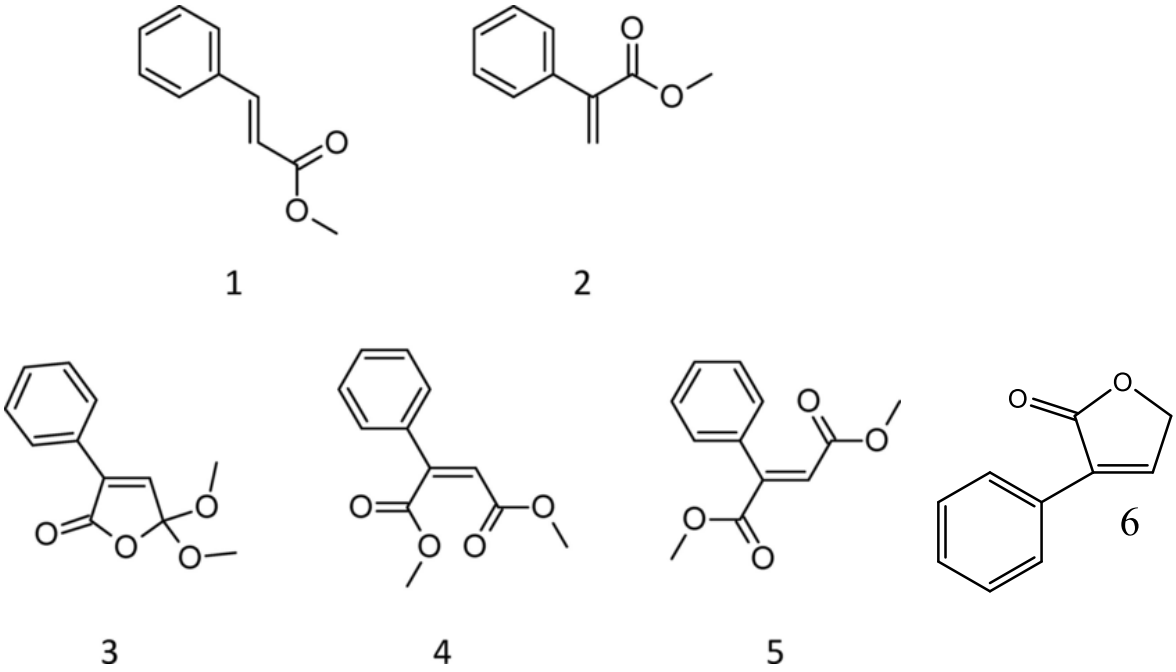

1. methyl (*E*)-cinnamate, (2-phenylacrylic acid methyl ester)
2. methyl atropate, 2 (E-3-phenylacrylic acid methyl ester)
3. 5,5-dimethoxy-3-phenyl-2(5*H*)-furanone
4. dimethyl (2Z)-2-phenyl-2-butenedioate (Z-isomer)
5. dimethyl (2E)-2-phenyl-2-butenedioate (E-isomer)
6. 3-phenyl-5H-furan-2-one

Figure 3.8. Products reported to occur in the oxidative carbonylation of phenyl acetylene [8, 10, 30, 31].

In addition to these six, two other products have been identified (3-phenylfuran-2,5-dione and Z-2-phenyl-2-butenedioic acid; Chapter 2 Section 2.4), however, these other two products are reported as least likely and were not easily detected by GC-MS analysis [8, 175]. Carbonylation reaction in phenyl acetylene occurs at the functional end with terminal alkyne, hence, it is presumed that oscillatory carbonylation of alkyne functionalised polyethylene glycol would occur in the same manner. Based on this analogy, it is then possible to analyse the spectra obtained from oscillatory carbonylation of the alkyne functionalised polymer by focusing on the moieties (groups) attached to the phenyl backbones in Figure 3.8. The structures in Figure 3.9 were generated for this purpose by substituting phenyl acetylene with the functional methoxy polyethylene glycol backbone.

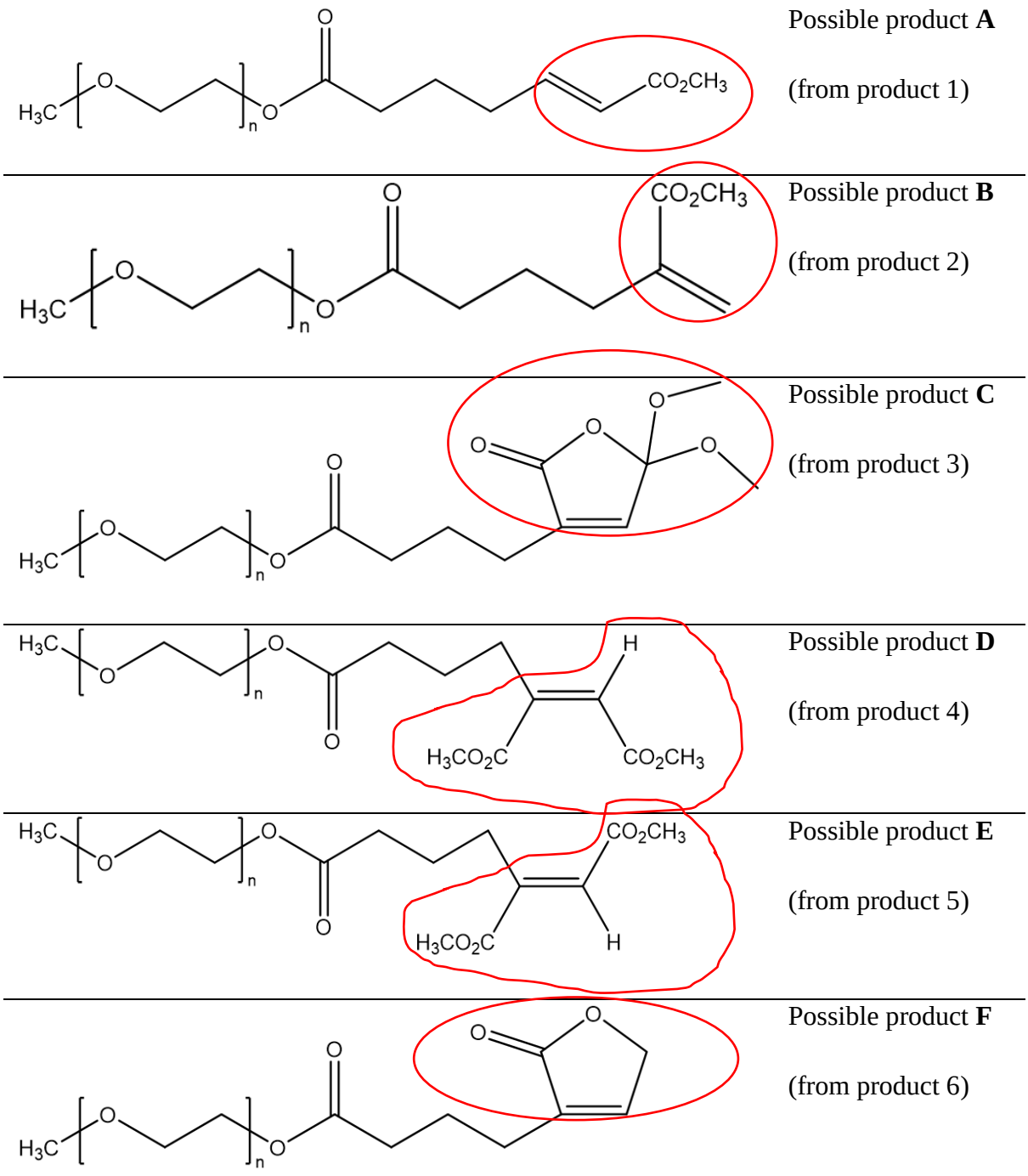

Figure 3.9. Proposed products from the carbonylation of mono alkyne methoxy polyethylene glycol based on known products from oxidative carbonylation of phenyl acetylene. Encircled groups are from products in Figure 3.8.

The macromolecules in Figure 3.9 are the proposed products from the carbonylation of alkyne functionalised methoxy polyethylene glycol. A range of typical NMR shifts, interactions and methods for spectral assignments of individual groups attached to the end of the polymer to form polymer products are available in literature and textbooks dedicated solely to spectroscopy studies [233-237, 244]. These were used as reference in suggesting potential

products responsible for the shifts observed in the spectra obtained from analysis of the mixture of products. The proton NMR spectrum in Figure 3.10 was obtained from a mixture of products following termination of the carbonylation reaction. Since product separation and quantification is not possible at this time, NMR analysis of the product mixture is aimed at identifying possible products.

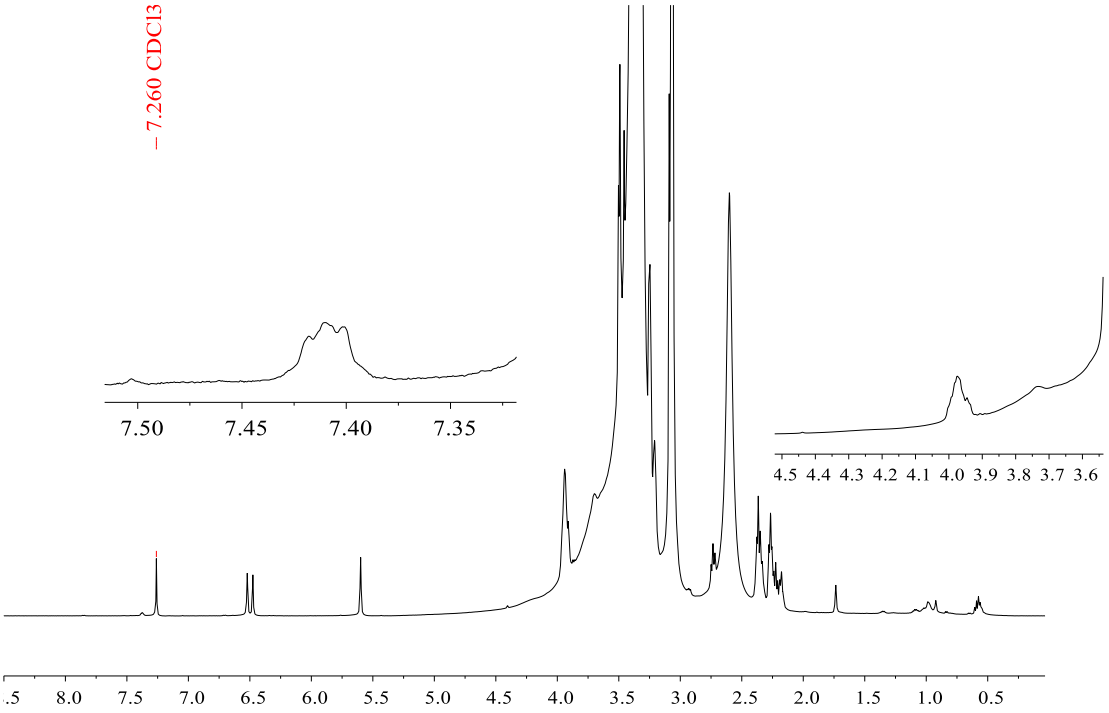

^{1}H NMR (500 MHz, Chloroform-*d*) δ 7.47 – 7.38 (m, 1H), 6.53 (d, *J* = 22.8 Hz, 11H), 5.63 (s, 9H), 3.97 (td, *J* = 10.6, 9.8, 5.3 Hz, 69H), 3.97 (s, 1H), 3.72 (s, 9H), 3.39 (s, 7281H), 3.11 (t, *J* = 7.7 Hz, 403H), 2.77 (t, *J* = 7.9 Hz, 14H), 2.63 (s, 409H), 2.39 (q, *J* = 7.4, 6.6 Hz, 44H), 2.34 – 2.25 (m, 34H), 2.22 (d, *J* = 8.5 Hz, 16H), 1.77 (d, *J* = 2.9 Hz, 5H), 1.02 (d, *J* = 6.6 Hz, 4H), 0.96 (s, 2H), 0.64 – 0.59 (m, 7H).

Figure 3.10. ^{1}H NMR spectrum from mixture of products obtained from oscillatory carbonylation of alkyne functionalised methoxy polyethylene glycol.

The shift between 7.47 ppm and 7.38 ppm suggest resonance from proton attached to a cyclic structure since typical shifts from protons on aromatic rings range from 6 ppm to ≈ 8 ppm [233-237, 244]. Possible products **C** and **F** have pendant ring structures from the 2 (5H) furanone thus, both are considered as potential products causing the shift. This resonance is possible in product **C** because of the interaction (H > C=C < CH-H) from the single H attached at the cis end of the ethylene carbon on the ring. Alternatively, product **F** could also occur at this shift since it has a furanone ring and proton attached to 1-ethylene. However, if product **F** is the source of the shift between 7.47 ppm and 7.38 ppm, an additional shift from methylene proton in the ($(RO_2)C\underline{H}_2$) position on the ring is expected [233-237, 244]. The typical shift for protons

from the said group is around 4.8 ppm (±0.1 ppm). Since a shift around this range is absent in the spectrum in Figure 3.10, the most likely product generating this resonance is product **C.** In addition, the formation of 5,5-dimethoxy-3-phenyl-2(5H)-furanone (product 3) occurs frequently in the oscillatory carbonylation of phenyl acetylene [8, 31, 173, 175]. It is more likely that product **C** with a comparable pedant group to 5,5-dimethoxy-3-phenyl-2(5H)-furanone is the source of the shift observed.

The chemical shift at 6.53 ppm and 5.63 ppm is typical for proton resonance from alkene, with an average range between 4 ppm and 7^{+} ppm [233, 236, 244]. Amongst the products proposed, products **A**, **B**, **D** and **E** may account for these shifts due to the 1-ethylene bond present in each of them. Products **D** and **E** both have dimethyl groups, while products **A** and **B** each have single methyl group. The shift at 6.53 ppm has a double peak, while a single peak was obtained at 5.63 ppm. If the shifts arise from proposed product **D,** the protons resonating at 6.53 ppm arise from the H on 1-ethylene and interactions from –C(=O)O-CH_3 at the trans[1] and geminal[2] positions. Alternately, if the shift is attributed to product **E,** then the peak at 6.53ppm may be from H node on the 1-ethylene and coupling from –C(=O)O-CH_3 at the cis[3] and geminal locations. The assumption for products **D** and **E** is supported by the presence of proton shift at 3.72 ppm (Figure 3.10) from the methyl group in the –C(=O)O-C$\underline{H}_3$ pendant. Products **A** and **B** may have also contributed to the resonance at 6.53 ppm because they also have hydrogen attached to the ethylene bond; interacting with protons from –C(=O)O-C$\underline{H}_3$ at cis and geminal positions (product **A**) and trans position (product **B**). It is more likely that products **D** and **E** are largely responsible for the shift at 6.53 ppm because the phenyl acetylene products (4 and 5 Figure 3.8) with the same moieties are known to have high conversion rates in oscillatory modes (conversion to 4 (Z-isomer > conversion to 5 (E-isomer)) [8, 10, 31, 175, 177]. Products **A** and **B** are assumed to be present because of the shift at 5.63 ppm, which is only possible in products with a single methyl group attached to –C(=O) O-CH_3. The presence of one methyl group in products **A** and **B** would allow for proton interaction between neighbouring H's on 1-ethylene and the –C(=O)O-C$\underline{H}_3$ at the geminal (product **A**) and trans (product **B**) positions, giving the resonance at 5.63 ppm. The chemical shifts from 4 ppm to 1 ppm are associated with methylene C$\underline{H}_2$ and methyl C$\underline{H}_3$ groups and interactions of protons on these groups with other protons around -O-C; -OC(=O)-C; -OC(=O)-C=C; -C; -C=C; -C(=O)O-C present in the long chain polyethylene glycol backbone.

[1] Trans: coupling between hydrogen on adjacent carbons (present due to stereoisomerism)
[2] Gem (geminal):coupling between hydrogens at the same carbon ($^2J_{HH}$).Generates through two bonds
[3] Cis: coupling between hydrogen on adjacent carbons (present due to stereoisomerism)

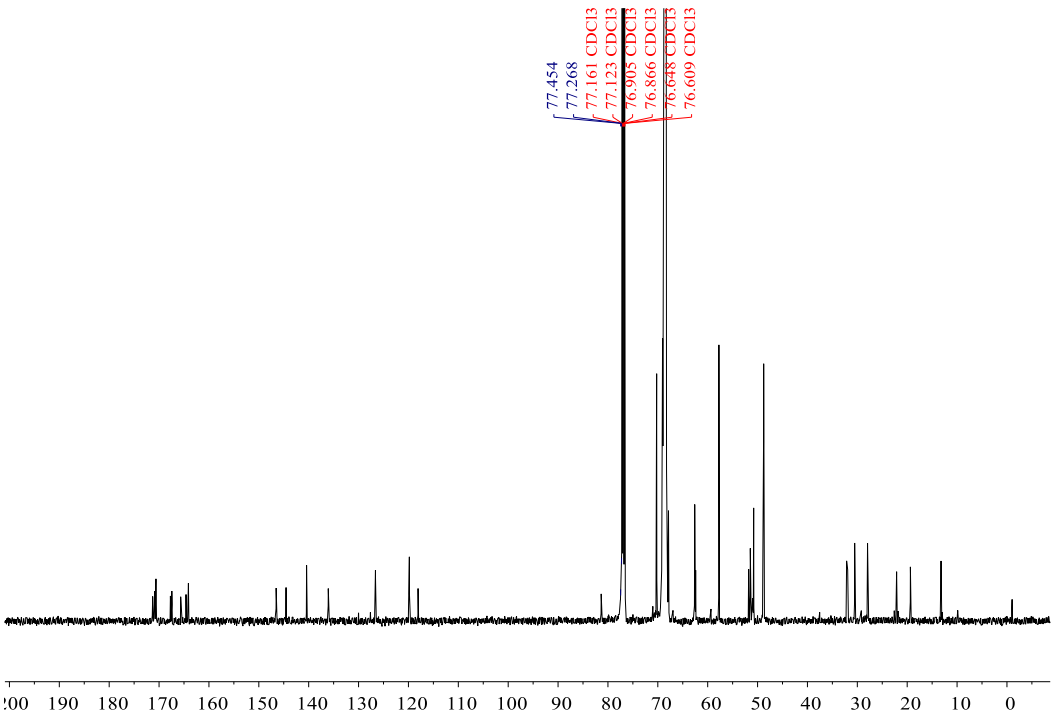

^{13}C NMR (126 MHz, Chloroform-*d*) δ 172.14, 171.76 – 171.20 (m), 168.44 (d, *J* = 35.3 Hz), 166.52, 165.45, 164.97, 147.38, 145.39, 141.28, 136.93, 127.47, 120.67, 118.93, 82.21, 70.63 – 68.78 (m), 63.97 – 62.92 (m), 58.61, 52.08 – 51.28 (m), 49.64, 32.90 (d, *J* = 27.0 Hz), 31.36 (d, *J* = 7.8 Hz), 28.81, 22.98, 20.22, 14.07.

Figure 3.11. ^{13}C NMR spectrum from mixture of products obtained from oscillatory carbonylation of alkyne functionalised methoxy polyethylene glycol.

The carbon NMR spectrum in Figure 3.11 was obtained from the same mixed product sample as the proton NMR spectrum. Carbonyl groups are known to resonate between 160 ppm and 220^{+} ppm [233, 236]. The position of the shift depends on the group present. Ketones and aldehydes containing H have chemical shifts ranging from 180 ppm to 220^{+} ppm, while carboxylic acids, anhydrides, esters, amides and acid chlorides without H have chemical shifts between 160 ppm and 180 ppm. Since proposed products are carboxylic esters and acids with varying degrees of saturation, the shifts within 160 ppm and 180 ppm agree with potential products. The resonance at 172.14 ppm is attributed to the carboxyl group at the position where pentynoic acid pendant is attached to the methoxy polyethylene glycol backbone. The carboxyl carbon is attached to C-C-C chain. The multiple peak from 171.76 to 171.20 ppm is also from a carboxyl group and is suggested to arise from carbon attached to –C=C-C in the furanone product **C**.

The shifts at 166.52, 165.45, 164.97 ppm are attributed chiefly to the carboxyl group in –C(=O)O-CH_3 pendant on possible products (**A, B, D** and **E**). These shifts are lower than previous carboxyl groups because of the hydrogen present. Alkene group chemical shifts occur approximately between 110 and 160 ppm and the shifts of ethylene is lower due to the hydrogen attached to the ethylene carbon [233-236]. The shifts at 147.38, 145.39, 141.28, 136.93, 127.47, 120.67 and 118.93 ppm are thus attributed to ethylene groups formed during the carbonylation reactions. In addition, interactions from -C-C-C and -C(=O)OC also contribute to the chemical shift obtained in the alkene region. Chemical shifts between 70.63 – 68.78 ppm and 63.97 – 62.92 ppm arise from aliphatic CH_2 carbon groups at alpha, beta, gamma, and delta positions, on the polymer chain while the shifts at 58.61 ppm and 52.08 – 51.28 ppm originate from aliphatic CH_3 groups. The other shifts in the carbon spectrum are CH_2 groups attached to either polymer back bone, carbon in the pendant group from pentynoic acid following functionalisation or from methylene groups introduced after the oscillatory carbonylation. Since iodine was not completely removed, it is also possible that iodide attached to carbon contributes to the chemical shift between 15 and 45 ppm [245].

In summary, if the catalysed carbonylation (insertion and addition polymerisation) process is assumed to occur via similar pathways for small molecule and polymeric substrates, given that the end functional groups are the same (alkyne ends), the most likely products formed are **C, D** and **E**, since the small molecule analogues of the aforementioned polymeric products achieve higher yields than other products (**A, B** and **F**).

Chapter 4. Results and Analysis of Reaction Profiles from the Oscillatory Carbonylation of Mono-Alkyne Functionalised Methoxy-Polyethylene Glycols

4.1 Introduction

In Section 2.4 of Chapter 2, oscillations arising from oxidative carbonylation reaction was discussed. Small molecule substrates such as phenyl acetylene [6, 8-10, 30, 32, 103, 173, 175-177, 242], non-1-yne [33], methyl acetylene [38], 2-methyl-3-butyn-2-ol [7], 2-propyn-1-ol [7], propargyl alcohol [38] etc. and polymeric substrate including mono-alkyne functionalised methoxy-polyethylene glycols (molecular weights of 2000 g/mole and 5000 g/mole) [29] employed in this form of oscillating reaction were examined. The application of polymeric substrates in oscillatory carbonylation reactions is a new development [28, 29] and existing knowledge on oscillatory carbonylations with alkyne functionalised polymeric materials as substrate is currently limited to a study [29]. Developing applications based on this oscillatory system lies in understanding its dynamics under various conditions, and in altering these conditions to suit desired purposes. Hence, this chapter follows on from the previous study [29] by extensively investigating reaction profiles generated under a variety of conditions, using the recently identified mono alkyne functionalised methoxy-polyethylene glycol (A-PEG_{2000}) as reaction substrate (polymeric substrate with single alkyne end group functionality). This chapter expands on existing knowledge by studying how various catalyst (PdI_2), catalyst promoter (KI) [246-252] and polymeric substrate (A-PEG_{2000}) concentrations effect oscillatory and non-oscillatory modes in the oxidative carbonylation reaction. Studies are designed to assess:

1. The influence of the catalytic mixture (KI/PdI_2) on reaction profiles at constant substrate concentration.
2. Impacts of extra potassium iodide on the reaction dynamics and profile features as a function of addition time.
3. The effects of varying potassium iodide or palladium iodide concentration at constant mono alkyne substrate concentrations.
4. Effects of halving the substrate concentration at various potassium iodide concentrations and palladium iodide concentrations
5. Influence of a wider range of polymer substrate concentrations at constant concentrations of potassium iodide and palladium iodide.

By implementing these studies, the expectation is that results obtained will provide a clearer representation of the non-linear dynamics in this system.

4.2 Effect of Varying Concentrations of the Catalytic Mixture (PdI_2/KI) in the Carbonylation of Mono Alkyne Functionalised Methoxy-Polyethylene Glycol

The influence of the concentration of the catalytic mixture (PdI_2/KI) at constant substrate concentration (A-PEG_{2000}) was investigated according to Table 4.1. A stock catalytic solution prepared as described in Chapter 3, Section 3.3 was employed in the study presented here. The catalytic mixture consists of palladium iodide dissolved in methanol with the aid of potassium iodide. This first study was essential to establish a broader PdI_2/KI range for which the substrate condition ([A-PEG_{2000}] = 2.03 mM) employed by Donlon and Novakovic (2014), would yield oscillatory profiles.

Table 4.1. Conditions for preliminary studies on the influence of catalytic mixture at constant substrate concentration. (CO/air flowrates = 15 mL/min; Total initial methanol volume = 90 mL, Additional methanol = 5 to10 mL aliquots; Reaction temperature = 20^oC ± 2; Ratio of [KI]/ [PdI_2] = 198±2)

[PdI_2] (μM)	[KI] (mM)	[A-PEG_{2000}] (mM)	[KI] / [A-PEG_{2000}]	[A-PEG_{2000}] / [PdI_2]
15.1	3.00	2.03	1.48	134.45
22.7	4.52	2.03	2.23	89.45
26.6	5.29	2.03	2.61	76.32
30.2	6.00	2.03	2.96	67.29
37.8	7.58	2.03	3.73	53.70
45.4	8.92	2.03	4.39	44.71

The pH and [H^+] adjusted profiles in Figure 4.1(a) and 4.1(b) were obtained from the carbonylation of mono alkyne functionalised polyethylene glycol ([A-PEG_{2000}] at 2.03 mM) based on the conditions in Table 4.1. Oscillations were recorded across all [KI]/ [PdI_2] employed in the studies, although the amplitudes and periods varied with concentration of catalytic system (KI/PdI_2). A representation of "period" and "amplitude" referred to throughout this thesis is exemplified in Figure 4.1(c). Oscillations were also present in all replicate experiments with some variations in periods and amplitudes. A comparison of some replicate experiments with the profiles given in Figure 4.1(a) is given in Figure 4.2(a-c). Larger amplitudes and periods were obtained at [KI]/ [PdI_2] = 5.29 mM/ 26.6 μM and 6.00 mM/ 30.2 μM and remained consistent in replicate runs. pH profiles were recorded through the experiments, while the [H^+] adjusted profiles were calculated from experimentally obtained pH values.

a

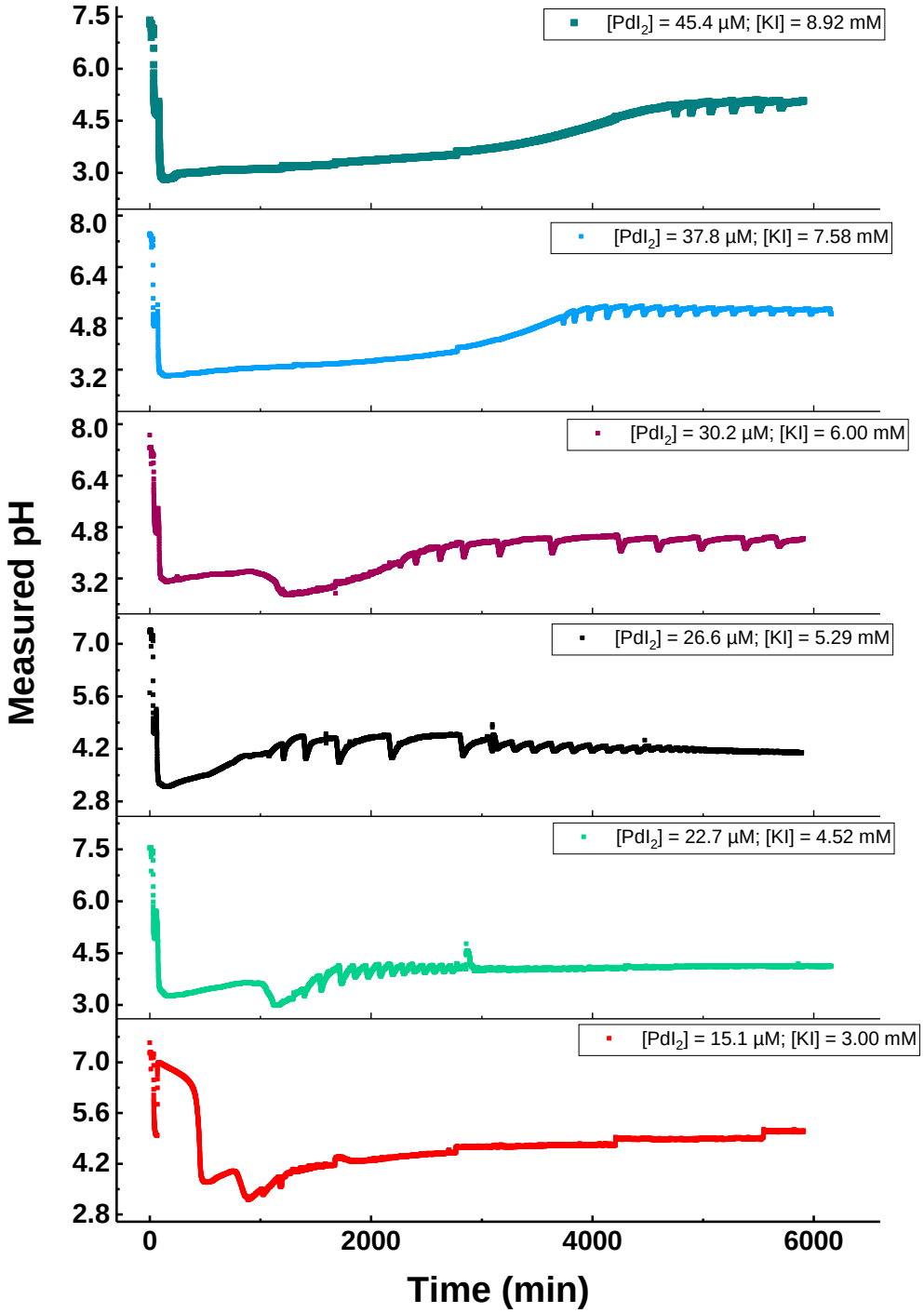
[PdI2] = 45.4 µM; [KI] = 8.92 mM
[PdI2] = 37.8 µM; [KI] = 7.58 mM
[PdI2] = 30.2 µM; [KI] = 6.00 mM
[PdI2] = 26.6 µM; [KI] = 5.29 mM
[PdI2] = 22.7 µM; [KI] = 4.52 mM
[PdI2] = 15.1 µM; [KI] = 3.00 mM
Measured pH
Time (min)
0
2000
4000
6000

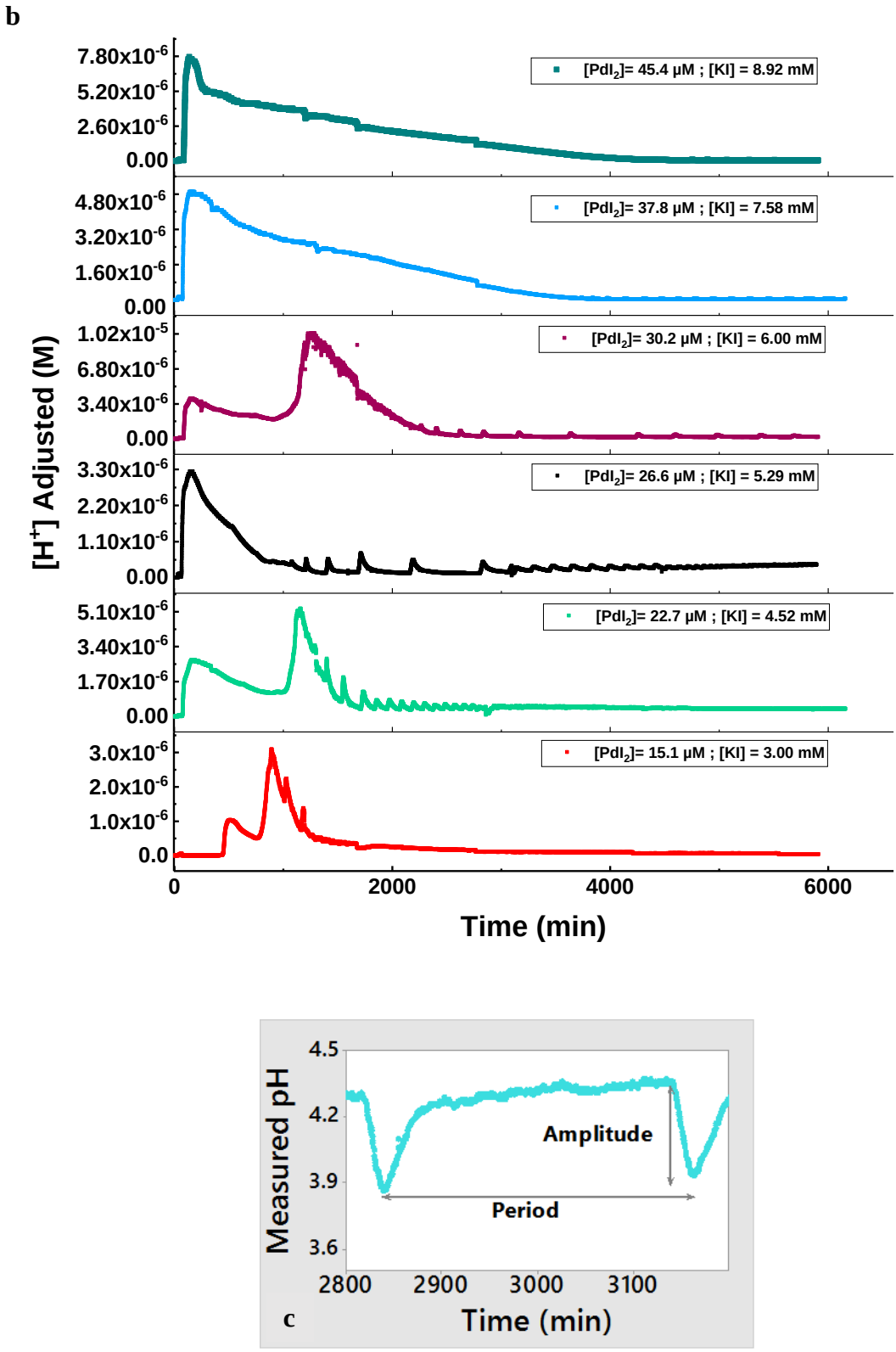

Figure 4.1. Full reaction profiles from the carbonylation of mono alkyne functionalised methoxy-polyethylene glycol at various KI/PdI_2 concentrations. (a) pH profiles (b) [H^+] adjusted profiles. (c) Representation of amplitude and period. (CO/air flowrates = 15 mL/min; total initial methanol volume = 90 mL; reaction temperature = 20°C ± 2; [A-PEG_{2000}] = 2.03 mM)

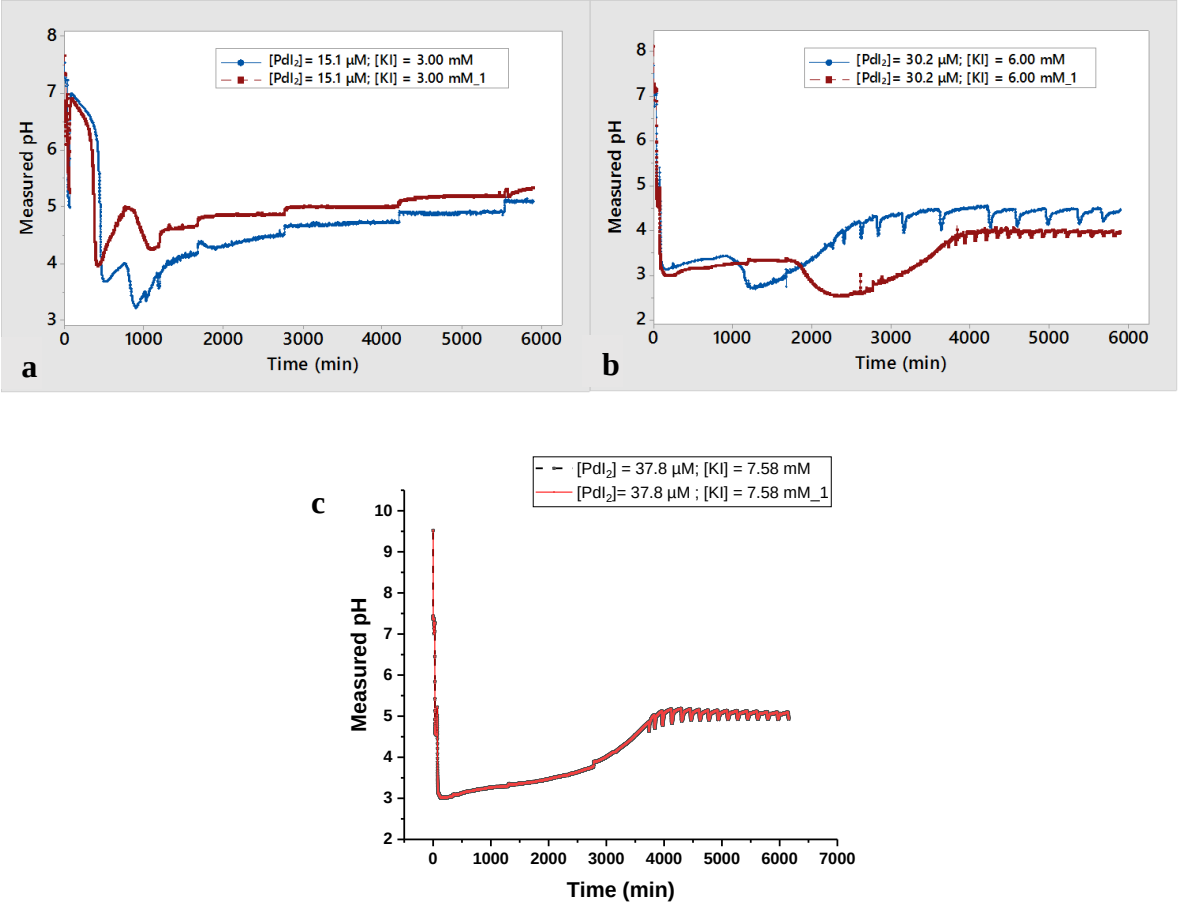

Figure 4.2. Replicate samples of reaction profiles from the carbonylation of mono alkyne functionalised methoxy-polyethylene glycol at various KI/PdI_2 concentrations. (CO/air flowrates = 15 mL/min; total initial methanol volume = 90 mL; reaction temperature = 20°C ± 2; [A-PEG_{2000}] = 2.03 mM)

pH is a measure of hydrogen ion concentration and is usually attributed to measurements made in aqueous solutions [253]. Although pH measurements are quite common in non-aqueous solvents, direct calculations of $[H^+]$ in such situations do not give accurate values, unless solvent effects and junction potentials are accounted for [254-258]. Previous studies in which pH measurements were performed in methanol [258] found that; adding 2.3 pH units to pH values obtained in methanol was a reasonable adjustment for the aqueous/non-aqueous effect. Since current studies were conducted in methanol and aqueous buffers were similarly used for electrode calibration (same with literature [258, 259]), the adjustment for the influence of methanol was performed by adding 2.3 pH units per pH value, before converting to $[H^+]$ values as proposed in literature [258]. The $[H^+]$ adjusted profiles in Figure 4.1(b) were obtained according to Eq. 4.1. The accuracy of the $[H^+]$ adjusted values obtained by converting the pH profiles from the carbonylation reactions of A-PEG_{2000} is not confirmed, however, it offers particularly useful approximations and aids in discussions hence, Eq. 4.1 is applied in generating the $[H^+]$ adjusted profiles throughout this thesis.

$$[H^+]_{adjusted} = 10^{(-(pH_{recorded}+2.3))}$$ Eq. 4.1

In this chapter and later chapters, the full reaction profiles such as the profiles given in Figure 4.1(a) and (b) are quite compressed due to lengthy experimental durations. As a result, full profiles are divided into key segments of the carbonylation reaction and discussed in further details. The segments include the initial phase (reactants addition) and oscillatory/non oscillatory modes observed.

pH and [H^+] adjusted profiles during the initial stages of the reactions investigating effects from varying the concentration of the catalytic mixture are given in Figure 4.3(a) and (b). The first dip in pH in Figure 4.3(a) which reverts almost immediately to ≈ initial pH values, occur on addition of the catalytic mixture (PdI_2, KI in methanol) to bulk methanol for the reactions. This drop is proposed to be of ionic nature, since adding the catalytic mixture introduces ions (from KI, PdI_2, CH_3I, I^- etc.) of different species to methanol in the reaction vessels (Erlenmeyer flasks). The alteration of the total concentrations of ions present is assumed to interfere with the ionic strength [176, 260-268] of methanol which is observed as the dip in pH. Change in ionic strength is known to increase [H^+] values [265] which supports the observed dip in pH values. The slight differences in the initial pH values following the catalyst addition as observed in Figure 4.3(a) is attributed to the variations in concentrations of ions in the catalytic mixture required for each experiment, since this would alter the ionic strength of each run. It is also possible that the slight variations in initial values of the pH probes following calibration (average pH value of 7.5 ± 0.07 pH units) contributed to the differences.

a

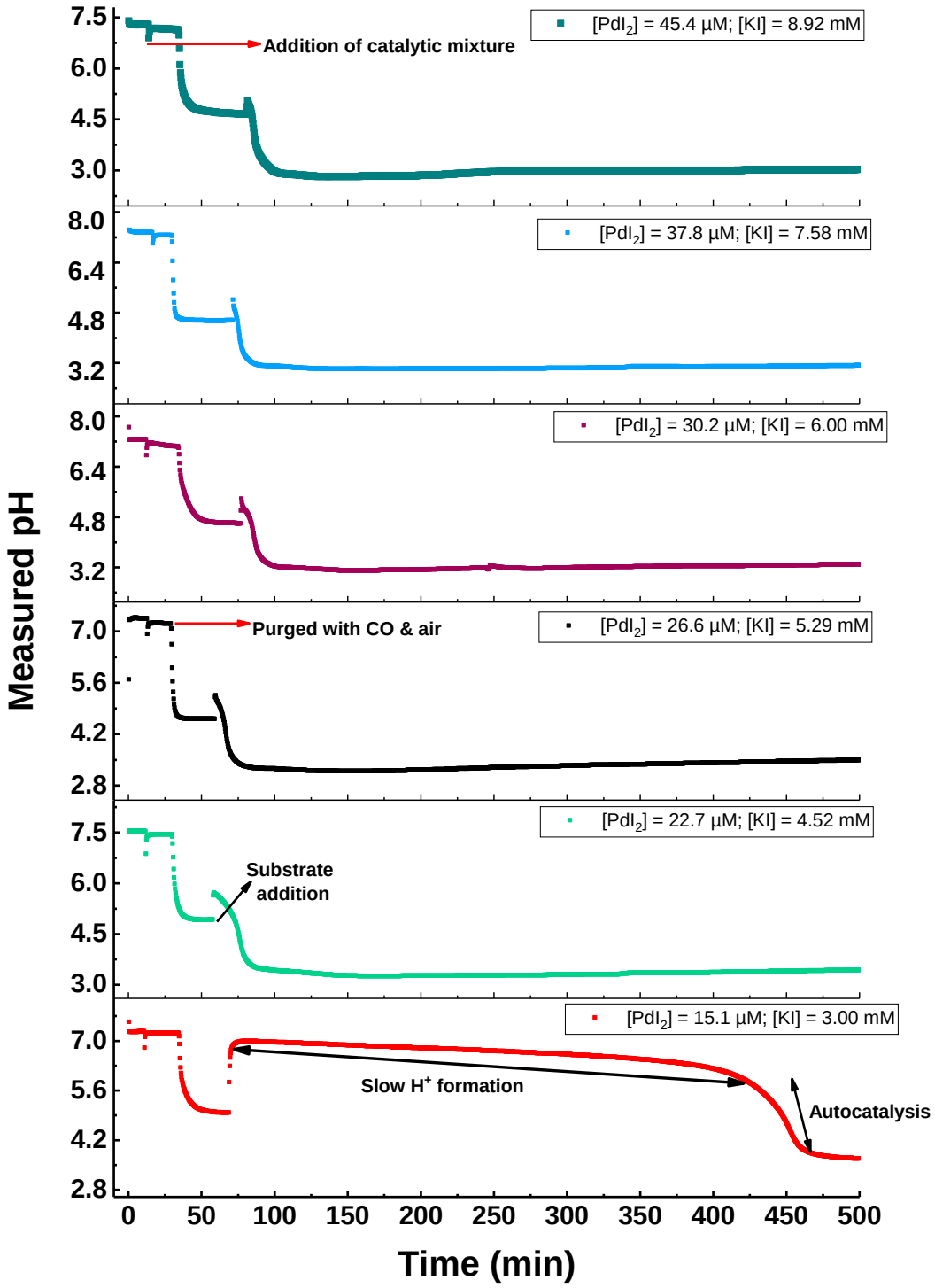
Measured pH
Time (min)
[PdI2] = 45.4 µM; [KI] = 8.92 mM
Addition of catalytic mixture
[PdI2] = 37.8 µM; [KI] = 7.58 mM
[PdI2] = 30.2 µM; [KI] = 6.00 mM
Purged with CO & air
[PdI2] = 26.6 µM; [KI] = 5.29 mM
[PdI2] = 22.7 µM; [KI] = 4.52 mM
Substrate addition
[PdI2] = 15.1 µM; [KI] = 3.00 mM
Slow H+ formation
Autocatalysis

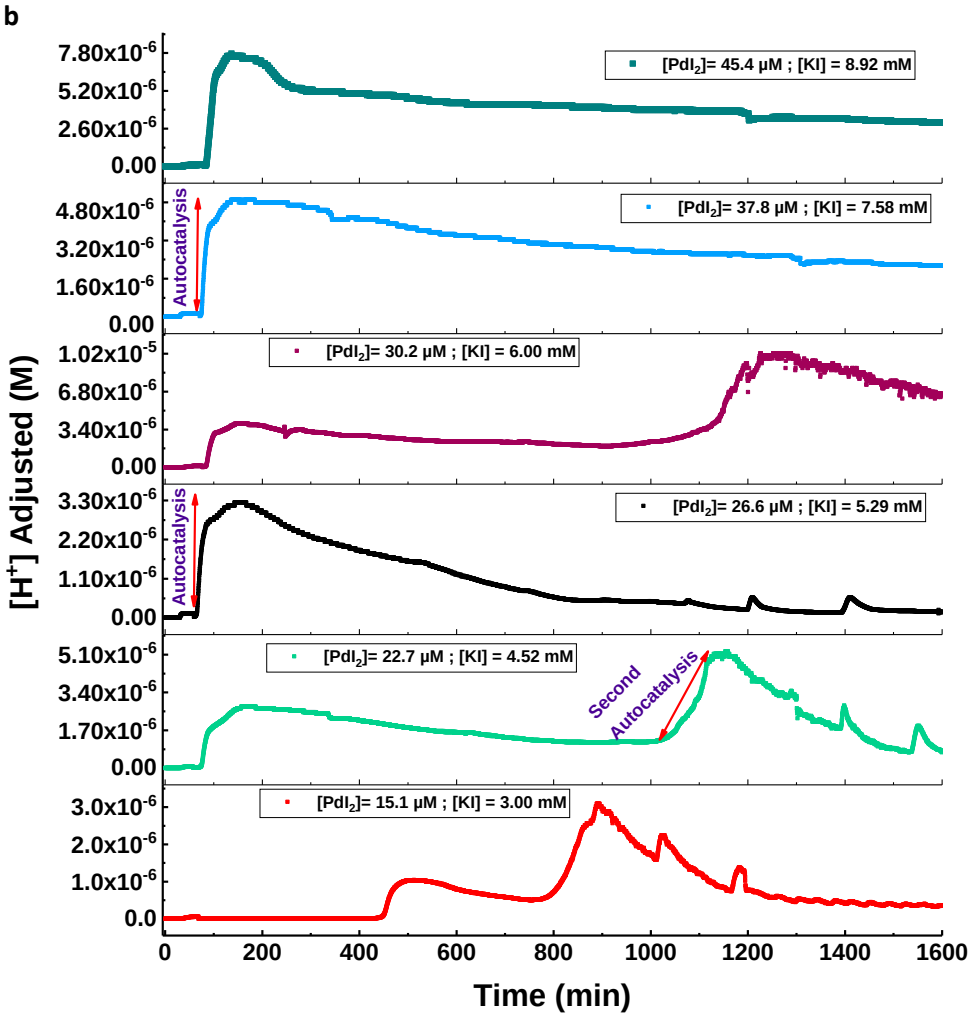

Figure 4.3. pH and [H^+] adjusted profiles recorded during the initial stages of the carbonylation reaction at various catalyst concentrations. (a) pH profiles (b) [H^+] adjusted profiles. (CO/air flowrates = 15 mL/min; total initial methanol volume = 90 mL; [A-PEG_{2000}] = 2.03 mM; reaction temperature = 20^{o}C ± 2)

The pH values were allowed to equilibrate for 20 - 35 min after the catalytic mix was introduced, before each reaction was purged with CO and air at 15 mL/min as indicated in Figure 4.3(a-b). On purging, the pH decreased, corresponding to the rise in [H^+] adjusted profiles (Figure 4.3(b)) obtained. The decrease in pH, which gradually stabilized (equilibration) suggests the presence of proton donating reactions. Previous oscillatory carbonylation studies in methanol [8-10, 29, 30, 32, 173-175, 177, 242] which share initial stages of the process studied here, displayed similar pH changes on purging. Eq. 4.2 to 4.4 proposed for carbonylation of methanol and water in oscillatory [8, 11, 29, 30, 32, 38, 103, 198] and non-oscillatory modes [269-271] are suggested to account for the increase in H^+ concentration.

$$PdI_2 + CO + H_2O \rightarrow IPdH + HI + CO_2 \qquad \text{Eq. 4.2}$$

$$PdI_2 + CO + H_2O \rightarrow IPdCOOH + HI \quad \text{Eq. 4.3}$$

$$PdI_2 + CO + CH_3OH \leftrightarrow IPdCOOCH_3 + HI \quad \text{Eq. 4.4}$$

The HPLC grade methanol used in the reactions as received from *Sigma Aldrich* have small amounts of water (< 0.03% H_2O content[4]*) and is assumed to be the source of water in Eq. 4.2 and 4.3. It is important to say that gases used in this study were not dried and that the system was not completely isolated from the atmosphere (parafilm was used to seal the Erlenmeyer flasks as much as possible however breaches remained around the probes), therefore, these may introduce moisture to the system.

As purging continued, the pH generally decreased (Figure 4.3(a)) with increasing concentration of catalytic mixture present. Similar decrease in pH as a function of PdI_2 concentration was observed in a previous study with phenyl acetylene [242], when the amount of PdI_2 was increased at constant KI concentration. It is tempting to ascribe the decreasing pH value with increasing concentration of catalytic mixture to PdI_2 since previous studies reported such dependence for Pd catalysed carbonylation. However, in this instance, concentration of KI also varied, hence, it is plausible that differences in concentrations of iodide ions may have also contributed to the reaction dynamics and observed differences in pH across runs on purging. KI is considered as it improves the efficiency of the catalytic cycle by promoting PdI_2 solubility and providing iodide ions that keep palladium in desired ionic salt forms [156, 157, 172, 247, 250, 269-274].

Furthermore, the reaction according to Eq. 4.2 (for catalytic conversion of water impurity in methanol and possible moisture from gases) was proposed to alternatively proceed according to Eq. 4.5 [275], wherein more proton is formed, which could also account for the variation.

$$PdI_2 + CO + H_2O \rightarrow Pd + 2HI + CO_2 \quad \text{Eq. 4.5}$$

Thus, the differences in rates of competing reactions occurring in each experiment according to Eq. 4.2 to 4.5, may have steered the variations in $[H^+]$, leading to the dissimilarity in pH drops given in Figures 4.3(a).

Equal concentrations of mono alkyne functionalised methoxy-polyethylene glycol (2.03 mM) were introduced to the reactions as the pH gradually equilibrated from purging (Figure 4.3(a)). The introduction of solutions of mono alkyne substrates (dissolved in 3.5±0.7 mL methanol[5]) was followed by increase in pH values and corresponding decrease in $[H^+]$ adjusted (Figure 4.3(a-b)). Since the mono alkyne substrates were dissolved in small volumes of methanol, the

[4] Residual water content in purchased methanol appeared to vary

[5] Volume of methanol used for dissolution depends on volume of catalytic mixture, such that total initial volume = 90mL.

sharp rise in pH may originate from the methanol introduced with the substrate, or from the substrate itself. The assumption that such rise originates from methanol is supported by some instances of increased pH on addition of more methanol in oscillatory carbonylation of phenyl acetylene [10, 32, 242]. Perturbation studies with methanol [243], addition of HPLC grade methanol following evaporative losses (higher reaction temperature (40^oC), experiments lasting several days) [9, 10, 32, 175], and oscillatory carbonylation in water-methanol solvent mixtures [176] are examples of such instances. As methanol is already in so much excess, literature [174, 175] suggests the residual water present in the methanol as the reason behind the rise in pH. Contributions to the observed rise in pH from the mono alkyne substrates is uncertain at this point because, functionalised polyethylene glycol is not likely to dissociate on dissolving under mild reaction conditions employed, despite its hydrophilic nature [276-283]. Also, possible products in the event of detached alkyne end groups were not identified via GC-MS in the previous study with mono-alkyne functionalised polyethylene glycol [29]. However, some interaction between the substrates and H^+ cannot be ruled out until more information becomes available. It is possible that substrate addition is followed by a fast consumption of H^+ via some pathway, which then facilitates the autocatalytic substrate conversion.

pH values before and after substrates were added is given in Table 4.2 and Figure 4.4. Maximum pH values following the addition of dissolved substrates appear to be dependent on the concentration of catalytic mixture present (Figure 4.3(a-b)) since, the pH value decreased at higher catalytic mix concentrations. The decrease in maximum pH values attained suggests that the reaction rate is proportional to [PdI_2/ KI], which is in agreement with the effects of catalyst (PdI_2) on rates of reaction [2, 284-286]. Also, since repeat samples had fairly similar values, especially at lowest and highest concentrations of the catalytic mixture, the proposed assumption appears feasible.

Table 4.2. Recorded pH values before and after the addition of constant concentrations of mono alkyne substrate (A-PEG_{2000}) at various concentrations of catalytic mixture. (CO/air flowrates = 15 mL/min; total initial methanol volume = 90 mL; [A-PEG_{2000}] = 2.03 mM; reaction temperature = $20^oC \pm 2$)

Concentration of catalytic mix (PdI_2 / KI) (μM / Mm)	pH values prior to substrate addition	Maximum pH on addition of substrate
15.1 / 3.00	4.98	6.99
22.7 / 4.52	4.93	5.72
26.6 / 5.29	4.62	5.28
30.2 / 6.00	4.6	5.27
37.8 / 7.58	4.56	5.22
45.4 / 8.92	4.65	5.05

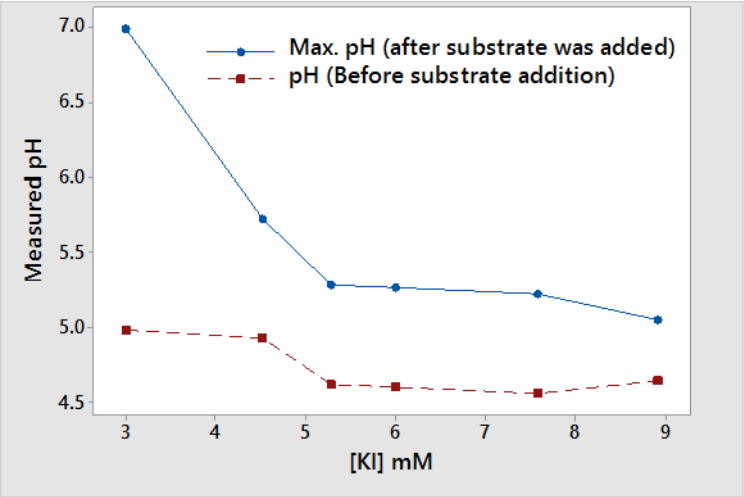

Figure 4.4. pH values before and after the addition of constant concentrations of mono alkyne substrate (A-PEG_{2000}) at various concentrations of catalytic mixture. (CO/air flowrates = 15 mL/min; total initial methanol volume = 90 mL; [A-PEG_{2000}] = 2.03 mM; reaction temperature = 20^{o}C ± 2)

A period of gradual formation of H^+ recorded as decreasing pH was seen following the pH rise on substrate addition. This phase is comparable to induction period/time prior to onset of oscillations, previously reported for other oscillatory systems [8]. Throughout the thesis, this period where H^+ is gradually formed is denoted as period of "slow H^+ formation" and is exemplified in Figure 4.3(a).

The gradual formation of H^+ is suggestive of reactions where H^+ is produced. Similar behaviour wherein, H^+ was formed on substrate addition was reported for large scale (reaction volume = 450mL) oscillatory carbonylation of phenyl acetylene at 20^{o}C and 40^{o}C [8, 9, 30, 32]. Eq. 4.2 to 4.5 (water / methanol carbonylation reactions and catalytic conversion of water) and Eq. 4.6 are proposed for the gradual decrease in pH and corresponding rise in H^+ (Figure 4.3 (a-b)). Eq. 4.6 is assumed to proceed in an autocatalytic mode; commencing slowly during the period of low H^+ ("slow H^+ formation") and subsequently faster as H^+ concentration increases auto-catalytically.

$$A - PEG_{2000} + 2CO + 2CH_3OH + PdI_2 \xrightarrow{HI} Pd + P - PEG_{2000} + 2HI \qquad \text{Eq. 4.6}$$

Where $P - PEG_{2000}$ stands for products from the oxidative carbonylation.

Duration of "slow H^+ formation" is given in Figure 4.5. The duration of gradual formation of H^+ decreased as the concentration of the catalytic mixture increased at constant substrate concentration (Figure 4.5). The highest duration of 425 min was observed at lowest concentration of catalytic mixture ([PdI_2] = 15.1 μM and [KI] = 3.0 mM). On increasing the

concentration of catalytic mixture, the duration of slow H^+ formation dropped significantly (by factors >10) and remained low (30 ± 6.5 min) at other catalytic concentrations. It appears that the reaction proceeds at a faster rate at higher concentrations of catalytic mix, given that other components of the reaction were kept constant.

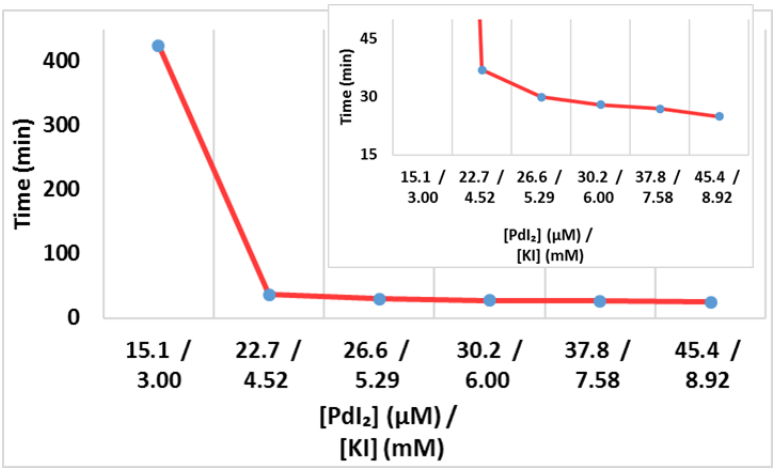

Figure 4.5. Duration of "slow H^+ formation" at constant concentration of mono alkyne (A-PEG_{2000}) functionalised methoxy polyethylene glycol. (CO/air flowrates = 15 mL/min; total initial methanol volume = 90 mL; [A-PEG_{2000}] = 2.03 mM; reaction temperature = 20°C ± 2)

As HI gradually accumulates during the period of "slow H^+ formation", it approaches a concentration (assumed to be determined by specific reaction constraints unique to each experimental condition) which prompts the autocatalytic production of HI, seen as the sudden drop in pH/ corresponding rise in [H^+] adjusted in Figure 4.3(a-b). Experimentally captured trends align with Eq. 4.6 (substrate conversion), postulated to proceed in an autocatalytic mode. The prompt fashion of the transition from slow H^+ production to rapid [H^+] formation agrees with autocatalysis assumption and HI is presumed to be the source of protons [29-32]. Modelling studies in the initial study on mono-alkyne polymer substrate also supports the autocatalytic formation of HI [29].

pH and adjusted [H^+] values after the first autocatalytic generation of HI according to Eq. 4.6 is given in Figure 4.5. H^+ concentration increased with increasing concentration of catalytic mixture at constant substrate concentration. The relative increase in [H^+] and corresponding decrease in pH with increasing KI/PdI_2 concentration suggests an influence on the rate of the carbonylation reaction (Eq. 4.6).

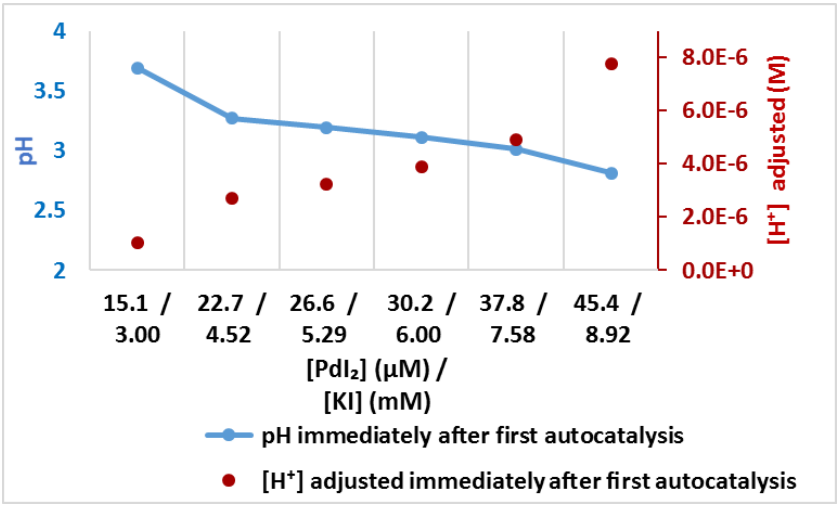

Figure 4.6. pH and H^+ adjusted values immediately after the first autocatalytic H^+ production / sharp fall in pH. (CO/air flowrates = 15 mL/min; total initial methanol volume = 90 mL; [A-PEG_{2000}] = 2.03 mM; reaction temperature = 20°C ± 2)

If the concentrations of methanol, CO and air (oxygen) are assumed to be in excess [9, 29, 30], and that purging the solution with CO/air greatly reduces mass transfer limitations [9, 179, 242], then the rate of the reaction "R" is postulated to be dependent on catalytic mix, substrate and HI concentrations according to Eq. 4.7

$$R \alpha [A\text{-}PEG_{2000}] [KI/PdI_2] [HI]^2 \quad \text{Eq. 4.7}$$

Thus, at higher [KI/PdI_2], the rate of the reaction increases, and more HI is produced (since it is autocatalytic), explaining the observed increase in [H^+] adjusted values with increasing catalyst concentration, immediately after first autocatalysis (Figure 4.6).

The autocatalytic increase in HI concentration was followed by periods of increase in pH with corresponding decrease in [H^+] in the profiles, given in Figure 4.2(a-b) and 4.3(a-b). This is suggestive of reactions where H^+ is consumed. Eq. 4.8 for the oxidation of HI previously reported in oscillatory and non-oscillatory carbonylation of alkyne terminated substrates such as phenyl acetylene [3, 29, 38, 156, 270, 271] and, the nucleophilic substitution of OH in methanol according to Eq. 4.9 which is proposed to occur in presence of excessive KI [30, 287-289] are offered as mechanisms for the decrease in [H^+].

$$\frac{1}{2}O_2 + 2HI \rightarrow I_2 + H_2O \quad \text{Eq. 4.8}$$

$$CH_3OH + HI \leftrightarrow CH_3I + H_2O \quad \text{Eq. 4.9}$$

In the reaction with [PdI_2] = 15.1 μM; 22.7 μM and 30.2 μM, second regions where additional H^+ is produced and consumed (represented by the number "2" in Figure 4.3(b)) occur before the onset of oscillations is observed. Eq. 4.8 in addition to Eq. 4.9 which is reversible, are suggested as possible reactions for this second region since, more water becomes available as reaction in Eq. 4.8 proceeds. An additional or alternate mechanisms for H^+ produced in this second region is proposed in literature [290-292] and an adaption to account for non-aqueous system is given in Eq. 4.10. Excess I^- from KI present in the reactions is suggested to promote Eq. 4.10.

$$I_2 + H_2O \leftrightarrow HOI + HI; \quad HI \leftrightarrow H^+ + I^- \qquad \text{Eq. 4.10}$$

It is also possible that substrate conversion (Eq. 4.6) may have contributed to HI production in the second region. It is interesting to note the occurrence of this second region at [PdI_2] = 15.1 μM and 30.2 μM as replicate samples (Figure 4.2(a-b)) also had similar second regions and the catalyst concentration is doubled.

Oscillations commenced in all runs after the period of H^+ consumption in reactions with and without the second region. The onset of oscillation was marked by sharp decrease in pH with according to Figure 4.7 and the rapid decrease is attributed to autocatalytic formation of HI agreeing with Eq. 4.6. Palladium iodide is important for reactions in Eq. 4.2 to 4.6 to proceed. It is especially important as it forms part of the feedback mechanism for the autocatalytic generation of HI during the oscillatory phase of the carbonylation reactions. Hence, Eq. 4.11 and 4.12 are offered for regeneration of palladium metal produced [3, 29, 156, 172, 271].

$$I_2 + Pd \rightarrow PdI_2 \qquad \text{Eq. 4.11}$$

$$I_2 + Pd \xrightarrow{PdI_2} PdI_2 \qquad \text{Eq. 4.12}$$

The regeneration of palladium is assumed to proceed via autocatalytic and non-autocatalytic routes whereby, the non-autocatalytic Eq. 4.11 has been suggested to produce PdI_2 in the event of complete consumption of the catalyst and also via continuous catalyst oxidation [29]. The autocatalytic regeneration of Pd is believed to occur as oscillations in turbidity (measure of particles in fluids) were reported in the carbonylation of mono alkyne functionalised polyethylene glycol at 2.03 mM substrate concentration and palladium iodide at 40.5 μM [29]. Likewise, fast transitions between clear solutions with floating black Pd particles to light brown solutions (PdI_2) observed visually, supports this assumption.

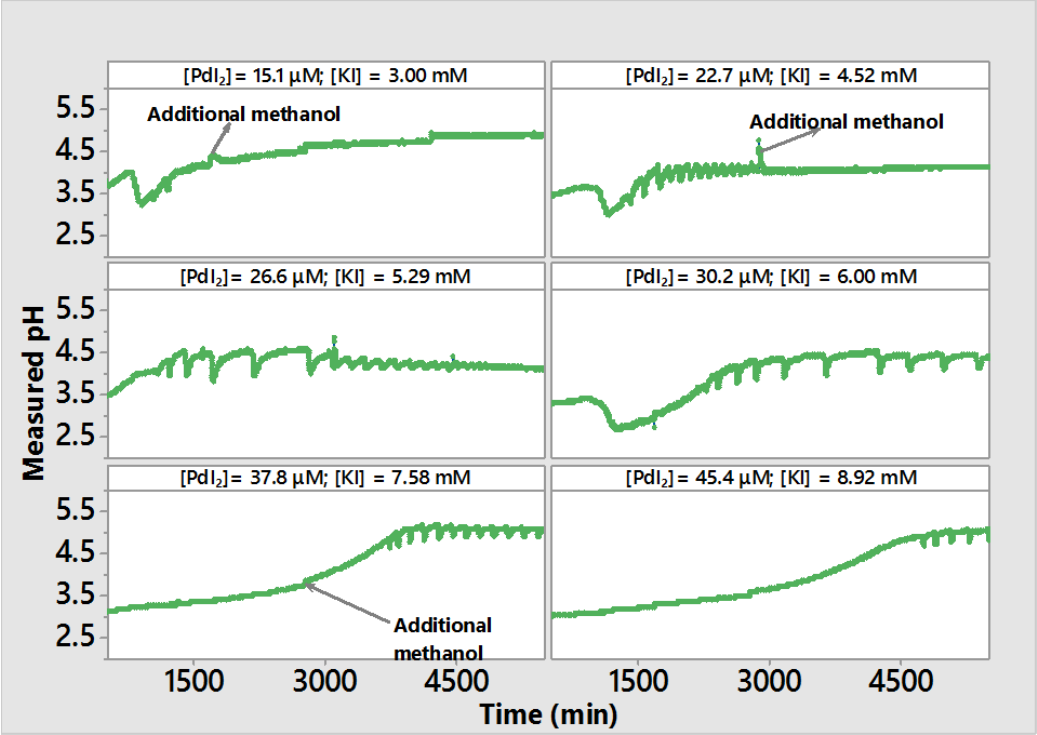

Figure 4.7. pH profiles indicating onset of oscillations and oscillatory attributes over the range investigated. (CO/air flowrates = 15 mL/min; total initial methanol volume = 90 mL; [A-PEG_{2000}] = 2.03 mM; reaction temperature = 20°C ± 2)

pH and [H^+] adjusted values at onset of oscillations is given in Figure 4.8. Oscillations commenced at lower pH values in reactions where the second region of HI formation and consumption (Figure 4.3(b), "second autocatalysis") was present ([PdI_2] = 15.1 µM; 22.7 µM and 30.2 µM), while higher pH values were recorded in the absence of this second region. It appears that higher H^+ produced during the second region contributed to lower pH at onset of oscillations, possibly because, the consumption of H^+ generated from the second region was ongoing at onset of oscillations.

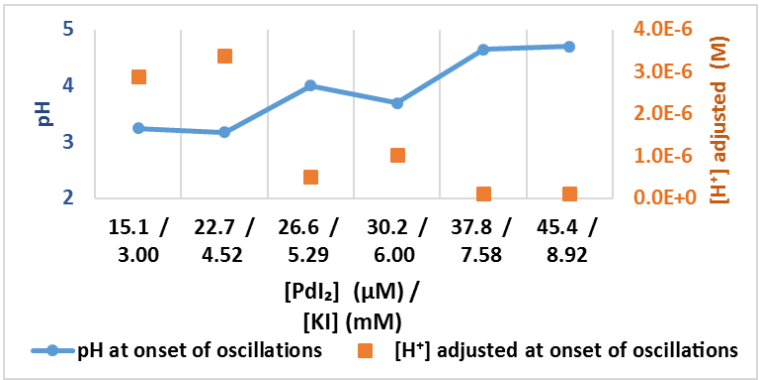

Figure 4.8. pH values recorded at onset of oscillations at constant concentrations of mono alkyne substrate (A-PEG_{2000}) and changing concentrations of catalytic mixture

Trends in time at onset of oscillations and duration of oscillations is given in Figure 4.9. Oscillations began earlier in reactions with less catalytic mixture and onset time increased with catalytic mixture, excluding the study at $[PdI_2]$ = 22.7 μM. The second region of HI production and consumption for reaction at $[PdI_2]$ = 22.7 μM may have delayed onset of oscillation at this concentration. The duration of oscillations across runs increased at lower concentrations of the catalytic mixture ($[PdI_2]$ = 15.1μM; 22.7 μM and 26.6 μM) and decreased at higher concentrations of the catalytic mixture ($[PdI_2]$ = 30.2 μM; 37.8 μM and 45.4 μM). However, since oscillations were still ongoing for runs at higher catalytic concentrations when the experiments were terminated[6], the actual duration of oscillations at these concentrations were not determined.

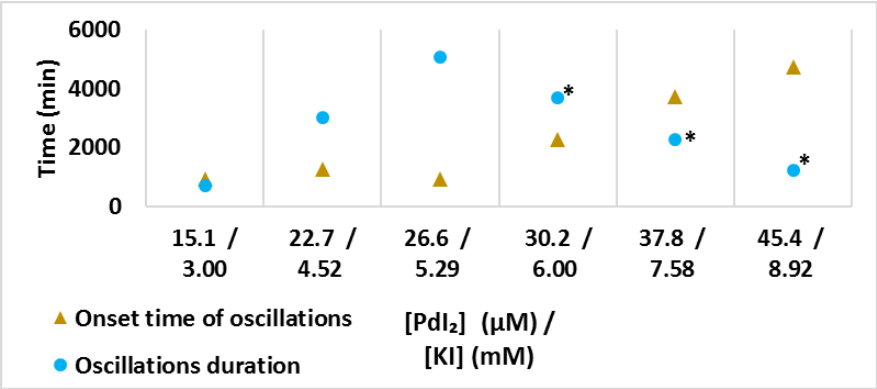

Figure 4.9. Onset of oscillations and oscillation duration at constant concentration of mono alkyne (A-PEG_{2000}) functionalised polyethylene glycol. (* indicate reactions where oscillations were still ongoing at point experiment was stopped)

Additional methanol was introduced to account for evaporative losses over the course of the study covered in this section. Examples of points of addition of extra methanol is shown in Figure 4.7 and the extracted profiles in Figure 4.10. The experiments were run for approximately 5 days during which the initial 90 mL of methanol gradually evaporated at an average of 6±1.2 mL/day. Thus, additional methanol was introduced at various points to keep the volume as close as possible to 90mL. The introduction of extra methanol to account for evaporative losses was reported in previous oscillatory carbonylation studies of phenyl acetylene at different scales and [9, 10, 32, 173, 177] for a range of temperatures (0 to 40^oC) [9, 32]. The additional methanol in these instances caused a rise in pH [242, 243].

[6] Due to long experiment durations, it was necessary to stop experiments after some days to allow for equipment maintenance and rehydration of probes.

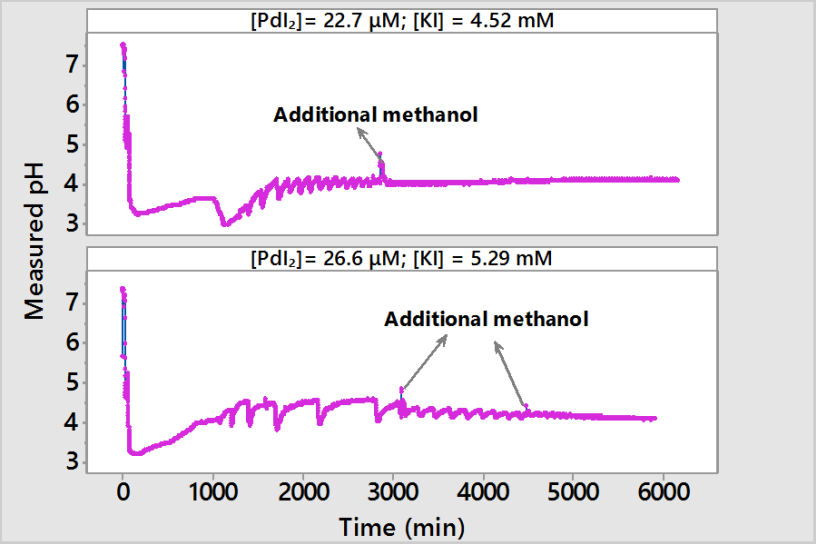

Figure 4.10. Changes in oscillatory pattern with additional methanol (Arrows specify additional methanol in 5 to 10 mL aliquots) (CO/air flowrates = 15 mL/min; total initial methanol volume = 90 mL; [A-PEG$_{2000}$] = 2.03 mM; reaction temperature = 20^{o}C ± 2)

Additional methanol was reported to restart oscillations in phenyl acetylene carbonylation at 40^{o}C and also increased the amplitude of oscillations when introduced during oscillatory cycle [9, 32]. The residual water impurity introduced with additional methanol was suggested as driving force behind these pH changes and is presumably correct since, water has been reported as an important factor in oxidative carbonylation reactions [293, 294]. However, a different reason for the changes in pH, restarting of oscillations and increased oscillation amplitudes after extra methanol is added could be dilution. As the reaction proceeds, concentrations of the species increase following solvent evaporation, hence, influencing the pH and trends recorded. The addition of more methanol dilutes the solution and may return the concentration of certain species to some earlier state where oscillations are possible, which may explain the restart of oscillations and increased amplitudes seen with the phenyl acetylene system. Consequently, a study comparing changes in the presence and absence of extra methanol was completed to assess the impact of additional methanol.

4.2.1 Assessment of the Effects of Additional Methanol on Reaction Dynamics

In Section 4.2, the influence of varying catalyst concentration at constant substrate concentration was assessed. The introduction of more methanol to account for evaporative losses over the course of the reaction due to the long experimental durations appeared to have introduced some changes to the pH profiles recorded and the reaction dynamics. For this reason, the influence of additional methanol was investigated according to the conditions in Table 4.3. Assessing changes from additional methanol was necessary to clarify and support the choice to perform all other experiments with or without additional methanol. Although a

single condition is presented here, additional data is included in appendix A, (A1 and A2) and same trends as shown and discussed here are observed at other conditions.

Table 4.3. Studies on the influence of additional methanol on the carbonylation reaction profile (CO/Air flowrates = 15 mL/min; total initial methanol volume = 90 mL, total additional methanol = 25 mL (added in 7.5 to 10 mL aliquots); Temperature = 20^{o}C±2)

Extra Methanol	[PdI_2] (μM)	[KI] (mM)	[A-PEG_{2000}] (mM)
Yes	26.6	5.29	2.03
No	26.6	5.29	2.03

The pH profiles obtained from studies with and without additional methanol are given in Figure 4.11. The initial stages in both reactions from onset of the reaction were more or less synchronized; from addition of catalytic mix to purging and substrate addition till the first autocatalytic HI production following the slow H^+ formation phase. A difference of 0.25 pH units was noted after first autocatalytic HI formation and oscillations commenced 168 min apart.

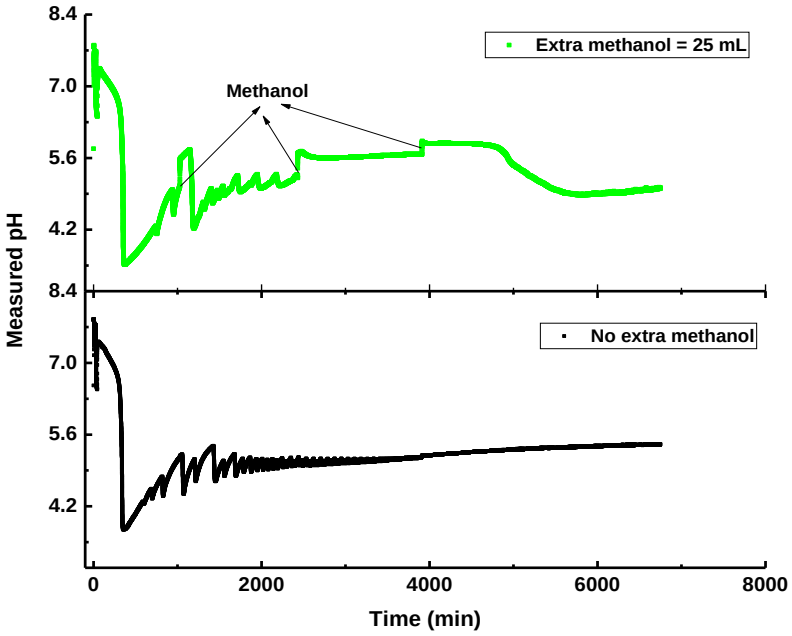

Figure 4.11. Influence of additional methanol on reaction profile obtained from carbonylation of A-PEG_{2000}. (CO/Air flowrates = 15 mL/min; total initial methanol volume = 90 mL, total additional methanol = 25 mL; Temperature = 20^{o}C±2)

Since volume is inversely proportional to concentration, loss of methanol with time may lead to increased concentrations of reactants and products in the solution. To limit the effect of evaporative losses on the reaction dynamics and determine the influence of additional methanol, extra methanol was added in one reaction at 1030 min, 2430 min and 3950 min (Figure 4.11). Maintaining the volume at roughly 90 mL in this reaction altered the oscillatory pattern and increased the pH value each time methanol was added. Introducing 10 mL of methanol at 1030 min during an oscillatory cycle as shown in Figure 4.12 was followed by a modification in oscillatory pattern and an increase in the amplitude of the affected oscillatory cycle.

Successive oscillations after more methanol was added had considerably less amplitudes and periods than the control experiment (without extra methanol). The pattern of successive oscillations also changed progressively with oscillations alternating between small and large period cycles. When additional 7.5 mL of methanol was introduced at 2430 min (Figure 4.12), a pH rise of 0.46 pH units was recorded. The addition of second aliquot of methanol was followed by loss of oscillations, while oscillations were still ongoing in the control run (No extra methanol, Figure 12 (below)). The run with extra methanol remained in stable steady state as shown in Figure 4.12, even after the last aliquot of 7.5 mL was added at 3950 min.

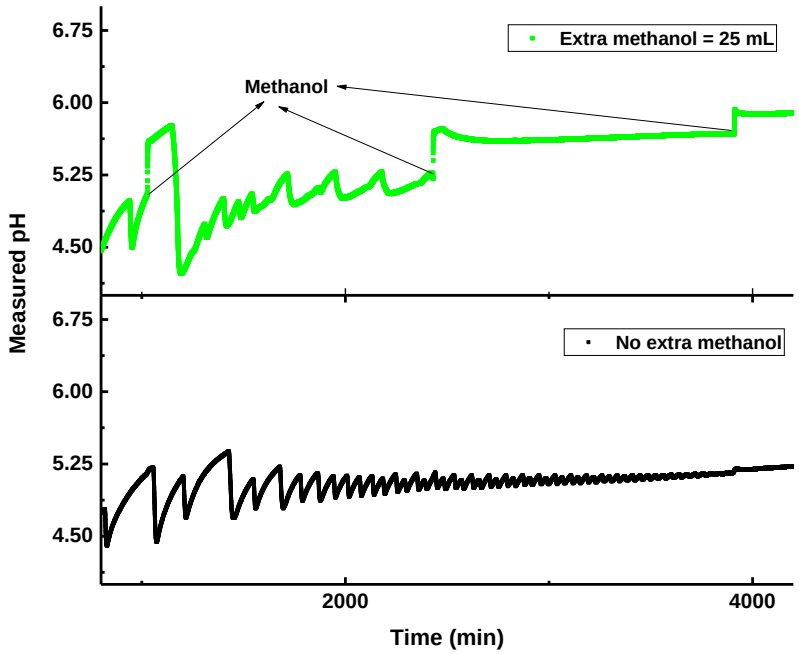

Figure 4.12. Alterations in oscillatory pattern and absence of oscillations on addition of extra methanol for evaporative losses (CO/Air flowrates = 15 mL/min; total initial methanol volume = 90 mL, total additional methanol = 25 mL) (a.) change in oscillations; (b.) absence of oscillation

The variation in oscillatory modes with the initial extra methanol and absence of oscillation after the second portion of methanol was added supports the proposition that addition of methanol to account for evaporative losses influences reaction dynamics. Replicate experiments also showed such behaviour. Supplementary Figures A2 and A3 in the appendix are further examples of the reaction profiles where extra methanol was introduced over the course of the reaction. The significant alterations in reaction profiles on introducing more methanol agree with the assumption. Consequently, profiles discussed in Section 4.2 have the added effects from extra methanol. While evaporative losses could change the reaction conditions by increasing concentration of reactants and products, the introduction of additional methanol to counteract evaporative losses evidently changes the reaction profile in several ways. For this reason, subsequent reactions and profiles reported in this thesis, unless otherwise stated, were obtained from reactions conducted in the absence of additional methanol. The effects of evaporative losses were minimized by sealing the reacting system as much as possible granting losses were still recorded. As the reactions are run for several days, losing 6±1.2 mL/day would amount to an average loss of 0.25±0.05 mL/hr. These loses appear minimal, but it could potentially affect the reaction profiles reported. Nonetheless, for consistency and ease of demonstrating a rather complex process, the choice was made to perform subsequent reaction without introducing additional methanol. It may also be easier to adjust for evaporative losses than deciphering how much dilution occurs each time with respect to reactants, products and intermediate species, since sampling during reaction was not done for the polymeric substrate. The influence of evaporative losses on oscillatory profiles in carbonylation of A-PEG_{2000} would require extensive work and is not examined in this report, instead, is proposed as a subject for future investigation.

4.2.2 Section Summary

Graphical summaries of trends observed on altering PdI_2/KI concentrations at constant substrate concentration is given in Figures 4.13 to 4.17. Increasing PdI_2/KI concentrations reduced the rise in pH on substrate addition as shown in Figure 4.13. The highest number of oscillations were recorded in reaction with moderate KI and PdI_2 concentrations. Higher PdI_2/KI concentrations did not favour more oscillations as given in Figure 4.14. The batch type bifurcation diagram (pH max/min vs PdI_2) illustrated in Figure 4.15 and trends in maximum amplitude and number of oscillations with increasing palladium iodide concentration reveal trends that suggest intermediate PdI_2 concentrations (22.7 μM and 26.6 μM) as desirable for maximum amplitudes and maximum number of oscillations. Increasing the catalytic

concentration supported a downwards shift in oscillations within the experimental duration investigated (Figure 4.17).

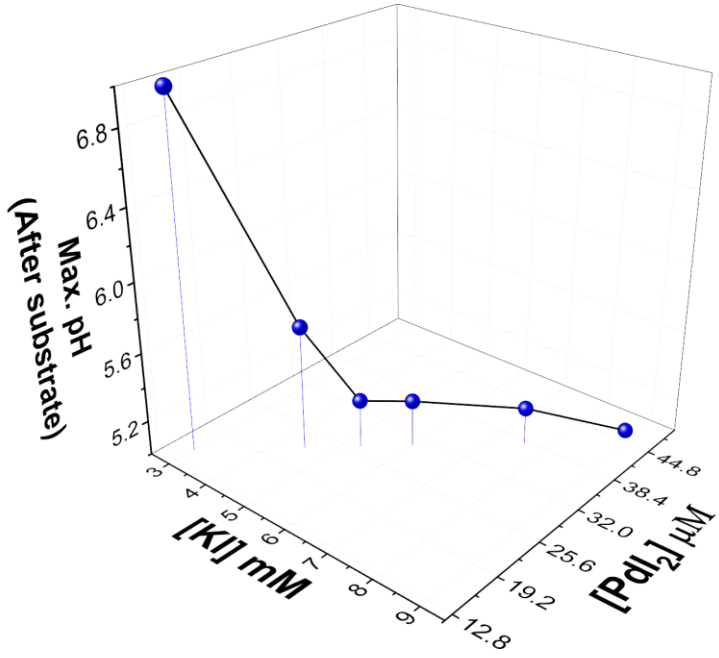

Figure 4.13. Trends in pH rise on substrate addition as a function of KI and PdI_2 concentrations

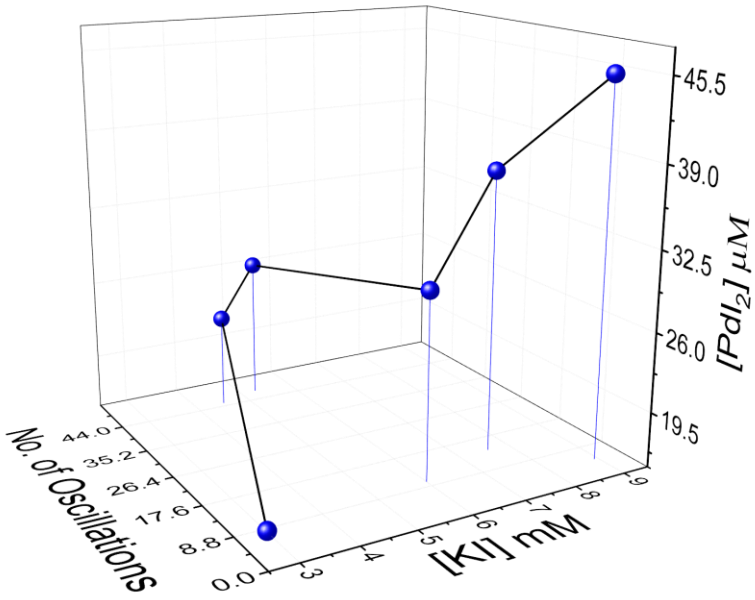

Figure 4.14. 3D illustration of drifts in number of oscillations as a function of KI and PdI_2 concentrations

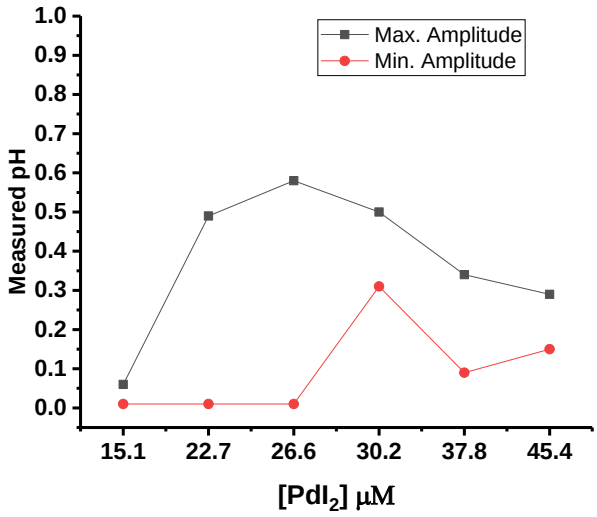

Figure 4.15. Changes in maximum and minimum pH amplitudes of oscillations recorded as PdI_2 concentrations increases

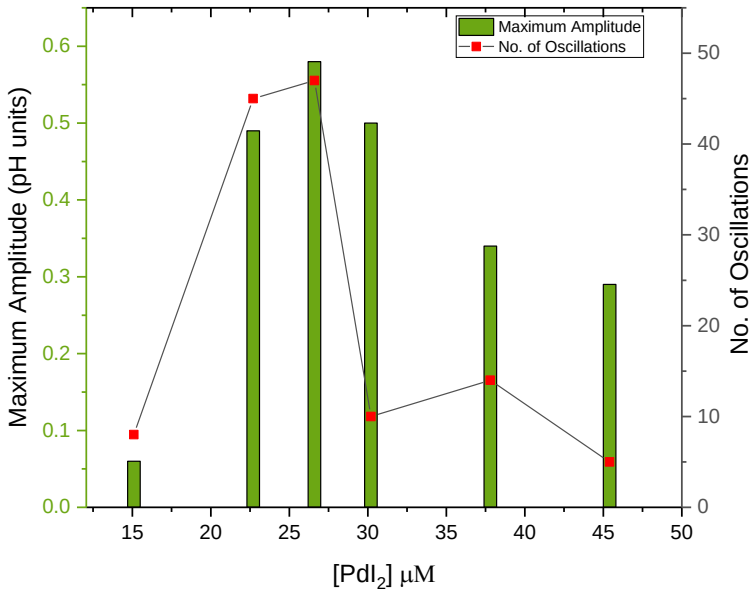

Figure 4.16. Variations in number of oscillations and maximum oscillatory pH amplitude as a function of increasing PdI_2 concentrations

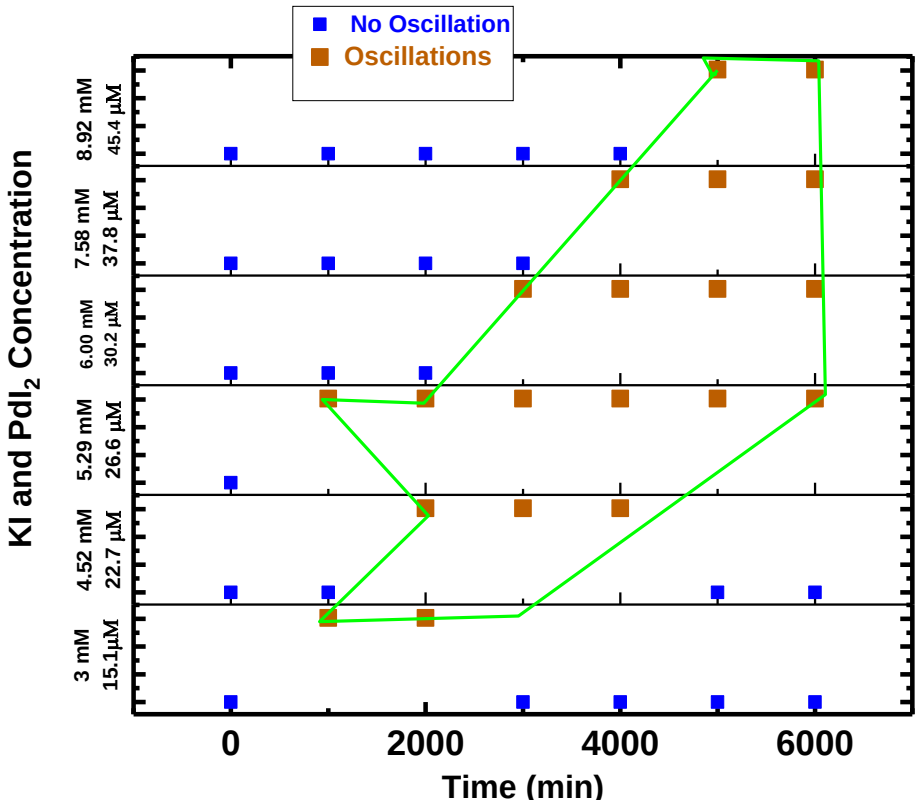

Figure 4.17. Phase diagram indicating regions of oscillatory and stationary phases as the reactions progress at different KI and PdI_2 concentrations and constant substrate concentration ([A-PEG_{2000}] = 2.03 mM)

In conclusion:

1. Reproducible oscillations are feasible at a given substrate concentration for the range of PdI_2 (15.1 - 45.4 µM) and KI (3 – 8.92 mM) concentrations studied.
2. Differences in the shapes, amplitudes and periods of the oscillations recorded was noted as the concentrations of PdI_2 and KI increased. Smaller oscillations were also obtained towards termination of reactions due to the semi-batch nature of the set-up.
3. Achieving oscillations in present study at reduced PdI_2 concentrations, in comparison to previous research in this area may prove useful for future applications and is cost effective.
4. Increasing the concentration of PdI_2/KI increased HI formation with respect to first autocatalytic H^+ formation in current and replicate samples.
5. Additional methanol changes oscillatory dynamics as it causes rise in pH.
6. Evaporation may influence nonlinear dynamics, thus, is suggested for further study.
7. KI is assumed to contribute to dynamics recorded by donating iodide and/or iodine.

4.3 Influence of Potassium Iodide Addition Times at Constant Palladium Iodide and Mono Alkyne Functionalised Methoxy-Polyethylene Glycol Concentrations

Potassium iodide is important in palladium iodide catalysed oxidative carbonylation reactions as it promotes dissolution, iodine availability and hence, efficient catalyst recycling [269-274]. In Section 4.2, the concentration of KI as well as PdI_2 was varied for each experimental run, hence, it was difficult to ascribe profile features to just PdI_2 or KI. Since KI is also necessary for dissolution of PdI_2, some KI is always introduced with the catalytic mix (KI/PdI_2/methanol). To address this challenge, the influence of KI was assessed as a function of KI addition time at conditions given in Table 4.4. The study in Table 4.4 was designed such that, minimal KI was used for dissolution and the rest of KI for the experiments were added at different times. Potassium iodide is not expressed as concentration in 90 mL (total initial volume) in this case as additional KI was introduced 24 hr and 48 hr into the reaction, at which point, some methanol had already evaporated. In this Section, excluding KI employed in catalyst dissolution, additional KI is termed "extra KI".

Table 4.4. Reaction conditions employed for studies on varying KI addition times. (CO/Air flowrates = 15 mL/min; total methanol volume = 90 mL; temperature = 20^{o}C±2)

[PdI_2] (μM)	Initial KI in catalytic mixture (mmol)	Extra KI (mmol)	Extra KI addition time (hr)			[A-$PEGA_{2000}$] (mM)
30.2	0.237	0.303	0	24	48	2.03
30.2	0.237	0.573	0	24	48	2.03

The pH profiles obtained by introducing additional KI at intervals (0, 24 and 48 hr) during the course of the reactions are given in Figures 4.18 and 4.19. 0.303 mmol of extra KI was added to the reactions in Figure 4.18, while 0.573 mmol of extra KI was added to profiles in Figure 4.19. Generally, increasing extra KI addition times reduced the chances of oscillations occuring, as oscillations were absent in both profiles (Figure 4.18 and 4.19) when extra KI was added 48 hr into the reaction. When the total moles of KI was added from onset of the reaction, oscillations were obtained in both profiles, however, small amplitudes oscillations were mostly present in the reaction with lower number of moles of extra KI (0.303 mmol), suggesting that KI may encourage larger sized of oscillations. It appears that increased KI concentration hinders the formation of HI as the lower pH values (more acidic, hence more H^+) in Figures 4.18 and 4.19 prior to adding "extra" KI at 48 hr increased (less acidic, less H^+) when extra KI was added. It is possible that additional iodide ions from the extra KI introduced creates an equilibrium state between H^+ and I^-, limiting dissociation of the HI acid which is then observed as increase in pH values. Similar trends are also observed for the 24-hr profile and are more

obvious when extra KI = 0.573 mmol is added. The reaction profiles are analysed in the rest of this section with respects to when extra KI is added.

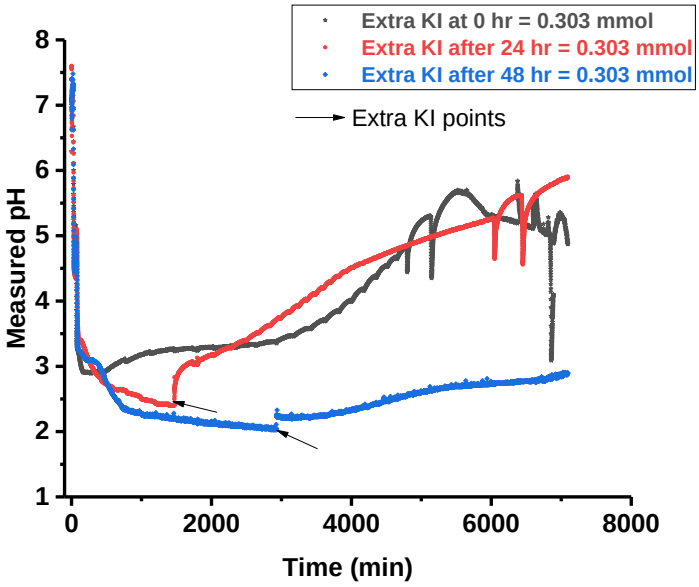

Figure 4.18. pH profiles from the carbonylation reactions with extra KI introduced at 0, 24 and 48 hr from onset of the reaction at constant PdI_2 and mono alkyne functionalised substrate concentrations. ([A-PEG_{2000}] = 2.03 mM; [PdI_2] = 30.2 μM; $KI_{initial}$ = 0.237 mmol; $KI_{additional}$ = 0.303 mmol CO/Air flowrates = 15 mL/min; total methanol volume = 90 mL; temperature = 20°C±2)

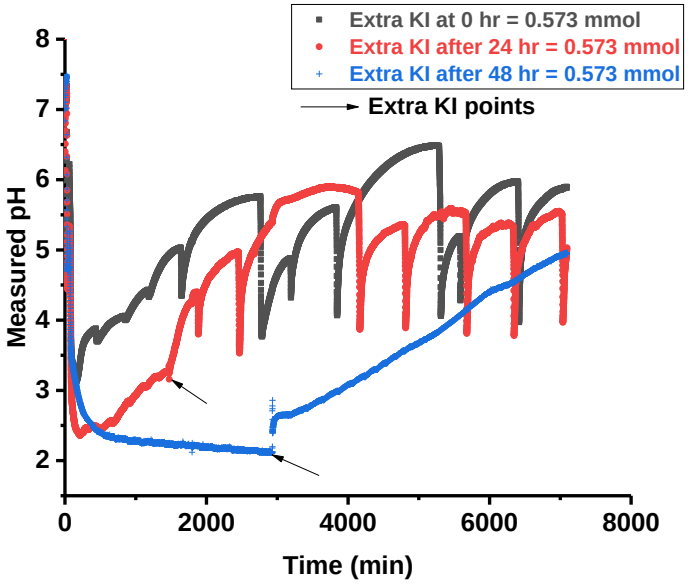

Figure 4.19. pH profiles from the carbonylation reactions with extra KI introduced at 0, 24 and 48 hr from onset of the reaction at constant PdI_2 and mono alkyne functionalised substrate concentrations. ([A-PEG_{2000}] = 2.03 mM; [PdI_2] = 30.2 μM; $KI_{initial}$ = 0.237 mmol; $KI_{additional}$ = 0.573 mmol CO/Air flowrates = 15 mL/min; total methanol volume = 90 mL; temperature = 20°C±2)

4.3.1 Analysis of Profiles where the Total Potassium Iodide was added at Onset of the Reaction

The pH and [H^+] adjusted profiles in Figure 4.20 was obtained from reaction at constant palladium iodide and mono alkyne substrate concentrations, when different amounts of extra KI were introduced at onset of the reaction (0 hr). Oscillations were recorded at both KI conditions, although at KI = 0.303 mmol, oscillations had smaller amplitudes and periods for an extended period (4403 min), before transitioning to larger amplitudes and periods. More oscillations were also recorded at this condition (extra KI = 0.303 mmol). The difference in number of oscillations and oscillatory pattern at both KI conditions (0.303 mmol and 0.573 mmol) agrees with the suggestion that KI influences reaction dynamics and oscillations. However, as total amount of KI was added at onset of reaction (0 hr), only a general idea of the influence of KI is appreciated.

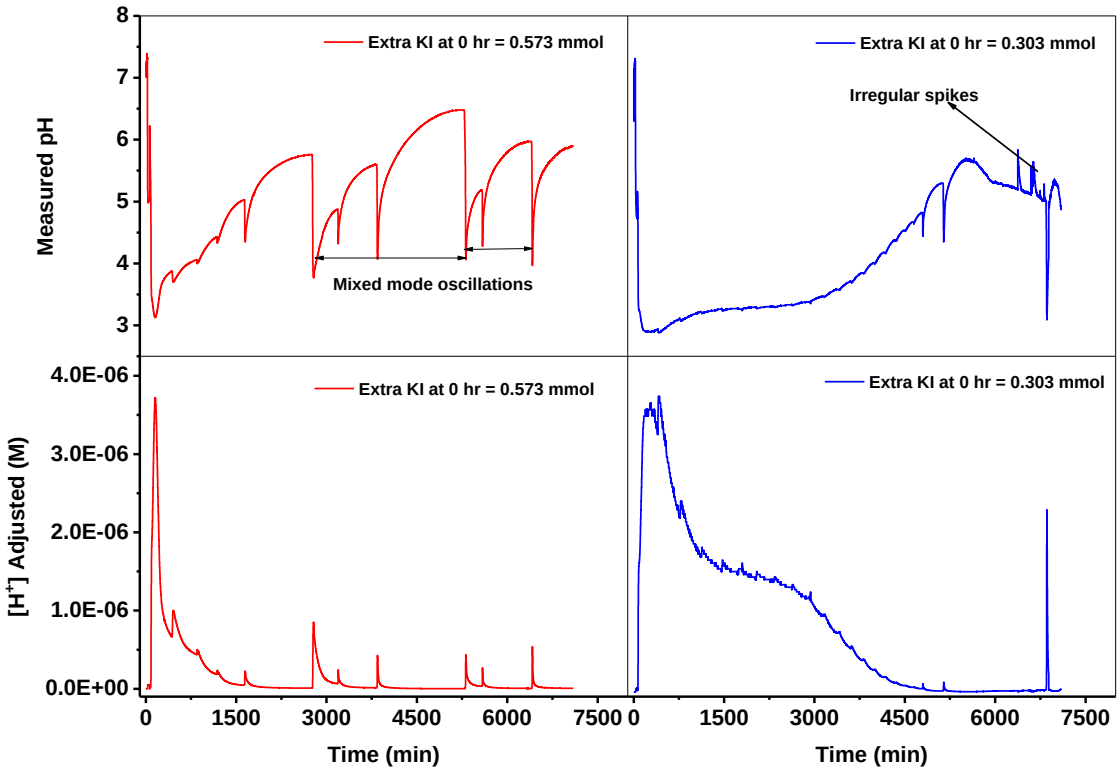

Figure 4.20. pH and [H^+] adjusted profiles from the carbonylation reactions at constant PdI_2 and mono alkyne functionalised substrate concentrations when total KI is added from onset. ([A-PEG_{2000}] = 2.03 mM; [PdI_2] = 30.2 μM; $KI_{initial}$ = 0.237 mmol; CO/Air flowrates = 15 mL/min; total methanol volume = 90 mL; temperature = 20°C±2)

The initial stages of the carbonylation reaction for samples where total KI was added at onset of the reaction at constant PdI_2 and A-PEG_{2000} concentrations proceeds in the same manner as results presented in Section 4.2. Summarily, the reaction profiles remained fairly similar from

onset until purging commenced 26 min into the reactions. On purging with CO and air, pH decreased with corresponding rise in [H^+] adjusted, signifying the onset of proton donating reactions. The reaction with extra KI = 0.303 mmol (Figure 4.20) produced more H^+ than reaction at 0.573 mmol, although solvent carbonylation time was extended by 5 min at extra KI = 0.573 mmol. The difference in [H^+] from solvent carbonylation may be attributed to competing reactions in Eq. 4.2 to 4.5. Initial pH values were very similar from onset of reaction, therefore, differences in pH probes after calibration is not considered as a contributing factor.

The pH rises on adding constant concentrations of mono alkyne substrate (2.03 mM) to both reactions was higher for reaction with extra KI = 0.573 mmol (4.95 to 6.22 pH units), and lower for reaction with extra KI = 0.303 mmol (4.73 to 5.16 pH units). The difference in pH rise following substrate addition in reactions with KI = 0.303 mmol and KI = 0.573 mmol is not credited to concentration of substrate, since equal concentrations were added to both reactions (2.03 mM each). The only other variable which may have contributed to the differences in pH rise in both reactions is KI, as the two experiments have different amounts of KI.
The rise in pH on substrate addition was followed by periods of "slow H^+ formation" as described in Section 4.2. This duration lasted for 8 min at extra KI = 0.303 mmol and 18 min at extra KI = 0.573 mmol. As HI gradually accumulates during the period of "slow H^+ formation", it approaches some concentration (presumed to be specific to each experimental condition), which prompts the autocatalytic production of HI, recorded as the sudden drop in pH/ corresponding rise in [H^+] adjusted. This change in both reaction profiles supports Eq. 4.6 (substrate conversion and HI formation), postulated to proceed in an autocatalytic mode. The prompt fashion of the transition from slow H^+ formation to rapid [H^+] formation agrees with autocatalysis assumption [295]. pH drop resulting from autocatalysis was higher in reaction with less overall KI (extra KI = 0.303 mmol), suggestive of potential damping effect on the amount of [H^+] generated from autocatalysis at extra KI = 0.573 mmol. However, there is no certainty to this claim and better understanding of the effect of KI on autocatalysis should become obvious when other conditions and addition times are examined.

The drop in pH from autocatalysis was followed by rise in pH, with corresponding decrease in [H^+] adjusted. The rate of consumption of HI formed appears slower in reaction with extra KI = 0.303 mmol, probably because more time was needed for consumption of higher HI produced during the initial autocatalysis. Oscillations begun at 396 min and 436 min for reactions with extra KI at 0.303 mmol and 0.573 mmol respectively. Onset of oscillations was marked by autocatalytic formation of HI and a period of slow consumption of HI, with this cycle

continuing for the duration of the experiment. Concentration of [H^+] remained higher in the reaction with extra KI = 0.303 mmol till 4600 min, at which point, the [H^+] reached concentrations closer to values obtained in the reaction with KI = 0.573 mmol. Oscillatory modes recorded for reactions where total KI was added from onset of the reaction is given in Figure 4.20. Oscillatory patterns differed with varying KI concentrations and, complex oscillatory phenomena in the form of mixed mode oscillations and irregular spikes within oscillations were recorded. These oscillatory phenomena are known to arise from complex nature of intermediates formed during the reaction [31, 109-112, 115]. The phenomena in Figure 4.20 in addition to other experimental observations in the rest of the chapter are discussed in greater details in Chapter 6, Section 6.5

4.3.2 Analysis of Reaction Profiles where Additional Potassium Iodide was Introduced Twenty-Four Hours from Onset of the Reaction

In Section 4.3.1, the influence of the moles of potassium iodide on the oxidative carbonylation reaction was assessed when total KI for the reaction was introduced from onset. This section analyses reaction profiles obtained when the same amounts of extra KI (0.303 mmol and 0.573 mmol) were added 24 hr into the reaction. Introducing extra KI into the reaction as a function of time, improves the likelihood of extracting the effect of KI on oscillations and the initial stages of the reaction. Reaction profiles obtained from experiments for extra KI at 24 hr is given in Figure 4.21. As with previous profiles, pH profiles were measured throughout the duration of the experiments, while [H^+] adjusted profiles were obtained from pH profiles according to Eq. 4.1.

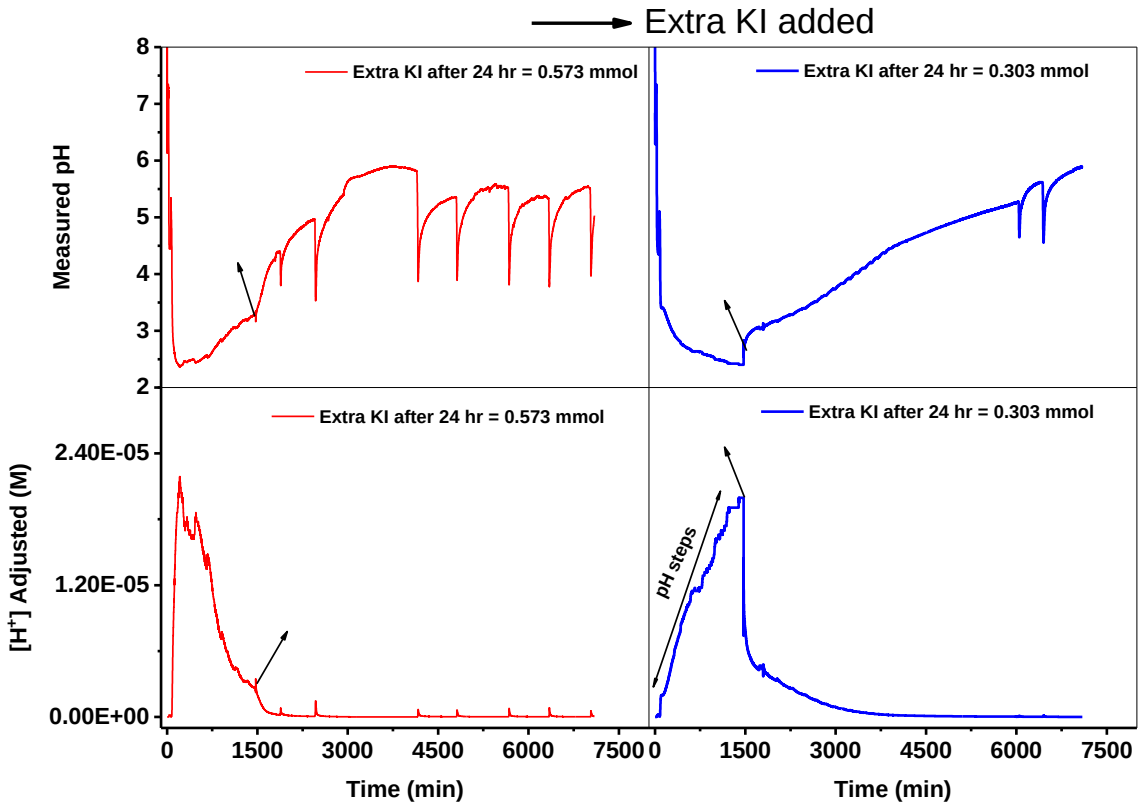

Figure 4.21. Full pH and [H^+] adjusted profiles when more KI was added 24 hours from onset of the carbonylation reaction at constant PdI_2 and mono alkyne functionalised substrate concentrations. ((top) pH profiles (bottom) [H^+] adjusted profiles; [A-PEG_{2000}] = 2.03 mM; [PdI_2] = 30.2 μM; $KI_{initial}$ = 0.237 mmol; CO/air flowrates = 15 mL/min; total methanol volume = 90 mL; temperature = 20°C±2). Arrows indicate where extra KI was added

Oscillations were obtained at both conditions investigated. Oscillations with larger amplitudes and periods were obtained in reaction with extra KI = 0.573 mmol. At KI = 0.303 mmol, decreasing step changes in pH were observed prior to small amplitude and period oscillations, before a final transition to larger amplitude oscillations. Oscillations were still ongoing when both experiments were stopped. Steps were absent in the reaction where extra KI = 0.573 mmol was added 24 hr later, however, onset of oscillations was marked with small amplitude oscillations.

After the reactions were purged and the pH following purging allowed to equilibrate, the pH drop varied slightly between runs, with a higher pH drop (0.06 pH units) in one of the runs. This slight difference was noted though the reaction conditions in both experiments remained identical, as such, the difference may arise from small variations in rates of the initial reactions (Eq. 4.2 to 4.5). Since this difference (0.06) was less than the difference in Section 4.3.1 (0.22 pH units), where different amounts of total KI was added at onset of the reaction, it appears to support the assumption that KI effects [H^+] formed during solvent carbonylation.

Constant concentration of mono alkyne substrate (2.03 mM) dissolved in methanol (≈ 3.7 mL) were added to each reaction, leading to rise in pH and corresponding decrease in $[H^+]$ adjusted as described in Section 4.2. Substrate addition was followed by periods where H^+ was formed gradually. The periods of slow H^+ formation lasted 9 min and 10 min at 0.303 mmol and 0.573 mmol, respectively. The similarity in duration is likely from the identical reactant concentrations (extra KI not yet added) and conditions. As the concentration of hydrogen ion slowly increased, a transition from slow mode to autocatalysis, recorded as rapid decrease in pH / sharp increase in $[H^+]$ adjusted (Figure 4.21) was present in both runs. More HI was formed from autocatalysis in one experimental run than the other with a difference of 1.75 x 10^{-5} M, based on the adjusted $[H^+]$ calculation. Such difference following autocatalysis was also noted when the total amount of KI was varied from onset of reaction and KI was then suggested as a possible reason. However, since KI was still constant (0.273 mmol) at this point in the reaction for current study, it is less likely that KI influenced the differences in autocatalytic HI formed here and in Section 4.3.1. If KI is less likely to have contributed to this difference, then the concentration of HI formed in the "slow H^+ formation" period is now proposed as reason for the variation in concentrations of HI subsequently formed via autocatalysis. This assumption holds for both current study and Section 4.3.1, since reactions with more HI in the "slow H^+ formation" period formed more HI in autocatalytic mode.

The reaction profiles were altered following the first autocatalytic HI formation. For the experiment where less HI was produced from autocatalysis, the pH steadily decreased in a step wise mode signifying further formation of H^+ and the duration between each pH step increased with time (Figure 4.21). Consumption of H^+ followed autocatalytic HI formation in the reaction where more HI was produced from autocatalysis. Continued rise in pH with H^+ consumption, was followed by onset of oscillations as shown in Figure 4.21.

Extra KI was added to both reactions 24 hr from onset of experiment as given in Figure 4.21. When 0.303 mmol KI was added to reaction with stepwise decrease in pH, a rise in pH with corresponding decrease in $[H^+]$ adjusted was noted. The rise in pH suggest reactions consuming H^+ and Eq. 4.8, in addition to reversible reactions given in Eq. 4.9 and 4.10 are suggested. The reaction with extra KI = 0.303 mmol transitioned from pH steps to small amplitude oscillations at this point. When 0.573 mmol extra KI was added to reactions where oscillations had already commenced (Figure 4.21), the oscillatory pattern transitioned from small amplitude to large amplitude oscillations. It seems like extra KI facilitated oscillations in both reactions, though adding 0.573mmol KI encouraged larger oscillations than 0.303 mmol extra KI. Nonetheless,

it is plausible that the higher [H^+] in reaction where 0.303mmol of KI was added, influenced the outcome of the reaction and delay in onset of larger oscillations.

Oscillatory patterns obtained in reactions where extra KI was added 24 hr into the reaction is shown in Figure 4.21. Simple oscillations were obtained, which is in contrast to mixed mode and spiked oscillations obtained when total KI was introduced from onset of reaction (at identical PdI_2 and mono alkyne substrate concentrations). The difference in oscillatory pattern suggests the possibility of altering the type of oscillation produced in carbonylation of mono alkyne functionalised methoxy-polyethylene glycol by varying KI addition times and KI concentration.

4.3.3 Analysis of Reaction Profiles where Additional KI was Introduced Forty-Eight Hours from Onset of the Reaction

Extending the time when extra KI was added to reactions from 24 hr to 48 hr, resulted in the full pH and [H^+] adjusted profiles in Figure 4.22. No oscillations were observed when the extra KI addition time was moved to 48 hr from onset of the reaction, contrasting the range of oscillations obtained at extra KI addition times of "0 hr" and 24 hr.

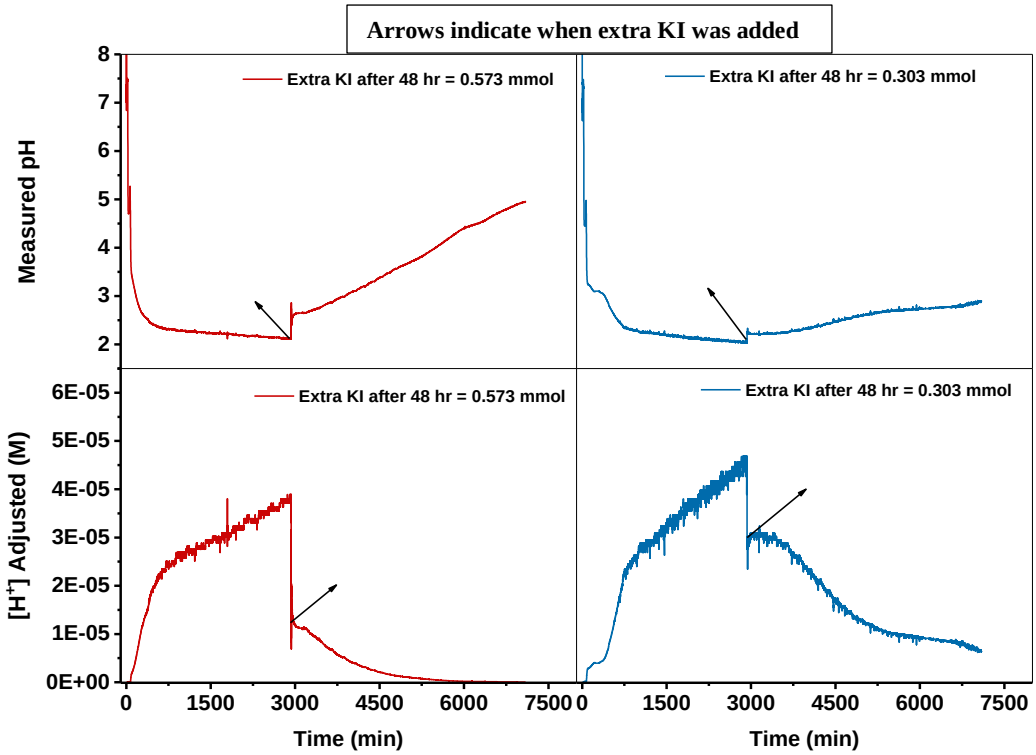

Figure 4.22. Reaction profiles when extra KI was added 48 hours from onset of the carbonylation reaction at constant PdI_2 and mono alkyne functionalised substrate concentrations. ((top) pH profiles (bottom) [H^+] adjusted profiles; [A-PEG_{2000}] = 2.03 mM; [PdI_2] = 30.2 μM; $KI_{initial}$ = 0.237mmol; CO/air flowrates = 15 mL/min; total methanol volume = 90 mL; temperature =20°C±2)

Both reactions appear to follow similar reaction pathways following initial stages of the reaction until different amounts of extra KI was added. Addition of extra KI (0.303 mmol and 0.573 mmol) lead to an increase in pH / decrease in $[H^+]$ adjusted. pH rise was comparable to the millimoles of extra KI added and the rise in pH remained significantly higher in reaction with more overall KI till both runs were terminated to allow for equipment maintenance.

A slight difference was observed in initial values of the pH probes following calibration which may have influenced the profiles obtained. The pH drops on purging remained smaller in the reaction where initial pH values were higher (reaction where 0.573 mmol of extra KI was eventually added) following pH probe calibration. Although this difference in pH drop on purging may arise from variations in rates of Eq. 4.2 to 4.4 and Eq. 4.5 (reactions for catalytic conversion of water), the influence from different initial pH probe values is not ruled out. Constant concentrations of mono alkyne substrates were added to both reactions leading to rise in pH. Substrate addition was followed by periods of gradually increasing hydrogen ion concentration (slow H^+ formation period) until the $[H^+]$ reached some concentration allowing for autocatalytic formation of H^+. Some disparity was observed in $[H^+]$ generated from autocatalysis, however, as the reaction continued, the H^+ concentrations remained steady and comparatively equal in both runs until extra KI was added.

4.3.4 Section Summary

Graphical summaries comparing key changes throughout the reactions where different moles of extra KI were added at various times is given in Figures 4.23 to 4.26. The heat map in Figure 4.23 illustrates the influence of extra KI addition times and number of moles of extra KI on the number of oscillations recorded. Achieving maximum number of oscillations appears to depend more on KI addition time than the number of moles of KI added. The trend shows that more oscillations are feasible at lower values of KI, as the maximum number of oscillations occur when KI is introduced between 10 and 20 hr into the reaction. Adding KI within the first 36 hrs supports the possibility of increased oscillations regardless of how much KI is present. The map in Figure 4.24 relates the period of oscillations with addition time and moles of KI added. Figure 4.24 shows a similar trend to that observed in Figure 4.23, with maximum periods within the same KI addition times as Figure 4.23. The maximum amplitude of oscillations achieved as a function of KI addition time and moles of KI added is given in Figure 4.25. The trend shows an increase in maximum amplitude of oscillations across all moles of

additional KI when extra KI is added earlier and is in line with previous trends in Figures 4.23 and 4.24, which support early addition of KI.

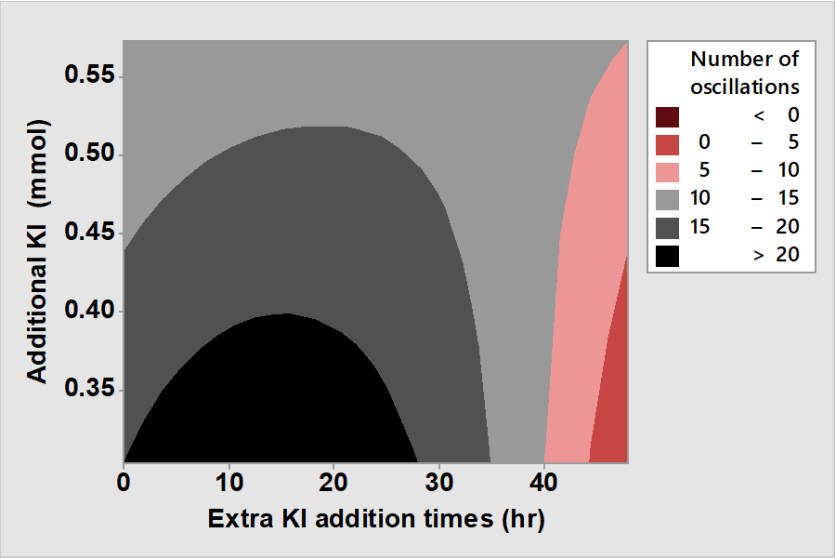

Figure 4.23. Heat map distribution of number of oscillations as a function of extra KI addition times and moles of KI added

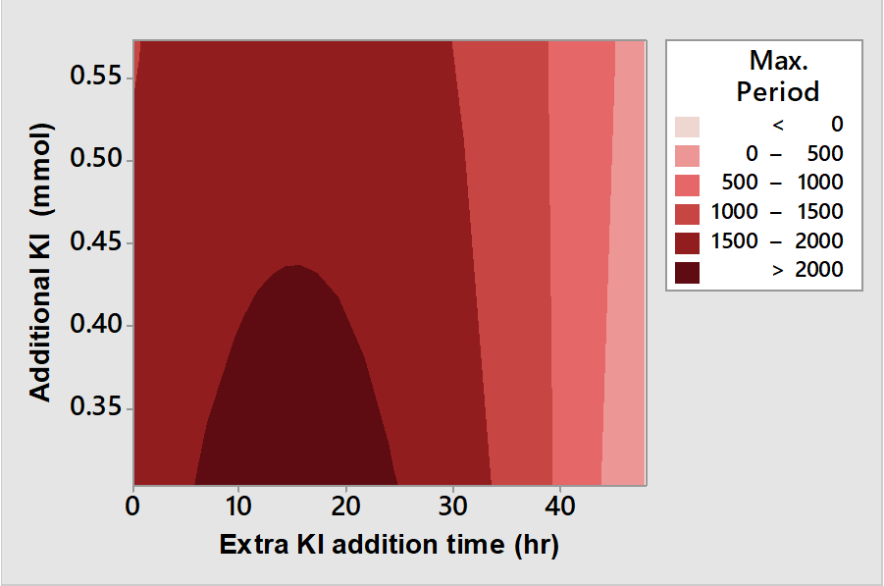

Figure 4.24. Heat map of maximum oscillation period as a function of extra KI addition times and moles of KI added

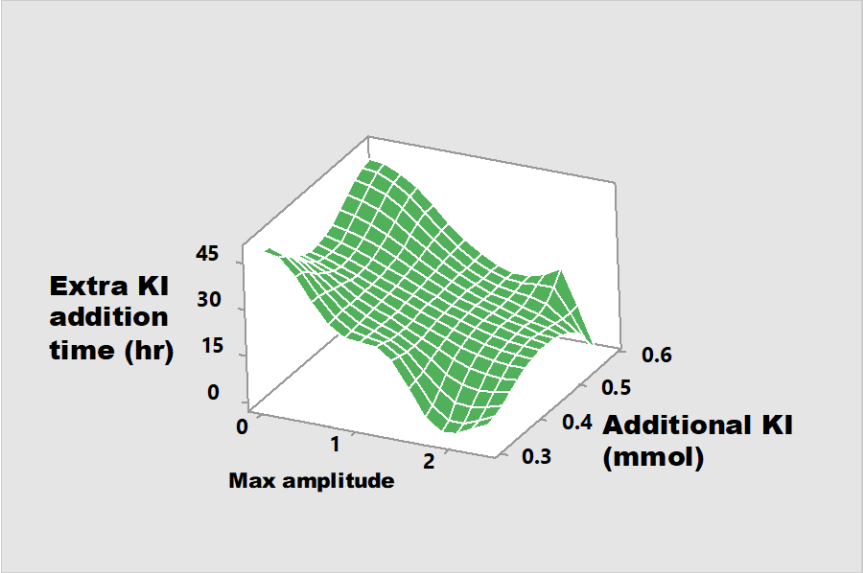

Figure 4.25. Changes in maximum pH amplitudes of oscillations recorded as a function of extra KI addition times and moles of KI added

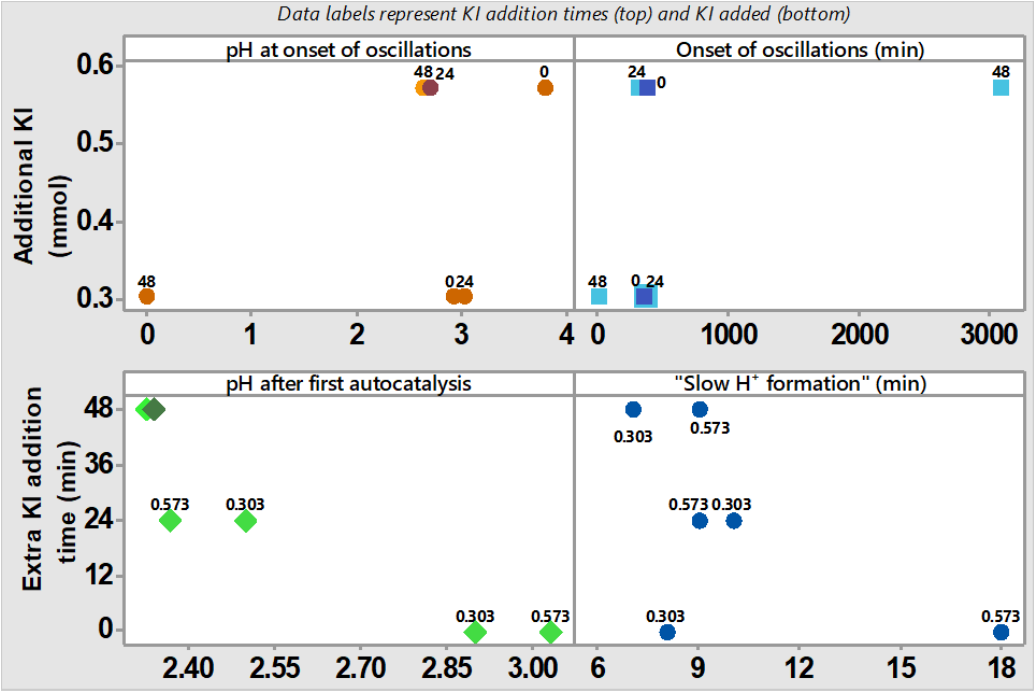

Figure 4.26. Graphical summary of key reaction attributes as a function of moles of KI added and extra KI addition times.

Variations in initial stages of the reaction, pH and time at onset of oscillations is given in Figure 4.26. The top left of Figure 4.26 shows the interdependence between pH at onset of oscillations, extra KI addition time and moles of additional KI. pH at onset of oscillation was similar at lower and higher moles of extra KI when added 24 hrs into the reaction while, a significant difference was observed for KI added at 0 hr (from onset). At 48 hr, oscillation was absent when 0.303 mmol of extra KI was added, but present when 0.573 mmol was added. This

suggests the need for increased concentrations of KI if later KI addition time and presence of oscillations are desirable factors and reduced concentration of KI if the absence of oscillation is needed. The time at onset of oscillations as a function of KI addition time and moles of extra KI is given in top right corner of Figure 4.26. The trend suggests that early onset of oscillations is promoted by earlier KI addition times irrespective of the concentration of KI present. pH after first autocatalysis (bottom left) is more acidic (increased HI formation) when KI is added from onset of the reaction than when it is added 48 hr into the reaction. No consistent trend was present during the period of slow H^+ formation (bottom right, Figure 4.26) as a function of extra KI addition times, but, identical durations were noted at 0.573 mmol when KI was added 24 hr and at 48 hr from onset of the reaction.

In conclusion

1. KI appears to promote large sized oscillations and facilitate onset of oscillations when it is added earlier than much later into the reaction.
2. The probability of achieving oscillations is significantly dependent on the initial concentration of KI present at onset of reaction for instances where extra KI is added much later in the reaction.
3. Amount of HI formed from initial autocatalysis following the region defined as "slow H^+ formation" increases when concentration of KI from onset of the reaction is reduced. Also, the addition of extra KI was followed by a reduction in H^+ concentration; suggesting that increased KI concentrations may limit HI formation.
4. KI may be used to alter oscillations and oscillatory patterns in the carbonylation reaction.
5. Increasing the initial amount of KI present may decrease pH drop achieved on purging.

4.4 Influence of Varying Palladium Iodide Concentrations at Constant Potassium Iodide and Mono Alkyne Functionalised Substrate Concentrations

In Section 4.3, total amounts of KI present at onset of the reaction, extra KI addition times and amount of additional KI introduced to the carbonylation reaction were found to influence oscillatory dynamics. When low concentrations of KI were employed from onset of the reaction, additional KI was required to promote oscillations but when additional KI was added much later into the reaction (48 hr), the ability of KI to promote oscillations appeared less successful. KI addition times seems significant from studies in Section 4.3 but, it is challenging to tune KI addition times without more information on reaction mechanisms. Thus, total

amounts of KI for other studies in this thesis were added at the onset of the reactions. Likewise, the KI study in Section 4.3 was performed at a single palladium iodide concentration, therefore, further studies were carried out at other PdI_2 concentrations with total KI added from the beginning. This was done to ensure that any deductions reached reflect the behaviour of the oscillatory system as much as possible. The amounts of KI and PdI_2 at onset of reactions were varied according to Table 4.6 and the reactions were performed at constant mono alkyne substrate concentration. Unlike earlier investigation in Section 4.2, (pre-made catalytic mixture), total initial concentrations of KI (Table 4.3) was obtained by adding fresh potassium iodide to the reaction vessels at start of reaction.

Table 4.5. Reaction conditions for evaluating the effects of potassium iodide concentration on oscillatory profiles obtained at various palladium iodide concentrations. (CO/air flowrates = 15 mL/min; total methanol volume = 90 mL; temperature = 20^{o}C±2)

[PdI_2] (μM)	[KI] (mM)			[A-PEG_{2000}] (mM)
17.0	3.00	6.00	9.00	2.03
22.7	3.00	6.00	9.00	2.03
30.2	3.00	6.00	9.00	2.03

4.4.1 Reaction Profiles at 3 mM Potassium Iodide Concentration and Constant Mono Alkyne Substrate Concentration

The pH and [H^+] adjusted profiles in Figure 4.27(a-b) were obtained from carbonylation of mono alkyne functionalised methoxy-polyethylene glycol (2.03 mM) at [KI] = 3 mM and a range of palladium iodide concentrations ([PdI_2] = 17 μM, 22.7 μM and 30.2 μM respectively). Oscillations were obtained at PdI_2 = 17 μM and 30.2 μM and were still ongoing at 17 μM when experiments were stopped. Oscillations were replicated at all 3 concentrations of PdI_2 investigated (Figure 4.28), contradicting the absence of oscillations at 22.7 μM in the experiment discussed herein. Other profiles feature in replicates were also similar to the results presented here, and small amplitudes oscillations were obtained in the original runs and in all replicate experiments. Amplitude of oscillations recorded at 22.7 μM and 30.2 μM, including the replicate samples, were also much smaller than amplitudes at 17 μM. The pH rise shown by the double arrow in Figure 4.27a at [PdI_2] = 22.7 μM is assumed to be intrinsic to the system since no perturbation such as additional methanol or KI was applied over the course of the reactions in this study (Table 4.5). This rise in pH and corresponding decline in [H^+] may be attributed to a phenomenon termed "bi-stability", where transitions between stable steady states in the reaction is observed as a "jump" in pH [26, 92, 94-96, 102, 195, 296]. The presence of a similar pH shift at about the same reaction time in the replicate run (Figure 4.28) at the

same concentration ([PdI_2] = 22.7 μM) seems to support the assumption that the shift in pH is intrinsic to the reaction. Nonetheless, in Chapter 3, Section 3.4, pH electrode poisoning which could present as an offset in pH values was mentioned as a potential limitation of observed trends. As only pH change was monitored during the reaction, bi-stability is only offered as hypothesis and will require additional characterisation to fully claim that this phenomenon has caused the transition. This characterisation requires detailed investigations and is thus recommended for future studies in Chapter 7. As with previous section, the [H^+] adjusted profiles were obtained by applying Eq. 4.1 for pH measurements in methanol [30, 258, 259] when the pH electrodes are calibrated with aqueous buffers.

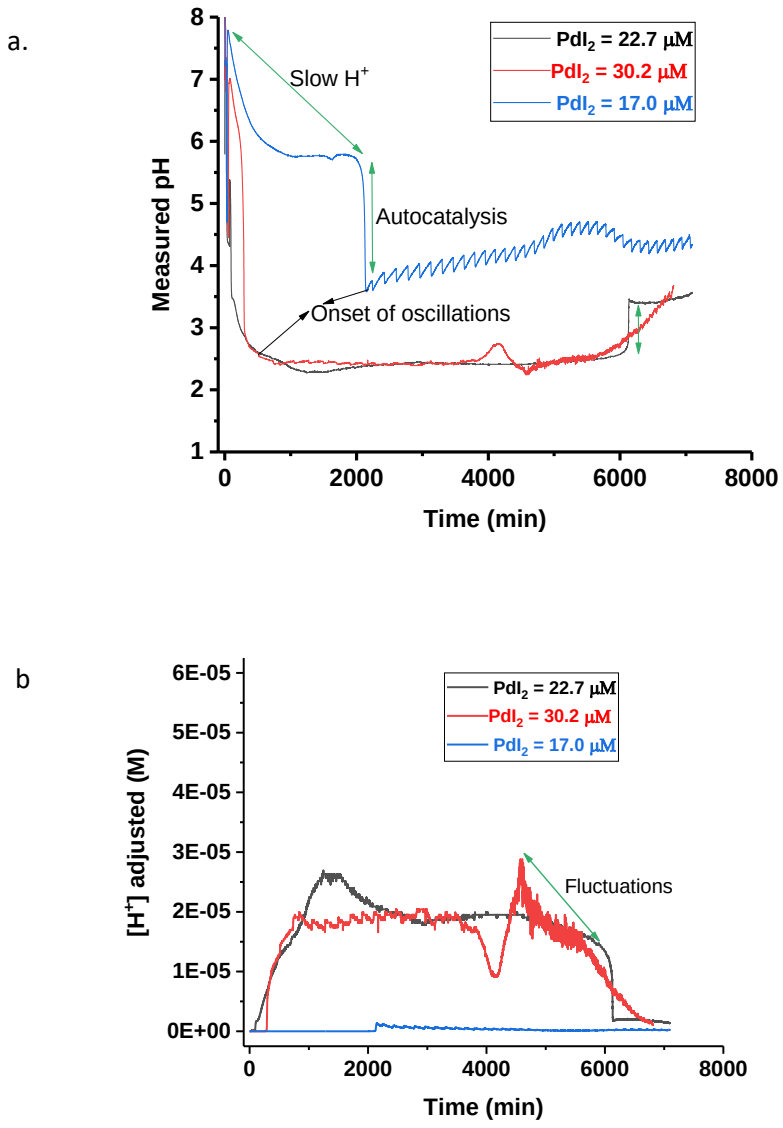

Figure 4.27. Full (a) pH and (b) [H^+] adjusted profiles from the oxidative carbonylation of mono alkyne functionalised substrate at various PdI_2 concentrations. ([A-PEG_{2000}] = 2.03 mM; [KI] = 3 mM; CO/air flowrates = 15 mL/min; total methanol volume = 90 mL; temperature = 20±2 ºC)

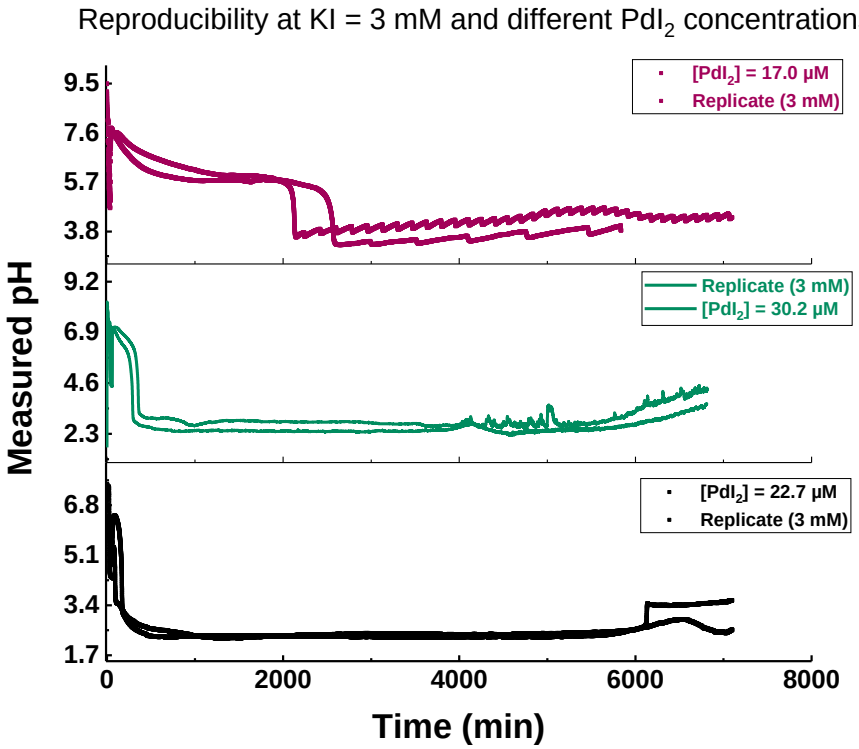

Figure 4.28. Replicate and original pH profiles from the oxidative carbonylation of mono alkyne functionalised substrate at various PdI_2 concentrations. ([A-PEG_{2000}] = 2.03 mM; [KI] = 3 mM; CO/air flowrates = 15 mL/min; total methanol volume = 90 mL; temperature = 20±2 ^oC)

At the onset of the reactions, small variations in pH occurred on addition of solid KI (bringing total concentration in each experiment to 3 mM) and the catalytic mix (PdI_2/KI) to bulk methanol for reaction. This change is ascribed to alterations in ionic strength [260-268] of the methanol and/or junction potential [253, 297-300] (non-aqueous) due to the ions from KI and the catalytic mix. The dilute catalytic mixture was purged with CO and air shortly after leading to decrease in pH and corresponding rise in $[H^+]$ adjusted. These initial features of the reactions follow the same pattern as reactions reported in Sections 4.2 and 4.3, and oscillatory carbonylation reactions with MeOH/KI/PdI_2 catalytic system are known to follow such pathways [29, 30, 174, 175].

The drop in pH on purging is consistent with prior studies in oxidative carbonylation of phenyl acetylene [8-10, 30, 32, 173-175] and the original study with mono-alkyne methoxy-polyethylene glycol [29]. Substrate was added to the reactions after purging till the pH started to equilibrate. Substrate addition was followed by increase in pH recorded. The increase in pH is proposed to arise from the methanol introduced with the substrate solution. [10, 32, 173-177] and this may have repressed measured H^+ concentration via dilution or other reactions which are currently unknown. Methanol was linked to the rise in pH under different conditions

with the phenyl acetylene oscillatory system [9, 10, 32, 173-177, 242, 243], which is consistent with rise observed.

A concept for pH rises from substrate interactions is not known yet, so contributions from A-PEG_{2000} cannot be ruled out. One theory could be the presence of hydrogen ion consuming/binding steps that precede the conversion of the alkyne functionality on the substrate. Such speculation would present as a decrease in free H^+ available and thus the rise in pH. pH rises following substrate addition at $[PdI_2]$ = 17 μM > 30.2 μM > 22.7 μM and the same pattern was seen in replicate samples (Figure 4.28). The differences in pH rise when equal volumes of constant concentrations of substrate were added may be attributed to different $[PdI_2]$ in each reaction since similar values were obtained with replicate samples. It is also possible that small differences in pH probes values at beginning of the reaction (0.1±0.04 pH units) and/or the resultant rates from reactions in Eq. 4.2 to 4.5 influenced the difference.

A period of gradual H^+ increase ("slow H^+ formation"), represented in Figure 4.27a, commenced after the rise in pH. The slow H^+ formation is proposed to occur according to Eq. 4.2 to 4.6 where HI formation is the bases of H^+ observed experimentally. Eq. 4.2, 4.3 and 4.5 account for HI formation from water [3, 38, 103, 198, 275] while Eq. 4.4 generates HI from the carbonylation of methanol [29, 30, 269-271]. Eq. 4.6 is assumed to proceed slowly initially in this region of slow H^+, and subsequently, at a faster rate. The end of the gradual H^+ increments was marked by autocatalytic formation of H^+ across runs and is exemplified in Figure 4.27a. The autocatalytic formation of H^+ is assumed to proceed according to Eq. 4.6, and is in agreement with autocatalytic pH drop following substrate conversion, reported for oscillatory carbonylation with phenyl acetylene [6, 10, 30-32, 38, 173, 175]. The autocatalysis is probably initiated once the $[H^+]$ formed during the "slow phase" reaches some internally determined concentration possibly driven by reaction conditions and intermediate specie concentrations. The likely existence of such minimum concentration agrees with the presence of a feedback cycle, which is one of the condition for the occurrence of oscillation [14].

Table 4.6. Duration of "slow H^+ formation" at constant mono alkyne functionalised polyethylene glycol and KI concentrations.

$[PdI_2]$ (μM)	17.0	22.7	30.2
"Period of slow H^+ formation" (min)	2084	15	197

Duration of slow H^+ formation is given in Table 4.6. Duration of slow H^+ varied with concentration of palladium iodide present ($[PdI_2]$ = 17 μM > 30.2 μM > 22.7 μM) and replicate samples (Figure 4.28) followed a similar trend. The long duration of slow H^+ formation at

$[PdI_2]$ = 17 μM suggests a slower rate of reaction in comparison to the other concentrations. It is possible that with reduced concentration of palladium iodide, the rate of formation of H^+ during the "slow H^+ formation" period at 17 μM and according to Eq. 4.6 (proposed to starts of slowly) is reduced and then takes longer to reach H^+ concentration required for autocatalysis. Also, the need for palladium regeneration during the reaction according to Eq. 4.11 and 4.12 increases when less PdI_2 is present in the reaction, which could also explain the relation between PdI_2 and the extended "slow H^+" duration. Autocatalysis was followed by a period of consumption of H^+ produced and then, onset of oscillations. The consumption of H^+ is proposed to proceed according to Eq. 4.8 and 4.9. Onset of oscillation for reactions with $[PdI_2]$ = 17 μM and 30.2 μM is shown in Figure 4.27a. Oscillations commenced earlier at higher palladium iodide concentration and more $[H^+]$ was present in the reaction when oscillation commenced. The higher $[H^+]$ is attributed to increased concentration of HI following first autocatalysis and is believed to occur due to higher $[PdI_2]$.

Time at onset of oscillations is given in Table 4.7. The delay in generating enough H^+ to trigger autocatalysis at $[PdI_2]$ = 17 μM is reflected in the longer duration it takes for oscillations to commence at this concentration. In experiment presented here, no oscillation was recorded at $[PdI_2]$ = 22.7μM, however, oscillations were present in a replicate run. In the replicate sample with oscillations, pH value following autocatalysis was lower (3.15 pH unit vs 3.39 pH units). The increased concentration of $[H^+]$ following autocatalysis is suggested to have moved the reaction conditions to a region where oscillations are possible.

Table 4.7. Time at onset of oscillations at constant KI concentration and changing PdI_2 concentrations

$[PdI_2]$ (μM)	17.0	22.7	30.2
Time at onset of oscillations (min)	2123	n/a	512

Experimentally observed oscillations and changes in profile patterns are given in Figure 4.27(a-b). In addition to the "jump" in pH mentioned earlier for $[PdI_2]$ = 22.7μM, nonperiodic/aperiodic changes in pH values were observed at $[PdI_2]$ = 30.2 μM. This irregular fluctuations are somewhat similar to what may be termed as a chaotic system or "chaos" in other oscillating chemical systems [12, 14, 97, 109, 119, 195, 301]. The double arrow in Figure 4.27b defines the main region of the reaction where this feature was observed. The onset of the aperiodic complex pH changes at $[PdI_2]$ = 30.2 μM was marked by a period of irregular oscillations, followed by rapid formation and consumption of $[H^+]$ 4000 min (Figure 4.27b) into the reaction and then, continuous aperiodic changes with downward pH trend. The

complex nonperiodic trend gradually thinned out and was not significantly present at the point the reaction was stopped.

4.4.2 Reaction Profiles at 6 mM Potassium Iodide Concentration and Constant Mono Alkyne Substrate Concentration

The reaction profiles in Figure 4.29(a-b) were obtained from studies where initial KI for the reaction was increased to 6 mM. Oscillations with varying degrees of complexity were recorded across palladium iodide concentrations investigated. Oscillations were also recorded in replicate samples as shown in Figure 4.30 and Figure 4.31 though some differences in degree of complexity was noted. Oscillations at [KI] = 6 mM displayed larger amplitudes and period in comparison to [KI] = 3 mM profiles in Section 4.4.1, supporting the prior assumption that KI promotes oscillations. The complexity of oscillations at [PdI_2] = 22.7 μM in Figure 4.29a, is comparable with complex oscillations obtained in the study where total KI was introduced at onset of reaction (Section 4.3.1, Figure 4.20). This complex oscillatory phenomena were small amplitude oscillations alternate with large amplitude oscillations are termed mixed mode oscillations and are suggested to arise from alternating reactions of intermediate species [109-115] occurring via different pathways in the same system. The oscillations at [PdI_2] = 30.2 μM also seems like a variants of complex oscillations known as “Canard oscillations” [113, 302-304]. These phenomena and potential routes that drive them are discussed in greater details in Chapter 6.

The initial stages of the reaction proceed the same way as discussed in previous sections. The addition of KI and catalytic mixture to methanol produced a dip in pH, which increased with increasing concentration of catalytic mixture, possibly because more palladium ions become available at higher concentrations. This is proposed to affect ionic strength [260, 268, 305] of the methanol solution, which is a measure of total ion concentration in solution. Ions with greater charge (Pd in this instance) is speculated to exert more influence due to increased electrostatic charge. The presence of excess KI may have also contributed to the ionic strength and changes in the junction potential of the pH electrode used for measurements [267]. pH stabilisation followed catalytic mixture addition before the reactions were then purged with CO and air. pH declined on purging, indicating onset of proton donating reactions. Eq. 4.2 to 4.5 are offered as reactions occurring at this point. The pH decline on purging was similar at the three concentrations of palladium iodide investigated with an average difference of 0.053 pH units. Due to the similarity in pH drop on purging, the overall rate of reactions (Eq. 4.2 to 4.5) are assumed to be alike in all 3 runs in this instance.

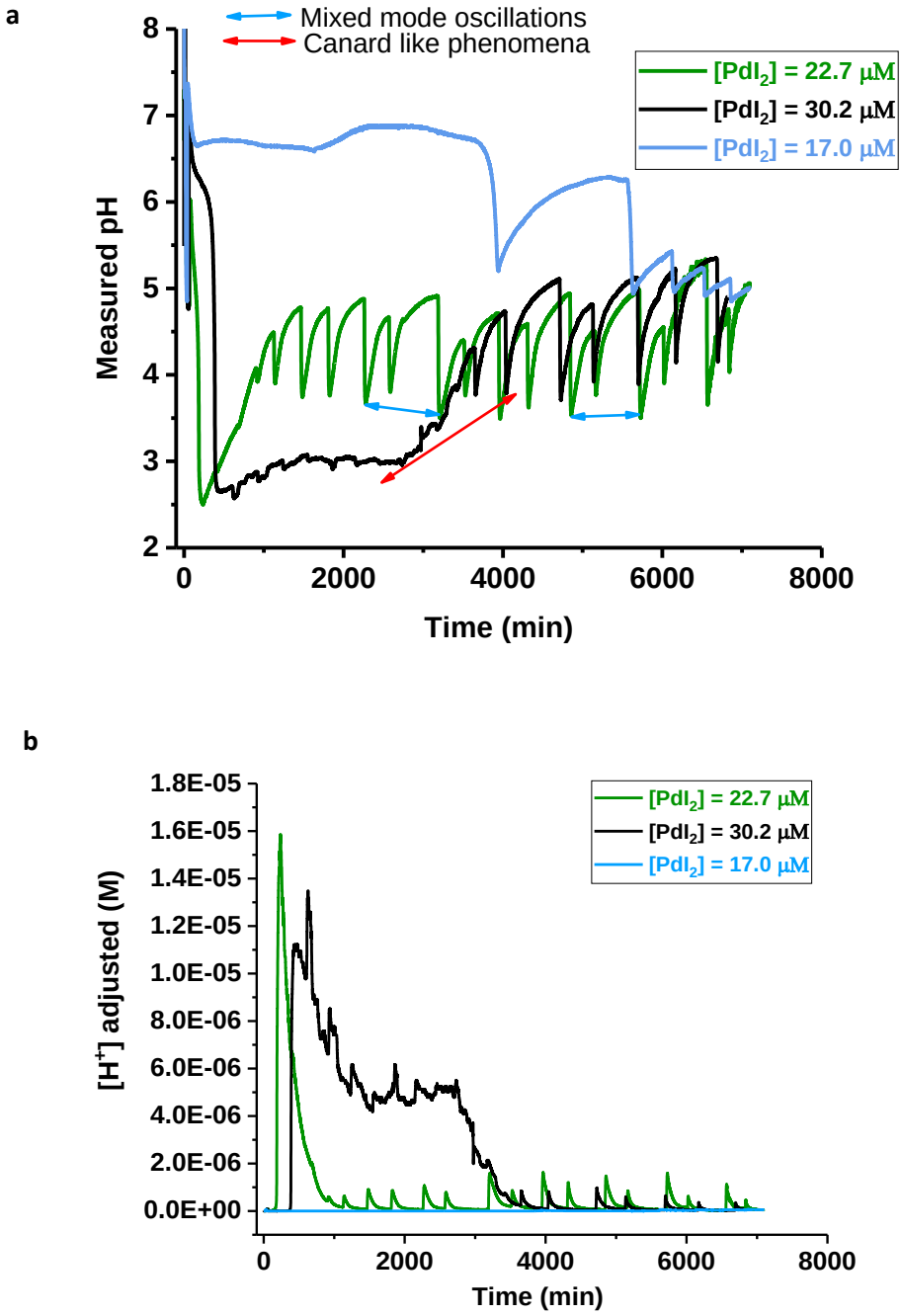

Figure 4.29. Reaction profiles from the carbonylation reactions of constant concentrations of mono alkyne functionalised substrate at various PdI_2 concentrations. ((a) pH profiles; (b) $[H^+]$ adjusted profiles; [A-PEG_{2000}] = 2.03 mM; [KI] = 6 mM; CO/air flowrates = 15 mL/min; total methanol volume = 90 mL; temperature = 20^oC±2)

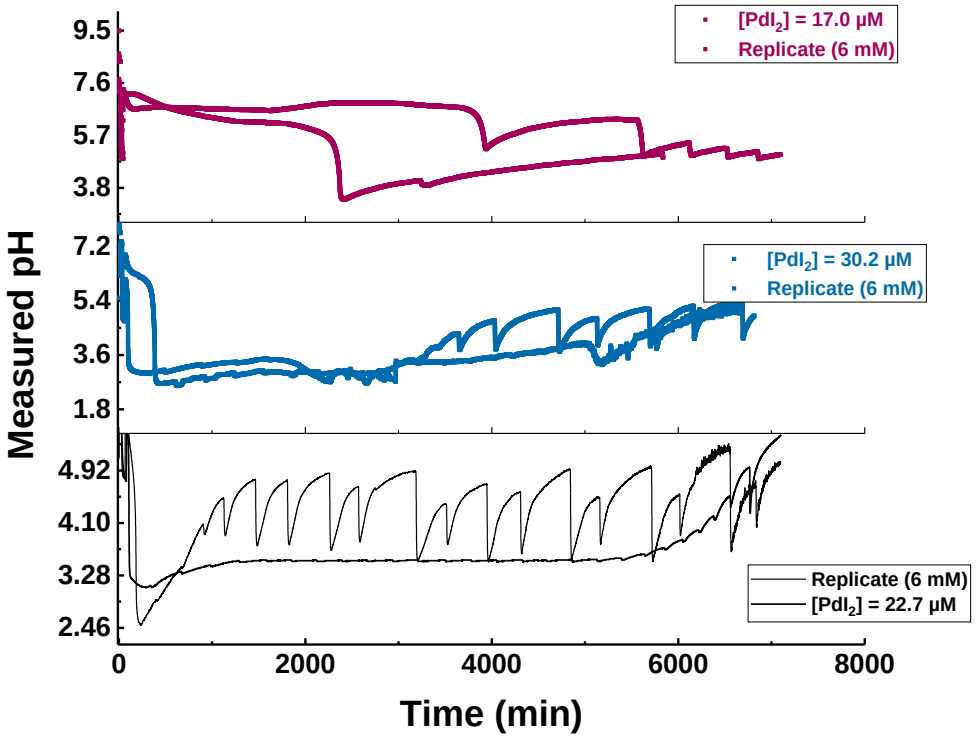

Figure 4.30. Replicate and original pH profiles from the oxidative carbonylation of mono alkyne functionalised substrate at various PdI_2 concentrations and [KI] = 6 mM

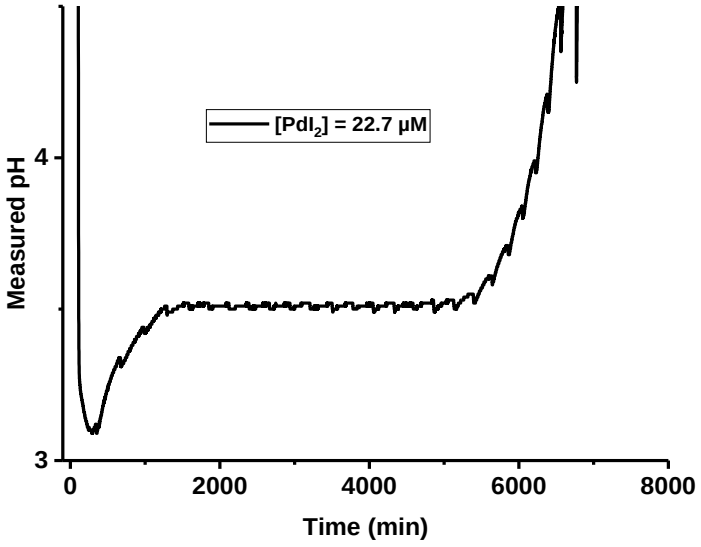

Figure 4.31. Excerpt of replicate pH profile showing oscillations present in the oxidative carbonylation of mono alkyne functionalised substrate at [PdI_2] = 22.7 µM and [KI] = 6 mM

pH rise from substrate addition was maximum at [PdI_2] = 17 µM, then 30.2 µM and lowest at 22.7 µM. This trend is similar to that observed with [KI] = 3 mM. It is not clear why this trend is consistent at both KI concentrations ([KI] = 3 mM and 6 mM), however, one common factor in both cases at [PdI_2] = 22.7 µM is the extended purging duration, thus, this is offered as a

possible reason. The rise in pH from substrate addition was followed by a period where H^+ was gradually formed. The duration of "slow H^+ formation" was 3724 min, 110 min and 295 min at [PdI_2] = 17 μM, 22.7 μM and 30.2 μM respectively. The duration of "slow H^+ formation" recorded at [KI] = 6 mM was more than the time recorded at [KI] = 3 mM, suggestive of potential influence of KI at this stage of the reaction. This is also consistent with increased durations in reaction with more KI in Section 4.3.1 when different amounts of total KI were added at onset of reaction. The duration of slow H^+ was followed by the autocatalytic formation of H^+ due to substrate consumption. Concentration of H^+ following autocatalysis was lowest at the least palladium iodide concentration (17 μM) and pH recorded (5.2) was higher (less acidic) than pH (3.59) for [KI] = 3 mM.

The reduction in autocatalytic [H^+] and longer time spent in "slow H^+" phase suggests that less H^+ accumulated at [KI] = 6 mM, which may be explained by the reduced palladium iodide concentration. It is also possible that increased KI concentration (from 3 mM to 6 mM) has some effect on the reaction, as only KI was altered in both studies. pH decrease from autocatalysis was followed by rise in pH / corresponding decrease in [H^+]. Initial oscillations at [PdI_2] = 22.7 μM and 30.2 μM had small amplitudes, which transitioned to larger amplitude oscillations. At [PdI_2] = 17 μM, the reverse was the case, as large amplitude oscillations were prior to small amplitude oscillations. The contrast in transitions between small and large amplitude oscillations is ascribed to the different concentrations of palladium iodide employed, as PdI_2 is a part of the feedback mechanism for the oscillatory cycles. An excerpt of oscillations captured in the carbonylation of mono alkyne functionalised substrate at [KI] = 6 mM is given in Figure 4.32. On amplifying the large amplitude oscillations, the estimated concentration of [H^+] becomes obvious in the adjusted profile, and the reduced concentration of [H^+] at [PdI_2] = 17 μM (10^{-7} to 10^{-8} range) is clear. Oscillations were still ongoing when the experiments were terminated, as such actual number of oscillations possible at these concentrations were not determined.

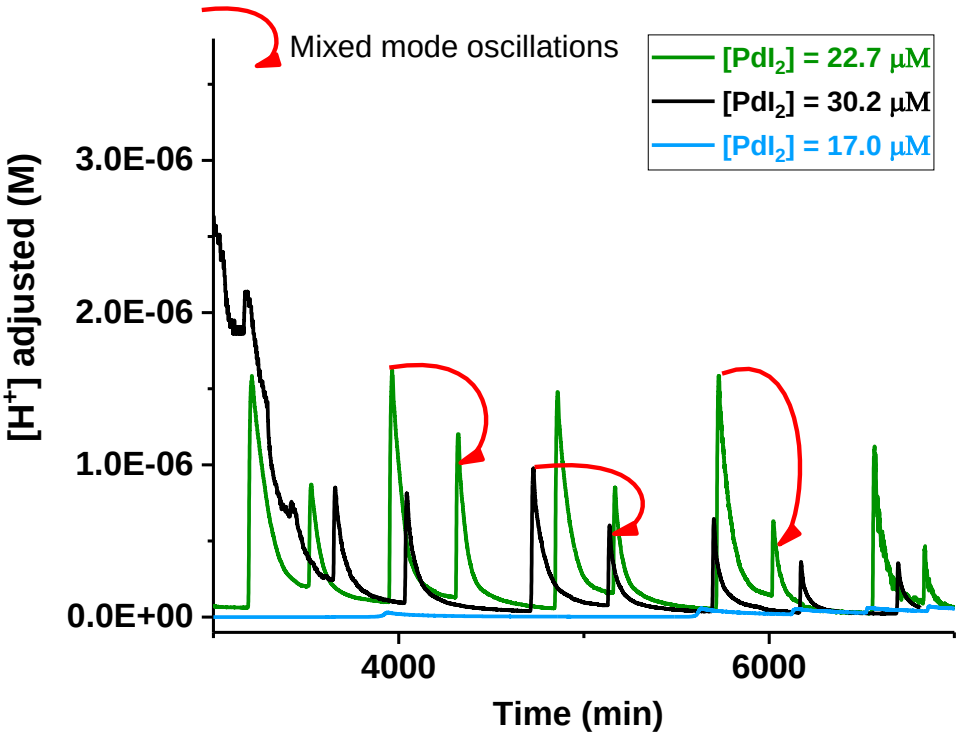

Figure 4.32. Oscillations and oscillatory features recorded at constant substrate and KI concentrations and varying PdI_2 concentrations. [A-PEG_{2000}] = 2.03 mM; [KI] = 6 mM; CO/air flowrates = 15 mL/min; total methanol volume = 90 mL; temperature = 20°C±2; 1. Mixed mode oscillations)

4.4.3 Reaction Profiles at 9 mM Potassium Iodide Concentration and Constant Mono Alkyne Substrate Concentration

In earlier subsections (Sections 4.4.1 and 4.4.2), increasing the concentration of potassium iodide from 3 mM to 6 mM, appeared to increase the amplitudes and periods of oscillation, and promote the manifestation of mixed mode oscillations. A further increase in potassium iodide concentration to 9 mM for the same range of concentrations of PdI_2 employed earlier, resulted in the pH and [H^+] adjusted reaction profiles in Figure 4.33(a-b). Reproducible oscillations with some variations in degrees of complexity were obtained at all concentrations investigated when [KI] = 9 mM and is given in Figure 4.34. Oscillations were still ongoing when experiment was stopped for all samples including the replicates. A range of complex oscillatory features were recorded for reactions at [KI] = 9 mM as shown in Figure 4.33. Spikes within oscillations, mixed mode oscillations and Canard like oscillations were experimentally captured at [KI] = 9 mM. These reactions, and all other results presenting with such complex phenomena in Section 4.4, were not subject to any external influences or perturbations. Thus,

the features are believed to be intrinsic to each reacting system and were probably determined by intermediate species and reactions occurring during the carbonylation process. Mixed mode oscillations were present in replicate experiments (Figure 4.34) but the spikes in oscillations at [PdI_2] = 17 μM was absent in its replicates. It should be noted that the duration of the experiment for replicate samples at 17 μM and [KI] = 9 mM was shorter (5900 min) than sample presented here for discussion. The possibility of spiked oscillations if the replicate reactions were left for the same duration is, hence, conceivable.

Initial features of the carbonylation reaction was also comparable to all other reactions described in earlier sections. The first drop in pH, which steadied around pH 7.5 (Figure 4.33a) is attributed to the addition of KI and catalytic mix to bulk methanol for the reaction. The drop in pH from catalytic mix and KI was more, in comparison to pH decrease when 6 mM and 3 mM potassium iodide concentrations were employed. The larger drop at [KI] = 9 mM supports the supposition that the increase is related to changes in ionic strength of the solution [176, 260-268]. Purging was initiated following pH stabilization after catalytic mix and KI were added. When the reaction pH equilibrated under continuous purging, dissolved solutions of constant concentration of mono alkyne functionalised substrates (2.03 mM) were added to reactions, leading to a rise in pH. The pH rises on substrate addition decreased with increasing palladium iodide concentration, and the pH rise at [PdI_2] = 17 μM was at least twice as much in comparison with other profiles. The differences in duration of purging, in addition to reduced concentration of palladium iodide is suggested as reason for the large difference in maximum pH reached after substrate addition.

Substrate addition was followed by a period of gradual formation of HI, lasting for 3288 min, 26 min and 16 min at [PdI_2] = 17.0 μM, 22.7 μM and 30.2 μM respectively. The decrease in the duration of "slow H^+" with increasing catalyst concentration was also observed in replicate samples. Like the reactions at [KI] = 3 mM and 6 mM, the longest duration of "slow H^+" was observed at least palladium iodide concentration. The "slow H^+" phase is assumed to proceed according to Eq. 4.2 to 4.5 and Eq. 4.6, which is expected to commence slowly during the "slow H^+" period and in an autocatalytic mode after this phase. Autocatalytic formation of H^+ according to previously postulated Eq. 4.6 [29] followed the period of slow increase in hydrogen ion concentration. The rate of HI formation following autocatalysis increased with increasing palladium iodide concentration for the reactions at [KI] = 9 mM and the trend hold for replicate samples.

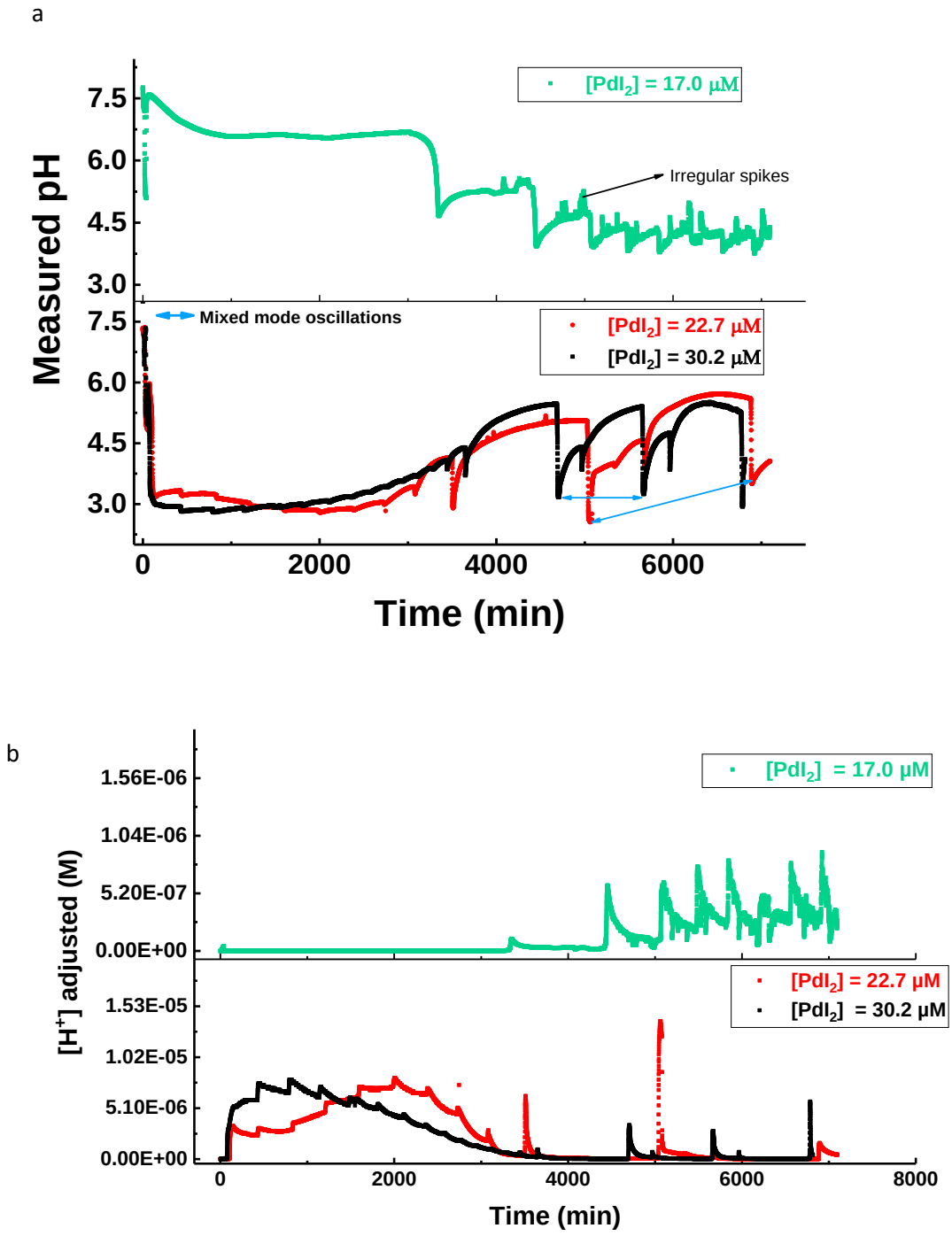

Figure 4.33. Full pH and [H^+] adjusted profiles obtained from reaction at constant mono alkyne functionalised substrate concentration and various PdI_2 concentrations. ((a) pH profiles; (b) [H^+] adjusted profiles; [A-PEG_{2000}] = 2.03 mM; [KI] = 9 mM; CO/air flowrates = 15 mL/min; total methanol volume = 90 mL; temperature = 20^{o}C±2)

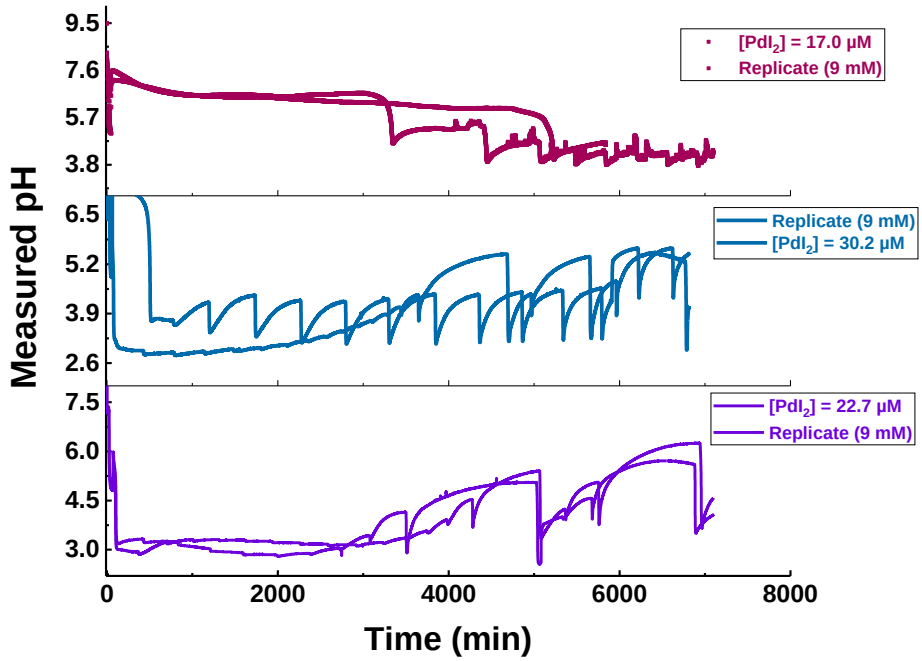

Figure 4.34. Reproducibility across pH profiles showing oscillations present in the oxidative carbonylation of mono alkyne functionalised substrate at different [PdI_2] and [KI] = 9 mM

Oscillations begun after the first autocatalytic formation of HI and pH at onset of oscillations decreased with increasing catalyst concentration. The decrease in pH as a function of catalyst concentration agrees with increased rate of reaction expected at higher palladium iodide concentration. Oscillations begun 3324 min into the reaction at [PdI_2] = 17.0 µM, 422 min at [PdI_2] = 22.7 µM and 425 min at [PdI_2] = 30.2 µM. Additional complexity was noted at [KI] = 9 mM in comparison to reactions profiles at [KI] = 6 mM and 3 mM. A possible justification for this increase in complexity is an increase in intermediate species probably facilitated by the presence of more iodide ions as KI concentration increases. The presence of intermediate reactions have been proposed as a contributing factor in other oscillatory systems with similar complex oscillations [31, 104, 117], hence, the same analogy could be applied in this instance.

4.4.4 Section Summary

Graphical summaries of trends and features of the reaction profiles across palladium iodide and potassium iodide concentrations investigated in Section 4.4 are shown in Figures 4.35 to 4.40. Changes in pH arising from substrate addition as a function of KI and PdI_2 concentration is given in Figure 4.35. The overall reduction in pH differential at [PdI_2] = 22.7 µM is attributed to the extended purging duration. Due to this, a direct comparison across [PdI_2] investigated is

less informative. Comparing [PdI_2] = 30.2 μM and 17.0 μM, a decreasing trend in differential is seen as [KI] increases from 3 to 9 mM. This trend suggests that [KI] interferes with [H^+] availability on substrate addition. This interference seems dominant at lower [KI] than at higher [KI] concentration and accounts for the converging trend noted at 30.2 μM and 17.0 μM. The comparable differences at [PdI_2] = 22.7 μM irrespective of [KI] also offers an insight into ways of controlling pH rise from substrate addition via extended purging before substrate addition.

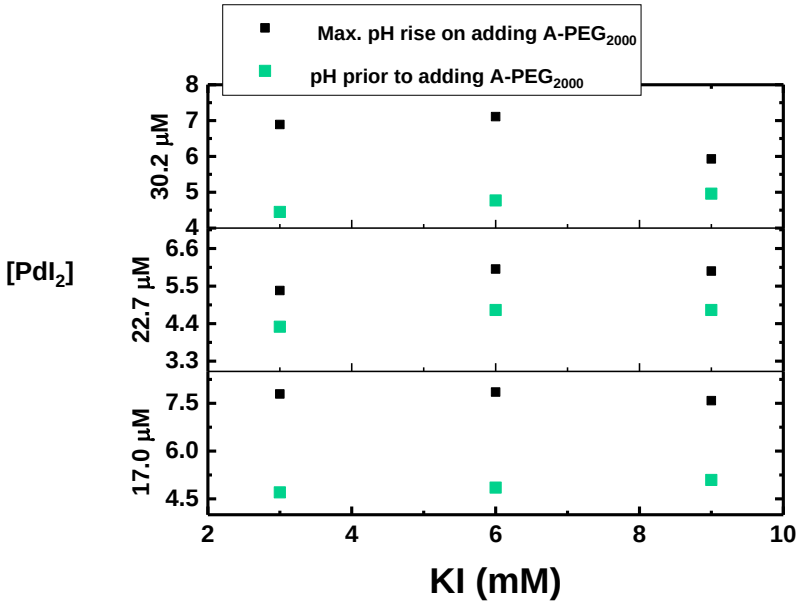

Figure 4.35. Variations in pH before and after mono alkyne substrate addition at various PdI_2 and KI concentrations. ([A-PEG_{2000}] = 2.03 mM; CO/air flowrates = 15 mL/min; total methanol volume = 90 mL; temperature = 20°C±2)

The pH following initial autocatalysis and at onset of oscillation did not show clear trends across [KI] and [PdI_2] concentrations investigated and given in Figure 4.36. Higher pH values were obtained at [PdI_2] = 17.0 μM, supporting reduced catalytic activity. The concave pH trends, with a maximum at [KI] = 6 mM when [PdI_2] = 17.0 μM, differs from the convex pH trends (pH from initial autocatalysis) at [PdI_2] = 22.7 μM and 30.2 μM, though the minima also occurred at [KI] = 6 mM. [KI] = 6 mM appears to be a dynamic point in the reaction with respect to pH drop from first autocatalytic HI formation. The concave / convex nature at different [PdI_2] is attributed to reduced / increased reaction rates as the catalyst concentration varies. pH at onset of oscillations did not significantly differ from pH after first autocatalysis in most instances, suggesting that HI formed from initial autocatalysis drives the reaction towards oscillations.

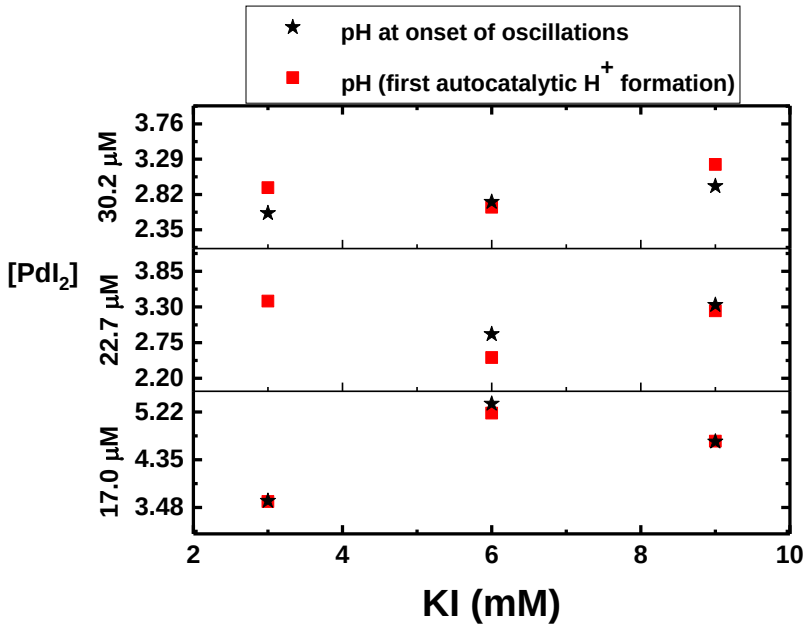

Figure 4.36. Comparison of pH following initial autocatalysis and pH at onset of oscillations at various PdI_2 and KI concentrations. ([A-PEG_{2000}] = 2.03 mM; CO/air flowrates = 15 mL/min; total methanol volume = 90 mL; temperature = 20°C±2)

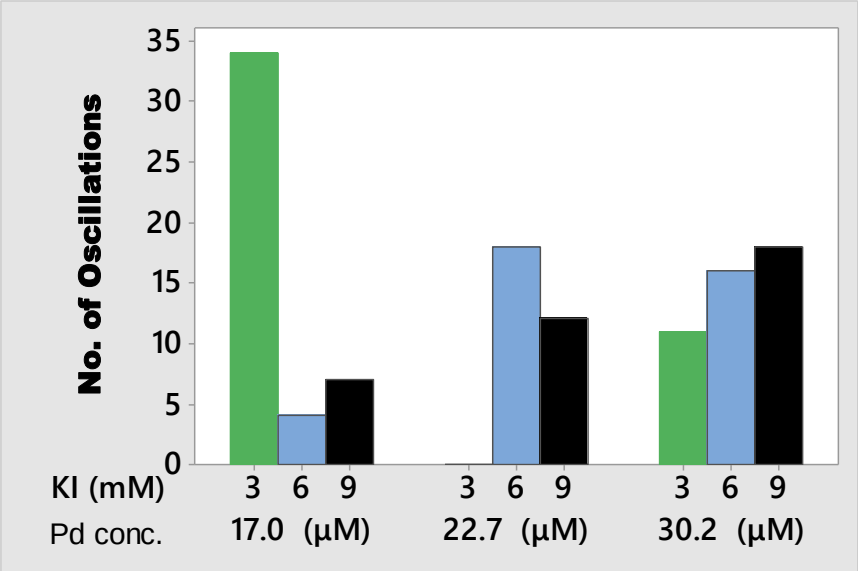

Figure 4.37. Number of oscillations recorded at equal reaction durations and various PdI_2 / KI concentrations. ([A-PEG_{2000}] = 2.03 mM; CO/air flowrates = 15 mL/min; total methanol volume = 90 mL; temperature = 20°C±2)

The number of oscillations recorded as a function of KI/PdI_2 concentration is shown in Figure 4.37. The highest and lowest number of oscillations were observed at lowest PdI_2 concentration. Increasing the catalyst concentration increased the number of oscillations at [KI] = 6 mM and 9 mM while a decrease occurred at [KI] = 3 mM. A comparison of Figure 4.37 and 4.38 for maximum period of oscillation reveals a relation between the period of oscillations

and number of oscillations. Maximum period was higher for reactions with smaller number of oscillations and vice versa. This trend is most obvious at [PdI_2] = 17.0 µM and 22.7 µM (Figure 4.37 and 4.38) and less apparent at 30.2 µM. The considerably higher maximum period at [KI] = 9 mM and smaller maximum periods at [KI] = 3 mM supports the assumption that KI may be used to tune properties of oscillations in the carbonylation reaction.

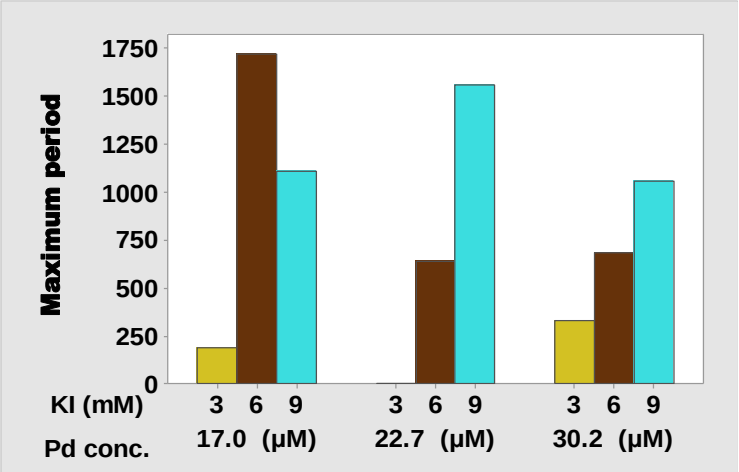

Figure 4.38. Maximum periods of oscillations at various PdI_2 and KI concentrations. ([A-PEG_{2000}] = 2.03 mM; CO/air flowrates = 15 mL/min; total methanol volume = 90 mL; temperature = 20°C±2)

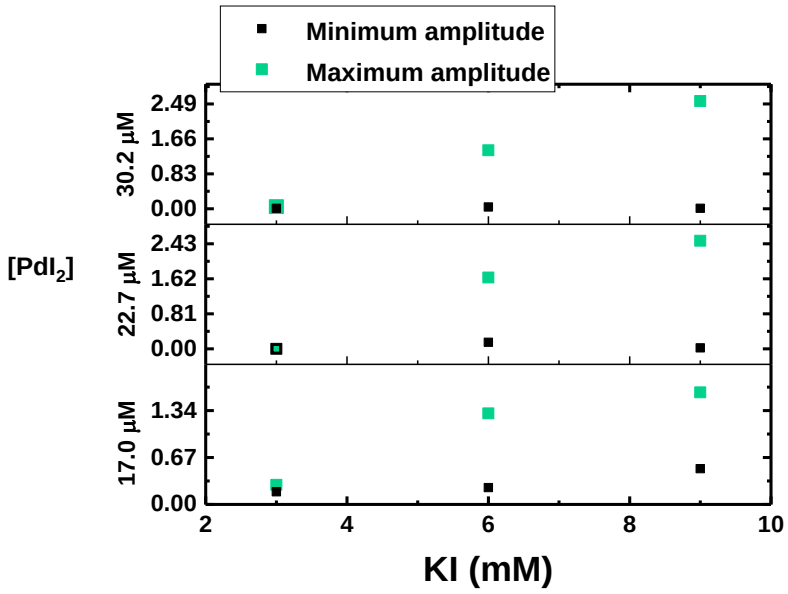

Figure 4.39. Maximum and minimum oscillatory pH amplitudes obtained at various PdI_2 and KI concentrations. ([A-PEG_{2000}] = 2.03 mM; CO/air flowrates = 15 mL/min; total methanol volume = 90 mL; temperature = 20°C±2)

The batch type bifurcation diagram for max/min oscillatory amplitudes at different KI and PdI_2 concentrations is given in Figure 4.39. Divergent (max/min) pH amplitude trends were noted as KI concentration increased from 3 mM to 9 mM. Increasing the concentration of KI and

PdI_2 increased the maximum amplitude achieved in oscillatory mode, with the maximum amplitudes occurring at [KI] = 9 mM and 30.2 μM. A phase representation of different oscillatory and non-oscillatory features recorded at various KI/PdI_2 concentration is given in Figure 4.40. Complex, mixed mode and Canard like oscillations were the most common features at higher KI and PdI_2 concentrations. This suggests the increased KI concentration supports the occurrence of more than one catalytic pathway within an oscillatory system. Regular or simple oscillations were present when either the catalyst concentration was lower (17.0 μM) and KI was moderate (3 or 6 mM) or, the catalyst concentration was high (30.2 μM) and KI was low (3 mM). This supports the assumption above, since a reduction in either KI/PdI_2 encouraged simple/ regular oscillations. Oscillations without irregularities such as "jumps" etc. was achieved when both KI and PdI_2 was increased.

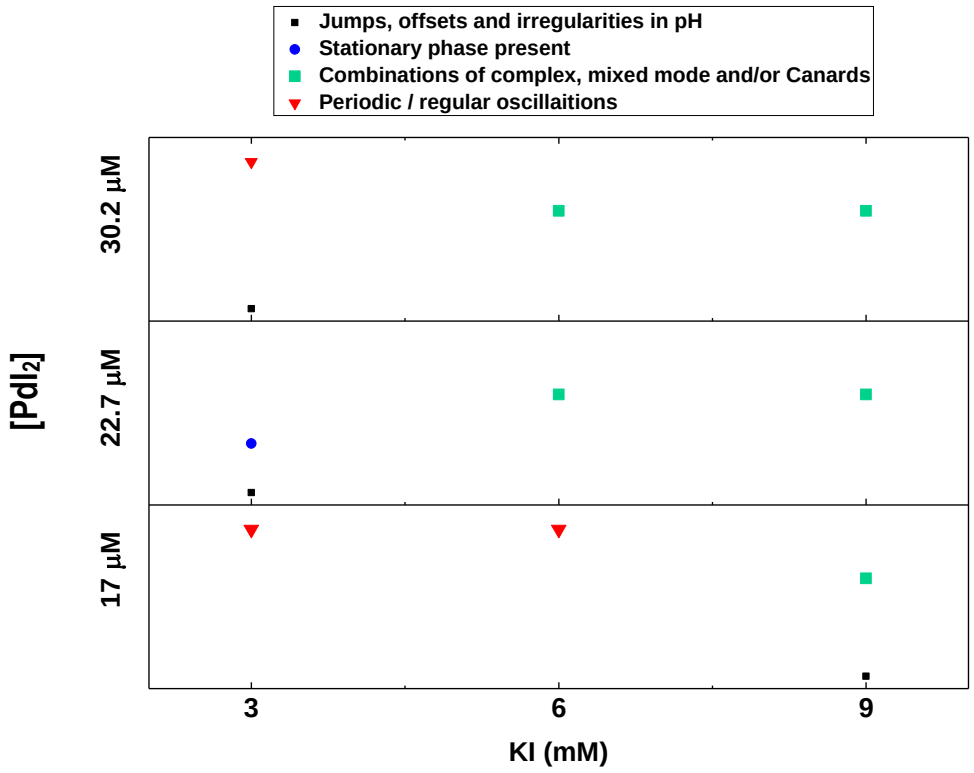

Figure 4.40. Oscillatory and non-oscillatory phenomena observed at various PdI_2 and KI concentrations. ([A-PEG_{2000}] = 2.03 mM; CO/air flowrates = 15 mL/min; total methanol volume = 90 mL; temperature = 20°C±2)

In conclusion,

1. Introducing total KI at the beginning of the reaction and increasing the concentration of KI promotes an increase in oscillation size (period and amplitude). This agrees with findings in Section 4.3.
2. Small amplitude pH oscillations are more likely to occur in regions with higher H^+ concentration; this usually occurs immediately after the initial autocatalytic HI formation. Perhaps PdI_2 is limited at this point (reduced to Pd, catalyst regeneration) and oscillation is dependent on HI formation.
3. Extended purging time decreases rise in pH (increased H^+ concentration) on substrate addition and the rise in pH on substrate addition seems dependent of the concentration of KI present. Conceivably, purging increases HI availability and reduces the shift in equilibrium or impact of substrate addition.
4. Lengthier durations in the region termed "slow H^+ formation" at smaller concentration of palladium iodide was not improved by increasing KI concentration. KI does not seem to reduce this duration, even in absence of extended purging time. The longer "slow H^+" phase also limits number of oscillations possible. Thus, at equal substrate concentration, duration of slow period is affected mainly by catalyst concentrations.
5. Overall $[H^+]$ adjusted concentration decreased with increasing KI concentration. Iodide ions may be suppressing H^+ via an equilibrium state in methanol. KI via excess iodide ions possibly contributes to the reduced reaction rate. Finally, kinetic salt effect may play a contributory role (kinetic salt effect describes the way salts stabilize reactants in this case, H^+ formed) [306-311].
6. pH drops on purging decreases with increasing KI concentration at constant catalyst and substrate concentrations. This may be attributed to increasing degrees of incomplete dissociation of HI as KI increases.

4.5 Influence of Mono Alkyne Substrate Concentration on Duration of Gradual $[H^+]$ Formation and Manifestation of Complex Oscillations

So far, this chapter has focused on elucidating the influence of potassium iodide and palladium iodide which constitute the catalytic mix. Less consideration was placed on substrate concentration which was held constant at 2.03 mM. The diversity of oscillatory and non-oscillatory profiles obtained echo the significance of palladium iodide and potassium iodide in the carbonylation of mono alkyne functionalised methoxy-polyethylene glycol. Changes in substrate concentration is expected to influence reaction dynamics since, the autocatalytic

formation of [H^+] in the feedback cycles, generates the experimentally captured oscillations. Thus, the rest of this chapter explores the effects of changing substrate concentrations.

In Section 4.4, at reduced concentration of palladium iodide (17 μM), the "slow H^+ formation" time was unusually lengthy (thousands of minutes) yet reproducible. This slow phase did not also improve on increasing the concentration of KI. Since the rate of the reaction postulated to occur in the slow H^+ phase (Eq. 4.6 - substrate conversion reaction), is dependent on substrate concentration (Eq. 4.7), the possibility of reducing this "slow" duration by exploring the substrate concentration was considered. The experiments in Table 4.8 were designed to study the influence of halving the original substrate concentration (from 2.03 mM to 1.02 mM) at same PdI_2 and KI concentrations investigated in Section 4.4. Two palladium iodide concentrations were considered; 17 μM and 22.7 μM. The former (17 μM) was selected for the abovementioned reason (lengthy "slow H^+"), while the later (22.7 μM) was chosen to investigate the influence of substrate concentration on development of mixed mode oscillatory phenomena [31, 104, 117]. Mixed mode phenomena are investigated as this oscillatory phenomenon was recorded at different PdI_2 and KI concentrations at constant substrate concentration, making it difficult to assign the phenomena to specific reactant/s. The influence of halving substrate concentration at these PdI_2 concentrations were studied at all concentrations of KI (Table 4.8) employed in Section 4.4.

Table 4.8. Reaction conditions employed in assessing the influence of halving the original substrate concentration at constant palladium iodide concentration and changing KI concentrations. CO/air flowrates = 15 mL/min; total methanol volume = 90 mL; temperature = 20^{o}C±2; agitation = 350 rpm)

[A-PEG_{2000}] (mM)	[PdI_2] (μM)	[KI] (mM)
1.02	17	3.00
1.02	17	6.00
1.02	17	9.00
1.02	22.7	3.00
1.02	22.7	6.00
1.02	22.7	9.00

4.5.1. Profiles at 17 μM Palladium Iodide Concentration and Various KI Concentrations – Effects of Halving Substrate Concentration on the Duration of "Slow H^+" Formation

The reaction profiles in Figure 4.41 (top 3) were obtained from halving the mono alkyne substrate concentration (from 2.03 mM to 1.02 mM) for the carbonylation reaction at constant palladium iodide ([PdI_2] = 17 μM) and various KI concentrations. The reaction profiles and replicate samples are given in Figure 4.42. Reproducibility varied, as replicates at [KI] = 3 mM

and 9 mM were more like the results presented here than the replicate at [KI] = 6 mM. A comparison of the profiles before and after reducing the substrate concentration is likewise given in Figure 4.41. A visual assessment of Figure 4.41 (top 3) immediately reveals the absence of the extensive "slow H^+" duration at [PdI_2] = 17 μM and [A-PEG_{2000}] = 1.02 mM. The absence of the longer "slow H^+" phase, hence, ensues from reducing the substrate concentration from 2.03 mM to 1.02 mM. The forms of oscillations and modes of onset of oscillations also changed in comparison to the profiles in Section 4.4 at [PdI_2] = 17 μM. At [A-PEG_{2000}] = 1.02 mM, oscillations commenced as small amplitude oscillations, before transitioning to large oscillations, while at [A-PEG_{2000}] = 2.03 mM (Section 4.4), the reverse was the case.

The overall pH values following pH drop from initial autocatalysis was also lower (more acidic) than when substrate concentration was 2.03 mM. The steady rise in pH prior to oscillations onset, may have occurred at reduced concentration of palladium iodide (17 μM), owing to the need for regeneration of PdI_2 from Pd. As iodine is necessary for Pd regeneration according to Eq. 4.11 and 4.12, the oxidation of HI wherein iodine (Eq. 4.8) is formed (captured as pH rise) is assumed to have occurred to allow for catalyst regeneration. These assumptions are supported by the shortened duration of increasing pH (prior to oscillations) when KI was higher (9 mM), as more iodide which could form iodine, was available. Another noteworthy observation was the mode of transition from small amplitude to large amplitude oscillations at [KI] = 6 mM and 9 mM. The transition appears to have been influenced by the concentration of KI (arrows in Figure 4.41) present. After the first sets of small oscillations lasting till 1227 min and 1046 min at [KI] = 6 mM and 9 mM respectively, the pH in both reactions steadily increased for 2555 min and 1380 min at [KI] = 6 mM and 9 mM respectively, before oscillations with large amplitudes and periods were obtained. This difference in duration required to transition to large oscillations is, thus, partly attributed to different concentrations of KI present.

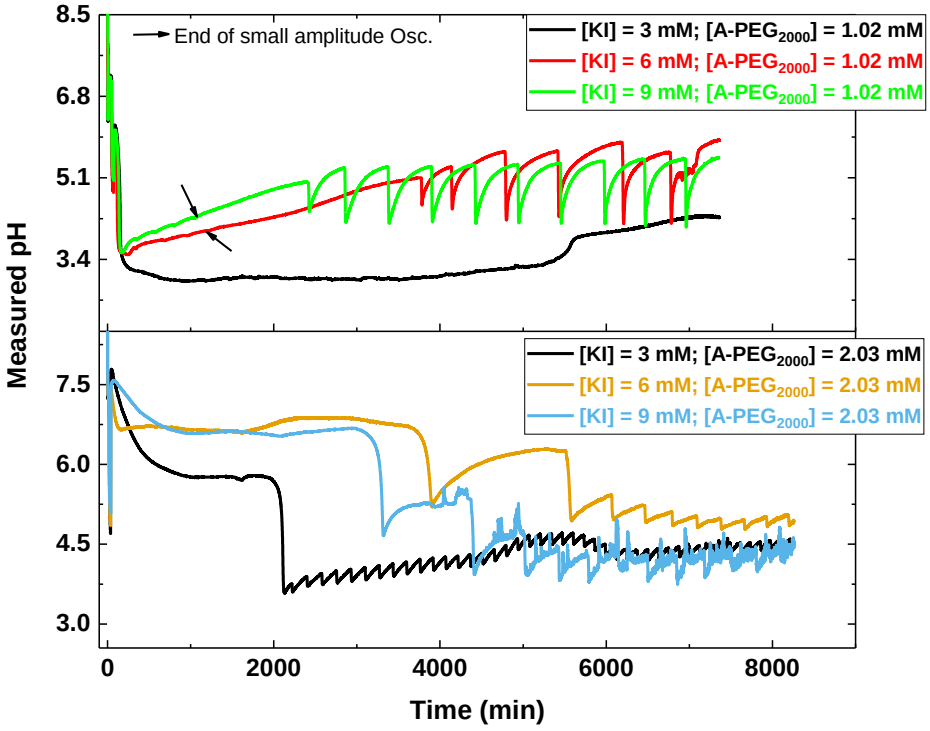

Figure 4.41. pH profiles obtained from the carbonylation of mono alkyne functionalised substrate. Top 3 - profiles on halving the substrate concentration. Bottom 3 - profiles at original substrate concentration in Section 4.4. ($[PdI_2]$ = 17 μM; $[A\text{-}PEG_{2000}]$ = 1.02 mM and 2.03 mM; CO/air flowrates = 15 mL/min; total methanol volume = 90 mL; temperature = 20°C±2; agitation = 350 rpm)

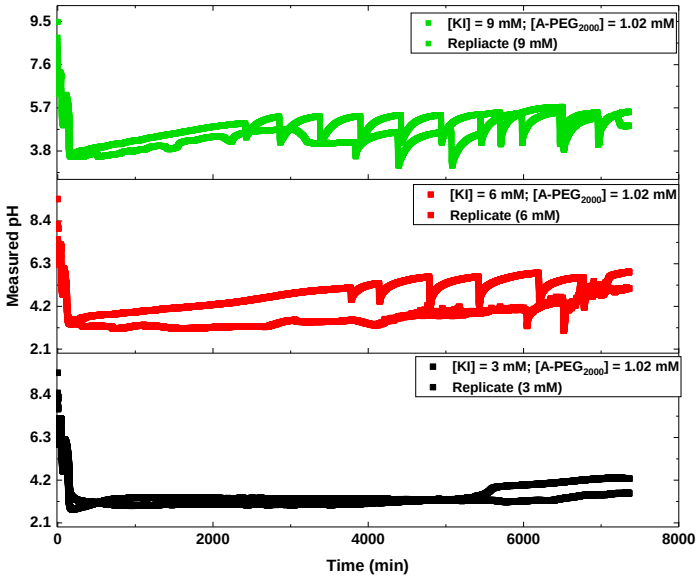

Figure 4.42. Original and replicate pH profiles obtained from the carbonylation of mono alkyne functionalised substrate ($[PdI_2]$ = 17 μM, $[A\text{-}PEG_{2000}]$ = 1.02 mM, temperature = 20°C±2)

Some complex oscillatory phenomena absent at [A-PEG_{2000}] = 2.03 mM, were recorded on halving the substrate concentration (1.02 mM) as shown in Figure 4.41. These complex changes occur before 6000 min and around 7000 min at [K1] = 3 mM and 6 mM respectively (Figure 4.41 – top 3). As the reaction was stopped, it is not possible to positively claim complex oscillations at [KI] = 6 mM, however, a similar mode of transition to complex oscillations was recorded at different conditions, reported elsewhere in this thesis (Chapter 5, Subsection 5.3.3). Complex oscillation was also recorded in replicate experiment at [KI] = 9 mM, supporting the assertion that, complex features are facilitated at reduced substrate concentrations. The only common phenomena observed at both substrate concentrations was occurrence of spikes in oscillations. Spikes in oscillation was recorded in a replicate sample of current study (Table 4.8 at [KI] = 6 mM and Figure 4.42) and in Section 4.4.3 at [A-PEG_{2000}] = 2.03 mM and [KI] = 9 mM.

In terms of kinetics mechanism, the initial steps remain the same. KI and catalytic mix were added producing the first drop which recovered (ionic effects [176, 260-268]). Purging commenced after pH stabilised and pH decreased on purging indicating proton donating reactions which are proposed to arise from reactions involving methanol and water impurities (Eq. 4.2 to 4.5). 1.02 mM of mono alkyne substrate was added to each reaction, causing a rise in pH. Although no trend was observed at maximum rise, the change in pH before and after substrate was added, decreased with increasing KI concentration. The rise in pH from substrate addition was followed by the period of "slow H^+ formation". No directly comparable trends were also observed as KI increased with respect to duration of slow H^+ formation.

Table 4.9. Trends in the carbonylation of mono alkyne functionalised substrate at [A-PEG_{2000}] = 1.02 mM and [PdI_2] = 17 μM. (** - oscillations were still ongoing in runs when experiments were stopped; [a] – after 8 small oscillations, pH changes turned irregular)

[KI] (mM)	3.00	6.00	9.00
pH following the first autocatalytic H^+ formation	3.27	3.59	3.54
Number of oscillations	8[a]	10**	13**

The period of gradual H^+ formation was followed by autocatalytic formation of H^+, experimentally captured as the rapid pH drop. Eventual pH values following the autocatalytic HI formation is given in Table 4.9 and no trend was noted. Oscillations commenced shortly after the autocatalytic formation of H^+ and continued until the reactions were stopped. A decrease in number of oscillations at KI = 3 mM was seen on halving the substrate concentration (2.03 mM to 1.02 mM), while, increased number of oscillations were noted at

[KI] = 6 mM and 9 mM and half the substrate concentration. This trend is representative of results presented in Figure 4.41.

4.5.2 Profiles at 22.7 μM Palladium Iodide Concentration and Various KI Concentrations - Influence of Halving Substrate Concentration on Complex Oscillatory Phenomena

In previous studies at the original substrate concentration (2.03 mM) in Sections 4.3 and 4.4, mixed mode oscillations were captured at various KI and PdI_2 concentrations, as such, it was challenging to credit the oscillatory phenomena to pathways driven by specific reactant/s concentration/s. At [PdI_2] = 22.7 μM, mixed mode oscillations were recorded at KI = 6 mM and 9 mM and [A-PEG_{2000}] = 2.03 mM. On halving the substrate concentration (1.02 mM), the reaction profiles in Figure 4.43 (top 3) were obtained. The absence of mixed mode oscillations in Figure 4.43 (top 3) suggests that substrate concentration significantly contributes to the manifestation of mixed mode oscillations. Other oscillatory phenomena including semblance of spikes in oscillations (around 8000 min in Figure 4.43 (top 3 profiles)) and "jumps" in pH (represented as "a" in Figure 4.43) were captured instead of mixed mode oscillation. Although the jumps in pH and spikes may have arisen partly or wholly from electrode differentials as discussed in Chapter 3, the absence of mixed mode oscillations appears to affirm the influence of substrate concentration on complex oscillatory phenomena. A comparison of profiles obtained on halving substrate concentration and at the original concentration is given in Figure 4.43 (top and bottom profiles respectively). Oscillations were recorded at [KI] = 3 mM and 6 mM and was absent at [KI] = 9 mM. 12 oscillations were recorded at [KI] = 3 mM, while 3 oscillations were recorded at [KI] = 6 mM. In both cases, oscillations were still ongoing when the experiments were stopped. In reactions with oscillations, the size of oscillations increased with increasing KI concentration and the time. pH at onset of oscillation similarly increased with an increase in KI concentration. Initial stages of the carbonylation reaction follows a similar pattern to initial stages of other reactions reported here. pH drops following purging with CO and air decreased with increasing KI concentration, suggesting some interference from iodide ions at higher KI concentrations. pH rises on substrate addition also increased with increasing KI concentration, although the difference in maximum pH rise at 6 mM and 9 mM was only 0.02 pH units. No trends were observed for the duration of "slow H^+ formation" however, change in pH following first autocatalysis increased with increasing KI concentration.

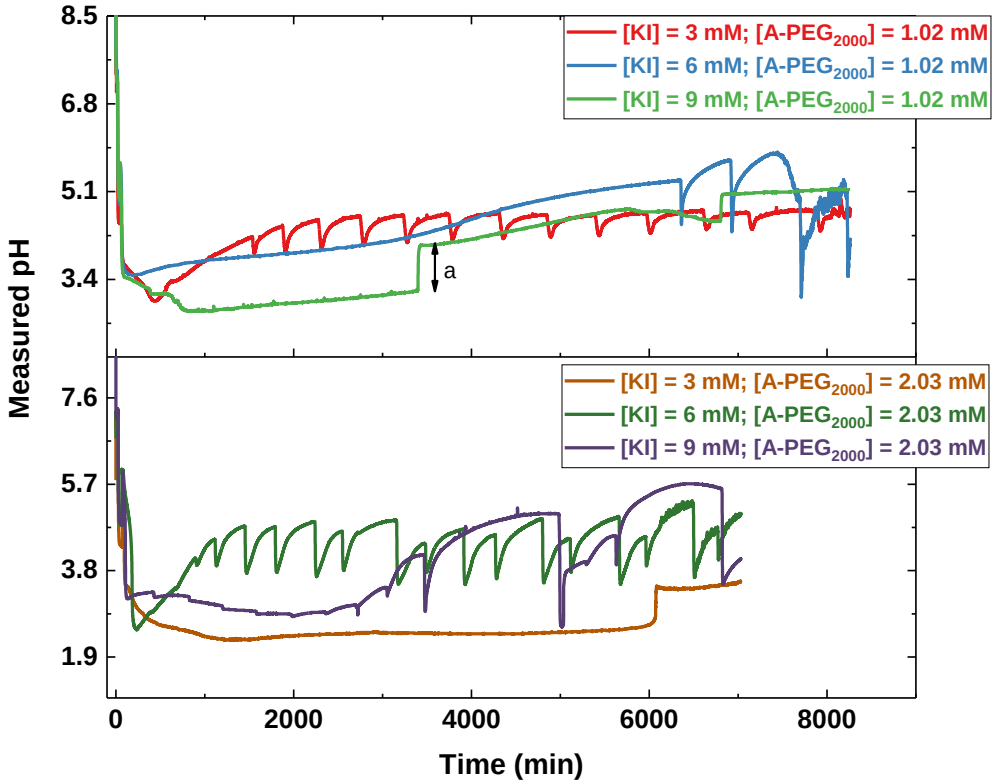

Figure 4.43. pH profiles obtained from the carbonylation of mono alkyne functionalised substrate. (Top 3 - profiles on halving the substrate concentration. Bottom 3 - profiles at 2.03 mM substrate concentration. ([PdI_2] = 22.7 μM; [A-PEG_{2000}] = 1.02 mM; CO/Air flowrates = 15 mL/min; total methanol volume = 90 mL; temperature = 20°C±2; agitation = 350 rpm; a – jump in pH)

4.5.3 Section Summary

Graphical summaries of key features of the carbonylation reaction investigated in this Section is given in Figure 4.44. pH before and after substrate addition was higher (less HI) when less catalyst was present in the reaction (bottom plots of Figure 4.44) and is consistent with general trends in earlier subsections. The duration of slow H^+ formation was also longer when less catalyst was present, although no trend was noted across KI concentrations investigated. The change in pH arising from the initial autocatalysis followed a convergent trend with a cross over at [KI] = 9 mM. Change in pH from autocatalysis pH and time at onset of the reaction increased with increasing KI and palladium iodide concentration.

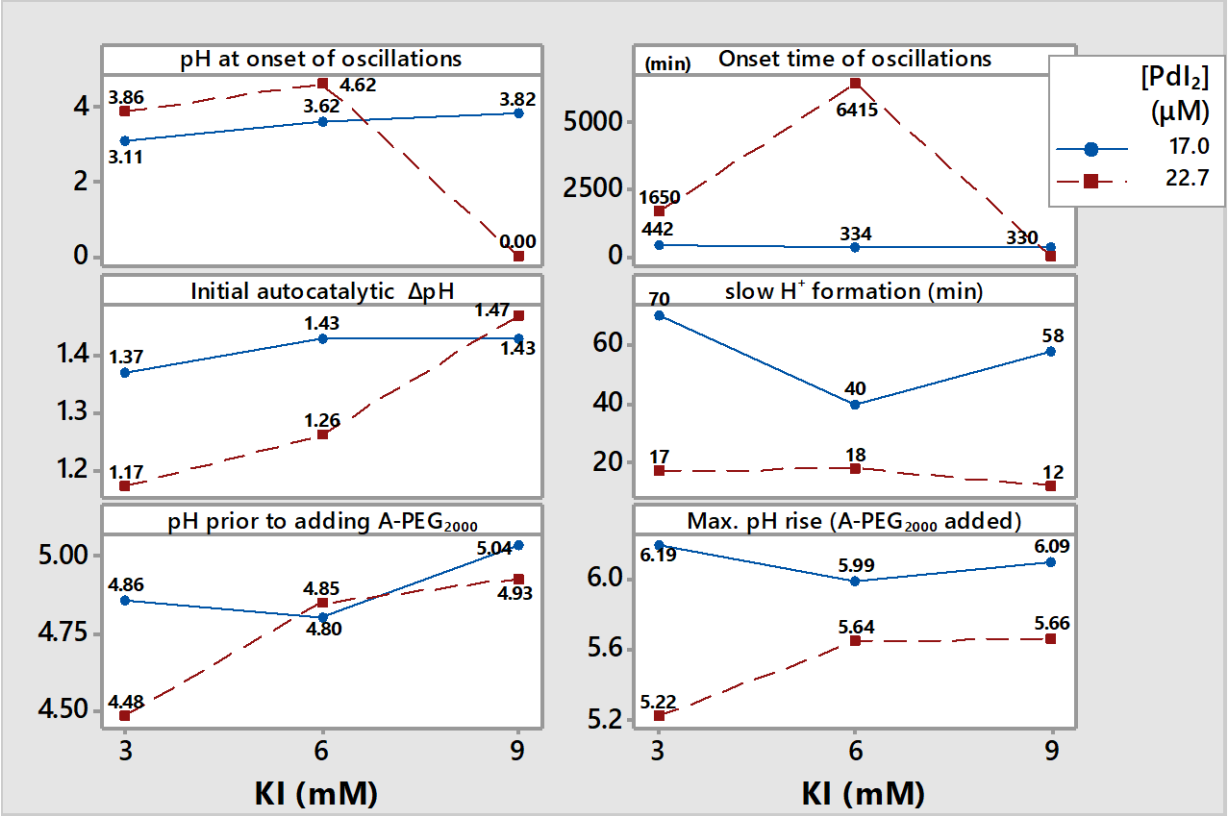

Figure 4.44. Summary of key stages of the carbonylation reaction at reduced substrate concentration

In conclusion,

1. Increased KI concentration appears to decrease pH drop on purging (limits HI formation) and encourages larger oscillations for reactions at $[PdI_2]$ = 17 μM.
2. Halving substrate concentration (2.03 mM to 1.02 mM) at reduced PdI_2 concentration (17 μM) reduces duration of phase termed slow H^+ formation from thousands of minutes (2084 – 3724 min) to tens of minutes (40 – 70 min).
3. Substrate concentration plays a significant role in manifestation of complex oscillatory features as evidenced by results in Section 4.5.2 & 4.5.1.
4. Ratio of palladium iodide to substrate concentration influences rate of reaction. As the ratio increases, the H^+ concentration (HI produced) reduces and vice versa.
5. Iodide from KI may interfere with measured HI concentration.

4.6 Effect of Varying the Concentrations of Mono-Alkyne Functionalised Methoxy-Polyethylene Glycol Substrate at Constant KI/PdI_2 concentration

In Section 4.5, halving the substrate concentration originally investigated by Donlon and Novakovic (2014) (2.03mM) [29] altered the reaction dynamics and appeared to influence a range of oscillatory phenomena. Based on the results obtained from reaction profiles at half substrate concentration, the study in Table 4.10 was designed to assess a range of substrate concentrations at constant PdI_2 and KI concentrations. In previous studies in Sections 4.3 to 4.5, the concentration of KI required for the reaction was augmented by dissolving fresh KI with catalytic mix at the beginning of each reaction. However, in this study (Table 4.10), a concentrated stock catalyst solution of PdI_2/KI in methanol devoid of fresh KI, was used.

Table 4.10. Reaction parameters for the carbonylation reaction at constant catalyst concentration and changing substrate concentration. (CO/Air flowrates = 15 mL/min; total methanol volume = 90 mL; temperature = 20^{o}C±2; agitation = 350 rpm)

[A-PEG_{2000}] (mM)	[PdI_2] (μM)	[KI] (mM)	Substrate to Catalyst Ratio ([A-PEG_{2000}] /[PdI_2])
0.508	29	5.7	17.52
1.02	29	5.7	35.17
1.52	29	5.7	52.41
2.03	29	5.7	70
3.05	29	5.7	105.17
3.55	29	5.7	122.41

The pH and [H^+] adjusted profiles obtained from experimental studies in Table 4.10 are given in Figures 4.45 and 4.46. Oscillations were recorded at all substrate concentrations investigated, and amplitudes and periods varied with substrate concentration employed. Oscillations were obtained in some replicate experiments but, variations in oscillatory patterns of replicate samples were noted. Oscillations were not reproduced at [A-PEG_{2000}] = 0.508 mM and 3.55 mM, instead stationary and "chaotic" profiles were obtained. Figure 4.47 illustrates the degree of reproducibility and typical variations in some replicate samples. The first stages of the replicate samples also varied in terms of duration of slow H^+ formation and pH rise on substrate addition, with the replicate samples showing smaller durations and reduced rise in pH on substrate addition. It is important to mention that these replicate experiments were completed more than a year after the original experiments discussed here (Figure 4.45), were performed. A different batch of catalytic mix (stock catalytic batch included), substrate, solvent and gases were used for the replicate runs. Additionally, the stock catalytic mix (KI/PdI_2/MeOH) used for the original experiment was stored for a longer period of time before

it was used (≥ 4 months), whereas, the stock catalyst for the replicate samples was prepared two weeks to one month before the experiments were conducted.

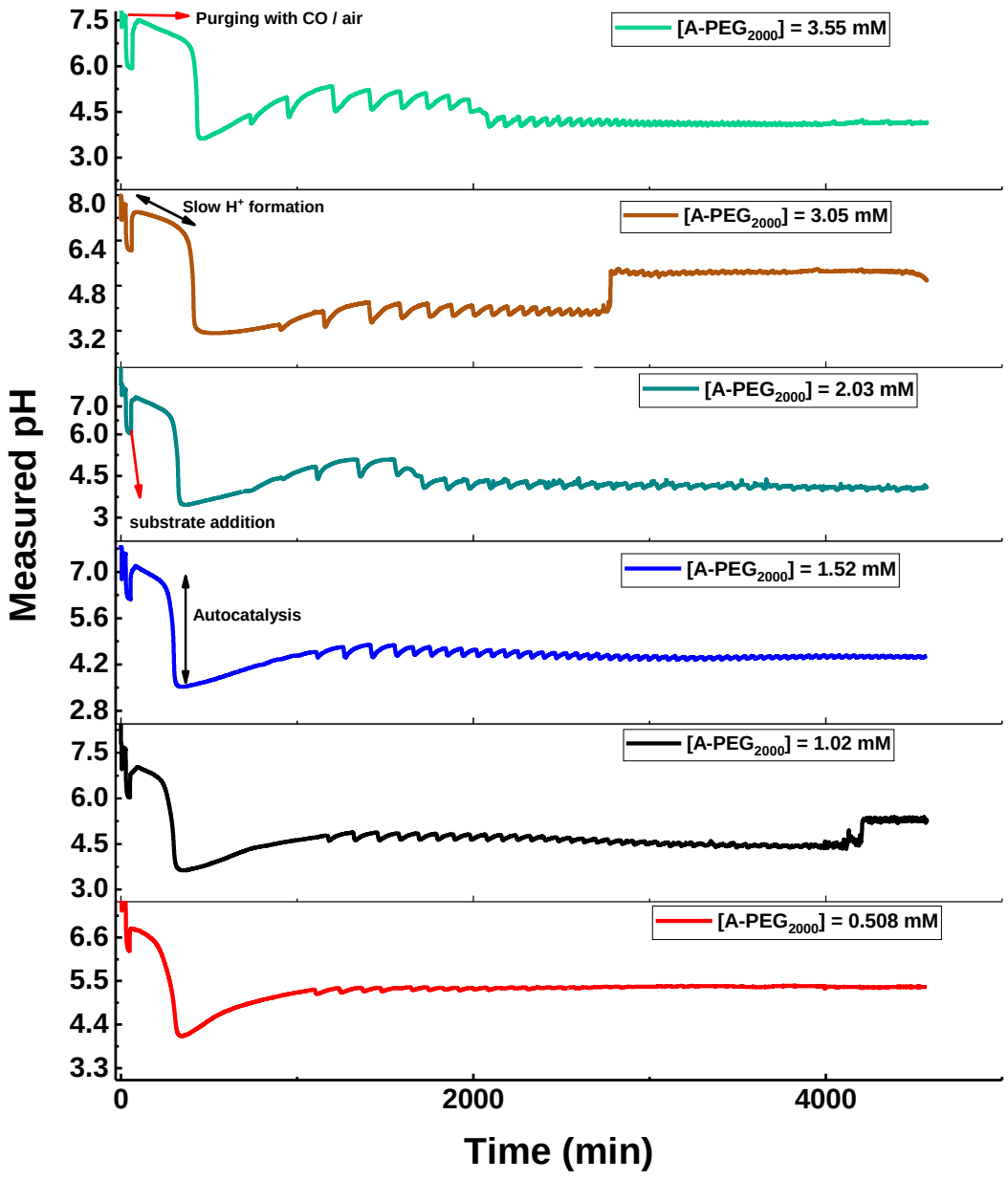

Figure 4.45. Measured pH profiles recorded in the carbonylation of mono alkyne functionalised substrate using pre-made PdI_2/KI catalytic mix. ([PdI_2] = 2.9 μM; [KI] = 5.7 mM; CO/Air flowrates = 15 mL/min; total methanol volume = 90 mL; temperature = 20°C±2 agitation = 350 rpm)

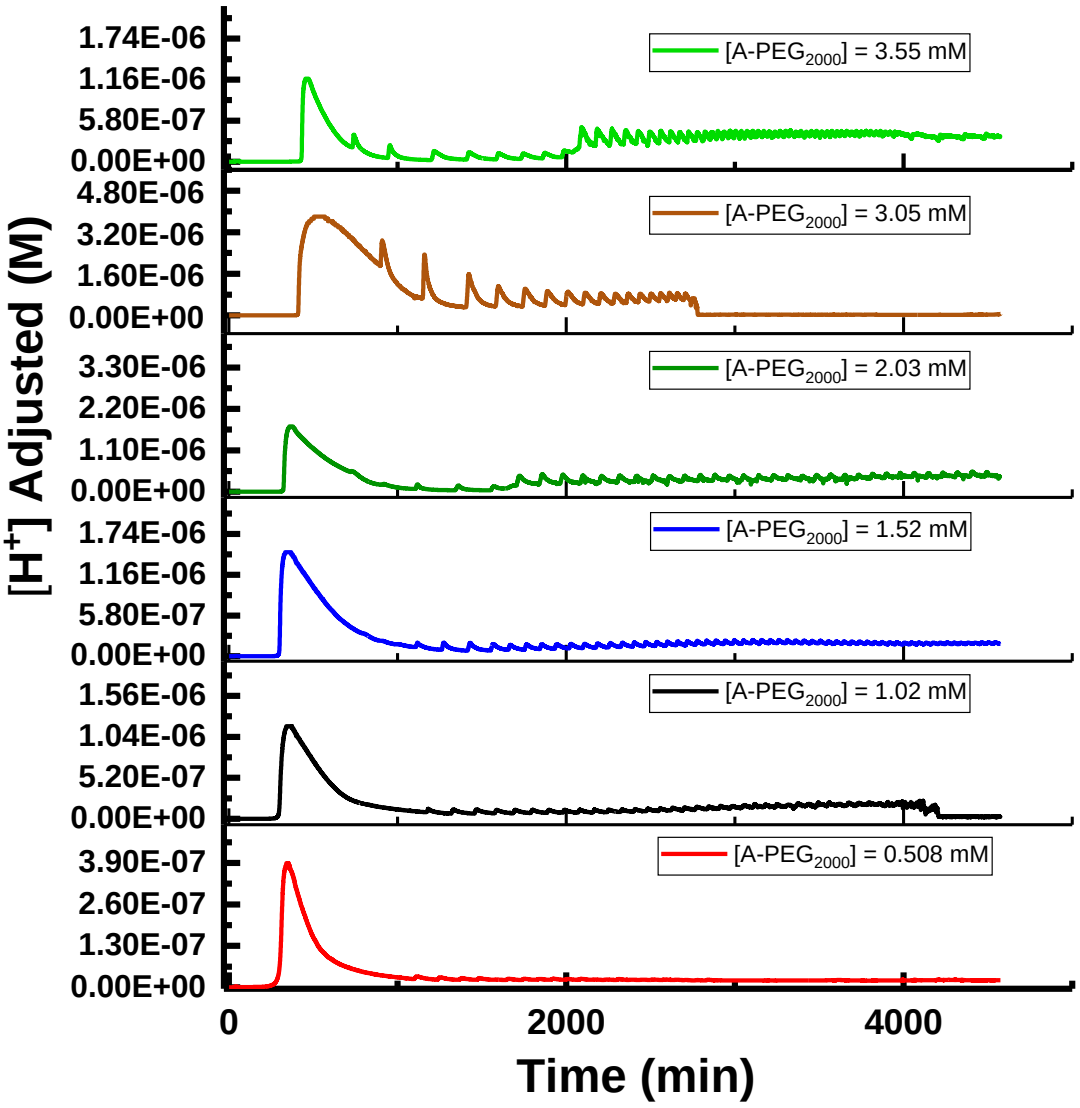

Figure 4.46. $[H^+]$ adjusted profiles obtained from the carbonylation of mono alkyne functionalised PEG substrate using pre-made PdI_2/KI catalytic mix. ($[PdI_2]$ = 2.9 μM; [KI] = 5.7 mM; CO/Air flowrates = 15 mL/min; total methanol volume = 90 mL; temperature = 20°C±2 agitation = 350 rpm)

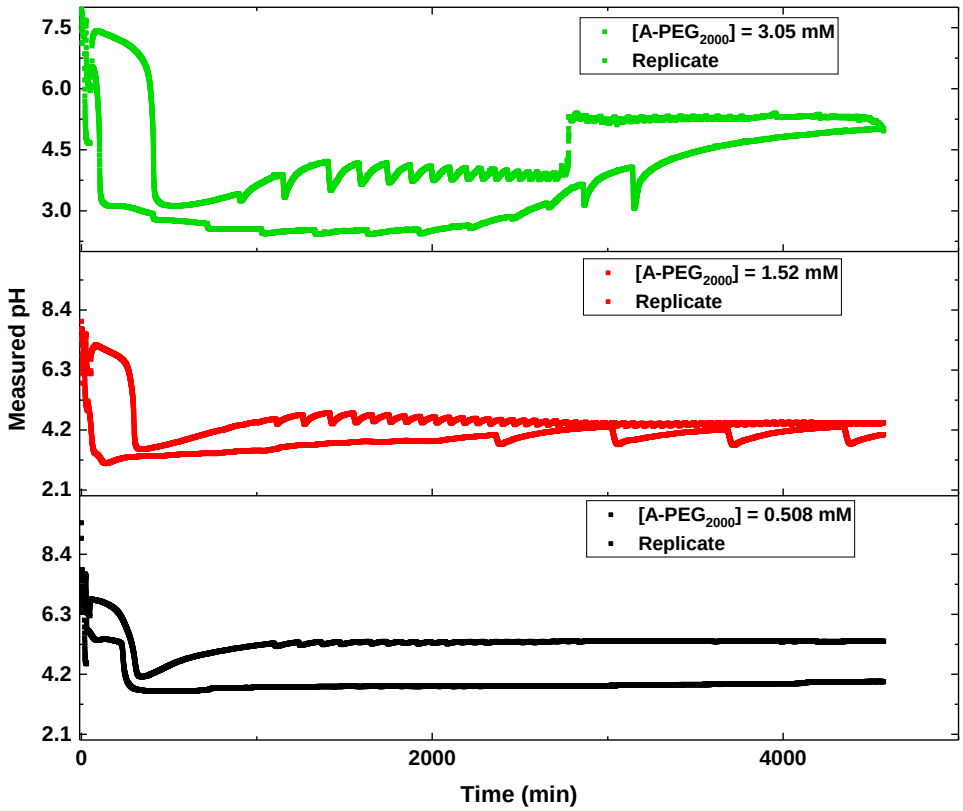

Figure 4.47. Variations in degrees of reproducibility achieved from the carbonylation of different concentrations of mono alkyne functionalised methoxy PEG ([PdI_2] = 2.9 μM; [KI] = 5.7 mM)

The initial stages of the profiles in Figure 4.45 was consistent with stages observed in previous sections of this chapter. Catalytic mixture for the reactions were added to methanol, producing a dip in pH, which is proposed as changes in the ionic strength [176, 260-268] of methanol. The dip in pH varied slightly between samples albeit constant catalytic concentration and is ascribed to slight differences in pH probe following calibration. The pH stabilised for 15 min before purging with CO and air commenced.

On purging, the pH decreased (Figure 4.45), indicating the onset of reactions producing hydrogen ions and agrees with the rise in [H^+] adjusted values in Figure 4.46. Previously proposed Eq. 4.2 to 4.5 for carbonylation of water and methanol and catalytic conversion of water are postulated to account for this pH decrease [8, 11, 29, 30, 32, 38, 103, 198, 269-271, 275]. The water stems from the HPLC grade methanol, which contains some residual water (as impurity) and possibly, the gases for reaction which were not pre-dried. The decrease in pH on purging varied across experiments, though the concentration of the catalytic mixture remained constant in all experiments. The differences in pH following purging are assumed to arise from

the different rates of competing reactions (Eq. 4.2 to 4.5) as this affects the overall [HI] formed, which in turn, influences measured rise in [H^+]. It is also possible that the slight differences in initial values of the pH probe contributed to the variation observed.

The next rise in pH and corresponding decrease in [H^+] adjusted profiles following purging occurred on addition of substrates (Figure 4.45 and 4.46). The substrates were dissolved in small volumes of methanol (3.8 mL) and added to the reactions. The rise in pH on substrate addition is attributed to methanol used for dissolution and the concentration of polymeric substrate present. This rise is partly attributed to methanol based on other instances of increase in pH on addition of more methanol in the oscillatory carbonylation of phenyl acetylene [242, 243]. Perturbation studies with methanol [243], addition of HPLC grade methanol following evaporative losses (higher reaction temperature (40^{o}C), experiments lasting several days) [9, 32], and oscillatory carbonylation in water-methanol solvent mixtures [176] are examples of such occasions. The mechanism of contributions to the observed rise in pH arising from the mono alkyne substrate is uncertain at this point because, functionalised polyethylene glycol is not expected to dissociate on dissolving despite its hydrophilic nature [276-283]. Also, products formed from detached alkyne end groups were not identified via GC-MS in the study with mono-alkyne functionalised polyethylene glycol [29].

The pH values before and after substrate addition is given in Figure 4.48. The rise in pH following substrate addition increased with increasing mono alkyne substrate concentration, supporting substrate interaction with H^+ as mentioned above.

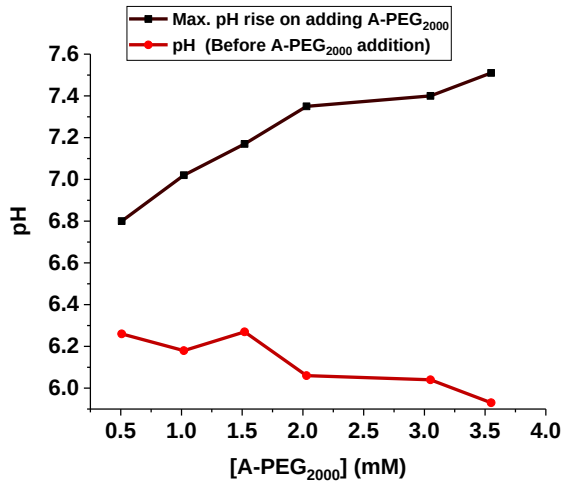

Figure 4.48. Measured pH values before and after the addition of various concentrations of mono alkyne functionalised substrate at constant KI and PdI_2 concentrations. ([PdI_2] = 2.9 μM; [KI] = 5.7 mM; CO/Air flowrates = 15 mL/min; total methanol volume = 90 mL; temperature = 20^{o}C±2; agitation = 350 rpm)

Substrate addition was followed by periods of gradual increase in [H^+], exemplified by the double arrow marked "slow H^+ in Figure 4.45. The gradual increase ("slow H^+ formation") is suggestive of reactions where H^+ is produced. Similar behaviour wherein H^+ forms on substrate addition was reported for large scale (reaction volume = 450 mL) oscillatory carbonylation of phenyl acetylene at 20^{o}C and 40^{o}C [9, 10, 32]. Eq. 4.2 to 4.5 (water / methanol carbonylation reactions and catalytic conversion of water) and Eq. 4.6 are suggested for the gradual decrease in pH corresponding to the rise in [H^+]. Eq. 4.6 is assumed to proceed in an autocatalytic mode; commencing slowly during the period of low H^+ ("slow H^+ formation") and subsequently faster as H^+ concentration increases auto-catalytically.

Durations of slow H^+ formation appear to increase with increasing substrate concentration and is given in Figure 4.49a. The period ranged from 135 min to 340 min and, durations at 1.02 mM and 1.52 mM (168 and 172 min respectively) were quite similar. This increasing trend suggests a slower rate of reaction as the substrate concentration increases, during this phase of the reaction. As the concentration of H^+ gradually increases during the period of "slow H^+ formation" (Figure 4.45), it appears to approach some concentration (presumably determined by reaction constraints at each experimental condition) which prompts the autocatalytic production of H^+, captured as the sudden drop in pH in Figure 4.45. Experimentally recorded trends align with Eq. 4.6 (substrate conversion), postulated to proceed in an autocatalytic mode. The prompt fashion of the transition from slow H^+ production to rapid [H^+] formation agrees with autocatalysis assumption and HI is presumed to be the source of protons [29-32, 295].

The pH values following autocatalytic formation of HI and shown in Figure 4.49b, was inconsistent. The change in pH from autocatalysis increased from 0.508 mM to 3.05mM (Figure 4.49b) and then, decreased at [A-PEG_{2000}] = 3.55 mM. The increasing trend agrees with increased H^+ concentration expected at higher substrate concentration (more alkyne end groups) however, the increase at [A-PEG_{2000}] = 3.55 mM is contradicting. It appears that the reaction at 3.55 mM proceeds differently or some interference occurs at this concentration. However, as replicate experiment at this concentration were quite different (oscillations were absent), this assumption may not hold. The autocatalytic increase in HI concentration was followed by periods of increase in pH with corresponding decrease in [H^+] in all profiles given in Figure 4.45 and 4.46. This is suggestive of reactions where H^+ is consumed. Eq. 4.8 for the oxidation of HI previously reported in oscillatory and non-oscillatory carbonylation of alkyne terminated substrates such as phenyl acetylene [3, 29, 32, 38, 156, 270, 271] and, the

nucleophilic substitution of OH in methanol according to Eq. 4.9 which is proposed to occur in presence of excessive KI [30, 287-289] are offered as reasons for the decrease in $[H^+]$.

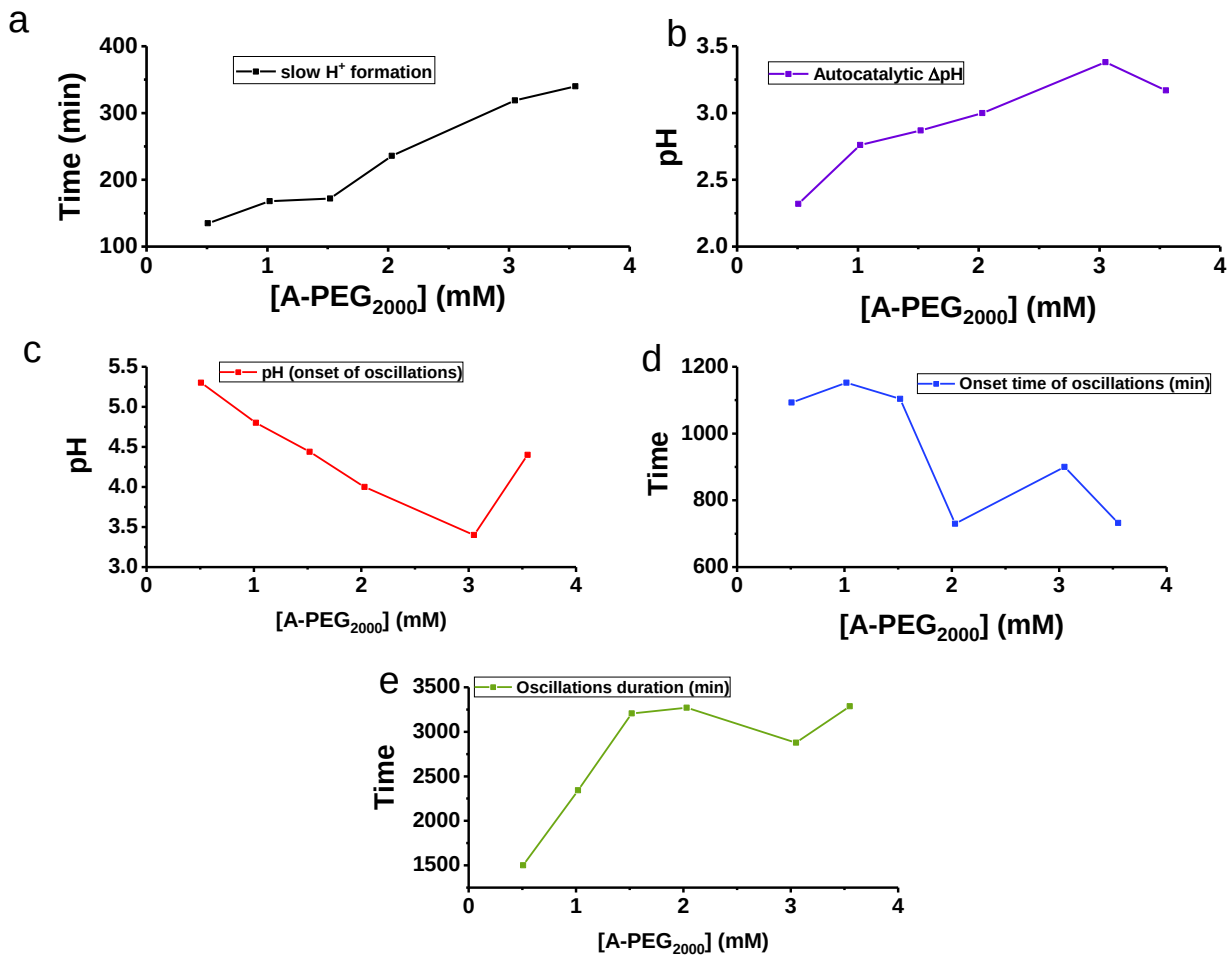

Figure 4.49. Trends obtained at different phases of the carbonylation reactions at various substrate concentrations. ($[PdI_2]$ = 2.9 μM; [KI] = 5.7 mM). CO/Air flowrates = 15 mL/min; total methanol volume = 90 mL; temperature = 20°C±2; agitation = 350 rpm)

Oscillations commenced in all runs after a period of H^+ consumption. The onset of oscillations was marked by rapid drops in pH with corresponding sharp rises in $[H^+]$ and is attributed to autocatalytic formation of HI (Eq. 4.6). pH and time at onset of oscillations are given in Figure 4.49c and 4.49d. The pH at onset of oscillations decreased with increasing substrate concentration excluding the reaction with $[A\text{-}PEG_{2000}]$ = 3.55 mM. At 3.55 mM concentration, the pH increased again, suggesting that less HI was present at onset of oscillations at this concentration despite having the highest substrate concentration. Onset time of oscillations varied across substrate concentrations investigated. It was higher at lower substrate concentrations but varied significantly at higher concentrations. Different forms of a complex oscillatory phenomena were observed at $[A\text{-}PEG_{2000}]$ = 1.02 mM, 2.03 mM, 3.05 mM and 3.55 mM. These complex features are discussed in greater details in Chapter 6.

Max/min pH amplitudes versus substrate concentration; number of oscillations recorded at various substrate concentrations; and separate graphical summaries of maximum and minimum amplitudes and periods are given in Figure 4.50 and Figure 4.51(a-e). The max/min pH amplitudes attained during oscillations versus substrate concentration in Figure 4.50 displays increasing divergence as substrate concentration increases. This divergence is typical of bifurcation diagrams [126, 312] and is consistent with other batch type bifurcation diagrams in previous sections of this chapter. Individual trends for max/min amplitudes and periods (Figure 4.51(a-d)) varied with increasing substrate concentration. The maximum amplitudes (Figure 4.51(a-b)) increased with increasing substrate concentration. This is attributed to higher HI formation via autocatalysis at higher substrate concentration. The minimum amplitudes increased initial till 2.03 mM substrate concentration and then decreased at much higher substrate concentrations (3.05 and 3.55 mM). Maximum and minimum oscillation periods differed at each substrate concentration investigated. The highest maximum periods occurred at 3.05 and 3.55 mM while the highest minimum period was at 2.03 mM substrate concentration (Figure 4.51 (c-d)). Oscillations were still ongoing at [A-PEG_{2000}] = 1.52 mM and 2.03 mM when the experiments were stopped, and the highest number of oscillations were obtained at highest substrate concentration and vice versa (Figure 4.51e).

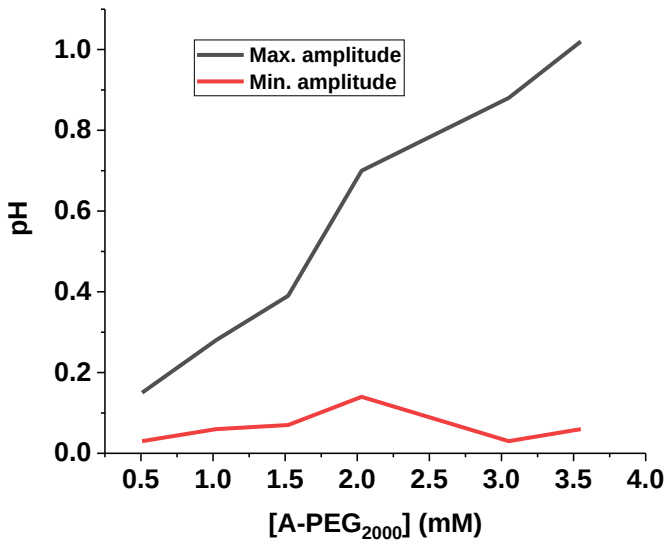

Figure 4.50. Max/min pH amplitude recorded across mono alkyne substrate concentrations investigated at constant PdI_2 and KI concentrations. (Batch type bifurcation diagram)

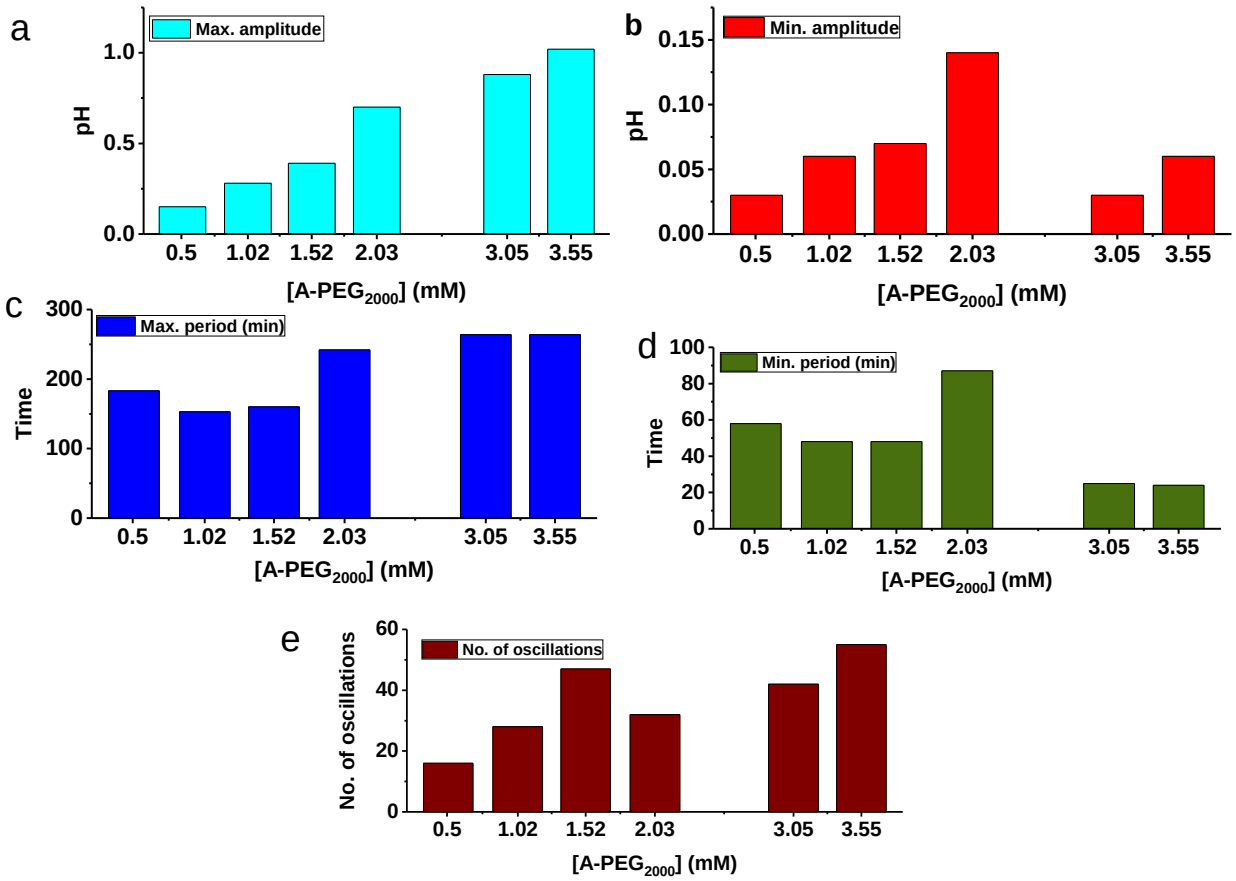

Figure 4.51. Maximum and minimum amplitudes and periods and number of oscillations recorded across mono alkyne substrate concentrations investigated at constant PdI_2 and KI concentrations. (Oscillations still ongoing at 1.52 and 2.03 mM when experiments were stopped)

4.6.1 Comparison of Reaction Profiles Obtained on Increasing Substrate Concentrations by Factors of Two at Constant PdI_2 and KI Concentrations

Further considerations of the substrate concentrations employed in the experimental study (Table 4.10) reveal a pattern of increasing substrate concentration by factors of 2. Substrate concentrations with such features are given in Figures 4.52 and 4.53. In Figure 4.52, increasing the substrate concentration from 0.508 mM to 1.02 mM and then 2.03 mM was followed by an increase in period of "slow H^+ formation", an increase in $[H^+]$ from first autocatalytic substrate conversion and increased size of oscillations.

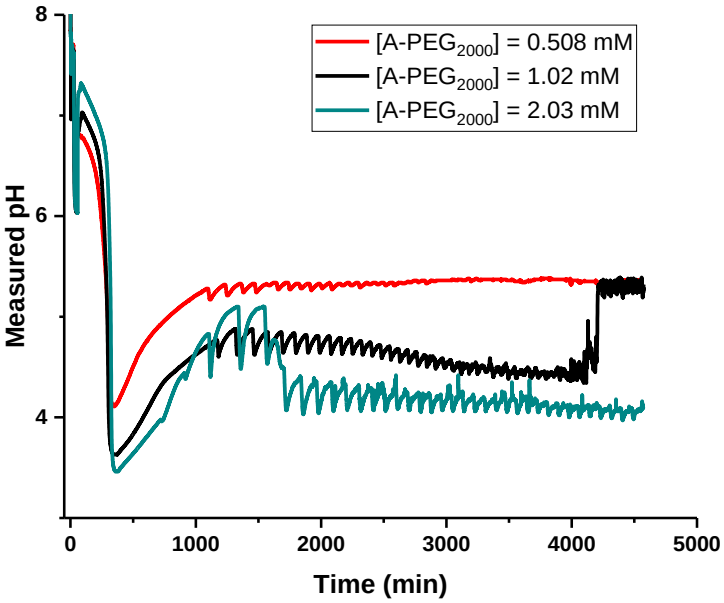

Figure 4.52. Reaction profiles obtained on increasing substrate concentration by factors of 2 at constant concentration of catalytic mixture. ([PdI_2] = 2.9 μM; [KI] = 5.7 mM)

The maximum and minimum amplitudes also increased by factors of 1.9 and 2.5 as the substrate concentration doubled. The overall increase seen suggests an increase in reaction rate as substrate concentration doubles and this is supported by lower pH (higher [H^+]) values observed at higher substrate concentration. An increasing trend in number of oscillations (Figure 4.51e) was also noted.

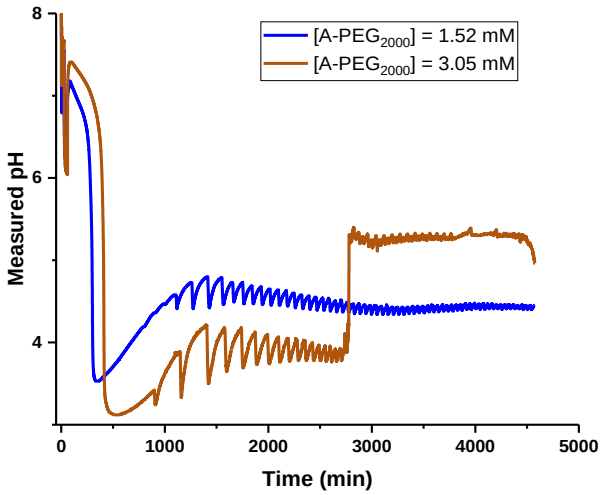

Figure 4.53. Reaction profiles obtained on increasing substrate concentration by a factor of 2 at constant concentration of catalytic mixture. ([PdI_2] = 2.9 μM; [KI] = 5.7 mM)

A similar pattern was also observed on doubling the substrate concentration from 1.52 mM to 3.05 mM at constant catalytic concentration, although the number of oscillations decreased at 3.05 mM. The decreases in number of oscillations is attributed to the "jump" like transition in pH from lower to higher values since oscillations became very irregular after this transition. Complex oscillatory phenomena were also present at other doubled substrate concentrations in Figures 4.52 and 4.53, supporting earlier assumption (Sub-section 4.5.2) that substrate concentration significantly contributes to the occurrence of complex oscillatory features.

4.6.2 Section Summary

At constant PdI_2 and KI concentrations,

1. Increasing substrate concentration from 0.508 mM to 3.55 mM increases oscillation size (amplitudes and period) and moves the pH profiles to more acidic regions, supporting proposed Eq. 4.6 (substrate autocatalysis). This observation becomes more obvious when the substrate concentrations are doubled (Subsection 4.6.1).
2. Compound transitions at double substrate concentration (0.508 mM to 1.02 mM and 1.52 mM to 3.05 mM) supports the influence of substrate concentration on formation of complex oscillatory phenomena.
3. Reproducibility across substrate concentration investigated was poorer than other studies in this chapter.
4. The period of gradual H^+ formation prior to initial autocatalysis and termed duration of "slow H^+ formation" increases as substrate to catalyst ratio increases. It seems that increasing substrate concentrations at constant catalyst concentration, prolongs this phase (same amount of catalyst vs increasing substrate concentration).

Chapter 5. Results and Analysis of Reaction Profiles from the Oscillatory Carbonylation of Bi-Alkyne Functionalised Polyethylene Glycols

5.1 Introduction

In Chapter 4, the influence of varying the concentrations of substrate, catalyst (PdI_2) and catalyst promoter (KI) employed in the carbonylation of mono-alkyne functionalised methoxy-polyethylene glycol was assessed. Oscillatory/non-oscillatory modes of the reaction were identified over the range of substrate and catalytic conditions studied. In this chapter, a new substrate, bi-alkyne functionalised polyethylene glycol (Alkyne-PEG_{2000}-Alkyne (A-PEG_{2000}-A)), is investigated. This new substrate differs from the mono-alkyne variant employed in Chapter 4 because, each polymeric chain has two alkyne end groups. Here, the influence of varying substrate, catalyst, and KI concentrations in oscillatory carbonylation reaction is also analysed, but, bi-alkyne functionalised polyethylene glycol (A-PEG_{2000}-A) is used as the reaction substrate instead of the mono functional substrate. The use of bi-alkyne functionalised polyethylene glycol as the reaction substrate in oscillatory carbonylation reactions is a novel subject, as such, very limited information is available in literature [28] and accessible information is credited to our research group. Consequently, studies in subsequent sections of this chapter are designed to demonstrate the potentials of A-PEG_{2000}-A (bi-alkyne functionalised PEG) substrate. The influence of varying A-PEG_{2000}-A substrate concentration at constant catalytic concentration and, the effects of the components of the catalytic mixture comprising potassium iodide and palladium iodide in methanol, at constant substrate concentration are investigated.

5.2 Effect of Varying Substrate Concentration at Constant Catalytic Concentration

The influence of altering the substrate concentration at constant catalytic concentration was investigated employing the conditions provided in Table 5.1. The catalytic concentration used in the study (Table 5.1) and the range of A-PEG_{2000}-A concentrations investigated were selected based on preliminary studies conducted with the mono-functional substrate. A-PEG_{2000}-A concentrations investigated ranged from 0.254 mM to 2.54 mM with the substrate to palladium iodide ratio increasing from 8.76 to 87.59 as substrate concentration increased.

Table 5.1. Range of substrate concentrations and substrate to catalyst ratios investigated at constant potassium iodide and palladium iodide concentrations. (Temperature = 20^{o}C±2, CO and air flowrates = 15 mL/min, [KI] / [PdI_2] = 196; V_{Total} = 90 mL)

[A-PEG_{2000}-A] (mM)	[PdI_2] (μM)	[KI] (mM)	Substrate to Catalyst Ratio (A-PEG_{2000}-A /PdI_2)
0.254	29	5.7	8.76
0.508	29	5.7	17.52
1.02	29	5.7	35.17
1.52	29	5.7	52.41
2.03	29	5.7	70
2.54	29	5.7	87.59

The pH and [H^+] adjusted profiles in Figure 5.1 and Figure 5.2 respectively, were obtained from experimental studies on the carbonylation of bi-alkyne functionalised PEG (0.254 mM to 2.54 mM) at constant palladium iodide and KI concentration as detailed in Table 5.1. Oscillations were captured for the full range of substrate concentrations employed in the carbonylation reaction. The size and duration of pH oscillations recorded over the course of the reaction varied with the substrate concentration, with all oscillations occurring between pH 3 and 5. The pH range within which oscillations were recorded using the bi-alkyne functionalised polymeric substrate is comparable with the range reported for oscillatory carbonylations where phenyl acetylene (small molecule) was the reaction substrate [6, 8, 10, 31, 32, 38].

The reactions were monitored by recording pH and temperature changes for the duration of the experiments. The experimentally obtained pH reaction profiles (Figure 5.1) were converted to [H^+] adjusted profiles since pH is a measure of hydrogen ion concentration. The profiles in Figure 5.2 were obtained from this conversion. The conversion is useful because it supports mechanism elucidation by relating H^+ generating reactions to pH changes occurring during the reactions. The conversion of pH profiles to [H^+] profiles was approached as discussed in Chapter 4, Section 4.2. In summary, the [H^+] profiles in Figure 5.2 were obtained by converting the corrected pH values to hydrogen ion concentrations. The pH values were corrected to account for the non-aqueous methanol solvent used for the reaction. The adjustment for non-aqueous methanol was performed by adding 2.3 pH units per pH value before the conversion to [H^+] as proposed in literature [258, 259]. The accuracy and precision of the [H^+] values obtained from the conversion of pH profiles from the carbonylation reactions of bi-alkyne functionalised PEG substrate is not established, however, it offers very useful approximations. Hence, was applied in generating the [H^+] adjusted profiles given in Figure 5.2 and in the rest

of this chapter. The adaptation for pH measurements in methanol is defined mathematically in Eq. 4.1 (Section 4.2).

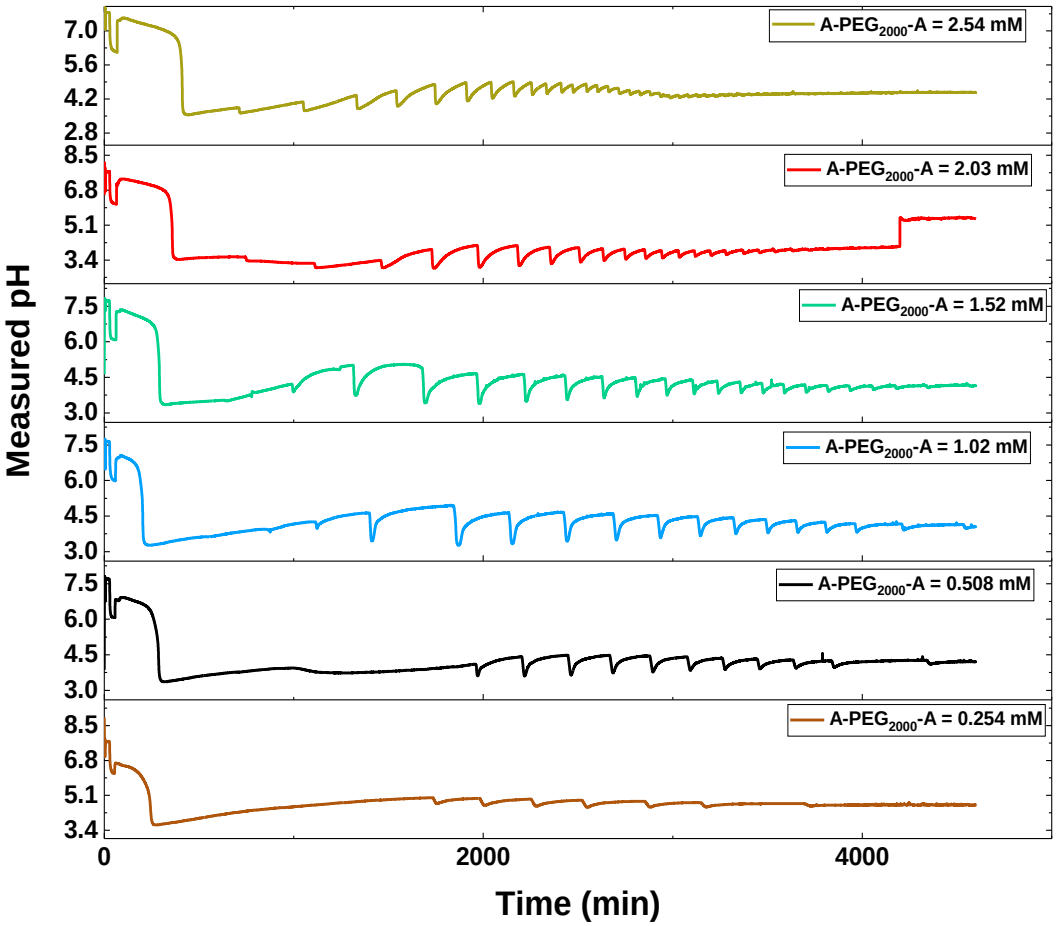

Figure 5.1. Experimentally recorded pH profiles from the oscillatory carbonylation of A-PEG_{2000}-A at constant catalytic concentrations. ([PdI_2] = 2.9 μM; [KI] = 5.7 mM; CO/air flowrates = 15 mL/min; temperature = 20°C±2)

As pH is a measure of hydrogen ion activity, the reaction profiles with more acidic pH values showed higher concentrations of hydrogen ion in Figure 5.2 and hence, greater [H^+] adjusted values. The highest [H^+] value (5.01 x 10^{-6} M) obtained during the oscillatory phase of the carbonylation reaction occurred at [A-PEG_{2000}-A] = 2.03 mM. On the other hand, the least [H^+] adjusted obtained in oscillatory mode was at [A-PEG_{2000}-A] = 1.52 mM with [H^+] adjusted value of 4.48x10^{-8} M, nevertheless, this value increased during further oscillations as the reaction progressed. Considering the full reaction duration (oscillatory and non-oscillatory regions), overall [H^+] adjusted values were lowest at [A-PEG_{2000}-A] = 0.254 mM. The low [H^+] value is credited to the smaller substrate concentration present. The assumption for

reduced substrate concentration (0.254 mM) resulting in lowest [H^+] was made because, constant PdI_2 and KI concentrations (PdI_2 = 2.9 μM; KI = 5.7 mM) were employed for the full range (0.254 mM to 2.54 mM) of bi-functional substrate concentrations investigated and, [H^+] values increased on increasing substrate concentrations.

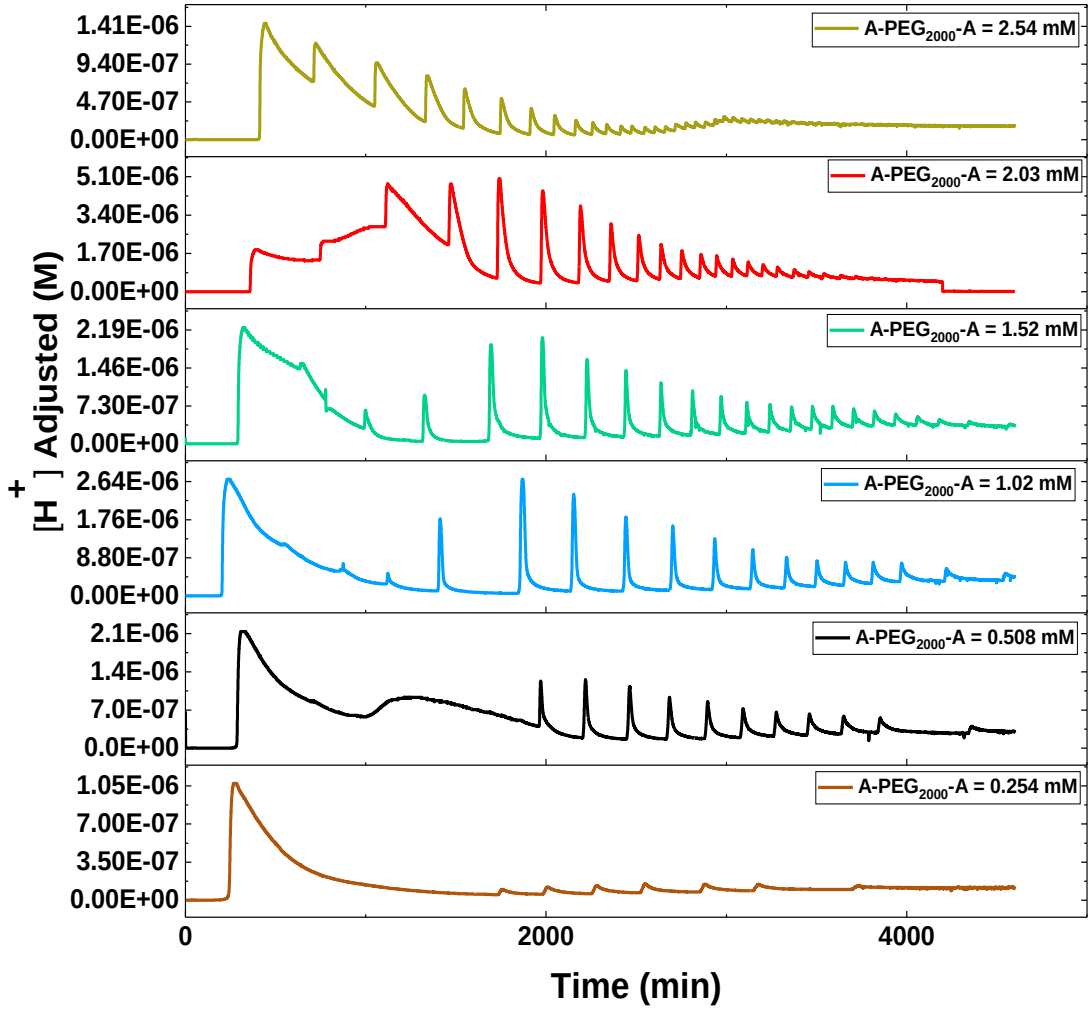

Figure 5.2. [H^+] adjusted profiles recorded in the oscillatory carbonylation of A-PEG_{2000}-A at constant catalyst concentration. ([PdI_2] = 2.9 μM; [KI] = 5.7 mM; CO/air flowrates = 15 mL/min; temperature = 20^{o}C±2)

pH changes recorded during the initial stages of the reaction is given in Figure 5.3. These stages are similar to stages for the mono alkyne substrate (Chapter 4) and some oscillatory carbonylation reactions with phenylacetylene as substrate. An initial reversible decline in pH occurred when defined volumes of the stock catalytic solution (PdI_2 and KI dissolved in methanol) to the reaction vessels containing only bulk methanol. The reversible nature of the

dip in pH suggests that the introduction of catalytic solution had a temporary effect on the concentration of H^+ present and/or the H^+ activity quantifiable by the pH electrodes (KI present in catalytic mix and the electrodes).

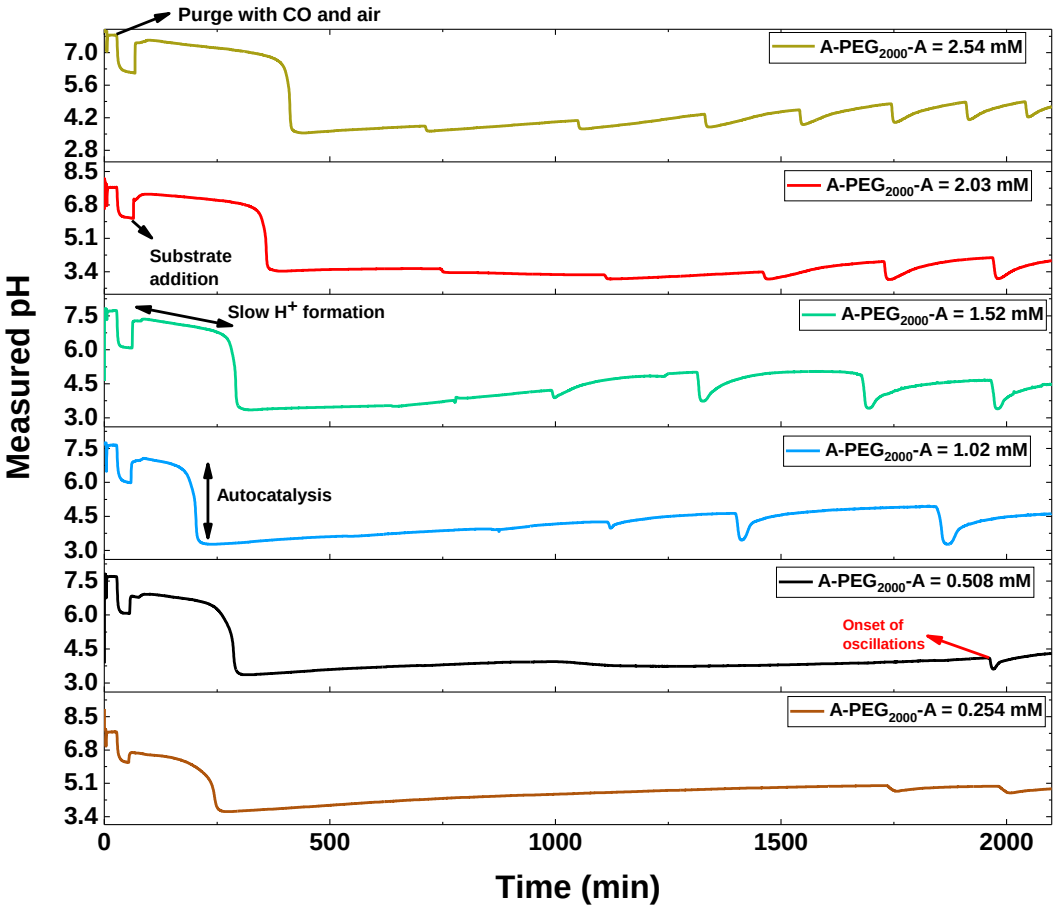

Figure 5.3. Reaction profiles showing the key stages of the oscillatory carbonylation reaction at various A-PEG_{2000}-A substrate concentrations and constant KI/PdI_2 concentration. ([PdI_2] = 2.9 μM; [KI] = 5.7 mM; CO/air flowrates = 15 mL/min; temperature = 20°C±2)

The first arrow from the top of Figures 5.3 indicates the onset of purging with CO and air at 15 mL/min following catalyst addition. On purging, a fast drop in pH which eventually levelled out was observed and is suggestive of the onset of hydrogen ions producing reactions. Such behaviour on purging was reported for the oscillatory carbonylation of phenyl acetylene [8-10, 30, 32, 173-175, 177, 242] employing the same catalytic system (PdI_2 and KI in methanol) applied in this study. Possible sources of protons from the reactants are methanol, CO, air and water (impurity) in the HPLC grade methanol used. Equations 4.2 to 4.4 (Section 4.2, Chapter 4) from studies on oxidative carbonylation reactions [3, 38, 103, 198, 174, 269-271] have been offered as pathways to hydrogen ion formation as HI and thus, the increased [H^+] values in

Figure 5.3. A comparison with previously reported pH drops on purging in other oscillatory carbonylation systems shows that the rapid fall in pH on purging (pH 7.5 to pH 6) in this study is less. When HPLC grade methanol used as received was purged, researchers found that the pH dropped from ≈ pH 7 to pH 2 at [KI] = 0.48 M and [PdI_2] = 2.22 mM in 25 mL of methanol [174]. Also, pH drops from ≈ pH 7 to pH 3 was reported in the carbonylation of mono alkyne functionalised polyethylene glycol at PdI_2 = 40.5 μM and KI= 2.28 mM in 90 mL methanol [29]. These differences in pH drop / increase in [H^+] is attributed to the difference in concentration of palladium iodide (29 μM) used in this study, which is less than any concentrations employed in previously reported oscillatory carbonylation reactions.

On further reflection, the rate of fall in pH on purging corresponding to an increase in [H^+], varied slightly between runs although catalyst concentration was kept constant. This variation may be a cumulative effect from the minute difference in pH values from onset of the reaction (different pH probes). It could also arise from competing reactions during the carbonylation of methanol and water in the reactions proposed in Eq. 4.2 to 4.4 [3, 38, 103, 198, 174, 269-271]. In case of competing reactions, the rate of H^+ production on purging would depend on the reactions present and the rate at which they proceed, hence, accounting for the small differences in pH witnessed across runs from purging at constant catalyst concentration. This rational is also supported by previous studies in carbonylation reactions where the presence of water interfered with catalytic activity (poisoning) via oxidation of CO to CO_2 [3, 174, 175] and was proposed to limit PdI_2 availability.

The addition of solutions of various concentrations of A-PEG_{2000}-A substrate to the reacting mixture indicated by the second arrow from the top of Figure 5.3 was followed by a rapid increase in pH of the reactions. This increase in pH is unexpected since the substrates have two alkyne end groups, as such, an increase in [H^+] (decreased pH) was anticipated. Since the bi-alkyne substrates were dissolved in small volumes of methanol (3.7 mL each), the rise in pH may be linked to the methanol introduced with the substrate, or from the substrate itself. The assumption that such rise in pH originates from methanol is supported by studies reported in Chapter 4, Section 4.2, where pH was shown to increase on addition of methanol to the reaction. Such behaviour was also reported in other instances on addition of more methanol in the oscillatory carbonylation of phenyl acetylene [9, 10, 32, 242, 243]. Perturbation studies with methanol [243] and oscillatory carbonylation in water-methanol solvent mixtures [176] are examples of such instances. Dilution of [H^+] (which would reduce measurable HI) is postulated to occur, however, as methanol is already in so much excess, previous studies [174-177] suggest residual water impurity present in the methanol as the source of the rise in pH.

Higher A-PEG_{2000}-A substrate concentrations promoted greater pH rise on substrate addition. This signifies that, the polymeric substrate has some effect on the pH of the reaction and HI concentration once the substrate is added. The only remote semblance to such rise in pH on substrate addition in oscillatory carbonylation reaction was reported by Gorodsky [33], where an increase in pH occurred on addition of non-1-yne substrate. He credited this behaviour to the backbone to which the alkyne end was attached, which was a heptyl [33] group for the non-1-yne substrate employed in his study. Applying a similar assumption in this case is speculative, since the influence of polyethylene glycol backbone on pH in methanolic reactions is not clear. This aspect of the application of polymeric substrate is thus recommended for future studies.

The increase in pH alkalinity following substrate addition was followed by a period of gradual H^+ increase (Figure 5.3, third arrow from top) termed "slow H^+ formation" phase in Chapter 4. A likeness to this slow H^+ phase was noted in the account by Gorodsky 2012 for non-1-yne carbonylation [33] and other accounts with phenyl acetylene as reaction substrates [8, 9, 32]. This period lasted between 83 and 331 min at the substrate concentrations investigated and, increased with increasing A-PEG_{2000}-A concentration. The only exception to this trend occurred in the experimental run at 1.02 mM (115 min) substrate concentration. This outlier behavior found in the experiment at A-PEG_{2000}-A = 1.02 mM may have some correlation with the higher H^+ concentration produced on purging the catalytic solution to which 1.02 mM A-PEG_{2000}-A was eventually added. The highest [H^+] following purging with CO and air was obtained at this concentration.

The gradual increase / "slow H^+ formation" suggest the presence of reactions where H^+ is produced. Similar behaviour wherein H^+ forms on substrate addition was reported for large scale (reaction volume = 450 mL) oscillatory carbonylation of phenyl acetylene at 20°C and 40°C [9, 10, 32]. Eq. 4.2 to 4.4 (water / methanol carbonylation reactions and catalytic conversion of water) and Eq. 5.1 below are proposed for the slow decrease in pH during this phase.

$$A - PEG_{2000} - A + 2CO + 2CH_3OH + PdI_2 \overset{HI}{\rightarrow} Pd + P - PEG_{2000} - P + 2HI \quad \text{Eq. 5.1}$$

Where $P - PEG_{2000} - P$ represents products from the carbonylation.

Eq. 5.1 is assumed to proceed in an autocatalytic mode; commencing slowly during the period of low H^+ concentration ("slow H^+ formation"), and subsequently faster, as H^+ concentration increases. The end of the "slow H^+ formation" phase was marked by a fast decline in pH and

is indicated by the fourth arrow from the top of Figure 5.3. This sharp drop in pH corresponding to a rapid increase in $[H^+]$ adjusted suggest the presence of reactions producing H^+ autocatalytically. The rapid mode of pH drops present in this study (Figure 5.3) is comparable to autocatalytic pH drop reported by Donlon and Novakovic (2014) [29] in the oscillatory carbonylation of the mono alkyne substrate. Such rapid decline in pH after a period of slowly decreasing pH values (albeit different from extended periods observed in this study) was similarly reported in semi-batch oscillatory carbonylation reactions with phenyl acetylene as reaction substrate [8-10, 31, 32, 175-177]. Hence, Eq. 5.1 is proposed as likely route. The initial HI for the autocatalysis is assumed to originate from ongoing carbonylation and HI accumulation during the slow phase.

Autocatalytic ΔpH ranged from 2.8 to 3.2 pH units at the end of slow H^+ phase. No trend was observed as substrate concentration increased instead; the autocatalytic pH change varied across substrate concentrations investigated. The absence of trends in ΔpH arising from the autocatalytic drop in pH due to HI formation suggests that, the autocatalytic Eq. 5.1 proceeds at a different rate for each substrate concentration investigated. The differences in the rates of the reaction depends on the concentration of the catalytic mixture, HI concentration, substrate concentration and, concentrations of other reactants and operating conditions. Considering Eq. 5.1 postulated for autocatalysis, if the concentrations of methanol, CO and air are assumed to be in excess [9, 29, 30], and it is also assumed that purging the solution with CO/air significantly limits mass transfer interferences [9, 179, 242], then, the rate of the reaction "R_1" for Eq. 5.1 is postulated to be dependent on catalytic mixture, substrate concentration and HI concentration according to Eq. 5.2.

$$R_1 \alpha [A\text{-}PEG_{2000}\text{-}A] [KI/PdI_2] [HI]^2 \qquad \text{Eq. 5.2}$$

Unlike the mono-alkyne substrate, the presence of two alkyne groups per polymeric substrate chain could influence the rate at Eq. 5.1 and hence, Eq. 5.2 proceeds. If both alkyne end groups on the bi-alkyne substrate are assumed to react at different rates, and the alkyne reactions are furthermore assumed to occur either concurrently (both alkyne ends reacting at same time via coordination with Pd) or successively (at different times), then, the rate of the overall reaction in Eq. 5.1 would also depend on intermediate substrate species present (in the event of successive alkyne reactions). The overall rate of the reaction (Eq. 5.1) under these conditions (presence of two alkyne groups) are hence proposed to be dependent on the original substrate (bi-alkyne), as well as the intermediate substrate species formed as the bi-alkyne substrate is consumed. Eq. 5.3 and 5.4 are postulated as possible variants of Eq. 5.1 if the intermediate

substrate species act as substrates for the reaction (autocatalytic conversion of substrate and HI formation). Based on these postulations, the rate of the reaction according to Eq. 5.1 which governs how much [H^+] is produced from autocatalysis then becomes a function of the effective rate "R_{eff}" of Eq. 5.1, 5.3 and 5.4 and is represented as Eq. 5.5.

$$A - PEG_{2000} - A + 2CO + 2CH_3OH + PdI_2 \xrightarrow{HI} Pd + A - PEG_{2000} - P + 2HI$$

$R_2 \alpha$ [A-PEG_{2000}-A] [KI/PdI_2] $[HI]^2$ Eq. 5.3

$$A - PEG_{2000} - P + 2CO + 2CH_3OH + PdI_2 \xrightarrow{HI} Pd + P - PEG_{2000} - P + 2HI$$

$R_3 \alpha$ [A-PEG_{2000}-P] [KI/PdI_2] $[HI]^2$ Eq. 5.4

R_{eff} = Function (R_1, R_2, R_3) Eq. 5.5

Where A-PEG_{2000}-P represent intermediate products from the carbonylation with an alkyne functional group at one end. The intermediate undergoes further autocatalytic conversion at which point it is effectively a reaction "substrate" as given in the rate expression.

Palladium iodide concentration is constant irrespective of substrate species present in this study. Therefore, the availability of active PdI_2 sites for autocatalytic conversion of substrate/intermediate substrate species remains constant as the number and concentration of reacting substrate species present in each experimental run increases. This invariably affects the total HI formed via initial autocatalysis, thus, supporting the variations in recorded pH. The decline in ΔpH following initial autocatalysis at lower bi-alkyne substrate concentrations (0.254 mM to 1.02 mM) and the subsequent rise in ΔpH at higher bi-alkyne concentration (1.52 mM to 2.54 mM) agrees with these postulations, since higher substrate concentration supports the chances of more intermediate species. The autocatalytic production of HI was followed by a gradual increase in pH. The increasing pH is attributed to the consumption of HI produced during the autocatalysis to generate products including iodine for palladium regeneration. In the original account on oscillatory carbonylation of mono-functional polyethylene glycol by Donlon and Novakovic 2014, [29] the regeneration of palladium iodide was also postulated to proceed according to Equation 4.11 and also, in an autocatalytic manner. Their postulation was supported by oscillations in turbidity during the reaction. Turbidity was not measured in this study, however, due to the reduced concentration of palladium iodide used, visual changes wherein the solution swiftly changed from very light brown/ pale yellow to colourless solutions with visible black particles of precipitated palladium (Pd) were observed at several points during the reactions. Images of the changes in the colour of reaction solution and palladium

particles are given in Appendix A (A3 to A7). As turbidity is a function of particles present in solutions, it is reasonable to assume that the reactions in this study could also oscillate in turbidity as proposed by Donlon and Novakovic 2014 [29], therefore, the autocatalytic recycling of palladium to palladium iodide is also proposed to occur in this study according to Eq. 4.12 given in Chapter 4. The initial palladium iodide required for the autocatalytic formation of PdI_2 is assumed to come from Eq. 4.11.

Oscillations started after the period of HI consumption as shown in Figure 5.3 (5^{th} arrow from the top). The onset time of oscillations and the pH at which oscillations commenced varied for each bi-alkyne substrate concentrations studied. The pH values at onset of oscillation ranged from 3.5 to 5 and onset time of oscillations ranged from 718 min to 1976 min. The range for pH and time at onset of oscillation in this study is moderately comparable to pH (2.27 and 3.13) and time (744 min and 2117 min) reported for phenyl acetylene at higher substrate and catalyst concentrations (0.124 M and 0.1414 M respectively) at the same reaction temperature [9, 32]. The maximum periods of oscillations ranged from ~ 4 to 9 hours, while the minimum periods ranged from 0.8 to ~ 4 hours. These periods are longer in comparison to 4 to 6-hour maximum periods and ~1-hour minimum reported by Donlon and Novakovic 2014 [29] for mono-functional PEG_{2000} substrate. Likewise, the amplitudes (0.34 to 1.7 maxima and 0.02 to 0.35 minima) for this study are also higher than the (0.4 to 0.7 maxima and 0.04 pH minima) amplitudes in previous study with the mono-alkyne substrate at 2.03 mM substrate concentration. These differences are assumed to arise from differences in substrate functionality (bi-alkyne functionalised against mono functionality), substrate concentration and catalyst concentrations.

Oscillations were still ongoing at [A-PEG_{2000}-A] = 1.02 mM and 1.52 mM when the reactions were stopped. The number of oscillations over the experimental duration increased with increasing substrate concentration from 0.254 mM to 2.54 mM. However, since oscillations were still ongoing at 1.02 mM and 1.52 mM substrate concentrations when the experiments were stopped, the increasing trend with increase in substrate concentration is inconclusive. At [A-PEG_{2000}-A] = 2.03 mM a jump in pH was recorded around 4250 min from onset of the reaction. This is similar to the pH transitions reported in Chapter 4, Section 4.6 using the mono-alkyne polymeric substrate at the same catalytic conditions ([PdI_2] = 2.9 μM; [KI] = 5.7 mM) reported here. This similarity irrespective of substrate type suggests that the jump in pH at [PdI_2] = 2.9 μM and [KI] = 5.7 mM is more reliant on the catalytic concentration than the substrate concentration or type.

To simplify the mechanistic description given in this section a simplistic oscillatory cycle is described. In a very simple oscillatory cycle, the carbonylation reactions switches between two pathways intermittently. Suppose the first pathway is the reaction according to Eq. 5.1, which produces HI in an autocatalytic manner (via Eq. 5.1, 5.3 and 5.4), then a second pathway which consumes the HI produced is required and this could be Eq. 4.8 and 4.9. The amplitude of the oscillation/concentration of HI is then determined by the concentration of one of the intermediates in reaction in the first pathway. In this case, the availability of PdI_2 serves this function or acts as the trigger governing the maximum HI produced via autocatalysis. Such that, when HI is low, PdI_2 facilitates the conversion to HI. The PdI_2 is reduced to Pd in this process which, then impedes HI production. The reaction switches to second pathway at this point to consume HI produced to form iodine, which regenerates the Pd to PdI_2 according to Eq. 4.11 and 4.12. When more palladium iodide is available, the reaction switches to the first pathway again and the cycle continues. Initial HI which drives the autocatalysis in Eq. 5.1 is assumed to be produced from solvent carbonylation (Equation 4.2 to 4.4). The process described above is for illustrative purposes and is much more complex than described.

5.2.1 Comparison of Reaction Profiles as a Function of Substrate Concentrations

In Table 5.1, details of substrate concentrations discussed in this section are given. From the table, some polymeric substrate concentrations employed in the experimental study were increased by factors of 2 and 10. Substrate concentrations with such features are given in Figures 5.4 and 5.5. In Figure 5.4, the substrate concentration was increased by a factor of 10; from 0.254 mM to 2.54 mM while in Figure 5.5, the concentration of bi-alkyne substrate was increased by a factor of 2; from 1.02 mM to 2.03 mM. The rates of reactions are affected by concentrations of reactants present, thus, changes in substrate concentration should influence the reaction rate and pH profiles obtained. An assessment of reaction profiles obtained by increasing the concentration of bi-alkyne polymeric substrate (A-PEG_{2000}-A) by a factor of 10 is given in Figure 5.4. Increasing the concentration of A-PEG_{2000}-A from 0.254 mM to 2.54 mM resulted in an increase in the concentration of hydrogen ions produced over the course of the reaction. An increase in substrate concentration by a factor of 10 drastically reduced the time of onset of oscillations from 1753 min to 718 min and led to an increase in the number of oscillations recorded from 6 to 33. Repeats of experiments at 0.254 mM did not produce oscillations hence, only single values are reported for increase in number of oscillations, instead of an average. Increased $[H^+]$ at constant catalyst concentration on increasing substrate concentrations by a factor of 10 suggests an increase in the rate of conversion of the substrate according to Eq. 5.1 and/or Eq. 5.3 and 5.4. Such increase in $[H^+]$ and in the number of

oscillations are in line with previous studies of oscillatory carbonylation system, wherein the addition of more substrates to the reaction improved [H^+] and/or prolonged oscillations [7, 38, 103].

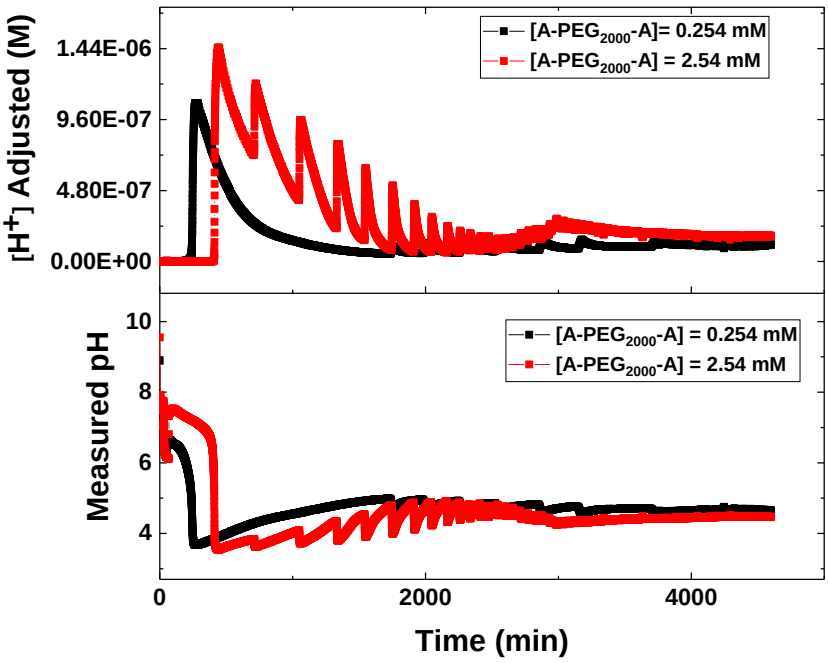

Figure 5.4. Comparison of reaction profiles on increasing the concentration of bi-alkyne substrate (A-PEG_{2000}-A) by a factor of 10 at constant catalyst concentrations. (bottom) - experimental pH profiles; (top) - [H^+] adjusted profiles; ([PdI_2] = 2.9 μM; [KI] = 5.7 mM; CO/air flowrates = 15 mL/min; temperature = 20°C±2)

Similarly, the longer oscillations periods and reduced [H^+] at $1/10^{th}$ substrate concentration (0.254 mM) (Figure 5.4(top)) suggests a slower reaction rate for Eq. 5.1 and/or Eq. 5.3 and 5.4 at this concentration. In contrast, increasing the substrate concentrations by a factor of 2 from 1.02 mM to 2.03 mM was followed by a reduction in initial H^+ from autocatalysis, although, this eventually changed as the reaction progressed. These results are given in Figure 5.5. The profiles obtained showed a decrease in onset time of oscillations from 883 min at 1.02 mM to 752 minutes at 2.03 mM. This difference is smaller than the difference observed when the change in substrate concentration was by a factor of 10. The number of oscillations also displayed a dependence on the concentration of the substrate, wherein more substrate generated more oscillations and vice versa. The [H^+] equally increased with increasing substrate concentration (Figure 5.5(top)) suggesting a higher substrate conversion rate at higher substrate concentration. Oscillations were still ongoing when the experimental run was stopped for the reaction at 1.02 mM substrate concentration. Continuing oscillations support proposed reaction

in Eq. 5.1 and reaction rates dependence on both PdI_2 and amount/species of substrate and substrate intermediates present (Eq. 5.2 to 5.5).

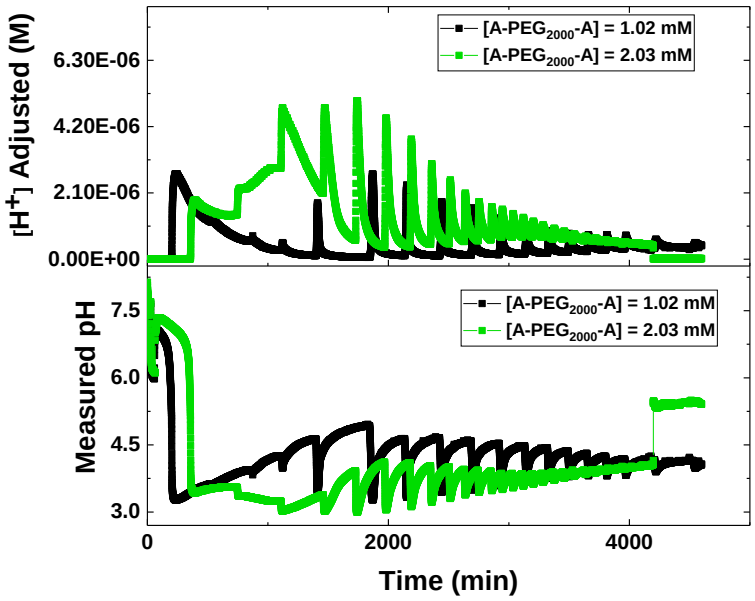

Figure 5.5. Comparison of pH profiles (bottom) and $[H^+]$ adjusted profiles (top) obtained on doubling the concentration of A-PEG_{2000}-A at constant catalyst concentrations

5.2.2 Section Summary

Graphical summaries of the features at different stages of the reaction and trends from pH profiles (Figure 5.1) obtained from the carbonylation of A-PEG_{2000}-A are provided in Figures 5.6 to 5.11.

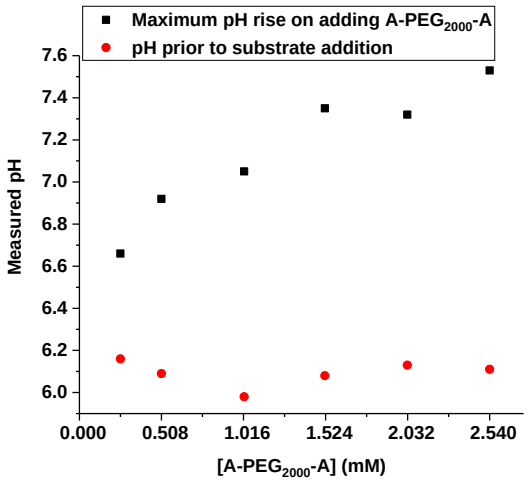

Figure 5.6. pH changes before and after substrate addition across A-PEG_{2000}-A concentrations investigated. ($[PdI_2]$ = 2.9 μM; [KI] = 5.7 mM; CO/air flowrates = 15 mL/min; temperature = 20°C±2)

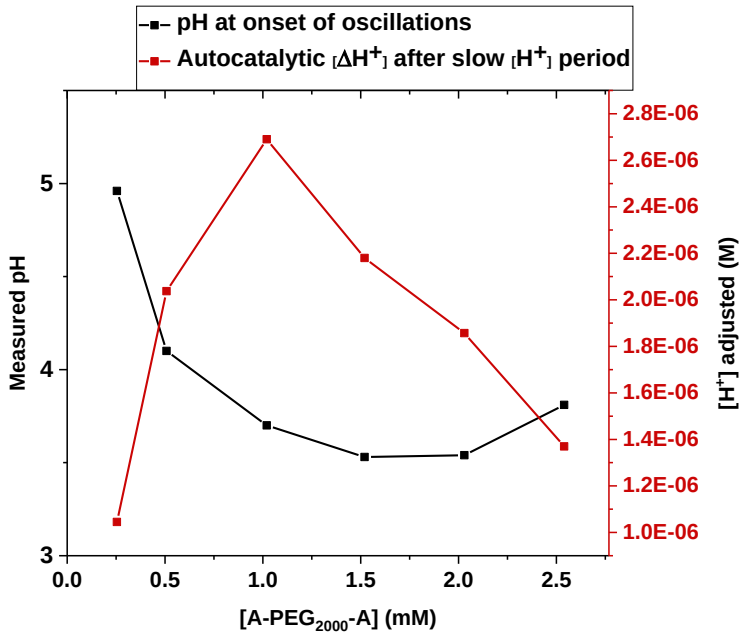

Figure 5.7. Trends in initial autocatalytic changes in hydrogen ion concentration following slow duration and pH at onset of oscillations at various A-PEG$_{2000}$-A concentrations investigated.

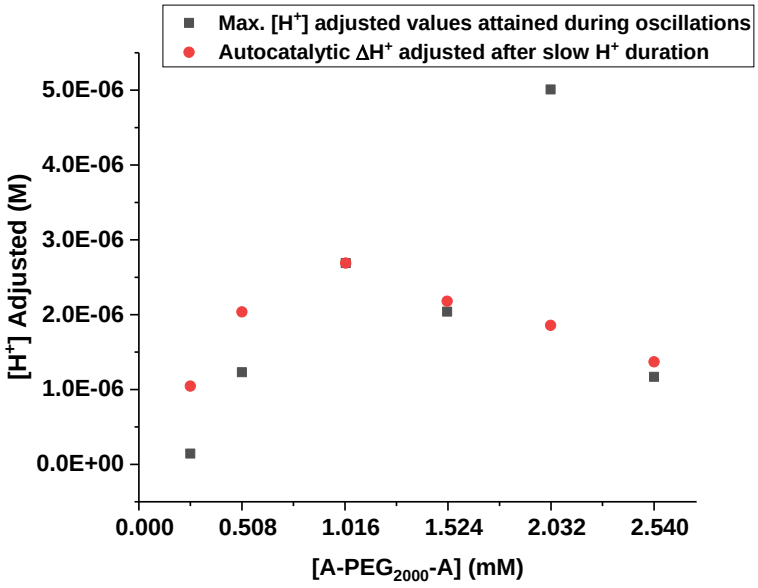

Figure 5.8. Initial autocatalytic changes in hydrogen ion concentration after the slow HI formation period and maximum hydrogen ion concentration achieved during oscillations at various A-PEG$_{2000}$-A concentrations. ([PdI_2] = 2.9 μM; [KI] = 5.7 mM; CO/air flowrates = 15 mL/min; temperature = 20^{o}C±2)

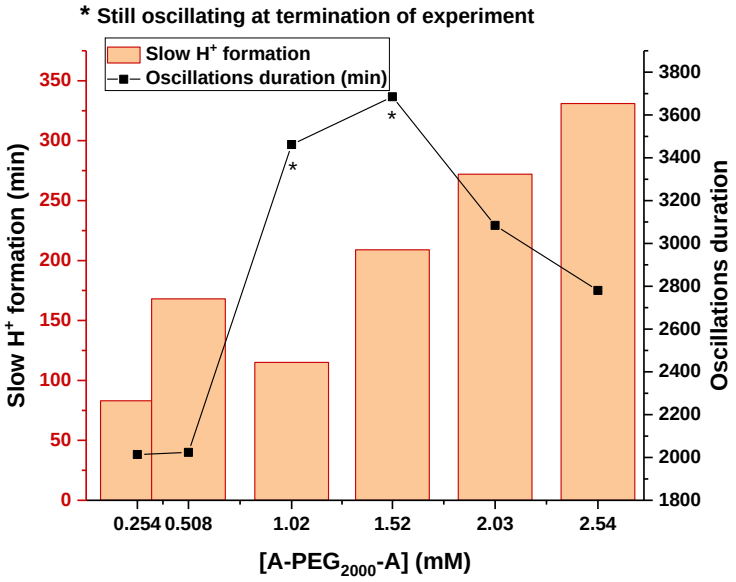

Figure 5.9. Durations of slow H^+ formation and oscillations at various A-PEG_{2000}-A concentrations investigated. ([PdI_2] = 2.9 μM; [KI] = 5.7 mM; CO/air flowrates = 15 mL/min; temperature = 20°C±2)

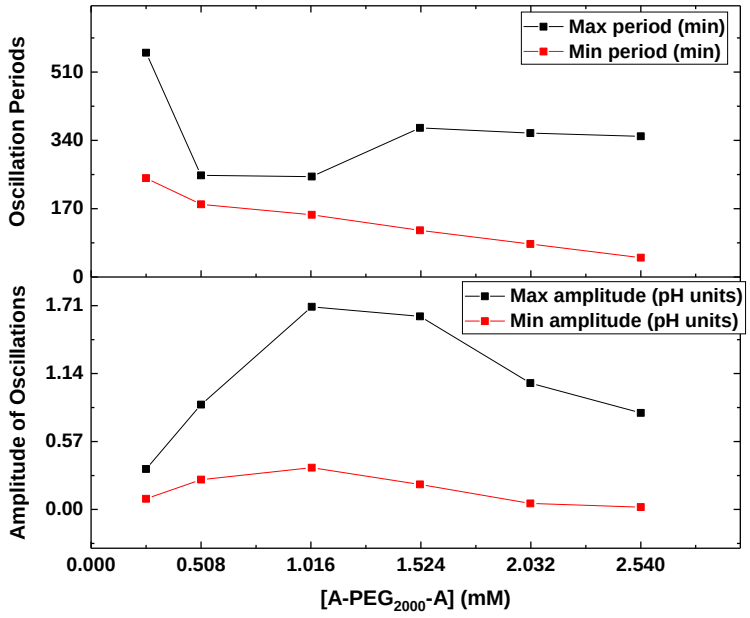

Figure 5.10. Maximum and minimum amplitudes and periods of oscillations recorded across bi-alkyne substrate concentrations investigated at constant PdI_2 and KI concentrations. ([PdI_2] = 2.9 μM; [KI] = 5.7 mM; CO/air flowrates = 15 mL/min; temperature = 20°C±2)

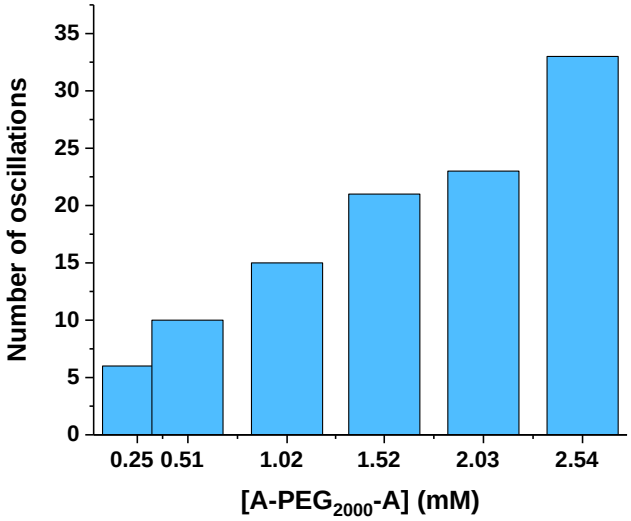

Figure 5.11. Number of oscillations recorded at constant PdI_2 / KI concentration, constant reaction durations and various substrate concentration

In conclusion,

1. Oscillations are possible with bi-alkyne functionalised polyethylene glycol substrate and were obtained at all concentrations investigated, which ranged 0.254 mM to 2.54 mM.
2. HI produced from purging reactions with CO and air at constant catalytic concentration (KI/PdI_2) appears to directly influence the duration of "slow H^+ formation". Increased HI from purging may reduce the period of "slow H^+ formation, irrespective of rise in pH on addition of solutions of substrate.
3. pH rises on substrate addition increased with increasing substrate concentrations suggesting some contribution from the substrate, though mechanism behind rise is still unclear at this point.
4. Initial autocatalytic formation of HI depends more on the rate of conversion of substrates than on the original substrate concentration present (skewed trend, with initial autocatalytic maxima at 1.02 mM), suggesting that, palladium iodide concentration and initial HI available to initiate autocatalysis (from solvent carbonylation) play significant roles in the pathway for autocatalysis.
5. The existence of optimal substrate concentrations at $[PdI_2]$ = 2.9 μM and [KI] = 5.7 mM for which, maximum HI is formed from initial autocatalysis is feasible. This inference was drawn after considering that, the maximum HI from initial autocatalysis

occurred at 1.02 mM (other substrate concentrations studied had less H^+) instead of higher substrate concentrations investigated.

6. Time at onset of oscillation is dependent on HI concentration from initial autocatalysis. As HI from first autocatalysis increases, more HI becomes available for oxidation to produce I_2, which in turn facilitates the regeneration of Pd^0 for the reaction, which then reduces the time of onset of oscillations.

5.3 Influence of Potassium Iodide and Palladium Iodide Concentrations in Oscillatory Carbonylation of Bi-Alkyne Functionalised Polyethylene Glycol

This section investigates the influence of components of the catalyst solution on oscillatory carbonylation at constant bi-alkyne functionalised substrate (A-PEG_{2000}-A) concentration. The amount of catalyst present is known to affect reaction rates [2, 284-286], but its effects on the oxidative carbonylation of bi-alkyne functionalised polyethylene glycol has never been studied. In addition, the effects of catalyst promoters [246, 250, 252, 313] such as KI, which support dissolution, catalytic activity and efficient recycling of palladium [3, 137, 172, 270] have also not been investigated for oscillatory reactions employing bi-alkyne polymeric substrate. The studies in subsequent subsections are therefore designed to assess the influence of KI and palladium iodide concentration via a series of one factor studies. The concentration of the bi-alkyne functionalised substrate (A-PEG_{2000}-A) was kept constant at 1.02 mM, while a range of palladium iodide and potassium iodide concentrations were employed for each study. In the following subsections, the concentration of potassium iodide is held constant at either 3 mM, 6 mM or 9 mM in addition to constant reaction conditions, while palladium iodide is varied at each KI concentration according to Table 5.2.

Table 5.2. Concentrations of individual components of the catalytic mixture investigated in the carbonylation of A-PEG_{2000}-A. Temperature = 20°C±2; CO and air flowrates = 15 mL/min; V_{total} = 90 mL; stirring speed = 350 rpm

PdI_2 (µM)	**KI - 1 (mM)**	**KI - 2 (mM)**	**KI – 3 (mM)**
17.0	3	6	9
22.7	3	6	9
34.0	3	6	9
60.4	3	6	9

5.3.1 Reaction Profiles at 3 mM Potassium Iodide Concentration

The influence of palladium iodide concentrations on the reactions were assessed at constant potassium iodide concentration (3 mM), according to Table 5.3. KI to PdI_2 and A-PEG_{2000}-A to PdI_2 ratios decreased with increasing PdI_2 concentration (3.55: 2.66: 1.78:1) for the range investigated.

Table 5.3. Range of reactant concentrations investigated in the carbonylation of A-PEG_{2000}-A. (Temperature = 20^oC±2; CO and air flowrates = 15 mL/min; V_{Total} = 90 mL; stirring speed = 350 rpm; [KI] / [A-PEG_{2000}-A] = 2.94)

[KI] (mM)	[PdI_2] (μM)	[A-PEG_{2000}-A] (mM)	Ratio of catalyst components [KI] / [PdI_2]	Substrate to catalyst ratio [A-PEG_{2000}-A] / [PdI_2]
3.00	17.0	1.02	176.47	60
3.00	22.7	1.02	132.16	44.93
3.00	34.0	1.02	88.24	30
3.00	60.4	1.02	49.67	16.89

The pH profiles in Figure 5.12 were obtained from the oxidative carbonylation reaction with the conditions given in Table 5.3. Visual inspection of the pH profiles in Figure 5.12 shows the presence of oscillations for experiments at 17 μM and 22.7 μM while oscillations was absent at 34 μM and 60.4 μM. Repeat experiments given in Figure 5.13 followed the same pattern, as oscillation were recorded at lower PdI_2 concentrations (17 μM and 22.7 μM) and absent at higher PdI_2 concentrations (34 μM and 60.4 μM). Mixed mode oscillations with extended periods (Figure 5.12) were obtained at constant substrate concentrations and 22.7 μM PdI_2 concentration, while the oscillations at [PdI_2] = 17 μM started off as simple oscillations with small amplitude till 6400 min when oscillations transitioned to mixed mode oscillation. Complex oscillations were present in replicate samples at 22.7 μM and oscillatory pattern at 17 μM (small amplitude preceding larger amplitude oscillations) was also reproduced. In both experimental runs, oscillation was still ongoing at point of termination. The pH profiles were similarly converted to [H^+] adjusted profiles by applying Eq. 4.1 and profiles obtained following conversion are given in Figure 5.14.

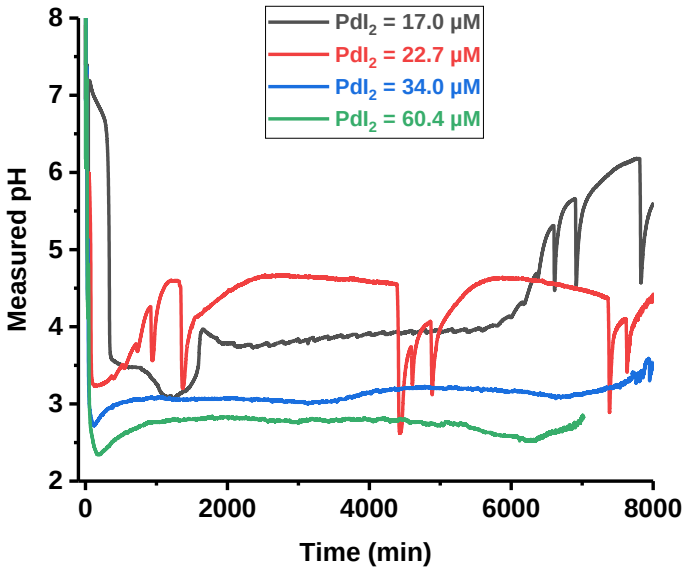

Figure 5.12. Measured pH profiles from the carbonylation of bi-alkyne functionalised polyethylene glycol at various palladium iodide concentrations and constant and KI concentration (3 mM). Temperature = 20°C±2; CO and air flowrates = 15 mL/min; [A-PEG$_{2000}$-A] = 1.02 mM

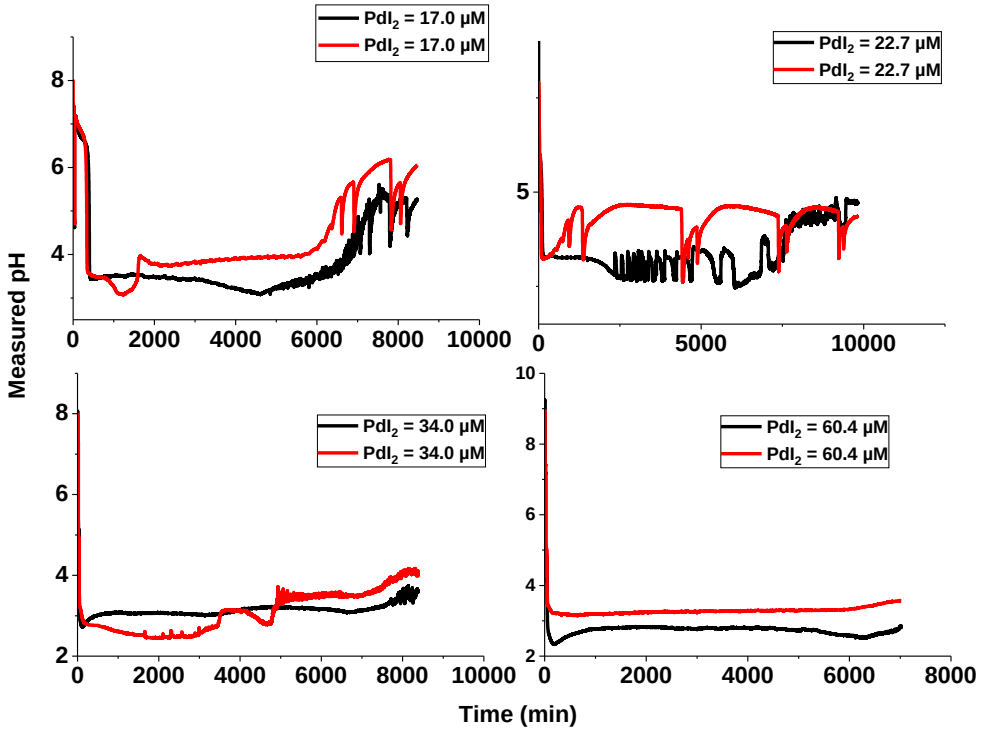

Figure 5.13. Degrees of reproducibility achieved from the carbonylation of different concentrations of PdI_2 at [KI] at 3 mM and [A-PEG$_{2000}$-A] = 1.02 mM

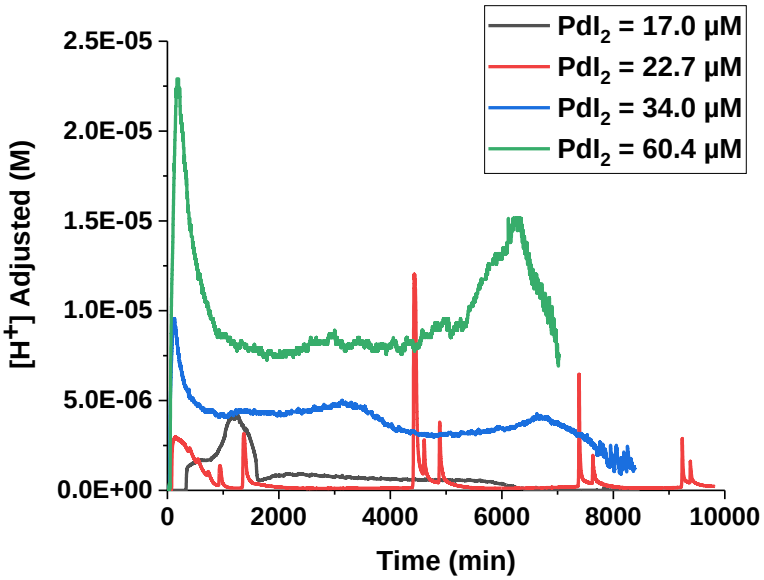

Figure 5.14. [H^+] adjusted profiles from the carbonylation of bi-alkyne functionalised polyethylene glycol at various palladium iodide concentrations and constant and KI concentration (3 mM). Temperature = 20°C±2; CO and air flowrates = 15 mL/min; [A-PEG_{2000}-A] = 1.02 mM

The trends and transition steps occurring during the reactions for the profiles in Figures 5.12 and 5.14 are comparable to profiles discussed in preceding sections and in Chapter 4. Concisely, the addition of catalytic solution (palladium iodide and KI in methanol) to bulk methanol for the reaction resulted in reversible drops in pH. The pH fell from ≈ 8.22 to 6.06 pH units and, recovered almost immediately with a range from 7.38 to 7.18 pH units. Reactions with higher palladium iodide concentration (34 µM and 60.4 µM), required more time to equilibrate (revert) unlike reactions with less palladium iodide (17 µM and 22.7 µM). The final pH values after stabilization following the catalytic mixture addition also decreased with increasing catalyst concentration. In Section 5.2, and results in Chapter 4, such behaviour was observed and, ionic strength effects arising from the introduction of potassium and palladium iodide ions to methanol was postulated.

The proposition that the dip in pH arises from the introduction of KI and PdI_2 ions to methanol (changing the ionic strength of methanol) is supported by the differences in pH drop, since the dip in pH increased as the amount of stock catalyst solution present increased. Similar drops in pH were observed in phenyl acetylene oscillatory system on addition of KI (pH changes from ≈ 8.5 to 7) and PdI_2 (pH changes from ≈ 7 to 6) [9]. These dips are not substantial, hence, the change in hydrogen ion concentration from catalyst addition is quite small, with a range of 4.37 $x10^{-9}$ M to 3.02 x 10^{-11} M according to the adjusted [H^+] values.

On purging the methanol-catalytic mixture, an increase in $[H^+]$ and equivalent reduction in pH values which increased with increasing PdI_2 concentration was noted. This change in $[H^+]$ agrees with Eq. 4.2 to 4.4 for solvent carbonylation in Section 4.2, Chapter 4 and is further supported by independent studies [174, 242] on the influence of the concentrations of palladium iodide on purging HPLC grade methanol [174, 175, 242]. In this instance, an increase in pH drop following purging occurred when the PdI_2 concentration was increased from 3 mg to 48 mg and then, 70 mg, at [KI] = 0.693 M and 50 mL/min of CO. Adding bi-alkyne substrates to the reactions similarly led to an increase in pH as seen in Section 5.2 and Chapter 4 on adding substrate solutions. pH values prior to substrate addition and the rise in pH values after substrate addition is given in Figure 5.15. The maximum rise in pH was found to decrease with increasing PdI_2 concentration and, the degree of rise in pH on comparing pH values before and after substrate addition, reduced as PdI_2 concentration increased. Since substrate concentration kept was constant here, the variations in degrees of rise (Figure 5.15) is credited to the concentration of HI formed during purging (Eq. 4.2 to 4.4), which depends on the concentration of PdI_2. It appears that the presence of more HI supresses the change in pH on addition of small volumes of methanol to the reactions, which could explain the absence of this feature in phenyl acetylene reactions (higher catalyst concentration used hence, more HI for phenylacetylene reactions).

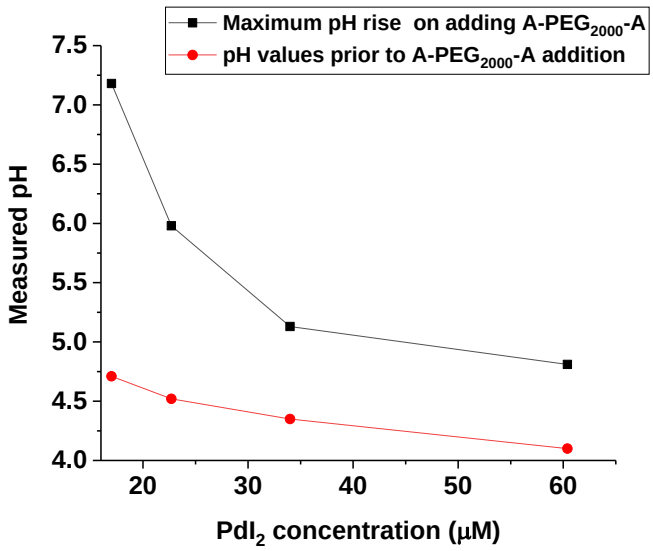

Figure 5.15. Variations in pH values recorded before and after substrate addition as a function of palladium iodide concentration. (Temperature = 20°C±2; CO and air flowrates = 15 mL/min; [A-PEG_{2000}-A] = 1.02 mM; [KI] = 3 mM)

The rise in pH on substrate addition was followed by "slow H^+ formation" phase and then, a rapid (autocatalytic) fall in pH. The periods of gradually increasing hydrogen ion concentration (slow H^+ formation period) corresponding to slowly decreasing pH in Figure 5.16 progressed gradually until enough [H^+] accumulated, allowing for autocatalytic formation of H^+. The "slow H^+ formation" and subsequent autocatalytic formation of H^+ is presumed to follow Eq. 5.1 and/or 5.3, which proceeds slowly initially and then, auto-catalytically. The duration of "slow H^+ formation" was observed to be dependent on the concentration of palladium iodide, such that increasing the palladium iodide concentration reduced the duration of the slow phase. This agrees with the rate equations postulated in Eq. 4.2 to 4.4, 5.1, 5.3 and 5.4, as an increase in PdI_2 is expected to increase these rates and produce more HI, which would be observed as a decrease in the duration of "slow H^+" phase. The duration of slow H^+ across runs is given in Figure 5.16 (bottom) and ranged from 305 min at PdI_2 = 17 µM to 18 min at PdI_2 = 60.4 µM.

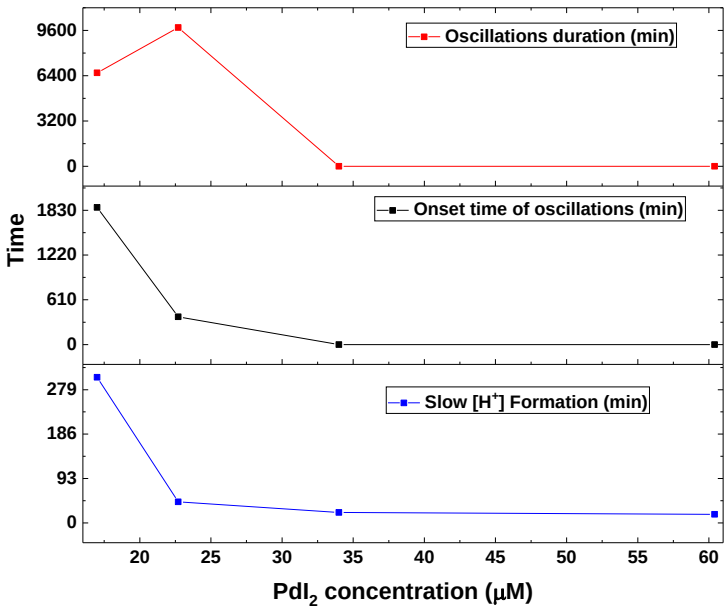

Figure 5.16. Variations in the duration of "slow H^+ formation", onset time of oscillations and oscillation duration as a function of palladium iodide concentration. (Temperature = 20°C±2; CO and air flowrates = 15 mL/min; [A-PEG_{2000}-A] = 1.02 mM; [KI] = 3 mM)

The rate of rapid drop (autocatalysis) in pH following the transition from "slow H^+ formation" period is presented in the profiles in Figure 5.17 and the trends in Figure 5.18. This fall in pH corresponds to an increase in [H^+] as shown in [H^+] adjusted profiles in Figures 5.17. The rapid increase in [H^+] is proposed to arise from the HI produced from the autocatalytic conversion of bi-alkyne functionalised PEG substrate according to Equation 5.1 and/or 5.3 from Section 5.2. A comparison of the rates of production of HI across runs at [KI] = 3 mM shows that, as the

palladium iodide concentration increased, concentration of HI (Figure 5.17 and 5.18) also increased. This is in agreement with recognized properties of catalysts [2, 284-286], and with the effect of PdI_2 in oxidative carbonylation reactions in oscillatory and non-oscillatory modes [3, 33, 103, 172, 269-271].

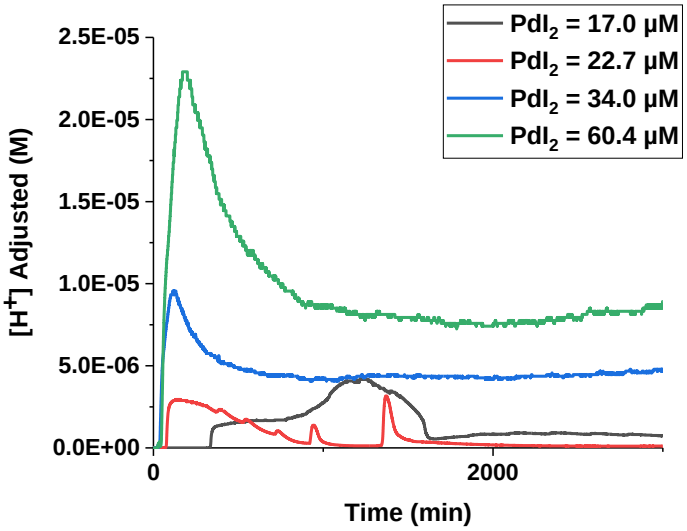

Figure 5.17. [H^+] adjusted reaction profiles showing variations in [H^+] adjusted from the first autocatalytic formation and consumption of HI as a function of palladium iodide concentration at constant KI and bi-alkyne substrate concentrations. (Temperature = 20°C±2; CO and air flowrates = 15 mL/min; [A-PEG_{2000}-A] = 1.02 mM; [KI] = 3 mM)

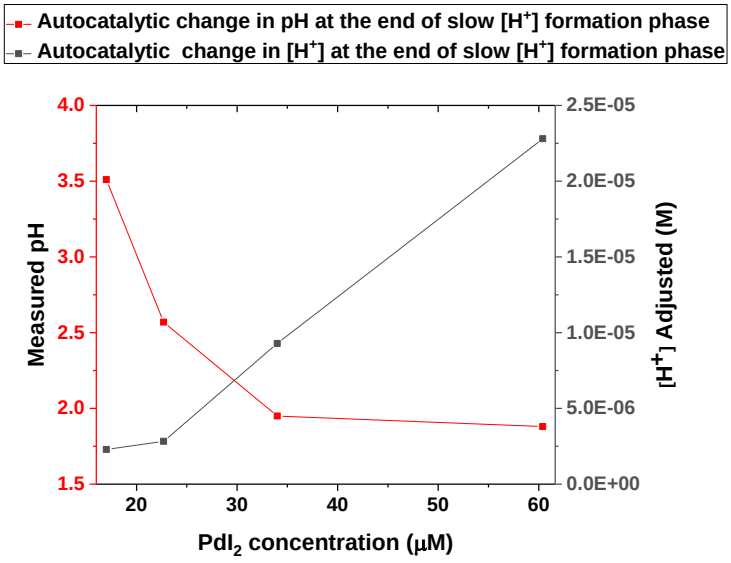

Figure 5.18. Changes in measured pH and [H^+] adjusted from first autocatalysis formation of HI following the slow HI phase. (Temperature = 20°C±2; CO and air flowrates = 15 mL/min; [A-PEG_{2000}-A] = 1.02 mM; [KI] = 3 mM)

The rapid rise in [H^+] (autocatalysis) was followed by a period of gradual decrease in [H^+] for runs with palladium iodide concentrations equivalent to 22.7 µM, 34 µM and 60.4 µM (Figure

5.17) indicative of reactions where HI is consumed. Eq. 4.8 for the oxidation of HI to form iodine and water and, the reversible Eq. 4.9, for the nucleophilic substitution of "OH" in methanol on reacting with HI (Chapter 4) accounts for this change. The overall rate of HI consumption increased with increasing palladium iodide concentration, as these reactions had more HI. In reactions with palladium iodide concentrations equivalent to 34 µM and 60.4 µM, the conversion of HI was fast initially, before it stabilized. A visual inspection of Figure 5.17 reveals that at [PdI_2] = 22.7 µM, the initial fast HI consumption observed at higher PdI_2 concentrations was absent, rather, a gradual rate of HI consumption was maintained. The different rates of HI conversion following autocatalysis for PdI_2 at 22.7 µM, 34 µM and 60.4 µM (Figures 5.17) are ascribed to the differences in the reaction rates for Eq. 5.1 and/or 5.3, arising from the different amounts of catalyst present in each reaction.

An entirely different profile trend was seen at [PdI_2] = 17 µM (Figure 5.17). At 17 µM PdI_2 concentration, the autocatalytic production of [H^+] was followed by periods of slow and then, faster production of extra [H^+] lasting for 587 min and 295 min respectively. Both phases were immediately followed by another period of gradual consumption of [H^+] lasting for 340 min; and finally, a fast consumption of [H^+] lasting for 9 min, after which, the [H^+] values remained steady.

The first autocatalytic production of H^+ is proposed to proceed according to Eq. 5.1 or 5.3 (autocatalytic in HI), which is the same for other PdI_2 concentrations investigated, with the hydrogen ion originating from HI. The next periods, consisting of slow and then slight faster production of [H^+] suggests the presence of competing reactions where H^+ is produced in the absence of autocatalysis. As such, Eq. 4.2 to 4.4, Eq. 5.1 and/or 5.3 (assumed to be slow at this point) and Eq. 4.9 (reversible formation of HI from methyl iodide and water) are proposed to account for these changes and HI patterns.

The period of gradual consumption of [H^+], corresponding to a decrease in [H^+] adjusted and lasting for 340 min, is proposed to proceed according to Eq. 4.4 (reversible carbonylation of methanol, Eq. 4.8 (oxidation of HI) and Eq. 4.9 (formation of methyl iodide and water facilitated by excess KI). And finally, the fast decline/consumption of [H^+] after the period of gradual consumption is assumed to occur during the regeneration of palladium to palladium iodide according to Eq. 4.12 and this is based on the assumption that a complete reduction of palladium iodide occurs at this point since the concentration of PdI_2 is low (17 µM) for this profile.

The period of HI consumption and stable [H^+] adjusted was followed by onset of oscillations at [PdI_2] = 22.7 µM. Oscillations commenced 379 min into the reaction at this concentration, starting off as small oscillations with amplitude equivalent to 0.04 pH units. Oscillations did not occur in reactions with [PdI_2] = 34 µM and [PdI_2] = 60.4 µM, while onset of oscillations was delayed at [PdI_2] = 17 µM.

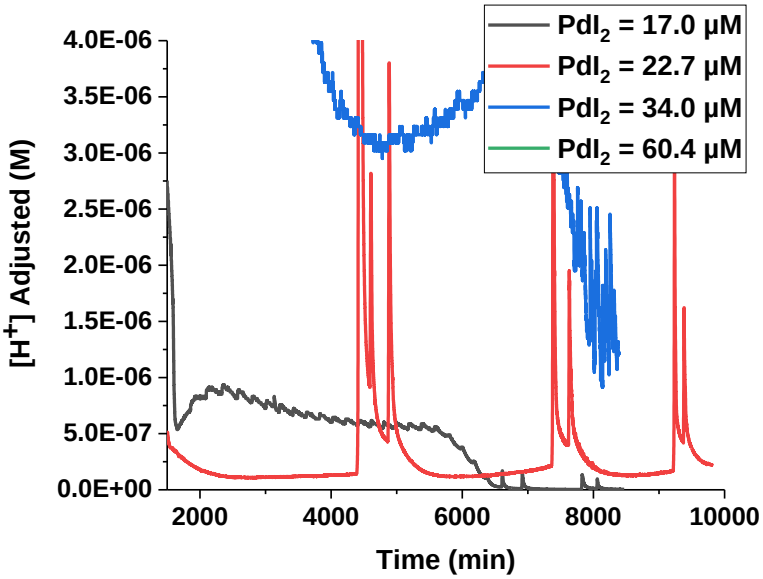

Figure 5.19. Excerpt of [H^+] adjusted profiles highlighting oscillatory modes (mixed mode) at different palladium iodide concentrations. (Temperature = 20°C±2; CO and air flowrates = 15 mL/min; [A-PEG_{2000}-A] = 1.02 mM; [KI] = 3 mM)

Although oscillations were absent at [PdI_2] = 34 µM and [PdI_2] = 60.4 µM, complex fluctuations in pH and [H^+] adjusted were observed in both profiles at various points until the experiments were terminated (Figure 5.12 and 5.14). The fluctuations are not discussed in depth as they need better characterisation to ascertain if they are present due to electrode inconsistencies or are inherent to the system. The absence of oscillations at certain reactant concentrations and reaction conditions in systems which are known to oscillate is known [10, 103] and is thought to occur when reactant concentrations and/or conditions fall outside boundaries of oscillation [103]. The small amplitude oscillations at [PdI_2] = 22.7 µM transitioned into oscillations with larger amplitudes (maxima = 1.93 pH units), presenting as mixed mode oscillations [31, 109, 110] (Figures 5.12 and 5.19) consisting first of triple peaks, and then, double peaks per oscillatory cycle. Oscillations were still ongoing when the experiment was stopped. Slightly similar mixed mode oscillations was observed in oxidative carbonylation with phenyl acetylene substrate (e.g. reacting conditions; [KI] = 0.4 M; [PdI_2] = 0.22 mM; [phenyl acetylene] = 0.1 M) [6] and from experimental and modelling studies in some biochemical systems which oscillate in mixed mode fashion [44, 98, 114, 301, 303].

The oscillations at [PdI_2] = 17 µM eventually started at 1868 min with 0.02 pH unit amplitudes and periods at 261±44 min. These small amplitude oscillations lasted for 4740 min, before transitioning to mixed mode oscillations (Figure 5.19) with double peaks per oscillatory cycle Maximum [H^+] adjusted concentration of the mixed mode oscillations was 1.69 x 10^{-7} M and generally, [H^+] at this concentration remained the least. Repeat run at this concentration was also similar, with small amplitude oscillations first and then larger amplitude oscillations (fluctuations in pH also present).

5.3.2 Reaction Profiles at 6 mM Potassium Iodide Concentration

In Section 5.3.1 the effect of varying palladium iodide concentration at constant substrate concentration was assessed at [KI] = 3 mM. The rate of formation of HI (observed as increased pH acidity) increased with increasing palladium iodide concentration irrespective of the presence or absence of oscillations. Oscillations were recorded at lower palladium iodide concentrations ([PdI_2] = 17 µM and 22.7 µM) while they were absent at [PdI_2] = 34 µM and 60.4 µM. This section follows on by assessing the influence of increasing palladium iodide concentrations at a higher KI value at the same bi-alkyne substrate concentration (1.02 mM). The concentration of KI is increased by a factor of 2 (6 mM), while the same range of PdI_2 concentrations are kept. Experimental conditions for this study are given in Table 5.4.

Table 5.4. Range of catalyst concentrations investigated in the carbonylation of bi-alkyne functionalised PEG (A-PEG_{2000}-A) substrate. (Temperature = 20^oC±2; CO and air flowrates = 15 mL/min; [KI] / [A-PEG_{2000}-A] = 5.88; V_{total} = 90 mL; stirring speed = 350 rpm)

[KI] (mM)	[PdI_2] (µM)	[A-PEG_{2000}-A] (mM)	Ratio of catalyst components [KI] / [PdI_2]	Substrate to catalyst ratio [A-PEG_{2000}-A] / [PdI_2]
6.00	17.0	1.02	352.94	60
6.00	22.7	1.02	264.32	44.93
6.00	34.0	1.02	176.47	30
6.00	60.4	1.02	99.34	16.89

Experimental pH profiles obtained from the initiation until termination of reactions for the conditions in Table 5.4 is given in Figure 5.20. A conversion of the pH profiles in Figure 5.20 by applying the method proposed in literature for non-aqueous solvents measurements following calibration with aqueous buffer [258, 259] (Eq. 4.1), gives the [H^+] adjusted profiles in Figure 5.21. Oscillations were obtained at three out of the four PdI_2 concentrations investigated. Repeats of the experimental runs in Figures 5.20 showed comparable profile

patterns and features at each palladium iodide concentration investigated and were generally reproducible. Samples of replicate runs compared with the profiles discussed in this section are given in Figure 5.22.

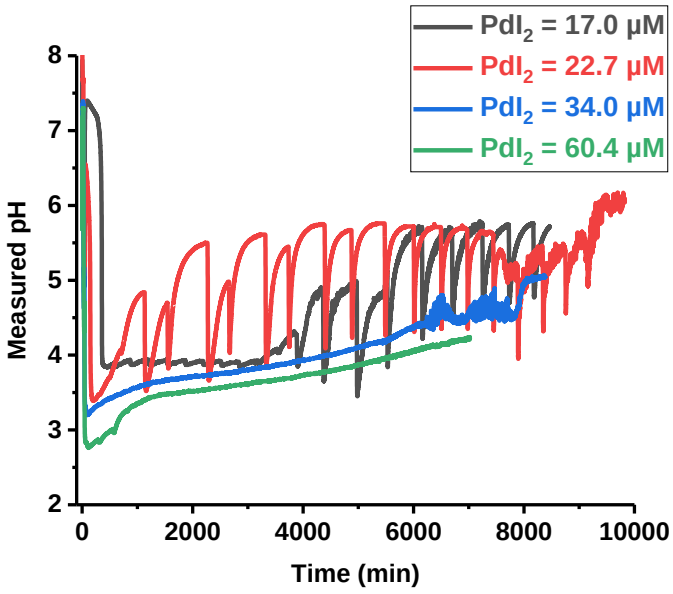

Figure 5.20. pH profiles from the carbonylation reactions of bi-alkyne functionalised polyethylene glycol substrate at various palladium iodide concentrations. ([KI] = 6 mM; [A-PEG_{2000}-A] = 1.02 mM; temperature = 20°C±2; CO and air flowrates = 15 mL/min)

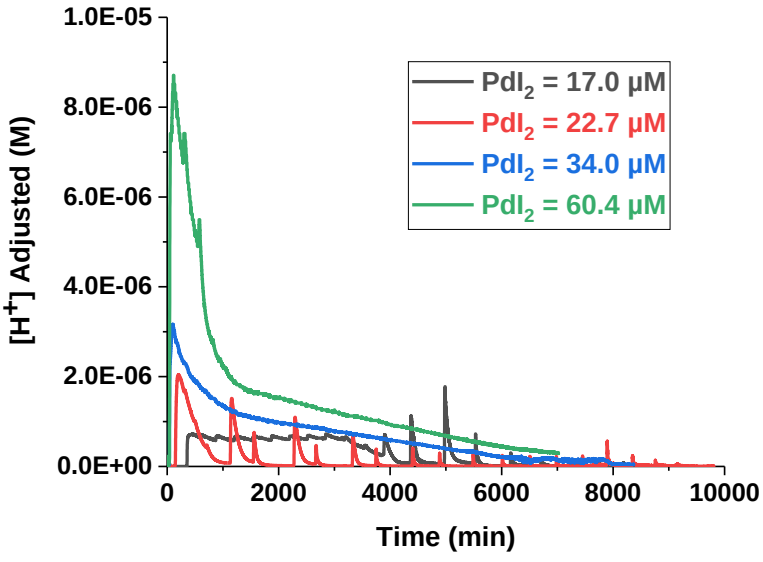

Figure 5.21. $[H^+]$ adjusted profiles from the carbonylation reactions of A-PEG_{2000}-A at various palladium iodide concentrations. ([KI] = 6 mM; [A-PEG_{2000}-A] = 1.02 mM; temperature = 20°C±2; CO and air flowrates = 15 mL/min)

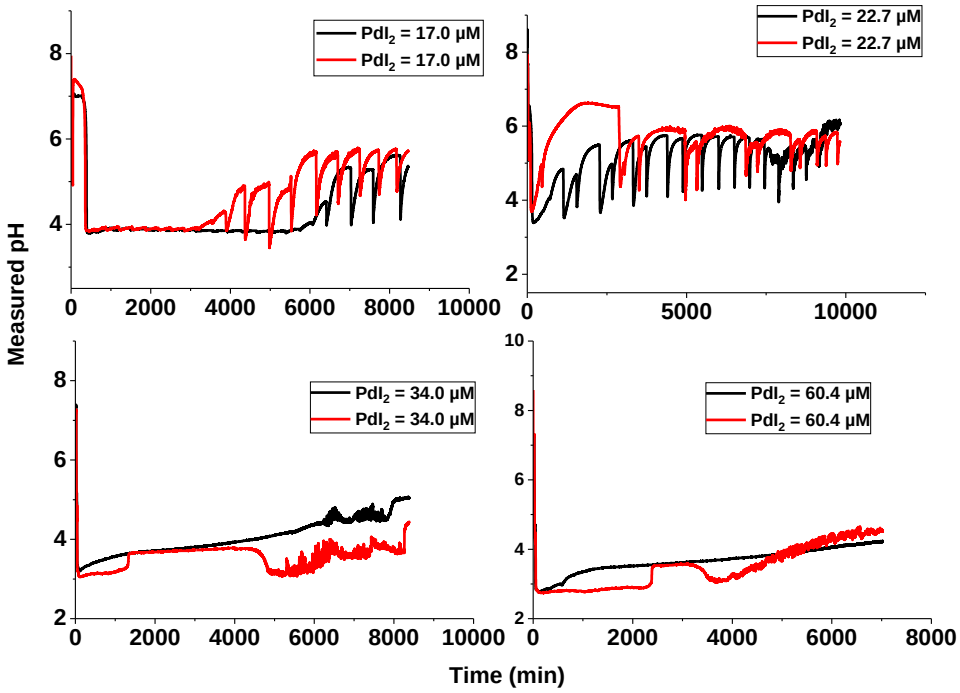

Figure 5.22. Comparison of replicate experiments with original runs obtained from the carbonylation of bi-alkyne functionalised PEG at different concentrations of PdI_2. ([KI] = 6 mM and [A-PEG_{2000}-A] = 1.02 mM)

Mixed mode oscillations (22.7 µM), complex oscillations (17 µM) and irregular pH variations within oscillations (22.7 µM after 7800 min) were recorded at [KI] = 6 mM as shown in the profiles with oscillations (Figure 5.20), while irregular pH changes (after the first 6000 min) and a "jump" / offset in pH (around 8000 min) was recorded at [PdI_2] = 34 µM. The reactions in this study proceed in a manner typical to previous discussions in earlier sections. Prior to adding catalytic mixture, solid KI was added to the methanol to bring final concentration in 90 mL of methanol to 6 mM. Addition of predefined amounts of stock catalyst solution for the reaction to methanol, caused a dip in the initial pH values (Figure 5.23) in a manner comparable to dip in pH recorded at [KI] = 3 mM. The pH of the reacting mixture was allowed to stabilize for briefly following catalyst addition, before the mixture was purged with CO and air (15 ml/min), ~ 20 minutes from onset of the reactions. pH acidity (Figure 5.23) increased on purging the reaction mixture (methanol, PdI_2 and KI); signifying the onset of reactions producing hydrogen ions.

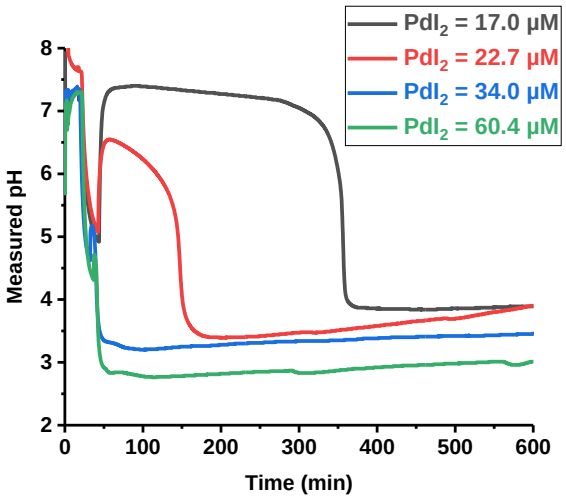

Figure 5.23. Variation in initial reaction features as a function of palladium iodide concentration at constant KI and bi-alkyne PEG concentration. ([KI] = 6 mM; [A-PEG$_{2000}$-A] = 1.02 mM; temperature = 20^{o}C±2; CO and air flowrates = 15 mL/min)

The role of catalyst in the reaction is clear as increasing the concentration of PdI_2 present in the reaction improved the rate of solvent carbonylation, thus, producing more HI (lower pH values following carbonylation). These pH drops from purging at [KI] = 6 mM were considerably less than previously reported changes when, methanol was purged in presence of PdI_2 and KI [174, 175]. However, the pH values at [PdI_2] = 60.4 µM and [PdI_2] = 34 µM (4.31 and 4.48 pH units respectively at 6 mM) are closer to reported value of ~ 3pH units at [PdI_2] = 40.5 µM and [KI] = 2.28 mM [29]. This suggests that the differences in amount (ratio) of KI in relation to PdI_2 concentration present may have affected the rate of HI formation from purging. It is also likely that other factors such as quality of methanol (quantity of residual water present), varying degrees of moisture in the gases (CO and air) used, differences in electrode type and reaction setup, contributed to differences in pH drop in this study.

A-PEG$_{2000}$-A (1.02 mM), equal to the concentration employed at [KI] = 3 mM, was added to each vessel as dissolved substrate solutions (dissolution with small methanol) following purging. Adding substrate solutions to the reactions led to decreases in [H^+] and corresponding rises in pH (Figure 5.23). As with the previous sections (Section 5.2 and 5.3.1), this decline in H^+ concentration is assumed to arise from the substrate and the small volumes of methanol introduced with the dissolved substrate. The influence of the substrate at this point requires further investigation, however, it is plausible it has an underlying effect based on the studies in Section 5.2 and Chapter 4, where degrees of rise following substrate addition increased with increasing substrate concentration. The proportion of pH rise following substrate addition decreased with increasing palladium iodide concentration as given in Figure 5.24. Reactions

with substantially higher [PdI_2] (60.4 µM and 34 µM) showed less susceptibility towards substrate addition, suggesting that the concentration of HI present prior to substrate addition further influences the degree of rise from substrate addition.

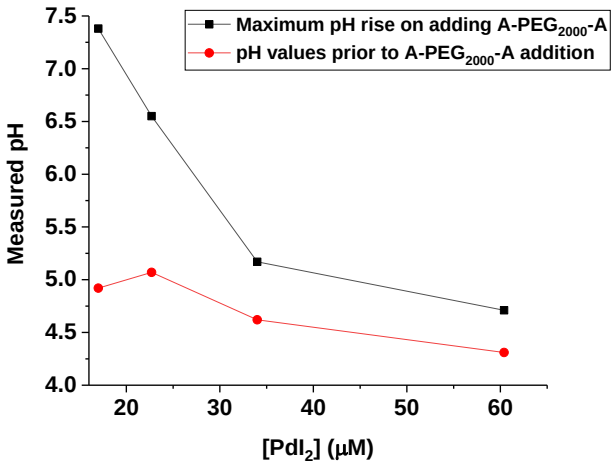

Figure 5.24. Variations in pH values recorded before and after substrate addition as a function of palladium iodide concentration. (Temperature = 20°C±2; CO and air flowrates = 15 mL/min; [A-PEG_{2000}-A] = 1.02 mM; [KI] = 6 mM)

After the substrates were added, the "slow H^+ formation" phase commenced (plateau like region of Figure 5.23). The duration for which the reactions remained in this slow phase is given in Figure 5.25 (first figure from the bottom) and, the duration of slow H^+ formation decreased as the concentration of PdI_2 increased. The maximum duration of "slow H^+ formation" occurred at [PdI_2] = 17 µM, lasting for 322 min, while the least "slow H^+ formation" duration lasted for 9 min at [PdI_2] = 60.4 µM. The dependence of the duration of this slow phase at different palladium iodide concentration is attributed to the differences in the rates of the reaction occurring at this stage (Eq. 4.2 to 4.4, 5.1 and/or 5.3). At different concentration of PdI_2, the concentrations of H^+ generated in the slow period will vary since, HI produced in these reactions is the sources of H^+ recorded experimentally.

A rapid drop in pH corresponding to increased [H^+] adjusted values marked the end of the "slow H^+ formation" phase (Figure 5.23). The autocatalytic change in pH and [H^+] values captured as rapid drop/rise respectively is given in Figure 5.26 (autocatalytic [ΔH^+] – top; autocatalytic ΔpH – bottom). The rate of rapid pH drop / rise in [H^+] values increased with increasing palladium iodide concentration and, the increased H^+ concentration suggest autocatalytic formation of HI as discussed in previous sections. Eq. 5.1 and/or Eq. 5.3 for substrate conversion, which are autocatalytic with respect to HI are assumed to account for the sharp increase in [H^+].

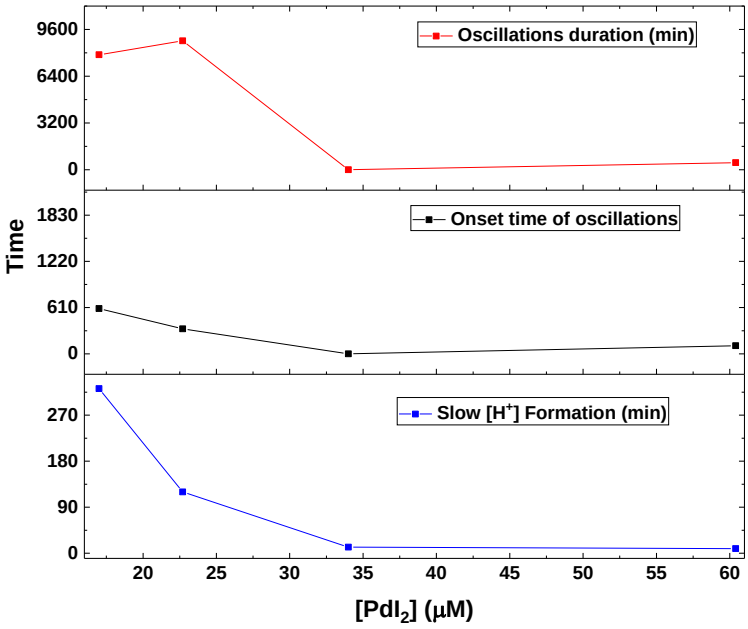

Figure 5.25. Variations in the durations of the "slow H^+ formation" phase, onset time of oscillations and length of oscillations as a function of palladium iodide concentration. ([KI] = 6 mM; [A-PEG_{2000}-A] = 1.02 mM)

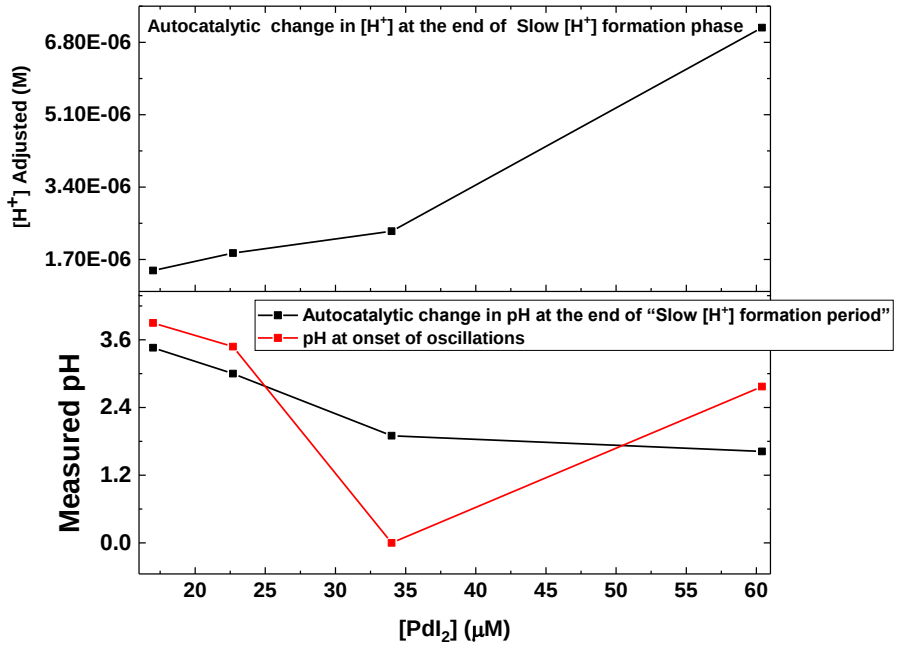

Figure 5.26. Profiles showing variations in pH and $[H^+]$ following initial autocatalysis and pH at onset of oscillations/absence of oscillations as a function of palladium iodide concentration. ([KI] = 6 mM; [A-PEG_{2000}-A] = 1.02 mM; temperature = 20°C±2; CO and air flowrates = 15 mL/min)

A period of declining H^+ (HI) concentration succeeded the rapid rise in $[H^+]$ due to autocatalysis. This fall in $[H^+]$ suggests reactions where HI is consumed and, consumption of HI based on Eq. 4.8 and 4.9 (Section 4.2, Chapter 4) support this assumption [3, 29, 30, 38, 153, 270, 271, 287-289]. The overall rate of HI consumption increased with increasing palladium iodide concentration (Figure 5.21), since the reactions with more palladium iodide generated more HI following initial autocatalysis in HI. Increased HI concentration (from autocatalysis) in these reactions (high PdI_2) is assumed to promote its conversion in this phase (HI consumption and catalyst regeneration).

In reactions with [KI] = 6 mM and palladium iodide concentrations equivalent to 22.7 µM, 34 µM and 60.4 µM, the conversion of HI was initially fast, before stabilizing (Figure 5.21). The trend at these KI and PdI_2 concentration is very similar to trends observed at [KI] = 3 mM and $[PdI_2]$ = 34 µM and 60.4 µM. A visual inspection of Figure 5.21 at $[PdI_2]$ = 17 µM and [KI] = 6 mM, reveals an absence of such initial fast rate of HI consumption observed at other PdI_2 concentrations (and [KI] = 6 mM), rather, a gradual rate of HI consumption was maintained. This trend at $[PdI_2]$ = 17 µM and [KI] = 6 mM is likewise, similar to the trend at [KI] = 3 mM and $[PdI_2]$ = 22.7 µM. The varying rates of HI consumption represented by the profiles in Figures 5.21 are credited to differences in the rates of reaction according to Eq. 4.8 and 4.9. These differences arise from the different amounts HI produced during the initial autocatalysis, which is in turn, dependent on concentration of catalytic mixture, in particular, $[PdI_2]$ present. At increased catalyst concentrations, more HI was produced via autocatalysis (Eq. 5.1 / 5.3). As the rate of Eq. 4.8 and 4.9 are dependent on concentration of HI present, increased HI concentration would increase the rate of these reactions, hence, the experiments with higher HI (from first autocatalysis) were marked with faster HI consumption rates and observed as faster decline in $[H^+]$ adjusted values (Figure 5.21).

Consumption of HI leading to decreased $[H^+]$ at [KI] = 6 mM was followed by onset of oscillations in reactions with palladium iodide concentrations equivalent to 17 µM, 22.7 µM and 60.4 µM (Figure 5.20 and 5.21). Visual inspection of reacting mixture at $[PdI_2]$ = 34 µM revealed the absence of oscillations. The presence of oscillations at $[PdI_2]$ = 60.4 µM and [KI] = 6 mM (Figure 5.20 and 5.21) contrasts the findings at $[PdI_2]$ = 60.4 µM and [KI] = 3 mM, were oscillations were absent. This trend in presence/absence of oscillations at both KI concentrations were also reproduced in repeat experiments, therefore, indicative of some reliability in the trend. Time at onset and duration of oscillations is given in Figure 5.25 (middle and top graphs respectively). Oscillations started at 107 min and lasted for 482 min, within which only 2 oscillations were recorded at $[PdI_2]$ = 60.4 µM and [KI] = 6 mM. The two

oscillations occurred during the consumption of [H^+] generated during the initial autocatalytic substrate conversion. An increase in KI concentration by a factor of 2 seems to have enabled oscillations at [PdI_2] = 60.4 µM, although only two oscillations were recorded. Increase in KI concentration facilitated oscillations in the study conducted in Chapter 4, Section 4.3, as such, it is possible that the increase in KI concentration (from 3 mM to 6 mM) may have promoted oscillations The manifestation of only two oscillations is assumed to arise from oscillation boundaries due to limiting concentration of intermediate and reacting species (substrate and catalyst) [103, 314]. Since this oscillatory reaction is quite sensitive to small changes, it is possible that other factors including loss of methanol from evaporation may have driven concentrations away from oscillatory regions.

The absence of oscillations at [PdI_2] = 34 µM and [KI] = 6 mM (Figures 5.20 and 5.21) agrees with the findings at [PdI_2] = 34 µM and [KI] = 3 mM, where, oscillations were also absent. In replicate runs, oscillation was absent for both KI concentrations at 34 µM palladium iodide concentration. Both profiles progressed with similar trends, although the reaction at [KI] = 3 mM had higher overall [H^+] values in profile reported in Section 5.3.1 and its repeat run. The onset of oscillations at [KI] = 6 mM and [PdI_2] = 17 µM and 22.7 µM occurred at 597 min and 330 min respectively (Figures 5.20 and 5.25). Oscillations were still ongoing for the run at [PdI_2] = 17 µM when the experiment was stopped.

Regions of irregular pH patterns were recorded at [PdI_2] = 34µ M and 22.7 µM after 6000 min and around 7800 min from onset of the experiments. A likeness to the irregular behaviour observed during the oscillations in this study were reported in phenyl acetylene carbonylation reaction under different concentrations and reacting conditions (methanol contained 20% water; different temperature, absence of oxygen) [30, 32, 176]. Such irregularities in measured concentration of species and voltages were also present in some modelling and experimental studies of other chemical and biochemical oscillating systems [44, 61, 62, 116, 296, 315, 316]. Defining this region of irregular pH changes in this study and replicate samples would require added investigations due to the novelty of polymeric substrate backbones in oscillatory carbonylation reactions. Nonetheless, preliminary investigations aimed at explaining this irregularity as some external influence from the equipment used (e.g. poisoning of pH probes) seems to be unlikely. Repeat studies wherein the vessels and probes were interchanged, such that reactions without pH irregularities now had vessels and probes were irregular pH was observed, did not show any anomaly. On the other hand, it is difficult to experimentally verify such aperiodic changes in oscillating systems. Thus, more directed investigated is recommended.

5.3.3 Reaction Profiles at 9 mM Potassium Iodide Concentration

This section follows on from Sections 5.3.1 and 5.3.2 in assessing the influence of increasing the potassium iodide concentration by a factor of 4 (from 3 mM to 9 mM). KI is increased while the same range of palladium iodide concentrations and constant A-PEG_{2000}-A (bi-alkyne) concentrations are assessed. The studies were carried out according to the conditions given in Table 5.5.

Table 5.5. Range of reactant concentrations investigated in the carbonylation of A-PEG_{2000}-A. (Temperature = 20°C±2; CO and air flowrates = 15 ml/min; [KI] / [A-PEG_{2000}-A] = 8.82)

[KI] (mM)	[PdI_2] (μM)	[A-PEG_{2000}-A] (mM)	Ratio of catalyst components [KI] / [PdI_2]	Substrate to catalyst ratio [A-PEG_{2000}-A] / [PdI_2]
9.00	17.0	1.02	529.41	60
9.00	22.7	1.02	396.48	44.93
9.00	34.0	1.02	264.71	30
9.00	60.4	1.02	149.01	16.89

Figures 5.27 and 5.28 show pH and [H^+] adjusted profiles obtained in the carbonylation of bi-alkyne functionalised polyethylene glycol substrate (A-PEG_{2000}-A) for the range of PdI_2 concentrations given in Table 5.5. Oscillations were recorded at all conditions investigated when [KI] = 9 mM. This differs from the reaction profiles at lower potassium iodide concentrations (3 mM and 6 mM) as oscillations were absent at some palladium iodide concentrations (oscillations were absent at [PdI_2] = 34 μM and 60.4 μM for [KI] = 3 mM and absent at [KI] = 6 mM and [PdI_2] = 34 μM). The reactions mechanism at [KI] = 9 mM was also quite similar to previously described steps in prior sections and Chapter 4. Oscillations were reproduced in repeat experiments with some variation in oscillatory modes. A comparison of replicate samples and runs in Figure 5.27 are given in Figure 5.29. The reactant addition steps were also identical to previous studies; the catalytic mixtures are added to bulk methanol, then, the reaction mixtures are purged continuously, and finally, substrate solutions are added when the pH stabilises (pH is allowed to stabilise on purging the catalytic methanol solution). The catalytic mixture consists of KI and PdI_2 in methanol and the solutions were purged with CO and air at I5 mL/min. The pH drops on purging the methanolic/catalyst mixtures prior to substrate addition because, methanol, residual water in the HPLC grade methanol, moisture from atmosphere (sealant had leaks around the probes), and possibly from CO/air (these gases were not dried before purging), are sources of hydrogen ion. pH on purging decreased

(corresponding to an increase in $[H^+]$) with increasing catalyst concentration, which is expected as the rates of Eq. 4.2 to 4.4 (solvent carbonylation) are dependent on PdI_2 concentration.

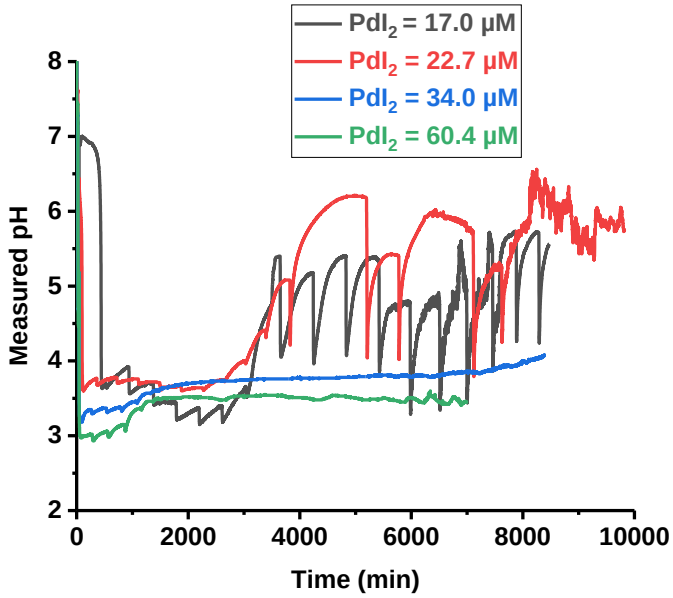

Figure 5.27. pH profiles from the carbonylation reactions of bi-alkyne functionalised polyethylene glycol at various palladium iodide concentrations. ([KI] = 9 mM; [A-PEG_{2000}-A] = 1.02 mM; temperature = 20°C±2; CO and air flowrates = 15 mL/min)

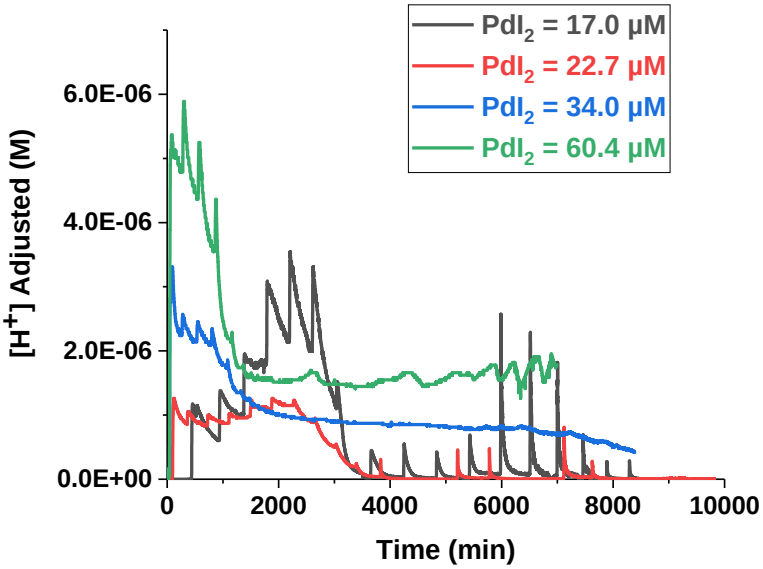

Figure 5.28. $[H^+]$ adjusted profiles from the carbonylation reactions of bi-alkyne functionalised polyethylene glycol at various palladium iodide concentrations. ([KI] = 9 mM; [A-PEG_{2000}-A] = 1.02 mM; temperature = 20°C±2; CO and air flowrates = 15 mL/min)

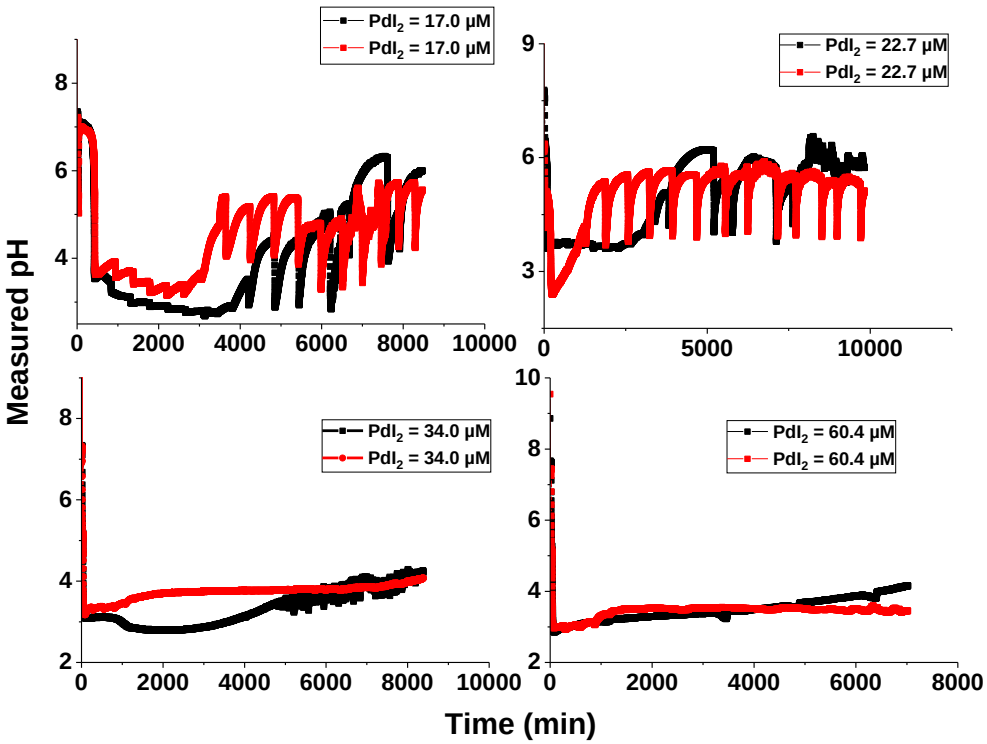

Figure 5.29. Comparison of replicate experiments with original runs obtained from the carbonylation of bi-alkyne functionalised PEG at different concentrations of PdI_2. ([KI] = 9 mM and [A-PEG_{2000}-A] = 1.02 mM)

The addition of substrates ([A-PEG_{2000}-A] = 1.02 mM) resulted in a decrease in H^+ concentration, corresponding to a rise in pH. The increase in pH after substrate addition is proposed to arise from the substrate and methanol introduced with the substrate solution. Additional methanol is assumed to facilitate the rise in pH as methanol has been linked to the rise in pH under different conditions with the phenyl acetylene oscillatory system [10, 32, 173-175, 177, 242, 243] and also, initial studies presented in Chapter 4, Section 4.2 support this postulation. The mechanism behind pH rises due to substrate interactions requires further investigations and is not discussed; instead, reference is made to Section 5.2 where, increase in substrate concentration led to increase in degree of pH rise on substrate addition. The rate of decrease in [H^+], corresponding to rise in pH on addition of substrate, decreased with increasing PdI_2 concentration. The trend showing this decrease as a function of palladium iodide concentration is given in Figure 5.30. The decreasing trend is suggested to occur because the reactions at lower PdI_2 concentrations already had less HI from purging, hence, the addition of substrate solutions produced more rise in pH. The decrease in H^+ concentration from substrate addition was followed by the "slow H^+ formation" phase wherein, the hydrogen ion concentration gradually increases. The durations of this slow hydrogen ion formation phase are given in Figure 5.31.

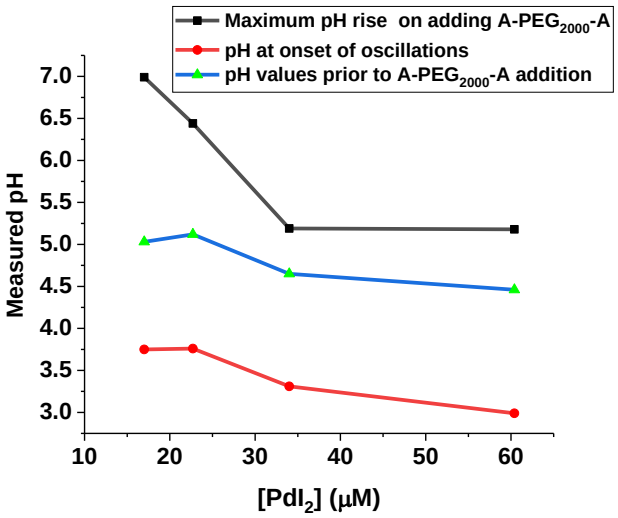

Figure 5.30. Changes in pH at key points in the oxidative carbonylation of bi-alkyne polyethylene glycol substrate at different palladium iodide concentrations. ([KI] = 9 mM and [A-PEG$_{2000}$-A] = 1.02 mM)

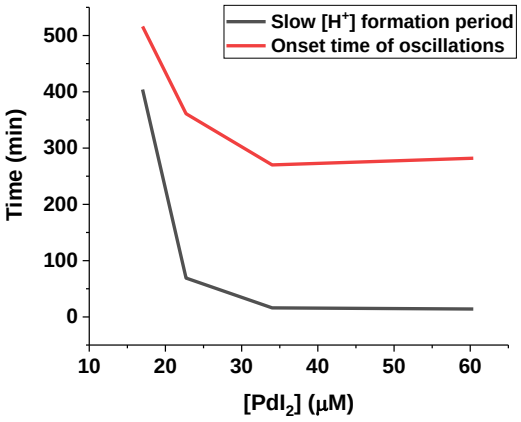

Figure 5.31. Variation in "slow H^+ formation" phase and onset time of oscillation at different palladium iodide concentration. ([KI] = 9 mM and [A-PEG$_{2000}$-A] = 1.02 mM)

The length of time each experimental run spent in the "slow H^+ formation" state decreased with increasing palladium iodide concentration at [KI] = 9 mM. This duration is smaller at higher PdI_2 concentrations since increased palladium iodide concentration improved the rate of HI formation. When HI is formed at a faster rate, less time is needed to overcome the slow phase. Initial autocatalytic HI formation from substrate consumption marked the end of the slow phase. This initial autocatalysis is observed as the first set of rapid increases in $[H^+]$ adjusted and sharp declines in pH before the onset of oscillations. The autocatalytic changes in pH at the end of the slow phase is given in Figure 5.32 as ΔpH and $[\Delta H^+]$. ΔH^+ concentration increased with increasing palladium iodide concentration at [KI] = 9 mM supporting Eq. 5.1/5.3 (autocatalytic substrate conversion) which proceed at faster rates when more PdI_2 is present [286] .

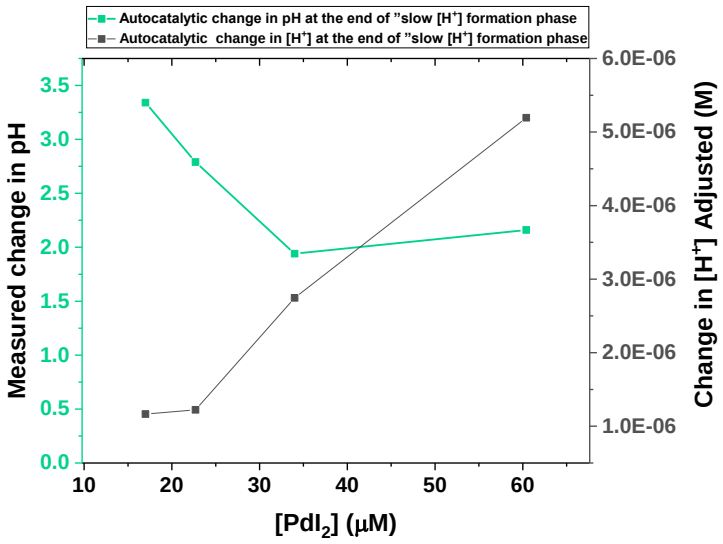

Figure 5.32. Changes in pH and [H^+] adjusted following the first autocatalytic HI formation as a function of palladium iodide concentrations at constant bi-alkyne functionalised polyethylene glycol and KI concentration

For reactions at [KI] = 9 mM, the autocatalytic production of HI was followed by short periods of decline in H^+ concentration before oscillations commenced. The decline in hydrogen ion concentration is assumed to proceed according to Eq. 4.8 and 4.9, where HI oxidation and nucleophilic substitution of hydroxyl group on methanol to form methyl iodide and water are suggested as reason for reduction in H^+ concentration. Oscillations commenced in all runs as HI consumption continued. Trends in Figures 5.30 and 5.31 show the pH and times at onset of oscillation respectively. pH and onset time of oscillations decreased as palladium iodide concentration increased suggesting that higher PdI_2 concentrations promote the onset of oscillations.

The presence of oscillations at [PdI_2] = 60. 4 μM and [KI] = 9 mM (Figures 5.27 and 5.28) agrees with oscillations at [PdI_2] = 60. 4 μM and [KI] = 6 mM, and both contrast the findings at [PdI_2] = 60. 4 μM and [KI] = 3 mM, were oscillations were absent. The oscillations at [KI] = 9 mM lasted for 1096 min, within which 4 visible oscillations were recorded, as against 482 min and 2 oscillations at [KI] = 6 mM and no oscillations at [KI] = 3 mM. The oscillations recorded also occurred during the decline in [H^+] (HI oxidation) after autocatalysis and this corresponds to the previously described initial regions of faster HI consumption (Section 5.3.2). An increase in KI concentration from 6 mM to 9 mM seems to have promoted oscillations at [PdI_2] = 60. 4 μM as the number of oscillations increased. Such increase was also noted in replicate experiments (Figure 5.29).

The presence of oscillations at [PdI_2] = 34 µM and [KI] = 9 mM (Figures 5.27 and 5.28) contrasts the findings at [PdI_2] = 34 µM and [KI] = 6 mM (Figures 5.20 and 5.21) and [PdI_2] = 34 µM and [KI] = 3 mM (Figures 5.12 and 5.14), where oscillations were both absent. The occurrence of oscillations seems to have been facilitated by the increase in KI, suggesting that, availability of extra iodide ions promotes the oscillatory mode of A-PEG_{2000}-A carbonylation at [PdI_2] = 34 µM. Similar trends were noted in replicate samples with respect to presence or absence of oscillations.

Oscillations were present at all KI concentrations investigated for [PdI_2] = 17 µM and 22.7 µM. The onset of oscillations at [KI] = 9 mM and [PdI_2] = 17 µM and 22.7 µM occurred at 516 min and 361 min respectively (Figure 5.31). Oscillations were still ongoing for the run at [PdI_2] = 17 µM when the experiment was stopped, while irregular pH behaviour similar to observations at [KI] = 6 mM (Section 5.2.3) was observed at [PdI_2] = 22.7 µM before the reaction was terminated.

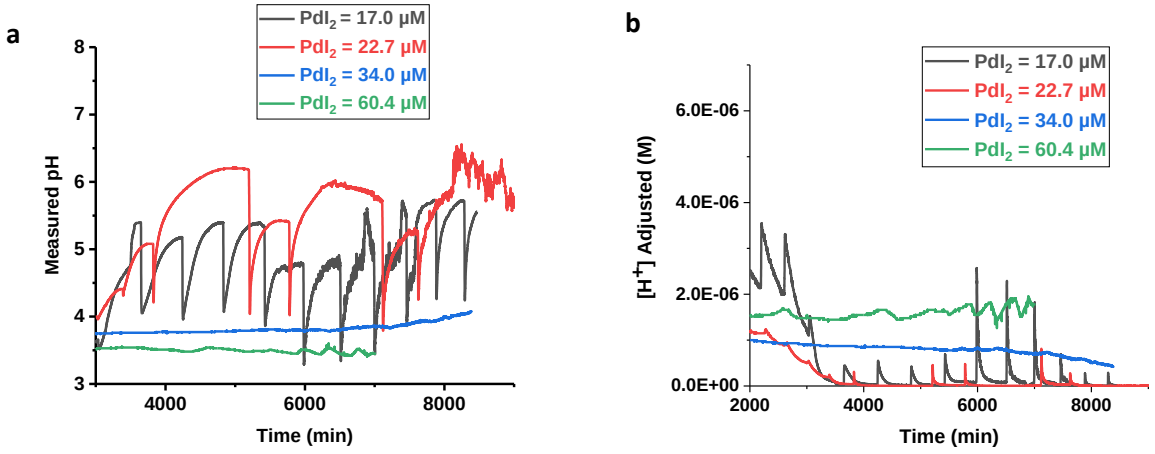

Figure 5.33. Segments of pH profiles highlighting oscillations during the carbonylation reactions at various palladium iodide concentration (a). Corresponding [H^+] adjusted profiles (b)

Figure 5.33(a-b) show the complexities of oscillations occurring at [KI] = 9 mM. Simple oscillations which transitioned to mixed mode oscillations [31, 109] with double peaks were observed at [KI] = 9 mM and [PdI_2] = 22.7 µM, while simple oscillations with brief intervals of complex oscillations [95] (≈ 3090 to 3660 min and ≈ 6995 to 7887 min) were recorded at [KI] = 9 mM and [PdI_2] = 17 µM. Complex/compound oscillations were observed in phenyl acetylene carbonylation reaction [30] and some coupled continuous oscillating reactions [95, 96]. These oscillations occurred when one of the oscillators from the coupled set becomes entrained in the other. This feature is explained in greater detail in Chapter 6.

5.3.4 Section Summary

Graphical summaries of studies in Subsections 5.3.1, 5.3.2 and 5.3.3 are presented in Figures 5.34 to 5.37 and discussed in this section. Comparison of slow phase prior to initial autocatalysis is given in Figure 5.34.

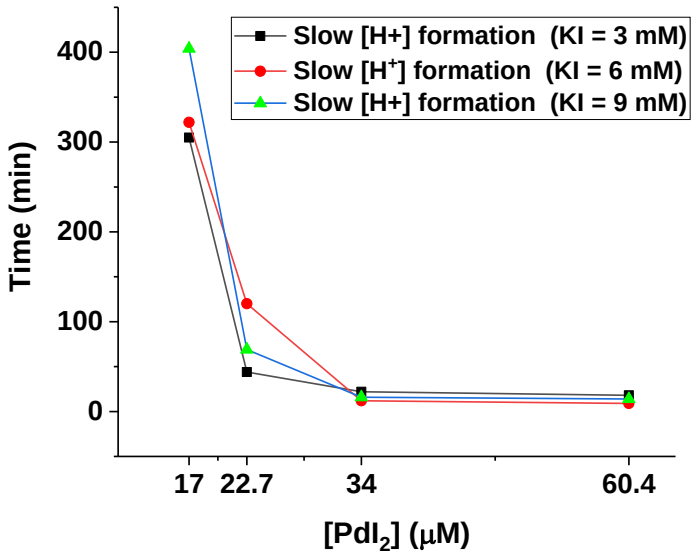

Figure 5.34. Comparison of duration of "slow H^+ formation" phase as a function of palladium iodide concentration at various KI concentrations. ([KI] = 9 mM; [A-PEG_{2000}-A] = 1.02 mM; temperature = 20°C±2; CO and air flowrates = 15 mL/min)

The duration recorded on increasing the KI concentration by a factor of 4 ([KI] = 9 mM) differed from duration at [KI] = 3 mM and [KI] = 6 mM. The duration of "slow H^+ formation" decreased with increasing PdI_2 concentrations and constant KI concentrations. Some differences were however observed on comparing "slow H^+ formation" durations at increasing KI concentration and constant PdI_2 concentrations. Increasing the KI concentration from 3 mM to 9 mM resulted in an increase in the duration of "slow H^+ formation" (time at [KI] = 3 mM < [KI] = 6 mM < [KI] = 9 mM) at [PdI_2] = 17 µM, with an average of time of 343.7±49.5 min (Figure 5.34). At PdI_2 concentration corresponding to 22.7 µM, the duration at [KI] = 3 mM < [KI] = 9 mM < [KI] = 6 mM with 77.7±38 min average time and deviation. A further increase in PdI_2 concentrations to 34 µM and 60. 4 µM resulted in comparable slow HI phase times and the duration at KI = 3 mM > KI = 9 mM > KI = 6 mM. The effects of increased KI concentration on the duration of slow H^+ formation at constant PdI_2 concentration is less obvious at higher palladium iodide concentrations (34 µM and 60. 4 µM), as indicated by the closeness of the data points in Figure 5.34. Average values of plateau times at 34 µM and 60. 4 µM PdI_2 concentrations were 16.7±5 min and 13.7±4.5 min respectively. The reduced influence and smaller periods observed at higher PdI_2 concentrations may be attributed to the increased HI

concentrations in these reactions from purging, which limited the rise in pH from substrate addition, and in effect, lessened time spent in "slow H^+" phase. Reproducibility in terms of duration of "slow H^+ formation" phase also improved with increasing palladium iodide concentration.

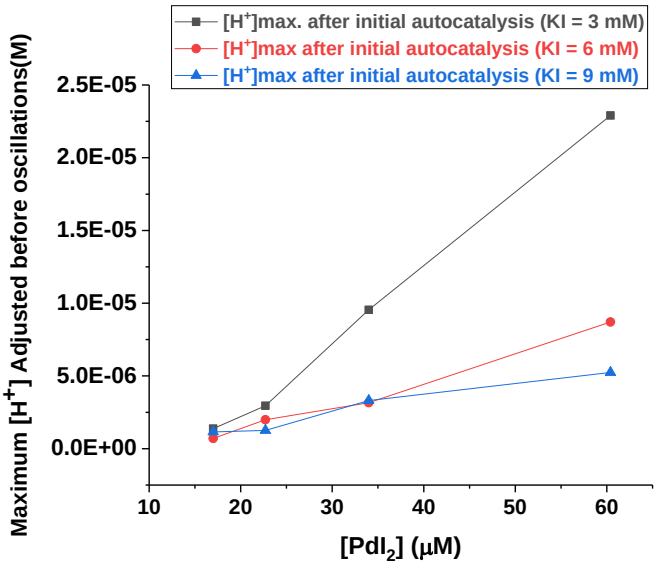

Figure 5.35. Maximum $[H^+]$ concentrations attained from initial autocatalytic HI formation at the end of the slow phase at different KI and PdI_2 concentrations. ($[A\text{-}PEG_{2000}\text{-}A]$ = 1.02 mM; temperature = 20°C±2; CO and air flowrates = 15 mL/min)

A comparison of the concentration of H^+ following the first autocatalytic formation of HI at the end of the slow phase as a function of concentration of KI present in the reaction is given in Figure 5.35. The rate of initial autocatalytic HI formation (according Eq. 5.1/Eq. 5.3) appears to be inversely proportional to the concentration of KI and directly proportional to the concentration of PdI_2. This assumption is made because H^+ concentrations decrease with increasing KI concentrations and, increase with increasing PdI_2 concentrations in Figure 5.35. The direct relationship between HI formation and palladium iodide concentration agrees with known influence of catalyst on chemical reactions [2, 284-286] which also supports Eq. 5.1 / Eq. 5.3. The inverse relation between autocatalytic HI formation and KI concentrations suggests that the presence of excess iodide ions and/or iodine from KI reduces the rate of autocatalytic HI formation. Some form of equilibrium condition may exist when KI is in so much excess, hence, limiting the dissociation of HI formed. Previous studies [3, 137, 148, 156, 172, 269, 270, 317] support the addition of KI since it promotes catalyst regeneration and dissolution, however, the trend presented in Figure 5.35 for oscillatory oxidative carbonylation appears to contrast this claim. The reduction in HI formed at higher KI and PdI_2 concentrations

suggest the possibility of some optimum concentration, above which KI concentration limits the autocatalytic formation of HI at substrate concentration investigated ([A-PEG_{2000}-A] = 1.02 mM). As smaller concentrations of KI (KI < 3 mM) were not assessed for the range of PdI_2 concentrations considered in this study, it is not possible to state or offer a suitable ratio or KI concentration to further support this assumption. Nonetheless, smaller KI to PdI_2 ratios (e.g. 10:1) which resulted in high product yields [137, 271, 318], were employed in oxidative carbonylation reactions at different conditions. This is significantly smaller than 100 parts equivalents employed in current study.

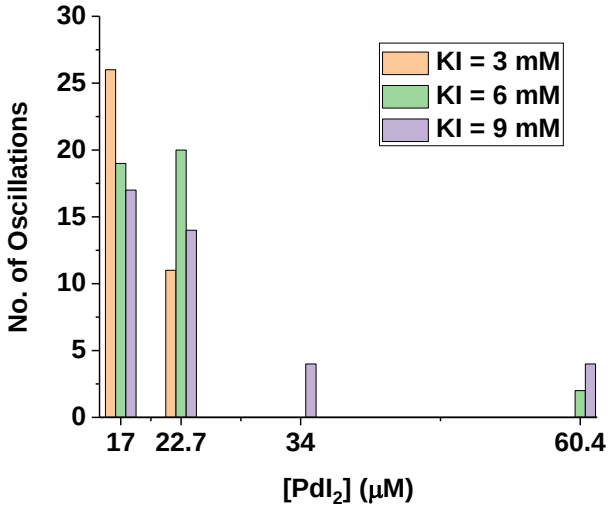

Figure 5.36. Number of oscillations in reaction profiles from the carbonylation of A-PEG_{2000}-A as a function of palladium iodide and potassium iodide concentrations

A summary of number of oscillations at various catalyst concentrations investigated is given in Figure 5.36. The general trend shows that more oscillations were recorded at lower palladium iodide concentrations, while the most frequent potassium iodide concentration that encouraged oscillations was at [KI] = 9 mM. At [KI] = 9 mM, the number of oscillations decreased with increasing palladium iodide concentration, though this trend was also observed at other KI concentrations. The frequency of oscillations at [KI] = 9 mM supports the postulation that KI promotes oscillations. The reduction in number of oscillations / absence of oscillations at higher palladium iodide concentrations and reduced KI concentrations also agrees this assumption. Number of oscillations in replicate samples differed, however, the overall trend was similar to Figure 5.36. Various complex features were observed in the studies discussed in Section 5.3. A phase diagram illustrating these oscillatory and non-oscillatory features is given in Figure 5.37.

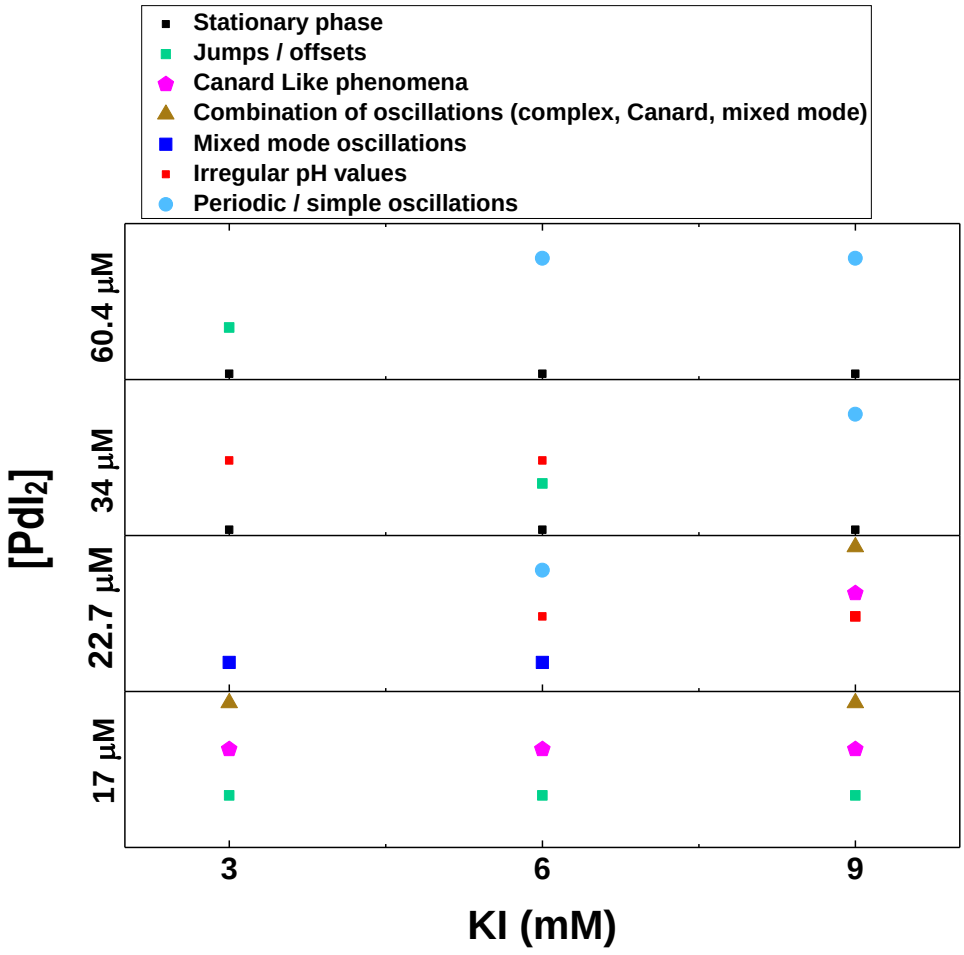

Figure 5.37. Phase diagram of oscillatory and non-oscillatory features in reaction profiles from the carbonylation of A-PEG$_{2000}$-A as a function of palladium iodide and potassium iodide concentrations

Non-oscillatory phases were present at higher catalyst concentrations irrespective of the KI concentrations employed. Jumps and pH offsets were prominent at various catalyst concentrations and cut across all KI concentrations investigated. Simple oscillations were found at higher KI concentrations and was absent at [KI] = 3 mM. Mixed mode oscillations occurred only when was [PdI_2] = 22.7 µM. Canard like phenomena (transition from small amplitude to large amplitude oscillations) and a combination of Canards and mixed-mode oscillations were presents at lower catalyst concentrations and cut across KI concentrations investigated. pH irregularities were also a common feature of the profiles at [PdI_2] = 22.7 µM and 34 µM.

In conclusion

1. Oscillations in the oxidative carbonylation reactions were absent at 34 µM catalyst concentration and [KI] = 3 mM and 6 mM at 1.02 mM bi-alkyne substrate concentration. Oscillations were present on increasing KI concentration to 9 mM.

2. At 1.02 mM bi-alkyne substrate concentration, oscillations were recorded at 17 µM and 22.7 µM catalyst concentrations and KI = 3 mM, 6 mM or 9 mM and at 60.4 µM catalyst concentration at KI = 6 mM or 9 mM.
3. Mixed mode and/or complex oscillations were recorded in oxidative carbonylation reactions employing bi-alkyne functionalised PEG substrate at 1.02 mM with catalyst concentrations at 17 µM and 22.7 µM.
4. KI appears to promote oscillations and increasing the concentration of palladium iodide reduced the number of oscillations recorded for the range studied (17 µM to 60.4 µM).
5. Duration of the phase termed "slow H^+ formation" decreased with increasing palladium iodide concentration due to increased rate of HI formation.
6. Increased KI concentration did not alter the duration of "slow H^+ formation" appreciably at higher palladium iodide concentrations (34 µM and 60.4 µM), however, at lower PdI_2 concentrations (17 µM and 22.7 µM), for [KI] > 3 mM an increase in duration of "slow H^+ formation" was observed.
7. Initial autocatalytic formation of HI was hindered at higher concentrations of KI ([KI] > 3 mM) and constant substrate concentration, suggesting the existence of some form of equilibrium condition on HI formation due to excessive KI (iodide) ions present.
8. Effective rate is proposed for autocatalytic generation of HI from substrate conversion due to presence of two alkyne groups.
9. pH rises on substrate addition decreased on increasing catalyst concentration, possibly due to the increase in HI concentrations generated in the reactions with higher catalyst concentrations during purging.

Chapter 6. Comparative Analysis of Reaction Profiles from the Carbonylation of Mono Alkyne and Bi-Alkyne Functionalised Polyethylene Glycols and Further Considerations of Complex Experimental Phenomena.

6.1 Introduction

Oscillatory and non-oscillatory modes in the oxidative carbonylation of mono alkyne functionalised polyethylene glycols and bi-alkyne functionalised polyethylene glycols were assessed in Chapters 4 and 5, respectively. A variety of phenomena including pH offsets / transitions / jumps in reaction profiles during stationary and oscillatory modes, mixed mode oscillations, complex oscillations and pH irregularities (aperiodic) were present in the diverse range of oscillations from experimental studies reported in both chapters. In this chapter, the effects of the number of alkyne functional groups per polymeric substrate chain is considered. The above-mentioned phenomena, and a comprehensive reaction scheme proposed for both substrates are likewise discussed. Studies on possible impacts from the number of alkyne groups per chain was accomplished by comparing profiles obtained from the carbonylation of mono alkyne (A-PEG$_{2000}$) and bi-alkyne (A-PEG$_{2000}$-A) functionalised polyethylene glycols substrate at selected substrate concentrations and constant catalyst (PdI_2) concentrations. As with earlier chapters, the catalyst used was introduced as a catalytic mixture consisting of palladium iodide dissolved with the aid of potassium iodide in methanol. The range of reactant concentrations, catalyst concentration and reacting conditions for the comparative analysis of number of alkyne end groups present is given in Table 6.1.

Table 6.1. Reactant concentrations employed in determining the influence of number of alkyne groups on oscillatory carbonylation reactions. (V_{total} = 90 mL; stirring speed = 350 rpm; CO and air flow rates = 15 mL/min; temperature = 20±0.2^{o}C).

[PdI_2] (μM)	[KI] (mM)	[A-PEG$_{2000}$-A] (mM) (Substrate)					[A-PEG$_{2000}$] (mM) (Substrate)				
29	5.7	0.254	0.508	1.02	1.52	2.03	0.508	1.02	1.52	2.03	3.05
22.7	6.0	1.02					1.02			2.03	
17	6.0	1.02					1.02			2.03	

6.2. Influence of Number of Functional Groups as a Function of Substrate Type at Various Substrate Concentrations and Constant Catalytic Concentration ([PdI_2] = 29 μM and [KI] = 5.7 mM).

The influence of number of alkyne end groups per polymeric substrate chain at constant catalytic concentration ([PdI_2] = 29 μM and [KI] = 5.7 mM) was assessed by considering two instances. The first case considers the influence of the number of alkyne end groups in the substrate chains at equal concentrations of mono alkyne and bi-alkyne functionalised polyethylene glycol substrates. By keeping equal concentrations of both alkyne polyethylene glycol substrates, the intention is to have twice as much alkyne ends in one reaction. This means that, the actual concentration of the alkyne end functionality in the bi-functional polyethylene glycol (A-PEG_{2000}-A) substrate becomes twice the concentration of alkynes in the mono-alkyne substrate (A-PEG_{2000}), in the first instance. The second case studies the effects of the number of alkyne end groups in both polymeric substrates by using twice as much mono alkyne substrate (A-PEG_{2000}) for any bi-alkyne substrate (A-PEG_{2000}-A) concentration investigated ([A-PEG_{2000}] ≈ 2 x [A-PEG_{2000}-A]). By using two times the concentration of mono alkyne substrate, the actual concentration of alkyne end functionality in both reactions with mono and bi-functional substrates is kept approximately constant.

6.2.1 Influence of Number of Alkyne Functional Groups – Case A: Equal Mono Alkyne and Bi-Alkyne Functionalised Polyethylene Glycol Substrate Concentrations

In this section, studies relating to the first scenario, wherein, equal concentrations of mono alkyne and bi-alkyne functionalised substrates are employed in carbonylation reactions at constant catalytic (PdI_2 and KI) concentrations, is investigated. This scenario at equal substrate concentration is denoted as "Case A" here and throughout this chapter. Concentrations studied at equal mono and bi-alkyne substrate concentrations and constant palladium iodide (catalyst) and KI concentrations are given in Table 6.2.

Table 6.2. Reactant concentrations employed in determining the influence of the number of alkyne groups at equivalent substrate concentrations. (V_{total} = 90 mL; stirring speed = 350 rpm; CO and air flow rates = 15 mL/min; temperature = 20±0.2^oC).

[PdI_2] (μM)	[KI] (mM)	[A-PEG_{2000}-A] (mM)	[A-PEG_{2000}] (mM)
29	5.7	0.508	0.508
29	5.7	1.02	1.02
29	5.7	1.52	1.52
29	5.7	2.03	2.03

pH and corresponding [H^+] adjusted profiles obtained from the carbonylation reactions at equal concentrations of both substrates for the range of concentrations investigated (Table 6.2) is given in Figure 6.1 and 6.2, respectively.

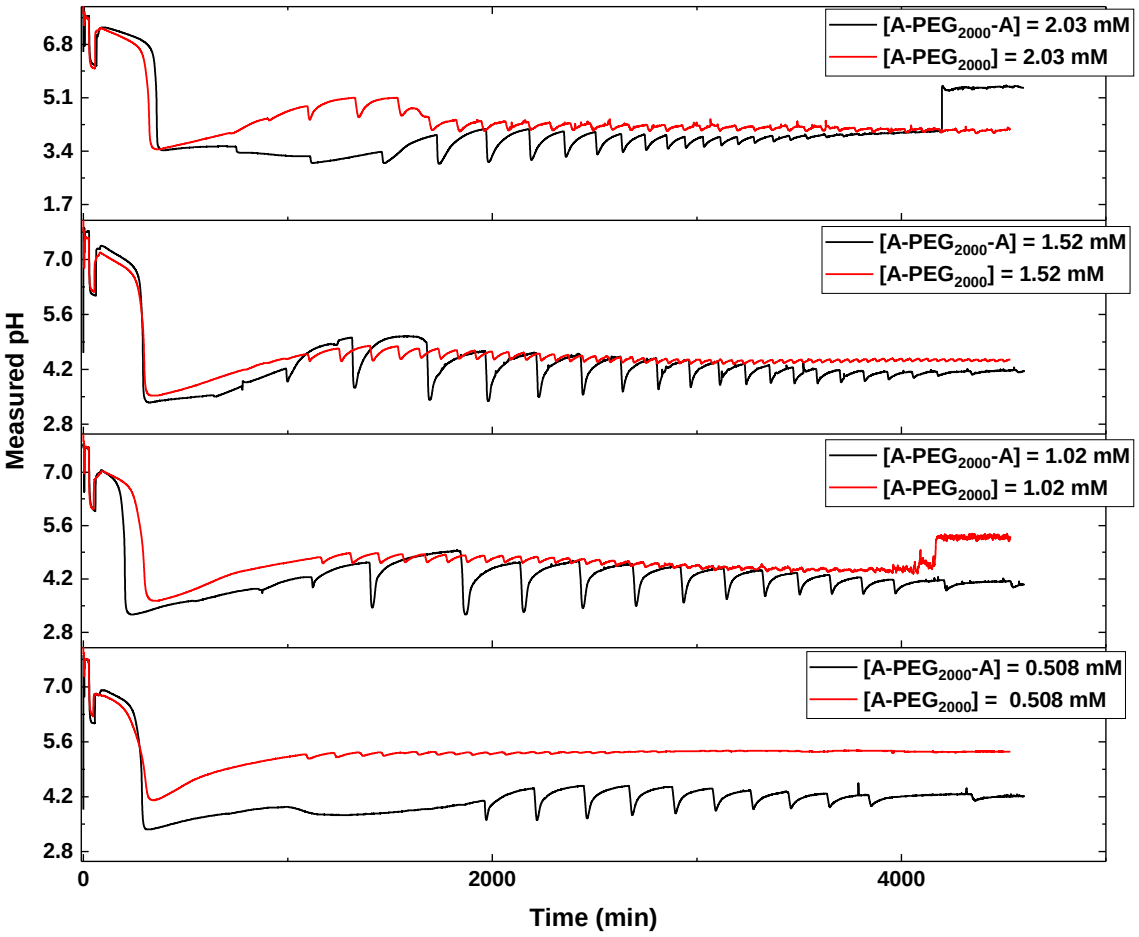

Figure 6.1. pH profiles recorded in the oscillatory carbonylation reactions employing equal concentrations of mono alkyne (A-PEG_{2000}) and bi-alkyne (A-PEG_{2000}-A) functionalised polyethylene glycol as reaction substrates at constant catalytic concentration. (V_{total} = 90 mL; CO and air flow rates = 15 mL/min; [KI] = 5.7 mM; [PdI_2] = 29 μM)

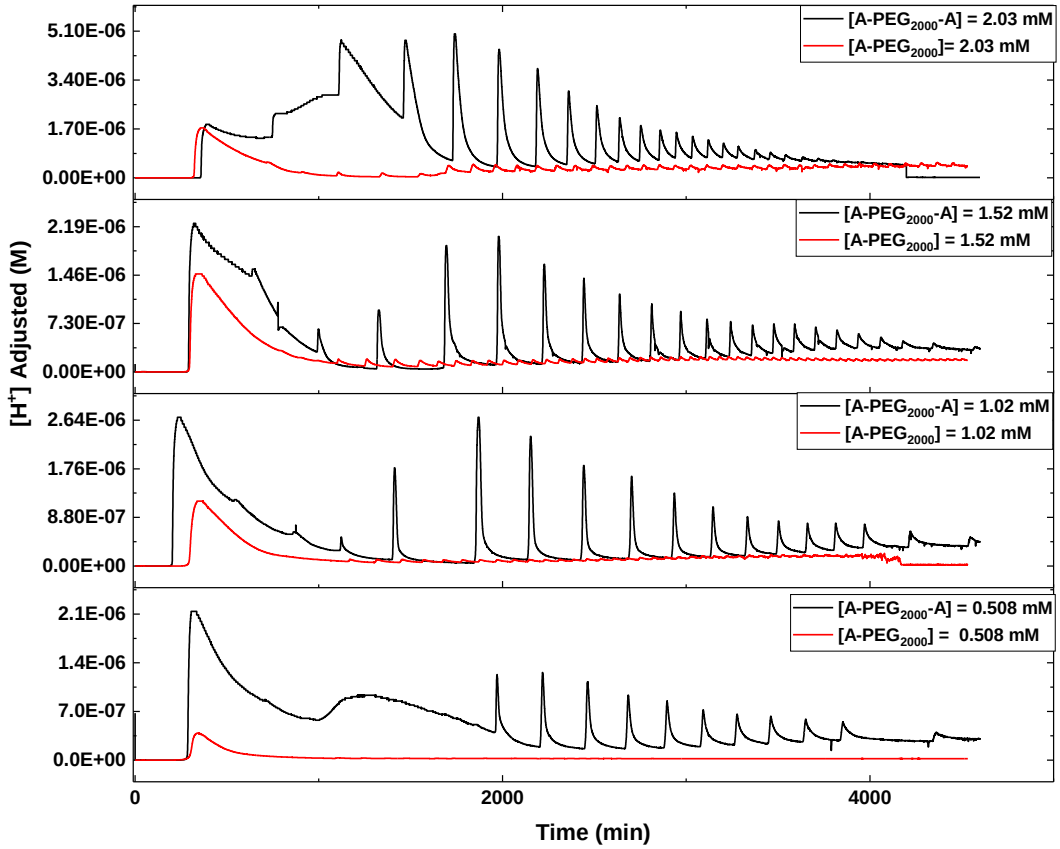

Figure 6.2. $[H^+]$ adjusted profiles obtained from carbonylation reactions employing equal concentrations of mono alkyne (A-PEG_{2000}) and bi-alkyne (A-PEG_{2000}-A) functionalised polyethylene glycol as reaction substrates at constant catalyst concentration. (V_{total} = 90 mL; CO and air flow rates = 15 mL/min; [KI] = 5.7 mM; $[PdI_2]$ = 29 μM)

Simple oscillations with varying amplitudes and periods were obtained at equal concentrations of mono and bi-alkyne functionalised PEG substrates. Larger amplitudes and periods were observed with bi-alkyne functionalised substrates, where the actual concentration of alkyne end groups was twofold. The amplitudes and periods for the mono alkyne functionalised substrate increased with increasing substrate concentration, however, the measured pH and calculated $[H^+]$ values were significantly less than the reactions with bi-alkyne functionalised substrates. Sudden transitions / jumps to higher pH values during oscillations [26, 89, 92, 94, 195, 296] were noted in mono alkyne substrates at 1.02 mM and 2.03 mM towards the termination of the reactions. This behaviour is discussed in detail in a later section of this chapter.

The profiles obtained at equivalent substrate concentrations follow similar reactant addition steps as profiles discussed in earlier chapters. pH trends during the initial stages of the reactions including reactant addition and transition to oscillatory phases are given in Figure 6.3. The

initial dip in pH, which reverts almost immediately to its original value in Figure 6.3 represented by the arrows labelled "1", occurs on addition of catalytic mixture (PdI_2, KI in methanol) to bulk methanol for the reaction. This dip is proposed to be of ionic nature since the addition of catalytic mixture introduces more ions to the methanol in the reaction vessel. The alteration of the total concentrations of ions present is assumed to change the ionic strength [260-268] of methanol, which is observed as dips in pH. A slight difference (0.07 pH units) in the initial pH values on initiating the reactions is observed in Figure 6.3 (1.52 mM substrate concentration) though the reacting vessels contained only methanol. This difference becomes more obvious after the catalytic mixture (KI /PdI_2) is added and allowed to equilibrate. The observed difference is attributed to small variations in the quality of the methanol, since it was used as received from Sigma Aldrich, and both experiments were performed on different days with different bottles of methanol. Additionally, slight variations between pH probes and values following calibration may have also contributed to the observed difference.

The addition of the catalytic mixture to each reaction was followed by a brief period of pH stabilisation, before purging with CO and air was commenced. The onset of purging is indicated by the arrow labelled "2" in Figure 6.3. pH decreased on purging due to H^+ production from carbonylation of methanol and residual water present. The HPLC grade methanol, which was used as received from Sigma Aldrich, contains small amounts of water (Chapter 3) and is assumed to be a source of water. It should also be noted that CO and air used in this study were not pre-dried and the system was not entirely isolated from the atmosphere (sealant had gaps round the pH and temperature probe), possibly introducing more water (moisture) to the system. Similar trends showing decrease in pH on purging were reported in oscillatory carbonylations with phenyl acetylene as reaction substrate [8-10, 30, 32, 173-175, 177, 242]. Since studies with phenyl acetylene share comparable initial stages to the process studied here, previously proposed reactions (Eq. 4.2 to 4.4, Section 4.2, Chapter 4) describing the drop in pH on purging [8, 11, 30, 32, 38, 103, 174, 198] are suggested as mechanisms for the rise in H^+ concentration.

As purging with CO and air continued, the increase in $[H^+]$ was similar, but not identical in all reactions though PdI_2 and KI concentrations remained constant. These variations in $[H^+]$ produced (see Figure 6.3, top and bottom profiles) are mostly ascribed to variances in water / moisture present in the methanol, gases, atmosphere etc. These differences in H_2O present affect the rates of Eq. 4.2 and Eq. 4.3 and consequently, the concentration of HI produced. Hence, for reactions with similar $[H^+]$ increment on purging (region indicated by arrow "2") (Figure 6.3, inner profiles (1.52 and 1.02 mM)), the water content and consequent reactions are

presumably fairly similar. Slight variation in pH values from using different pH probes is also considered as a minor contributor to variations in measured pH (H^+ activity) at this point.

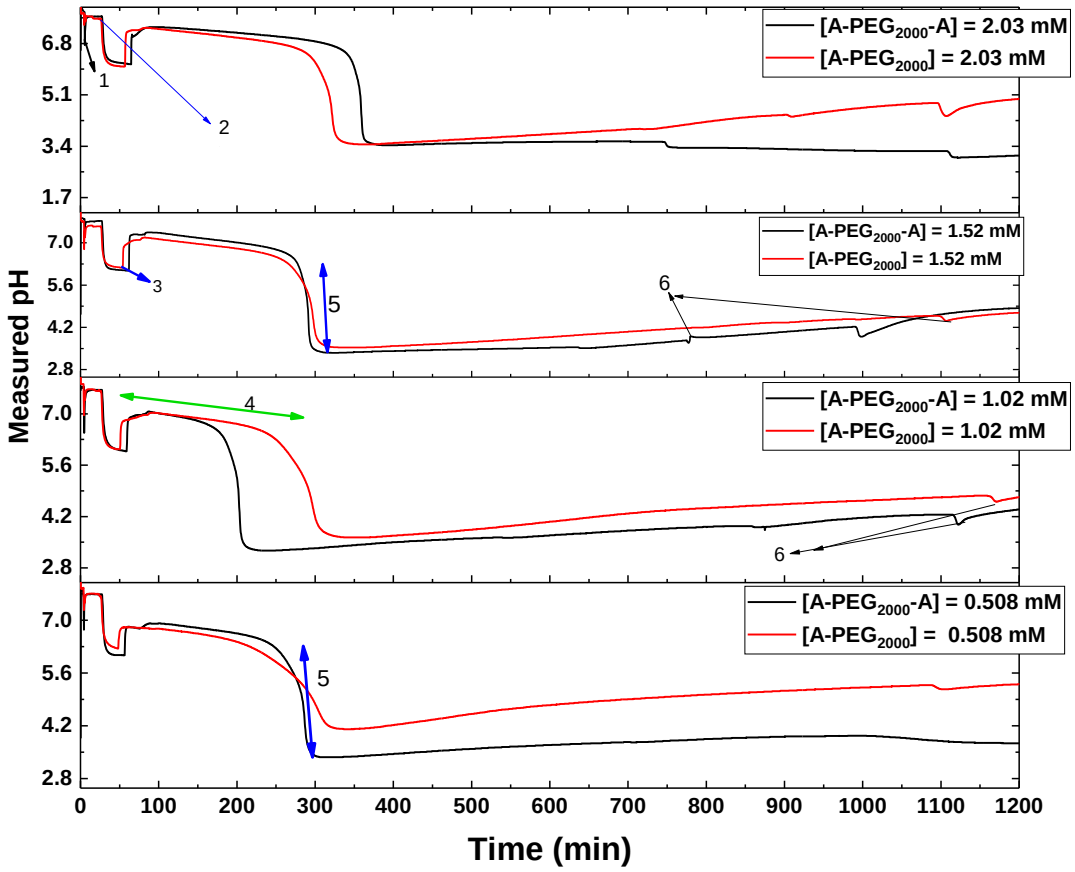

catalytic mix 1; purging 2; substrate addition 3; slow [H^+] formation 4; initial autocatalysis 5; onset of oscillation 6.

Figure 6.3. pH profiles of initial reaction conditions at equal concentrations of mono alkyne and bi-alkyne functionalised polyethylene glycol as reaction substrates and constant catalyst concentration. (V_{total} = 90 mL; CO and air flow rates = 15 mL/min; [KI] = 5.7 mM; [PdI_2] = 29 μM)

Equal concentrations (0.508 mM; 1.02 mM; 1.52 mM; 2.03 mM) of mono alkyne and bi-alkyne functionalised polyethylene glycol substrates were added to each reacting vessel after a brief period of purging, as exemplified by the arrow labelled "3" in the second figure from the top of Figure 6.3. The addition of respective polymeric substrates was followed by rises in pH in all profiles. Since the mono alkyne and bi-alkyne substrates were dissolved in small volumes of methanol (≈ 3.5 mL) before the solutions were added to the reacting vessel, the rise in pH may have partly originated from the methanol introduced with the substrate. This assumption is supported by pH rise from the addition of methanol in phenyl acetylene oscillatory carbonylation reactions following evaporative losses (higher reaction temperature (40°C),

experiments lasting several days) [10, 32], in perturbation studies [243], and carbonylation in water-methanol solvent mixtures (higher pH values with increasing water concentration) [176]. pH rises from methanol addition in Chapter 4, Subsection 4.2.1 also supports this assumption. The rise could also be partly attributed to dilution of HI present (thus affecting H^+ activity) which occurs when further methanol is introduced with substrate. Lastly, some interaction between the substrates and H^+ is speculated because, the pH rises on addition of mono alkyne and bi-alkyne substrates from studies at equal substrate concentration given in Figure 6.4 show trend in pH rise that appear dependent on substrate concentration and type. However, mechanisms supporting the observed rise in pH due to alkyne functionalised substrates is indeterminate at this point because, polyethylene glycol is unlikely to dissociate to any significant extent on dissolving in methanol [276-283]. Also, potential products in case of detached alkyne end groups were not identified via GC-MS in the original oscillatory carbonylation study with mono-alkyne functionalised polyethylene glycol [29].

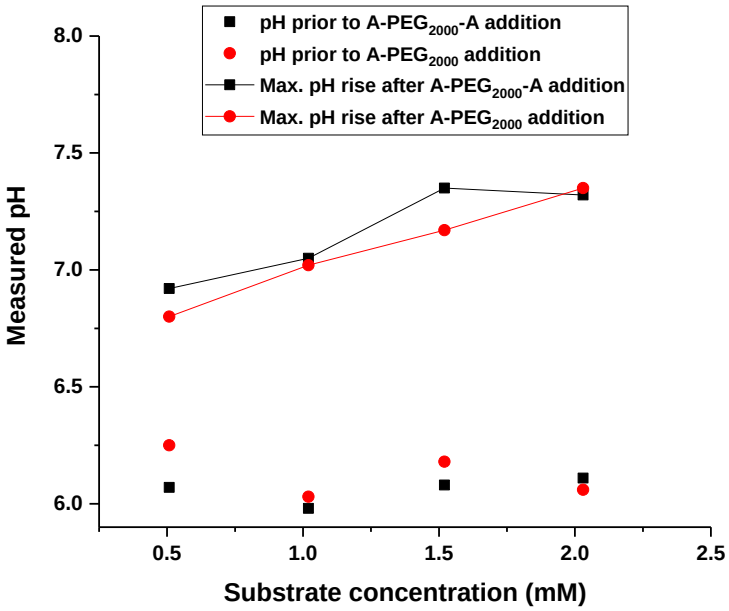

Figure 6.4. Comparison of pH prior to substrate addition and maximum rise in pH on addition of equal concentrations of mono alkyne (A-PEG_{2000}) and bi-alkyne (A-PEG_{2000}-A) functionalised polyethylene glycols. (Substrate concentrations = 0.508 mM; 1.02 mM; 1.52 mM; 2.03 mM)

The rise in pH on addition of mono alkyne (A-PEG_{2000}) and bi-alkyne (A-PEG_{2000}-A) substrates increased with increasing substrate concentration (from 0.508 mM to 2.03 mM). Deviations from this trend is observed at 2.03 mM bi-alkyne substrate concentration since pH values are recorded at 1.52 mM and 2.03 mM (7.35 and 7.34 pH units respectively) were approximately the same. As an overall trend, slightly higher pH values are observed when bi-

alkyne substrates are used (Figure 6.4). Higher H^+ concentrations were present in reactions with bi-alkyne substrate prior to substrate addition (lower pH values) yet, maximum pH on substrate addition was higher in reactions where bi-alkyne substrates were added. This trend therefore supports the above-mentioned speculation that substrate concentration and type contribute to pH rises on substrate addition.

A period of gradual increase in hydrogen ion concentration, defined as "slow H^+ formation" phase and exemplified in Figure 6.3 by the arrow labelled "4", succeeds the addition of alkyne functionalised substrates (this phase occurs in both reactions with mono alkyne and bi-alkyne functionality). This slow phase was described in previous chapters and, similar trend in slow H^+ formation upon substrate addition was reported for large scale (total methanol volume = 450mL) oscillatory carbonylation of phenyl acetylene at 20°C [8, 9] and 40°C [10]. Eq. 4.2 to 4.4 - for conversion of water and methanol and, Eq. 4.6, Eq. 5.1, and Eq. 5.3 - for mono alkyne and bi-alkyne substrate conversions, are proposed as reactions responsible for the gradual decrease in pH values and corresponding rise in H^+ concentrations. Eq. 4.6, Eq. 5.1, and Eq. 5.3 are assumed to proceed in autocatalytic mode; slowly during the period of low H^+ concentration ("slow H^+ formation") and, subsequently faster as H^+ concentration increases via autocatalytic substrate conversion.

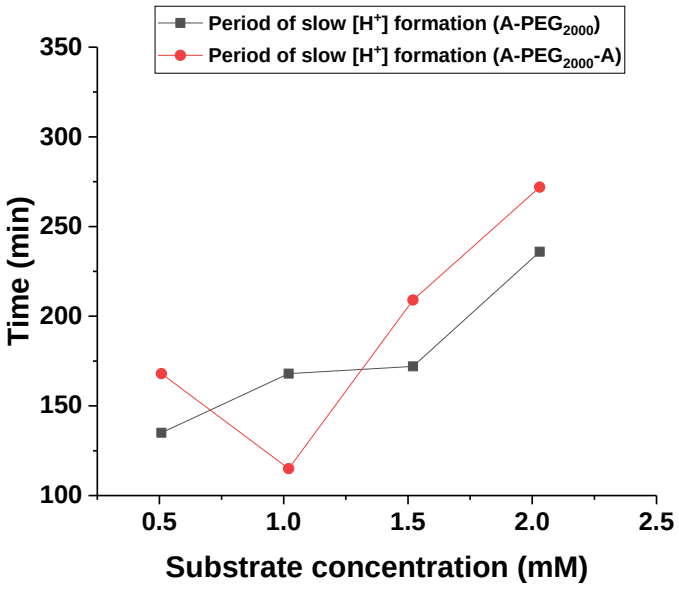

Figure 6.5. Duration of slow H^+ formation recorded for reactions with equal concentrations of mono alkyne (A-PEG_{2000}) and bi-alkyne (A-PEG_{2000}-A) functionalised polyethylene glycol. (Substrate concentrations = 0.508 mM; 1.02 mM; 1.52 mM; 2.03 mM)

The duration of "slow H^+ formation" in both substrates ranged from 115 min to 272 min and, trends in slow H^+ phase using mono and bi-alkyne substrates at four different concentrations (0.508 mM; 1.02 mM; 1.52 mM; 2.03 mM) is given in Figure 6.5. The period of slow H^+

formation for mono alkyne functionalised substrate appears to be slightly lower than the durations recorded with the bi-alkyne substrate. Exception to this trend is noted at 1.02 mM where the reverse occurs. This exception may have occurred since the highest H^+ concentration (from purging) prior to substrate addition was recorded in the reaction where 1.02 mM bi-alkyne substrate was eventually added. It is likely that the increased [H^+] from purging facilitated a reduction in the duration of "slow H^+ formation", as more [H^+] was already present in this reacting system to drive it away from the slow phase and towards autocatalysis.

On comparing reactions with mono alkyne and bi-alkyne substrates, PdI_2 and KI concentrations were held constant in both hence, the differences in rate of slow H^+ formation and overall longer duration in bi-alkyne system may be attributed to double alkyne groups in the bi-alkyne substrate. In Chapter 5, Section 5.2, the possibility of intermediate species influencing the effective rate (Eq. 5.5) of bi-alkyne substrate conversion was considered. Based on this prior postulation, the reduced availability of PdI_2 (after the first step, Eq. 5.3) for further conversions of the intermediate species (Eq. 5.4) from the bi-alkyne substrate may have impacted the rate of subsequent formation of HI (HI assumed as source of [H^+] measured experimentally), leading to the general increase in the durations of "slow H^+ formation" for bi-alkyne substrates as given in Figure 6.5.

As HI accumulates during the "slow H^+ formation" phase, it appears to approach a concentration, which prompts the autocatalytic formation of HI, seen as sudden decrease in pH / corresponding rise in [H^+]. The experimentally captured trends are linked to Eq. 4.6, Eq. 5.1 and 5.3, postulated to proceed via autocatalysis. The autocatalytic formation of HI corresponding to the sharp drops in pH are exemplified by double arrows marked as "5" in Figure 6.3. The prompt fashion of the transition from slow H^+ production to rapid [H^+] formation agrees with autocatalysis assumption and HI is presumed to be the source of protons [29-32, 295]. The increase in [H^+] / drop in pH from autocatalysis was greater in reaction with bi-alkyne substrate (Figure 6.3), suggesting that the higher concentration of alkyne groups in bi-alkyne functionalised substrates affect the rate of the autocatalytic substrate conversion reactions. Although the increase in [H^+] was generally higher with bi-alkyne substrates, at higher equivalent substrate concentrations (1.52 mM and 2.03 mM), the differences in pH decline (increased [H^+]) between both substrates following autocatalysis was smaller. The change in pH and [H^+] adjusted following the autocatalytic formation of HI is given in Figure 6.6. Autocatalytic change in pH and [H^+] adjusted increased with increasing mono-alkyne substrate concentration (Figure 6.6) while a curved trend was noted for the bi-alkyne functionalised substrates. As the bi-alkyne substrate concentration increased, the difference in

change in pH and [H^+] arising from initial autocatalysis reduced significantly, producing a convergence at 2.03 mM mono and bi-alkyne substrate concentrations.

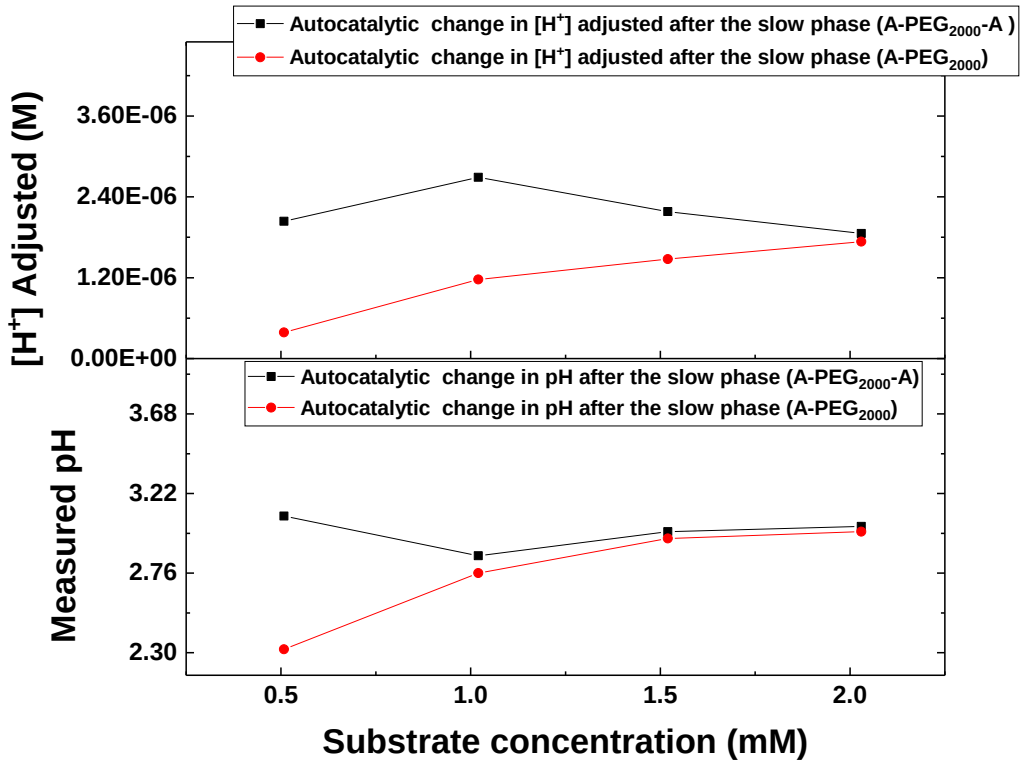

Figure 6.6. ΔpH and ΔH^+ adjusted from initial autocatalytic substrate conversion at equal concentrations of mono alkyne (A-PEG_{2000}) and bi-alkyne (A-PEG_{2000}-A) functionalised polyethylene glycol substrates. (Substrate concentrations = 0.508 mM; 1.02 mM; 1.52 mM; 2.03 mM)

The autocatalytic increase in HI concentration was followed by periods of decrease in [H^+] in both reactions with mono alkyne and bi-alkyne substrates (Figure 6.3). This decrease in H^+ is attributed to the oxidation of HI, previously reported in oscillatory and non-oscillatory carbonylation of alkyne terminated substrates such as phenyl acetylene [3, 29, 38, 156, 270, 271]. The nucleophilic substitution of OH in methanol forming methyl iodide according to Eq. 4.9 (proposed to occur in presence of excess KI [30, 287-289]) is also proposed as an alternate mechanism facilitating this decrease in [H^+].

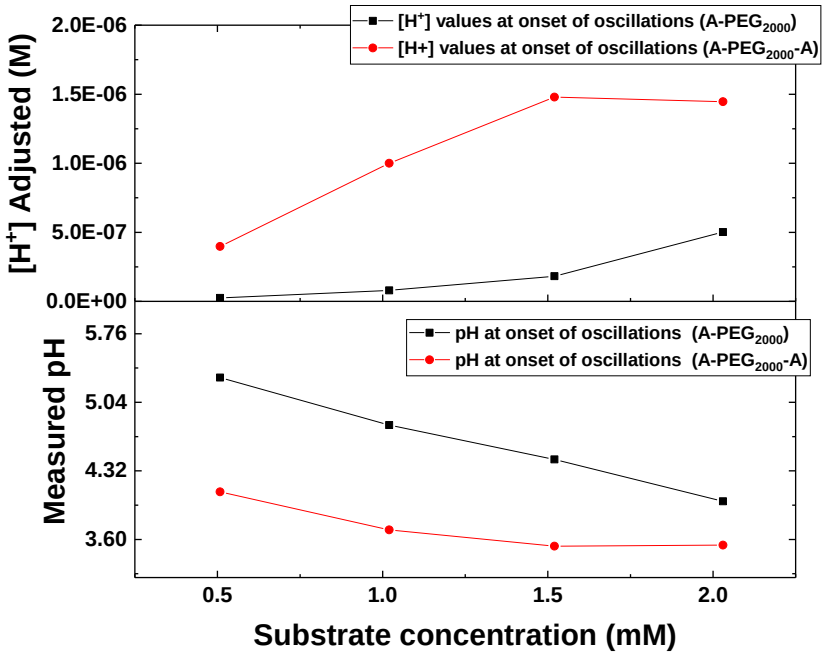

Figure 6.7. pH and [H^+] at onset of oscillations at equal concentrations of mono alkyne (A-PEG_{2000}) and bi-alkyne (A-PEG_{2000}-A) functionalised polyethylene glycol. (Substrate concentrations = 0.508 mM; 1.02 mM; 1.52 mM; 2.03 mM)

Subsequent rapid declines in pH (corresponding to swift rises in [H^+]) indicated by arrows "6" in Figure 6.3 marked the onset of oscillations. The sharp rise is attributed to autocatalytic formation of HI according to Eq. 4.6, 5.1 and 5.3 for substrate conversion. In the reaction with bi-alkyne substrate at 0.508 mM (Figure 6.1 and 6.2), a second region between 995 min and 1973 min where additional H^+ is produced and consumed, is observed. This region precedes the onset of oscillations which occurred 1976 min into the reaction where [A-PEG_{2000}-A] = 0.508 mM. Eq. 4.8, in addition to Eq. 4.9 which is reversible, are suggested as possible reaction mechanisms governing this second region. This supposition was made because, more water becomes available as Eq. 4.9 proceeds which could aid HI formation in this second region. pH and [H^+] adjusted trends in mono alkyne and bi-alkyne substrate at initiation of oscillation is given in Figure 6.7. The pH at onset of oscillation decreased as the concentration of both mono alkyne and bi-alkyne substrates increased. The decrease in pH agrees with the increase in H^+ adjusted concentration given in Figure 6.7 (top profiles). Mono alkyne substrates showed generally higher pH values, consistent with the smaller [H^+] adjusted values obtained (Figure 6.7), while lower pH values and higher [H^+] were recorded at equal bi-alkyne substrate concentrations. The higher pH values obtained in reactions with mono alkyne substrate is attributed to lower concentrations of H^+ as only one alkyne group is present per chain. The differences in [H^+] between mono alkyne and bi alkyne substrates at onset of oscillation at each

concentration investigated appears to increase with increasing substrate concentration, reaching a maximum at 1.52 mM, and then decreasing slightly at 2.03 mM. The increasing difference is attributed to increased HI formation via autocatalysis at increased alkyne group concentration (which increases as bi-alkyne substrate concentration increases). The slight decrease in the H^+ difference between mono and bi-alkyne substrate at 2.03 mM is attributed to the significantly higher mono alkyne concentration at this point and supports the assumption that alkyne concentrations regulates the pH at onset of oscillation.

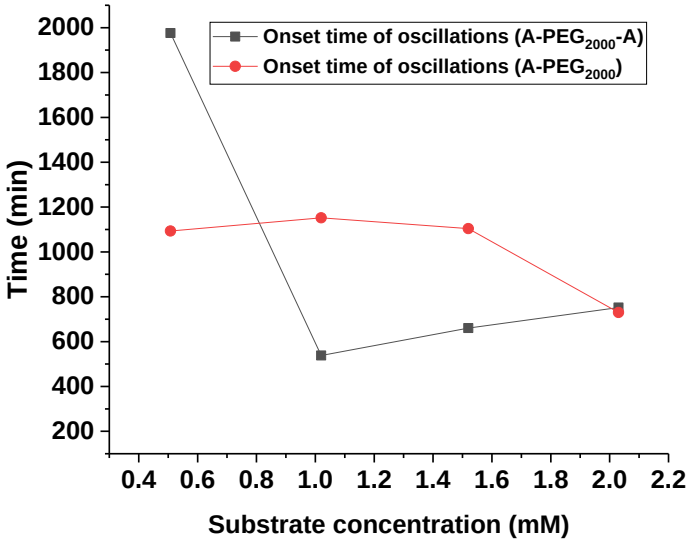

Figure 6.8. Reaction time at onset of oscillations for reactions at equal concentrations of mono alkyne (A-PEG_{2000}) and bi-alkyne (A-PEG_{2000}-A) functionalised polyethylene glycol

Time at onset of oscillations at equal mono alkyne and bi-alkyne substrate concentrations is given in Figure 6.8. As oscillations were not recorded in some replicate samples, comparison provided with respect to time at onset of oscillations is based on single experiments. Time at onset of oscillations varied across substrate concentrations and onset time was earlier for more bi-alkyne substrate reactions than mono-alkyne substrate reactions. Excluding the reaction with bi-alkyne substrate at 0.508 mM where an additional period of HI production and consumption preceded oscillations, increasing the bi-alkyne substrate concentration increased the duration required for initiation of oscillations. The increase in time at onset of oscillations is attributed to previously postulated serial reaction mechanism for bi-alkyne substrate conversion wherein the intermediate product serves as reaction substrate. For the mono alkyne substrate, time at onset of oscillations was similar at 0.508 mM, 1.02 mM and 1.52 mM as shown in Figure 6.8 with an average of 1116 min from start of the reaction while, the time at onset of oscillations at 2.03 mM was less. The reduced time at 2.03 mM mono alkyne substrate concentration is

attributed to increased H^+ concentration which is believed to promote earlier onset of oscillations.

Oscillatory modes recorded from investigations at equal substrate concentrations is given in Figure 6.9. Oscillations with larger amplitudes and periods were recorded in reactions with bi-alkyne substrate, while smaller amplitude oscillations were recorded for mono alkyne functionalised substrate. Maximum and minimum oscillatory amplitudes achieved during the oscillations is given in Figure 6.10. The increased concentration of alkyne end group in the bi-functionalised substrate (two alkyne ends per chain) is likely to have generated larger sized oscillations and higher maximum and minimum amplitudes. The assumption here is that HI formation per autocatalytic cycle in the reaction with bi-alkyne substrate is higher, supporting the larger amplitudes, while the larger periods of oscillations with bi-alkyne substrates are ascribed to increased reaction times required for conversion of both alkyne end groups and time for consumption of HI produced.

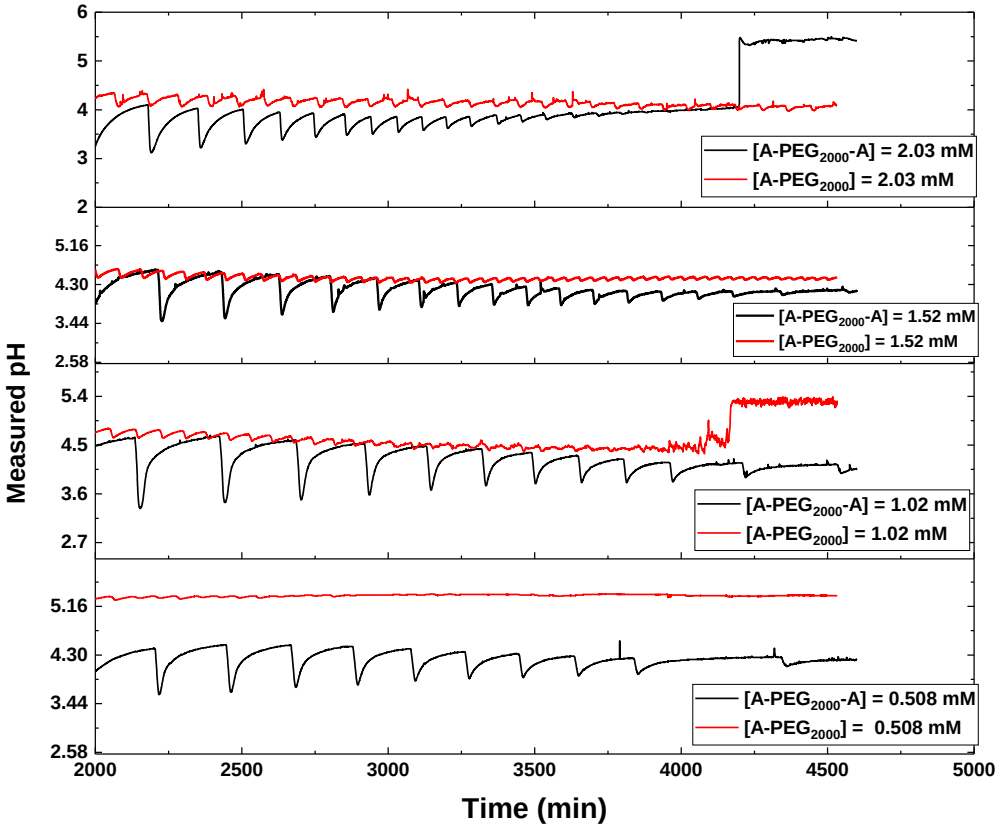

Figure 6.9. Oscillatory patterns recorded at equal concentrations of mono alkyne and bi-alkyne functionalised polyethylene glycol as reaction substrates and constant catalytic concentration. (V_{total} = 90 mL; CO and air flow rates = 15 mL/min; [KI] = 5.7 mM; [PdI_2] = 29 μM; Substrate concentrations = 0.508 mM, 1.02 mM, 1.52 mM, 2.03 mM)

The size of oscillations and adjusted [H^+] values increased with increasing substrate concentration for reactions with mono alkyne substrate. Nonetheless, the overall [H^+] values were significantly higher in reactions with bi-alkyne substrates, supporting the assumed influence of the additional alkyne groups in the bi-alkyne substrate. Oscillation lasted for over 3 days and had either stopped or presented with smaller amplitudes and period when the reactions were terminated, irrespective of the number of functional groups per chain.

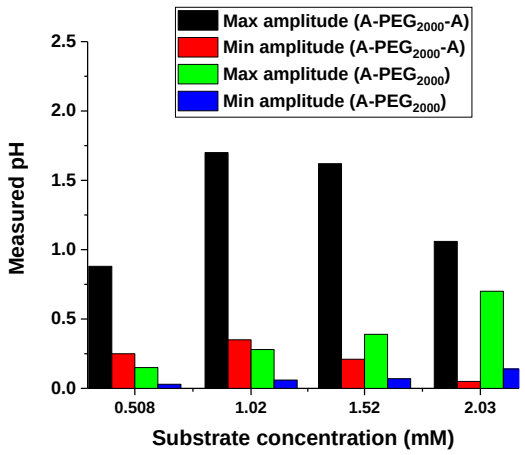

Figure 6.10. Maximum and minimum amplitudes recorded at constant catalytic concentration during the oscillatory carbonylation of equal concentrations of mono alkyne (A-PEG_{2000}) and bi-alkyne (A-PEG_{2000}-A) functionalised polyethylene glycol

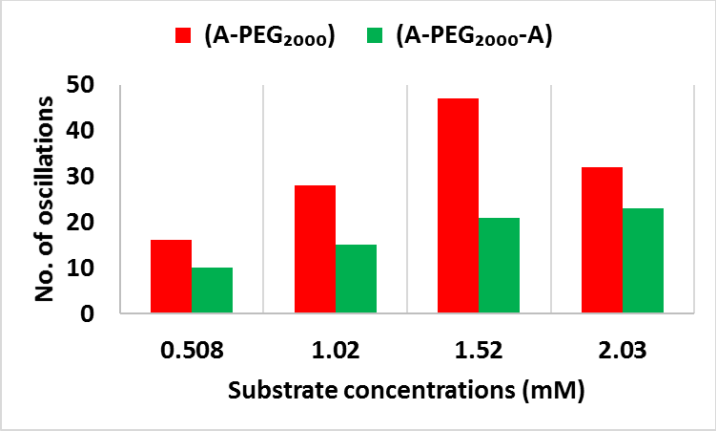

Figure 6.11. Number of oscillations recorded at identical experimental duration and constant catalytic concentration during the oscillatory carbonylation of equal concentrations of mono alkyne (A-PEG_{2000}) and bi-alkyne (A-PEG_{2000}-A) functionalised polyethylene glycol

The number of oscillations recorded at equal substrate concentrations are presented in the Figure 6.11. Significantly more oscillations were recorded in reactions with mono-alkyne substrate at each concentration investigated, with the largest difference in number of

oscillations between mono alkyne and bi-alkyne substrates occurring at 1.52 mM (47 and 21 respectively).The number of oscillations increased with increasing mono alkyne and bi-alkyne substrate concentration for the first three equivalent concentrations studied, while a decrease was noted at 2.03 mM for the mono-alkyne substrates. It is unclear why this decrease occurred at 2.03 mM, however, the transition from high pH to lower pH oscillatory state signified by the irregularly shaped oscillation around 1800 min in Figure 6.3 at 2.03 mM mono-alkyne substrate concentration may have contributed to decline in number of oscillations recorded in that reaction.

6.2.2 Sub-section Summary

1. Higher hydrogen ion concentrations were recorded in reactions with bi-alkyne functionalised polyethylene glycol (0.508 mM; 1.02 mM; 1.52 mM; 2.03 mM) than the mono-alkyne version (0.508 mM; 1.02 mM; 1.52 mM; 2.03 mM) at equal substrate concentrations and constant PdI_2 and KI concentration ([KI] = 5.7 mM; [PdI_2] = 29 μM). This agrees with higher concentration of alkyne groups in the bi-alkyne substrate.
2. The duration of gradual [H^+] increase following substrate addition defined as period of "slow H^+ formation" increased with increasing mono and bi-alkyne substrate concentrations. The duration was also generally higher in reactions with bi-alkyne substrates than mono alkyne substrates at equal substrate concentrations.
3. Initial HI formed from the autocatalytic conversion of equal concentrations of mono and bi-alkyne substrates was greater in reactions with bi-alkyne substrates supportive of increased reaction rate and substrate conversion at higher alkyne concentration. HI concentration also increased with increasing mono and bi-alkyne substrate concentration from 0.508 mM to 2.03 mM.
4. Increasing the number of alkyne end groups from one (mono alkyne substrate) to two (bi-alkyne substrate) at equal substrate concentrations increased the H^+ concentration at onset of oscillations and increased the onset time of oscillations.
5. Oscillations with larger amplitudes and periods were recorded in bi-alkyne substrate. Larger amplitudes are attributed to higher alkyne concentrations present (two end groups) while longer oscillation periods are possibly from extended times required for conversion of both alkyne groups per chain and time required for consumption of HI.

6.2.3 Influence of Number of Alkyne Functional Groups– Case B: Reactions where Mono Alkyne Substrate Concentration is Twice the Bi-Alkyne Substrate Concentrations

In Sub-section 6.2.1, equal concentrations of both substrates were employed in the reactions, hence, the concentration of alkyne end groups present in bi-alkyne functionalised substrate was double that of the mono alkyne substrate. In this section, a different scenario is assessed at the same catalyst ($[PdI_2] = 29$ μM) and KI (5.7 mM) concentrations. Here, the concentration of the alkyne end groups in both substrates are kept approximately constant by using twice the concentration of mono alkyne substrate for any concentration of the bi alkyne functionalised substrates investigated. Studies designed to study the influence of alkyne groups in the manner described above are denoted as "Case B" throughout this chapter. Concentrations investigated in this section are given in Table 6.3.

Table 6.3. Reactant concentrations employed in determining the influence of the number of alkyne groups at $[A\text{-}PEG_{2000}] \approx 2 \times [A\text{-}PEG_{2000}\text{-}A]$. ($V_{total}$ = 90 mL; stirring speed = 350 rpm; CO and air flow rates = 15 mL/min; temperature = 20±0.2°C)

$[PdI_2]$ (μM)	[KI] (mM)	$[A\text{-}PEG_{2000}\text{-}A]$ (mM)	$[A\text{-}PEG_{2000}]$ (mM)
29	5.7	0.254	0.508
29	5.7	0.508	1.02
29	5.7	1.02	2.03
29	5.7	1.52	3.05

pH and $[H^+]$ adjusted profiles obtained from the oxidative carbonylation studies employing reactant and catalyst concentrations given in Table 6.3 are given in Figure 6.12 and 6.13. Oscillations were recorded at all concentrations investigated with mono-alkyne and bi alkyne substrates. While the total alkyne content was kept constant by using twice as much mono alkyne substrate per bi-alkyne substrate, significant differences in the amplitude and periods of oscillation were still observed (Figure 6.12). Transitions from one oscillatory pH region to another occurred in mono alkyne substrate at 1.02 mM, 2.03 mM and 3.05 mM. Such transitions were absent for bi-alkyne substrates at corresponding alkyne end concentration.

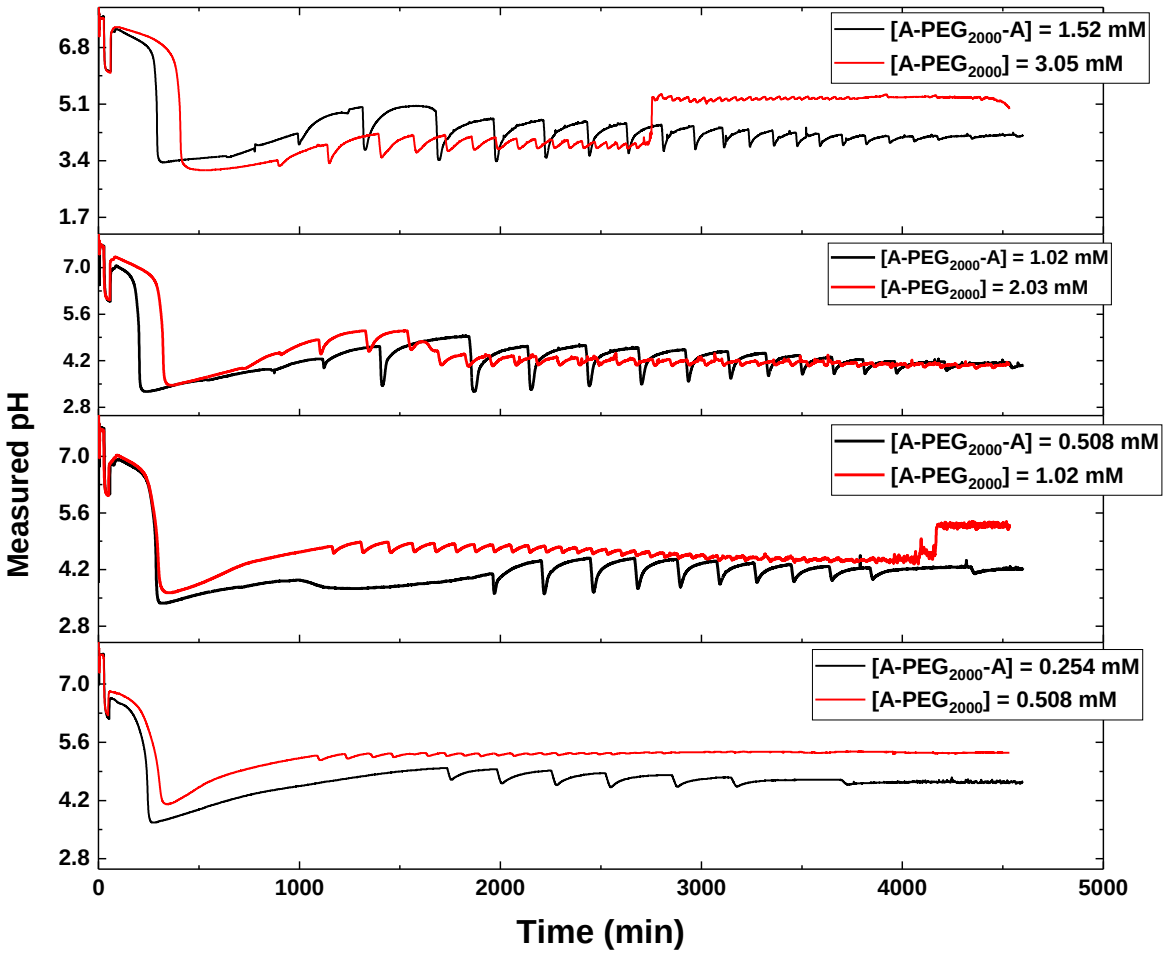

Figure 6.12. pH profiles from the oscillatory carbonylation reactions at constant catalyst concentration. Mono alkyne substrate concentration ([A-PEG$_{2000}$]) is twice the concentration of the bi-alkyne functionalised polyethylene glycol ([A-PEG$_{2000}$-A]) substrate. ([A-PEG$_{2000}$] ≈ 2 x [A-PEG$_{2000}$-A]). (V_{total} = 90 mL; CO and air flow rates = 15 mL/min; [KI] = 5.7 mM; [PdI_2] = 29 μM)

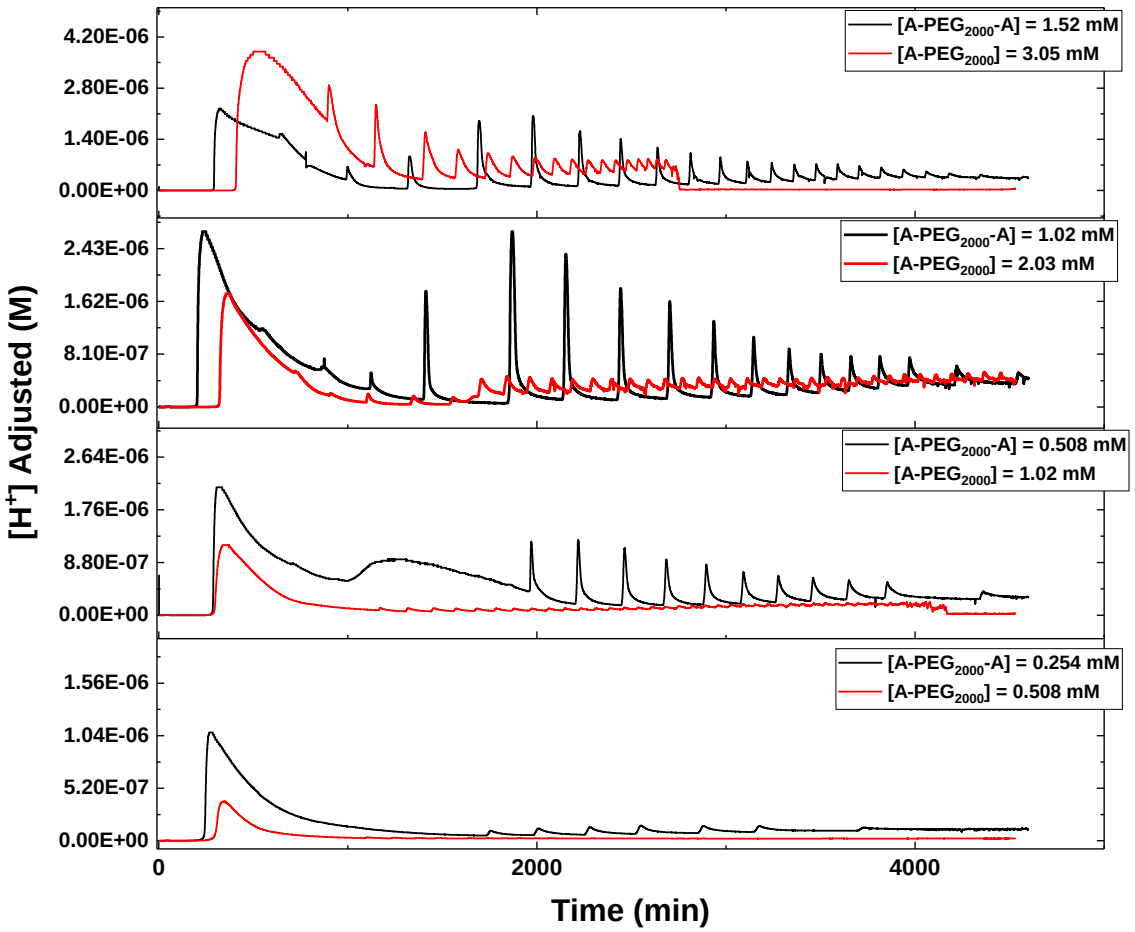

Figure 6.13. $[H^+]$ adjusted profiles obtained from the oscillatory carbonylation reactions at constant catalyst concentration. Mono alkyne substrate concentration [A-PEG$_{2000}$] is twice the concentration of the bi-alkyne functionalised polyethylene glycol [A-PEG$_{2000}$-A] substrate. ([A-PEG$_{2000}$] ≈ 2 x [A-PEG$_{2000}$-A]). (V_{total} = 90 mL; CO and air flow rates = 15 mL/min; [KI] = 5.7 mM; [PdI_2] = 29 μM)

pH changes during the initial stages of the carbonylation reaction is given in Figure 6.14. pH measurements begun after the probes were calibrated and bulk methanol for the reactions were added to flasks. The first drop and instant rise between pH 7 and 8, illustrated by the arrow labelled "1" in Figure 6.14 (at 1.52 mM and 3.05 mM), occurred on addition of the catalytic solution consisting of palladium iodide and potassium iodide dissolved in methanol. This dip was similarly noted across all profiles reported so far and has been attributed to changes in ionic strength [176, 260-268] of methanol in the reacting vessels following the addition of the catalytic solution. Following pH equilibration, the solutions were purged with CO and air at 15 mL/min. The pH decreases in Figure 6.14 (illustrated by the arrow labelled "2" at 1.02 mM and 2.03 mM)) as purging continued is indicative of HI formation owing to carbonylation of methanol and water. Water is present as impurity in the methanol and possibly, as moisture in the gases used for purging and from atmosphere. Increased $[H^+]$ and lower pH is assumed to

proceed according to Eq. 4.2 to 4.4 for carbonylation of water and methanol, and catalytic conversion of water.

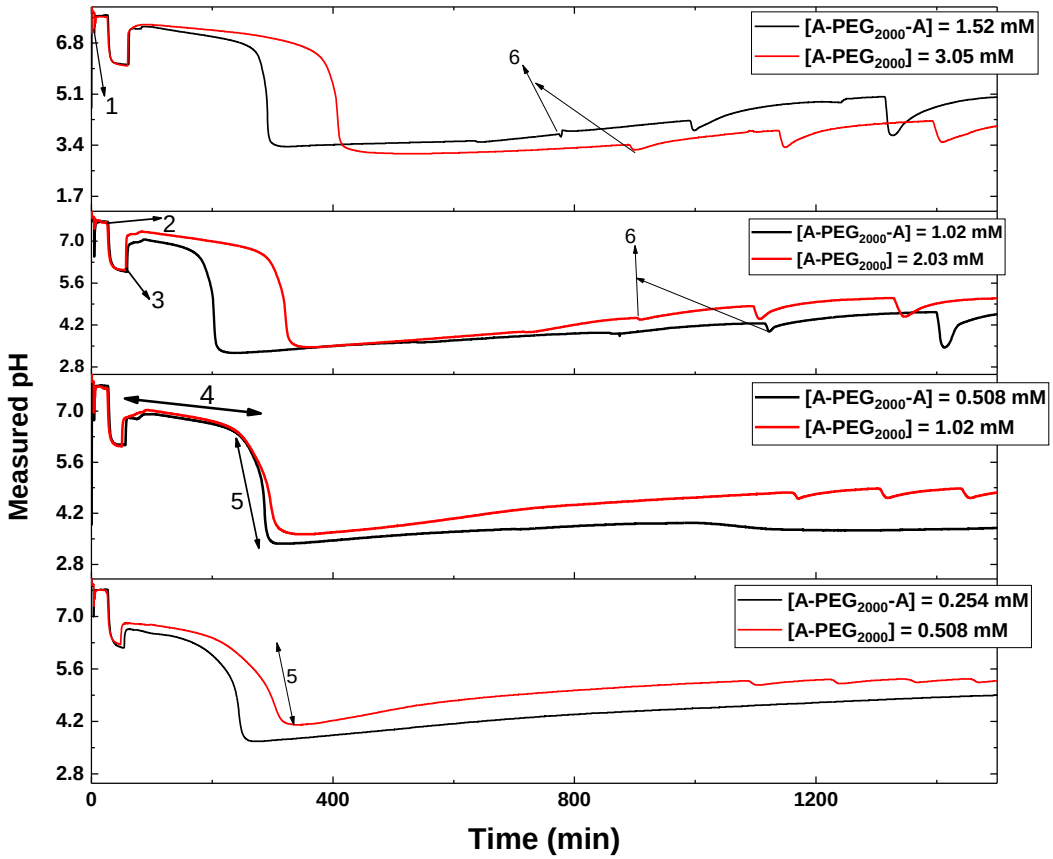

catalytic mix 1; purging 2; substrate addition 3; slow [H^+] formation 4; initial autocatalysis 5; onset of oscillation 6.

Figure 6.14. Initial profile features from the carbonylation reactions when the concentration of the mono alkyne substrate is twice the concentration of the bi-alkyne functionalised. ([A-PEG$_{2000}$] ≈ 2 x [A-PEG$_{2000}$-A]). ([KI] = 5.7 mM; [PdI_2] = 29 μM; CO and air at 15 mL/min)

Solutions of mono alkyne and bi alkyne substrates were added to the vessels after purging all reactions for short intervals (20-30 min). The addition of alkyne functionalised polyethylene glycol substrates, illustrated by the arrow "3" in Figure 6.14, was followed by rise in pH. This rise in pH was discussed in previous sections and is assumed to arise from methanol used for dissolution, dilution of the H^+ on adding substrate solutions and from interactions between the substrates and H^+ ions present in the solutions. Trends observed from rising pH on substrate addition is given in Figure 6.15. Higher pH values were obtained in reactions with mono alkyne substrates than bi-alkyne substrate and the pH values also increased with increasing substrate concentration. In Section 6.2.1 (for studies at equal concentration, Figure 6.4), slightly higher pH values were recorded in reactions with bi-alkyne substrate, which contrasts the finding here

(Figure 6.15). It appears that doubling the concentration of mono alkyne substrates to maintain constant alkyne concentrations in both reactions facilitated higher pH rise on mono-alkyne substrate addition. The observed increase suggests that, in addition to alkyne end concentration, the total mass of the polymeric substrate present has as an underlying effect on pH rise from substrate addition.

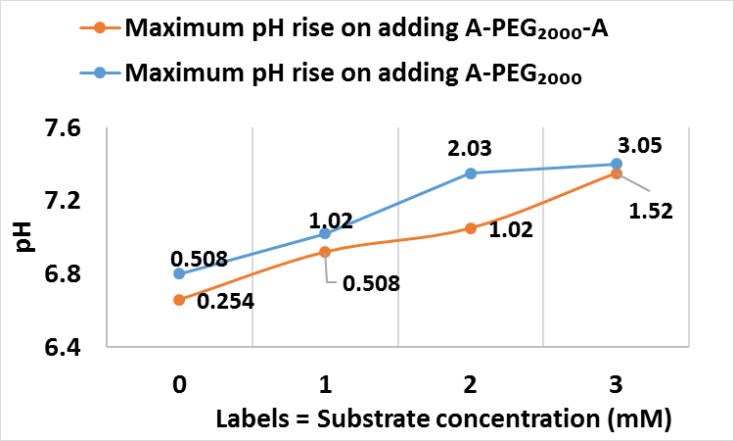

Figure 6.15. Comparison of maximum rise in pH values on addition of mono alkyne (A-PEG_{2000}) and bi-alkyne (A-PEG_{2000}-A) functionalised substrates for reactions where [A-PEG_{2000}] ≈ 2 x [A-PEG_{2000}-A] (CO and air flow rates = 15 mL/min; temperature = 20±0.2°C)

The addition of substrate was followed by periods of gradual formation of HI defined as "slow H^+ formation" phase and characterised by slowly decreasing pH values (Figure 6.14, exemplified by the double arrow denoted "4"). HI produced during this period is assumed to arise from Eq. 4.2 to 4.6, Eq. 5.1 and Eq. 5.3.

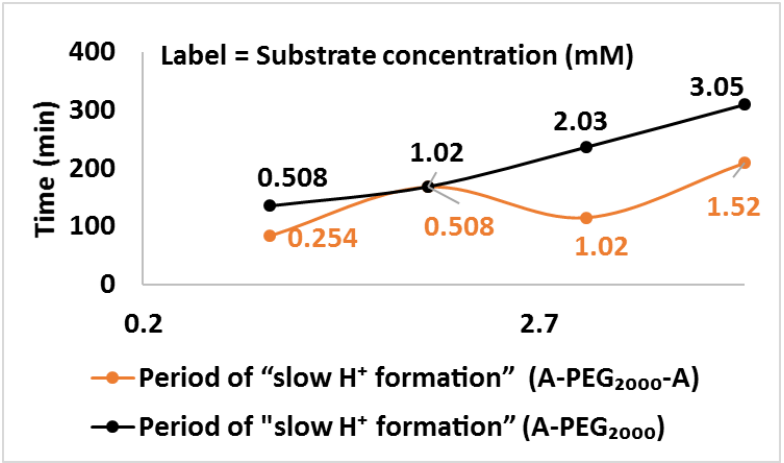

Figure 6.16. Duration of slow H^+ formation in reactions where mono alkyne substrate concentration is twice the bi-alkyne substrate concentration. (Actual alkyne concentration is ≈ constant) [A-PEG_{2000}] ≈ 2 x [A-PEG_{2000}-A] ([KI] = 5.7 mM and [PdI_2] = 29 μM)

The duration of slow H^+ formation at constant alkyne end concentration for substrates where [A-PEG_{2000}] ≈ 2 x [A-PEG_{2000}-A] is given in Figure 6.16. The duration increased with increasing

concentration of mono alkyne substrate concentration, but no correlation was found on increasing the bi-alkyne functionalised substrate concentration. Overall alkyne concentrations were kept constant irrespective of substrate type employed, yet, the periods of slow H^+ formation still differed by substrate type. The only exception occurred in reactions at 1.02 mM (mono alkyne) and 0.508 mM (bi alkyne) substrate concentrations, where the periods of slow H^+ formation following substrate addition were the same (168 min (Figure 6.16)). The observed differences by substrate type at approximately equal alkyne group concentration suggests that, the rate of HI formation in mono alkyne substrate reactions was slower than bi-alkyne substrate reaction during the slow H^+ phase. As higher pH values were obtained on adding mono alkyne substrate solutions (Figure 6.15), the HI concentrations at onset of the slow phase was lower in the mono alkyne reactions. Hence, further reaction time would be needed to increase HI concentration, which agrees with the longer duration of slow H^+ formation in mono alkyne reactions.

As the concentration of HI slowly increases during the slow phase, a threshold HI concentration which triggers the autocatalytic production of HI according to Eq. 4.6, Eq. 5.1 and/or Eq. 5.3 is presumed to occur. The assumption of the existence of intrinsically determined HI thresholds agrees with autocatalysis since more HI is produced in Eq. 4.6, Eq. 5.1 and/or Eq. 5.3 following the slow phase. This autocatalytic formation of HI, corresponding to the decrease in pH values given in Figure 6.14 following the slow phase and is exemplified by double arrows denoted "5" in Figure 6.14. The rapid drop in pH and corresponding rise in HI concentration following autocatalysis for reactions where $[\text{A-PEG}_{2000}] \approx 2 \times [\text{A-PEG}_{2000}\text{-A}]$ is given in Figure 6.17(a-b). The changes in $[H^+]$ adjusted due to autocatalytic formation of HI was higher in reactions with bi-alkyne substrate except for the reaction at 1.52 mM (Figure 6.17(b)). Experimentally recorded pH changes due to autocatalytic HI formation was higher in reactions with bi-alkyne substrate at lower substrate concentrations investigated (0.254 mM bi-alkyne to 1.02 mM mono alkyne, Figure 6.17a), while the reverse was the case at higher substrate concentrations (1.02 mM bi-alkyne to 3.05 mM mono alkyne, Figure 6.17a). Preserving constant alkyne concentration by using twice as much mono alkyne substrate appears not to have substantial influence in promoting similarities in the profile features at this stage. In reactions with mono alkyne substrate, the changes in pH and $[H^+]$ adjusted following autocatalysis increased with increasing substrate concentration. A curved trend indicating presence of maxima was noted in bi-alkyne substrate reactions, with maximum $[H^+]$ adjusted value from initial autocatalysis occurring at 1.02 mM substrate concentration.

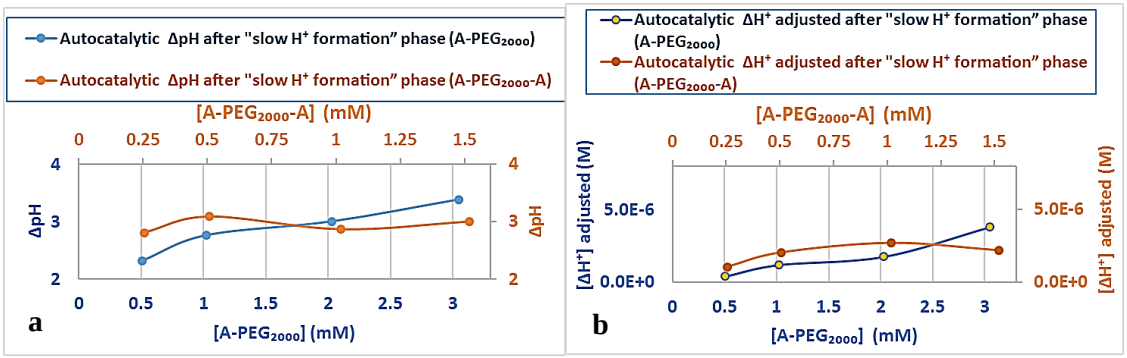

Figure 6.17. Autocatalytic pH and [H^+] changes observed in mono alkyne (A-PEG_{2000}) and bi-alkyne (A-PEG_{2000}-A) functionalised substrates at constant alkyne concentration

HI oxidation marked by periods of decrease in [H^+] in both reactions with mono alkyne and bi-alkyne substrates followed the autocatalytic formation of HI. H^+ concentration continued declining till rapid rises in [H^+], recorded as swift increase in pH acidity commenced, marking the onset of oscillations. Onset of oscillations is illustrated by arrows "6" in Figure 6.14. The sharp increase in pH acidity and onset of oscillations is attributed to autocatalytic formation of HI according to Eq. 4.6, Eq. 5.1 and/or Eq. 5.3.

pH, [H^+] adjusted and time at onset of oscillation are given in Figures 6.18(a-b) and Figure 6.19. At constant alkyne end concentrations ([A-PEG_{2000}] ≈ 2 x [A-PEG_{2000}-A]), increasing both substrate concentrations led to a decrease in pH at onset of oscillation. The decrease in pH and corresponding increase in [H^+] adjusted at onset of oscillations, observed in both substrate types, is likely from a faster rate of HI formation per autocatalytic cycle, which occurs as alkyne concentration increases at higher substrate concentration. H^+ concentration at onset of oscillations were higher for reactions with bi-alkyne functionalised substrate excluding the reaction at 1.52 mM bi-alkyne concentration (Figure 6.18b), where, the [H^+] was lower than its mono alkyne counterpart (3.05 mM, mono alkyne). The lower pH in bi-alkyne substrates corresponds to increased [H^+] and is linked to the number of functional groups per chain. This suggests that the number of alkyne end groups per chain has greater significance in the oscillatory carbonylation reaction than the total alkyne concentrations present at this catalytic concentration. It is likely that some differences which favour increased HI formation is present in the reaction routes when more than one alkyne group (bi-alkyne) is attached to a chain.

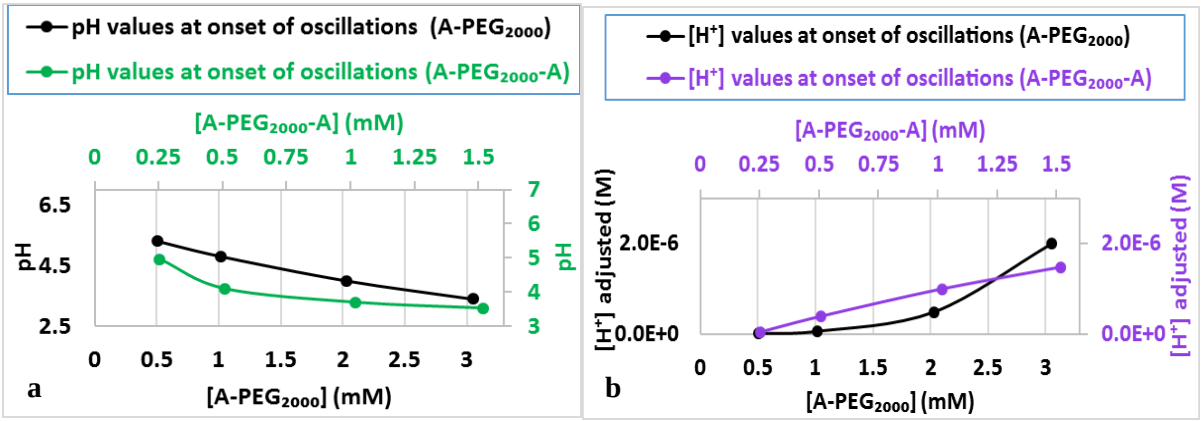

Figure 6.18 pH and [H^+] at onset of oscillations when concentration of mono alkyne substrate (A-PEG_{2000}) is double the bi-alkyne (A-PEG_{2000}-A) functionalised substrate concentration

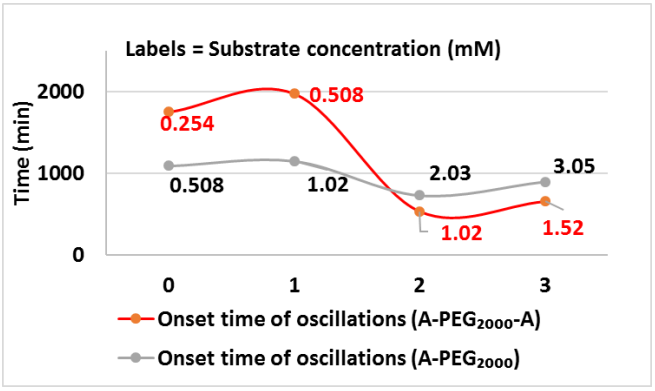

Figure 6.19. Time at onset of oscillations for the range of mono alkyne (A-PEG_{2000}) and bi-alkyne (A-PEG_{2000}-A) functionalised substrates studied where [A-PEG_{2000}] ≈ 2 x [A-PEG_{2000}-A]

The trend in Figure 6.19 showcasing time at onset of oscillation follows a similar pattern to trend in Figure 6.17a for changes in pH from initial autocatalytic HI production. The time at onset of oscillation was higher in reactions with bi-alkyne substrate at lower substrate concentrations (0.254 mM bi-alkyne to 1.02 mM mono alkyne), while the reverse was the case at higher substrate concentrations (1.02 mM bi-alkyne to 3.05 mM mono alkyne). The variation in times between both substrates decreased generally as concentrations increased at constant catalytic concentration. Range of oscillatory patterns recorded at constant alkyne group concentrations ([A-PEG_{2000}] ≈ 2 x [A-PEG_{2000}-A]) are given in Figure 6.20. Increasing the concentration of mono alkyne and bi-alkyne substrates increased the size of oscillations. However, smaller amplitudes and periods were still recorded for reactions with mono alkyne substrates despite doubling the alkyne end concentration. The smaller amplitudes and periods for mono alkyne substrate in Figure 6.20 supports the suggestion that maintaining constant alkyne concentration does not necessarily improve oscillation size at this catalyst concentration (PdI_2 = 29 μM) and prevailing reaction conditions.

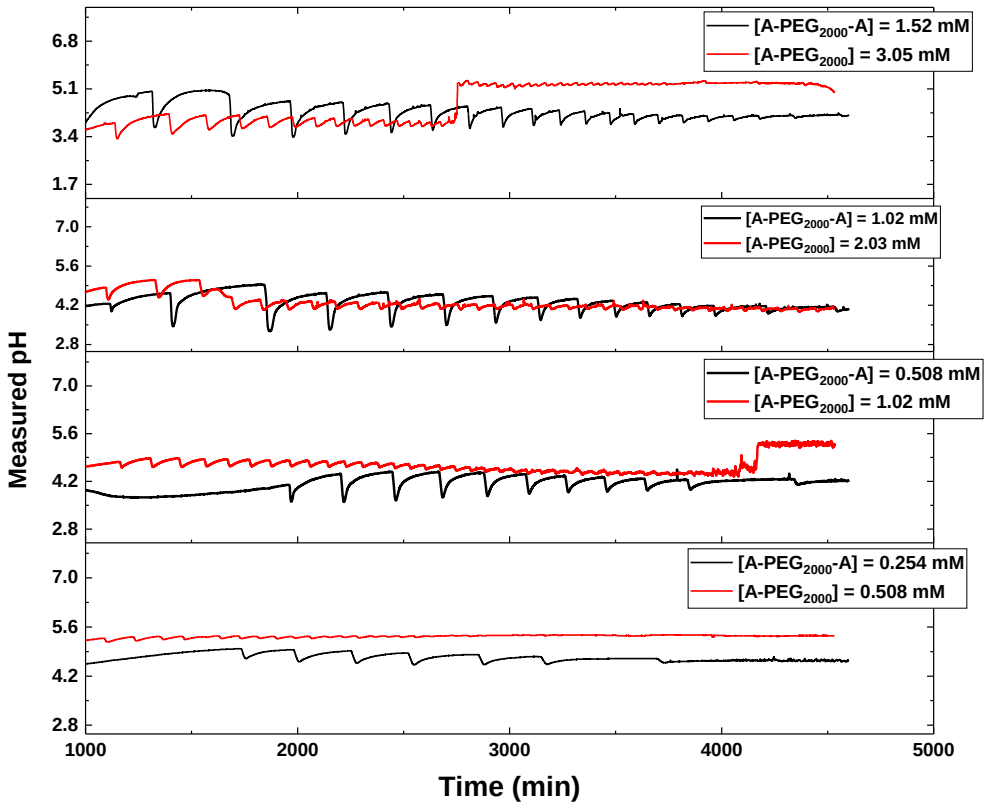

Figure 6.20. Oscillatory patterns recorded in reactions where mono alkyne substrate was twice the concentration of the bi-alkyne functionalised substrate ([A-PEG$_{2000}$] ≈ 2 x [A-PEG$_{2000}$-A]). ([KI] = 5.7 mM; [PdI_2] = 29 μM)

The number of oscillations recorded across runs is given in Figure 6.21. Number of oscillations increased with increasing substrate concentration and more oscillations were recorded for mono-functional substrates, despite having smaller oscillations size (smaller amplitudes and periods). It seems that some synergy exists between oscillation size and number of oscillations for reactions at ([A-PEG$_{2000}$] ≈ 2 x [A-PEG$_{2000}$-A]. This synergy is proposed because, the number of oscillations recorded for mono alkyne substrates reactions "A-PEG$_{2000}$" are ≥ 2 times the number of oscillations for bi-alkyne substrates "A-PEG$_{2000}$-A" for identical experimental durations. It seems that mono-alkyne substrates make up for smaller sized oscillations with increased number of oscillations. With the additional alkyne end groups in bi-alkyne functionalised substrates, the reaction in Eq. 5.1/5.3 (autocatalytic HI formation and product conversion) would have to convert two end groups on the polymer chain to final product. This may require more reaction time for bi-alkyne conversion and could proceed via different pathways. For mono alkyne substrate reactions, only one alkyne end group (Eq. 4.6) is available for reaction and is thus presumed to require less time per autocatalytic conversion cycle.

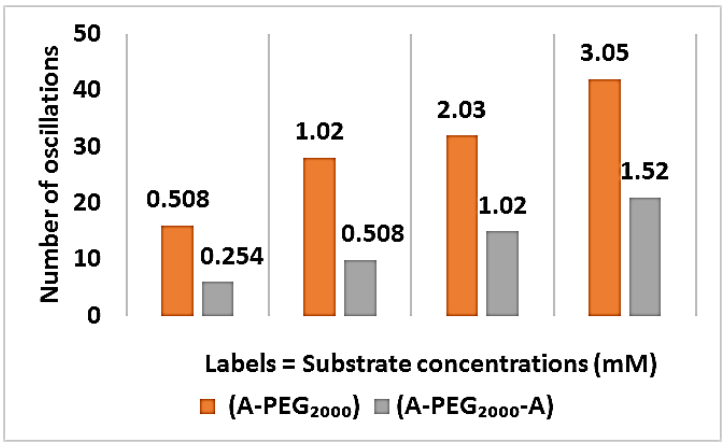

Figure 6.21. Number of oscillations for range of mono alkyne (A-PEG_{2000}) and bi-alkyne (A-PEG_{2000}-A) functionalised substrates studied where [A-PEG_{2000}] ≈ 2 x [A-PEG_{2000}-A]. [KI] = 5.7 mM and [PdI_2] = 29 μM

The oscillations in reactions with bi-alkyne substrates were still ongoing when the experiments were stopped, hence number of oscillations in Figure 6.21 is limited. As the duration of both experiments (mono alkyne and bi-alkyne) were the same, the increased frequency of oscillations in the reactions with mono-alkyne substrates suggests a faster rate of the autocatalysis (Eq. 4.6, Chapter 4 Section 4.2) when mono alkyne substrates are employed. The faster rate of reaction with mono alkyne substrates represented as greater number of oscillations for same reaction interval supports previously discussed possibility of increased reaction times / reduction in overall reaction rate (HI autocatalysis) arising from conversion of initial and intermediate alkyne species (Eq. 5.1 and/or Eq. 5.3, Chapter 5, Section 5.2) in reactions where bi-alkyne substrate is present.

6.2.4 Sub-section Summary

1. Oscillations were recorded for the range of mono alkyne (0.508 mM, 1.02 mM, 2.03 mM, 3.05 mM) and bi-alkyne substrates (0.254 mM, 0.508 mM, 1.02 mM, 1.52 mM) investigated for the studies where [A-PEG_{2000}] ≈ 2 x [A-PEG_{2000}-A].
2. Maximum pH rise on substrate addition was higher in reactions with mono-alkyne substrate. Overall pH rises also increased with increasing substrate concentrations (for both mono and bi-alkyne substrates). It appears that higher concentrations of the polymeric substrate backbone (PEG pendant) may have facilitated an increase in pH rise on substrate addition (This assumption was made since alkyne ends were equal in this study, yet mono alkyne substrates with twice polymeric backbone showed higher pH rise on substrate addition).
3. The period of gradual HI formation termed "slow H^+ formation" was higher in reactions with mono alkyne substrate, increasing with increasing substrate concentrations.

4. Doubling the mono alkyne substrate concentrations to maintain equal alkyne concentrations with the bi-alkyne substrate did not promote similarities between the reaction profiles recorded. A difference in reaction route and overall rates of reaction is postulated to occur when bi-alkyne substrates are used. The difference in profile features is attributed to the presence of more than one alkyne end group per polymer chain (Chapter 5, Section 5.2).
5. There is the possibility of a trade-off between the size and number of oscillations obtained and the rate of the autocatalytic substrate conversion reaction(s) (Eq. 4.6 and Eq. 5.1 and/or Eq. 5.3). This assumption is made since a larger number of smaller oscillations were recorded with mono alkyne substrate suggesting faster reaction rate per autocatalytic cycle, while a smaller number of large oscillations were obtained with bi-alkyne substrate at equal reaction times and constant catalyst / KI concentrations.

6.3 Influence of Number of Functional Groups on Polymeric Substrate at Constant Catalytic Concentration ($[PdI_2] = 22.7$ μM and [KI] = 6 mM)

The influence of number of alkyne functional groups per substrate chains at reduced catalyst concentration ($[PdI_2] = 22.7$ μM) and slighter higher KI concentration (6 mM against 5.7 mM in Section 6.2) was similarly investigated. Since carbonylation reactions are catalysed, the concentration of palladium iodide is expected to contribute to the oscillatory modes recorded for mono alkyne and bi-alkyne functionalised polyethylene glycol substrates. Altering the concentration of palladium iodide may also provide additional insight with respect to substrate choice for future studies. Reactions according to case "A" (equal substrate concentrations but twice as much alkyne concentrations are present in bi-alkyne substrate) and case "B" (mono alkyne substrate is twice as much as bi-alkyne substrate hence, equal alkyne concentration and different concentrations of polymeric backbone) are considered subsequently.

6.3.1 Case A: Reaction Profiles at Equal Mono Alkyne and Bi-Alkyne Substrate Concentrations

The influence of increasing the number of alkyne end groups per chain at constant catalytic concentration was assessed by employing mono alkyne and bi alkyne substrates at equal substrate concentrations (bi-alkyne substrate had twice as much alkyne groups) according to Table 6.4. Gas flow rates, total reaction volumes and temperature are identical to studies in

Section 6.2. A mini study at a single substrate concentration selected from the range of concentrations known to oscillate was explored.

Table 6.4. Reactant concentrations employed in determining the influence of the number of alkyne groups at equivalent substrate concentrations. (V_{total} = 90 mL; stirring speed = 350 rpm; CO and air flow rates = 15 mL/min; temperature = 20±0.2°C).

[PdI_2] (μM)	[KI] (mM)	[A-PEG_{2000}-A] (mM)	[A-PEG_{2000}] (mM)
22.7	6.0	1.02	1.02

The oscillatory profiles in Figure 6.22(a-b) were obtained from experiments performed at conditions in Table 6.4. The pH profiles were obtained by automatically recording pH changes in the reaction over time, while the [H^+] adjusted profiles were obtained by converting the pH profiles as previously described [258, 259] (Section 4.2). Oscillations were recorded in reactions with mono and bi-alkyne substrates, with more oscillations occurring in the reaction with bi-alkyne functionalised substrate. Mixed mode oscillations which transitioned to simple oscillations were recorded in reaction with bi-alkyne substrate.

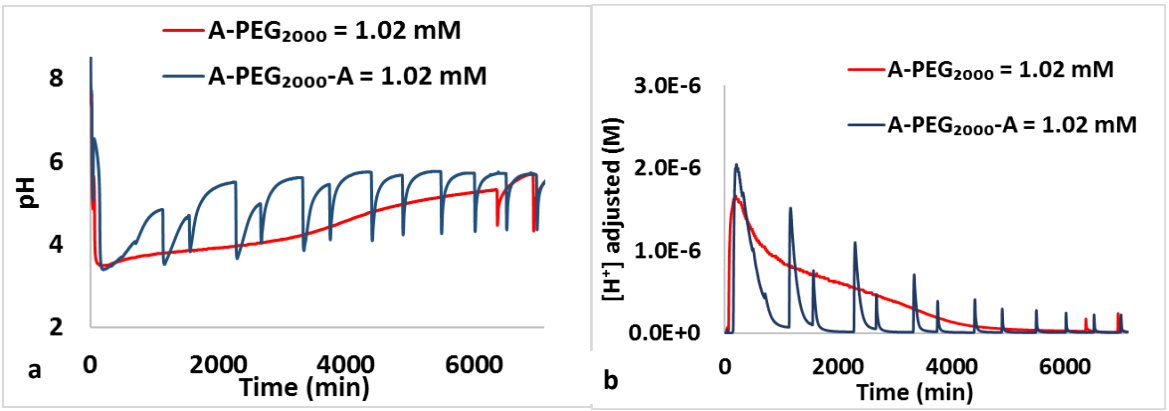

Figure 6.22. Reaction profiles obtained from oscillatory carbonylation reactions employing equal concentrations of mono alkyne and bi-alkyne functionalised polyethylene glycol as reaction substrates at constant catalyst concentration. (V_{total} = 90 mL; CO and air flowrates = 15 mL/min; [KI] = 6 mM; [PdI_2] = 22.7 μM). (a) pH profiles (b) [H^+] adjusted profiles

The initial features of the reaction profiles are given in Figure 6.23. Methanol and catalytic mixture were added and allowed to equilibrate for approximately 20 min before the methanolic mixtures were purged with CO and air at 15 mL/min. The initial difference in pH values prior to purging may be accredited to slight differences in pH probes, compounded by changes in ionic strength [176, 260-268] on addition of catalytic mixture and, the quality of HPLC grade methanol (used as received), as the reactions were carried out on separate occasions. The pH of both reactions decreased once purging commenced (represented as "1" in Figure 6.23), suggesting the onset of proton donating reactions. Eq. 4.2 to 4.4 proposed [8, 11, 29, 30, 32,

38, 103, 174, 198] for the carbonylation of the HPLC grade methanol and reactions with residual water contents in the methanol are thought to be responsible for the decrease in pH.

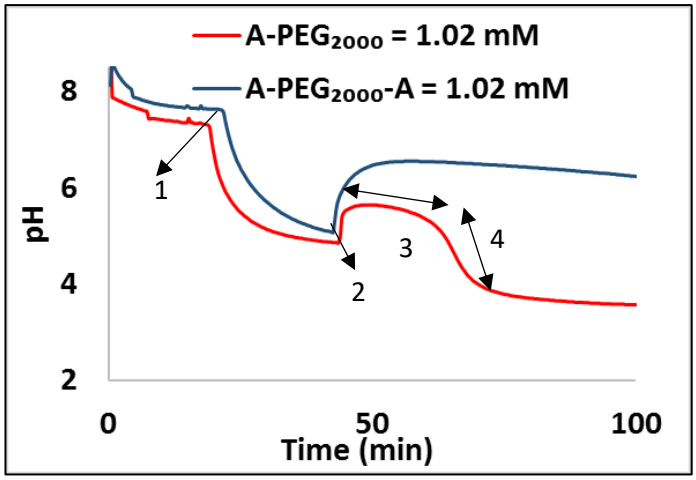

Figure 6.23 Initial features of the reaction profiles obtained at equal concentrations of mono alkyne and bi-alkyne functionalised polyethylene glycol substrate and constant catalytic concentration. (V_{total} = 90 mL; CO and air flowrates = 15 mL/min; [KI] = 6 mM; [PdI_2] = 22.7 μM) (1. Reaction purging; 2. Substrate addition; 3. Slow H^+ formation; 4. Initial autocatalytic substrate conversion)

Mono alkyne and bi-alkyne substrates were introduced to the reaction vessels as the pH drop from continuous purging slowed down. The addition of both substrates, indicated by the arrow "2" in Figure 6.23, was followed by rises in pH corresponding to reductions in [H^+] of the reactions. The decrease in [H^+] from substrate addition was followed by previously defined period of "slow H^+ formation" identifiable by the slowly decreasing pH trend in Figure 6.23 (double arrow labelled "3"). The slowly decreasing pH and gradual rise in [H^+] signify the onset of reactions forming HI. The HI formed from solvent and substrate carbonylation reaction discussed in previous sections of this thesis is assumed to donate the protons in this phase. The period of slow H^+ formation lasted 21 min for the mono alkyne substrate and 120 min for bi-alkyne substrate. The duration of slow H^+ formation recorded for mono alkyne substrate at [KI] = 6 mM and [PdI_2] = 22.7 μM is considerably less than duration (168 min) reported at same substrate concentration (1.02 mM) at [KI] = 5.7 mM and [PdI_2] = 29 μM (Sub-section 6.2.1). For the bi-alkyne substrate, the duration of slow H^+ formation was quite similar in both studies (120 min vs 115 min in Sub-section 6.2.1). The difference in slow H^+ phase recorded for mono alkyne substrate in this study is possibly from higher [H^+] obtained on purging the reactions ([H^+] in Sub-section 6.2.1 following purging was less). The comparable albeit slight increase in slow H^+ duration (115 to 120 min) noted in the bi-alkyne substrate reaction in this study and the study in Subsection 6.2.1 agrees with effects of reducing catalyst concentrations from 29 μM to 22.7 μM in this study.

The next rapid decrease in pH, given in Figure 6.23 (double arrow "4"), marked the end of period of slow H^+ formation phase. The sharp drop in pH is assumed to occur via autocatalysis and the autocatalytic production of HI according to Eq. 4.6 and Eq. 5.1 and/or 5.3 are proposed. An accumulation of HI in the slow H^+ formation phase is presumed to prompt the autocatalytic rise in $[H^+]$ (autocatalytic formation of HI) via the substrate conversion reaction given in Eq. 4.6, Eq. 5.1 and/or 5.3.

The increase in pH values (reduction in $[H^+]$) following the initial autocatalytic substrate conversion is assumed to arise from the consumption of the HI formed. The oxidation of HI forming iodine and water [3, 29, 38, 156, 270, 271] and, the reversible formation of methyl iodide and water from reactions between methanol and HI in excess KI [30, 287-289] are suggested as pathways supporting the rise in pH. The next rapid drop in pH with corresponding rise in $[H^+]$ adjusted marked the onset of oscillations. Oscillatory modes recorded at this catalytic concentration is given in Figure 6.24(a-b). Oscillations began 330 min into the reaction with bi-alkyne substrate, while it started at 6536 min from the initiation of reaction with mono-alkyne substrate. Small amplitude oscillations, which moved on to mixed mode oscillations (lasting over 2500 min), before transitioning finally to simple oscillations, were recorded in reaction with the bi-alkyne substrate. Amplitudes of the oscillations in bi-alkyne substrate reaction also decreased with increasing time and is attributed to the semi-batch nature of the reacting system. Only a single oscillation was recorded for the mono alkyne substrate over identical reaction time duration. A long non-oscillatory period with slowly rising pH (signifying H^+ consumption) preceded the oscillation.

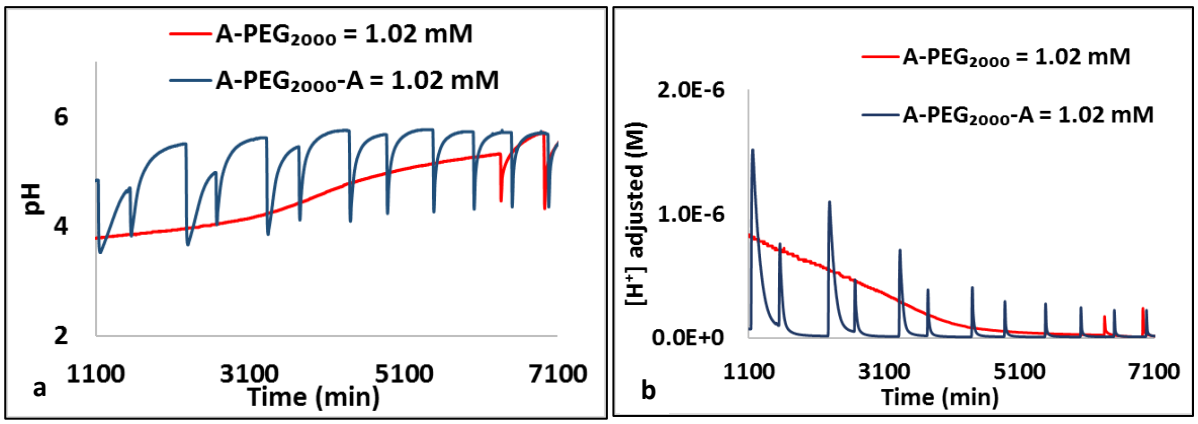

Figure 6.24. Oscillations at equal mono alkyne and bi-alkyne functionalised polyethylene glycol substrate concentrations and constant catalyst concentration (pH (a) and $[H^+]$ adjusted (b))

On assessing both studies (this study and Section 6.2.1) for reactions with equal substrate concentrations and twice the alkyne concentrations, a reduction in palladium iodide concentration and slight increase in KI concentration had visible effects on the oscillations in the mono alkyne substrate reaction. Significant declines in the number of oscillations and an increase in time at onset of oscillation were observed. At both palladium iodide concentrations, the reactions with bi-alkyne substrate displayed overall higher H^+ concentrations than mono alkyne version.

6.3.2 Case B: Reactions where the Mono Alkyne Substrate Concentration is Twice the Bi-Alkyne Substrate Concentrations (Constant Alkyne Concentration)

A similar study where single substrate concentrations of mono alkyne and bi-alkyne substrates were compared such that, the total alkyne concentration remained approximately the same, was investigated at $[PdI_2]$ = 22.7 μM and [KI] = 6 mM. The reaction conditions employed in the study for $[A\text{-}PEG_{2000}] \approx 2 \times [A\text{-}PEG_{2000}\text{-}A]$ are given in Table 6.5.

Table 6.5. Reactant concentrations employed in determining the influence of the number of alkyne groups at $[A\text{-}PEG_{2000}] \approx 2 \times [A\text{-}PEG_{2000}\text{-}A]$. ($V_{total}$ = 90 mL; stirring speed = 350 rpm; CO and air flow rates = 15 mL/min; temperature = 20±0.2°C)

$[PdI_2]$ (μM)	[KI] (mM)	$[A\text{-}PEG_{2000}\text{-}A]$ (mM)	$[A\text{-}PEG_{2000}]$ (mM)
22.7	6.0	1.02	2.03

The pH and $[H^+]$ adjusted profiles in Figure 6.25(a-b) compare oscillatory behaviours recorded during the carbonylation of mono alkyne and bi-alkyne functionalised substrates. Oscillations were recorded in both reactions, but largely smaller amplitude oscillations were obtained with mono-alkyne substrate. The presence of smaller oscillations (amplitude and period) in the reactions with mono alkyne substrate in comparison to oscillation size for bi-alkyne substrate, is similar to smaller oscillations obtained in studies in Sub-section 6.2.3 at higher PdI_2 concentration (29 μM). Also, in this instance, generally higher $[H^+]$ values were obtained with the mono functional substrate at the catalytic concentration in Table 6.5. This contrasts the lower $[H^+]$ in Sub-section 6.2.3 at same substrate concentration and is indicative of a difference in reaction pathways.

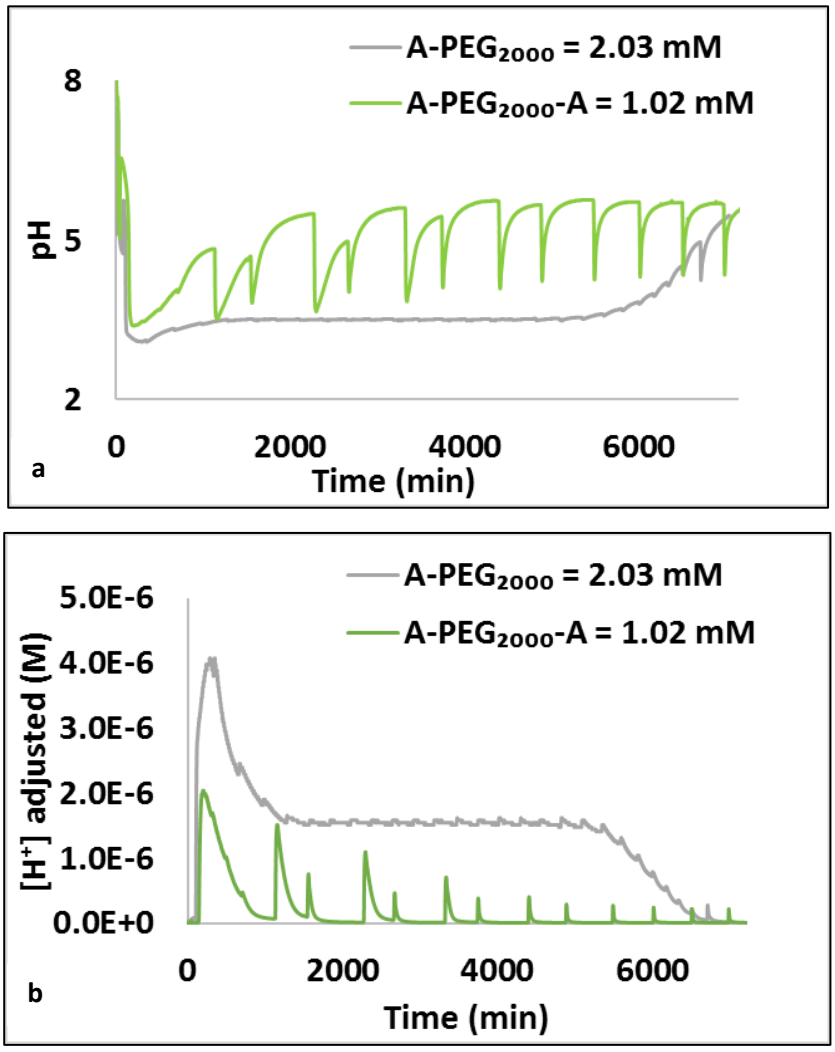

Figure 6.25. Reaction profiles from the oscillatory carbonylation reactions where mono alkyne substrate is twice the concentration of the bi-alkyne functionalised polyethylene glycol substrate ([A-PEG$_{2000}$] ≈ 2 x [A-PEG$_{2000}$-A]). ([KI] = 6 mM; [PdI_2] = 22.7 μM; CO and air flow rates = 15 mL/min; temperature = 20±0.2^{o}C). (a) pH and (b) [H^+] adjusted profiles

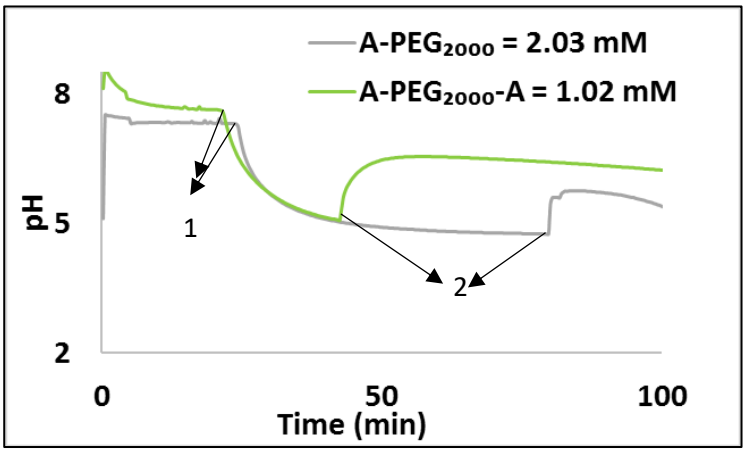

Figure 6.26. Initial profile features in the oscillatory carbonylation reactions. ([A-PEG$_{2000}$] ≈ 2 x [A-PEG$_{2000}$-A]). ([KI] = 6 mM; [PdI_2] = 22.7 μM; CO and air flow rates = 15 mL/min; temperature = 20±0.2^{o}C; 1. Reaction purging; 2. Substrate addition)

Profiles showing reaction conditions during the initial phase of the oxidative carbonylation and pH changes as reactants are added to methanol (solvent) is given in Figure 6.26. The initial difference in pH before the first set of arrows from the left of Figure 6.26 is attributed to variations in the quality of methanol (which was used as received), slight differences in pH probes and changes in ionic strength [176, 260-268] of the methanol on addition of catalytic mixture. Dilute solutions of methanol and catalytic mixtures were purged with CO and air at 15 mL/min, indicated by the arrows "1" in Figure 6.26. Purging each reaction caused a decrease in pH which is consistent with a rise in H^+ concentration. Proton donation at this stage is believed to proceed according to Eq. 4.2 to 4.4 and arises from methanol carbonylation and water-CO-PdI_2 reactions [8, 11, 29, 30, 38, 103, 174, 198, 269]. In this instance, the interval of purging for one of the reactions was left for a longer period (55 min) to gain some awareness on the duration required for Eq. 4.4 (methanol carbonylation) to approach equilibrium. When both substrates were added to the reaction at point "2" in Figure 6.26, the pH rose to maximum values of 5.74 and 6.55 pH units for mono-alkyne and bi-alkyne substrates, respectively. This rise in pH is ascribed to changes in the dynamics of the reacting system and may have risen from additional methanol introduced with substrate solution, dilution on adding the substrate solution and interactions between H^+ and the polymeric substrate. The substrates may play a contributory role to pH rise and considerations were given to concentration of PEG backbone in Sub-section 6.2.3 and addition of methanol during oxidative carbonylation reactions of phenyl acetylene is known to generate rise in pH [9, 10, 32, 175, 243].

The decrease in pH after substrate addition was followed by periods of gradual HI formation ("slow H^+" formation phase) and lasted for 26 min and 120 min in reactions with mono-alkyne and bi-alkyne substrates, respectively. This slowly decreasing pH and corresponding rise in H^+ is proposed to occur from gradual formation of protons due to the HI formed in Eq. 4.2 to 4.4, Eq. 4.6, and Eq. 5.1 and/or 5.3. Eq. 4.6, Eq. 5.1, and Eq. 5.3 are assumed to start slowly and are dependent on HI from Eq. 4.2 to 4.4. Such slowly decreasing pH trend on substrate addition has been observed following addition of phenyl acetylene under various conditions (higher and lower temperatures) albeit higher substrate concentrations (up to 100 times higher) were employed [8, 9, 30, 32] and it was also observed with mono-alkyne substrate at 2.03 mM and higher palladium iodide concentration (1.78 times) [29].

The period of slow accumulation of HI in both reactions was followed by the autocatalytic formation of HI due to substrate conversion and then, a very short duration of HI consumption according to Eq. 4.8 and 4.9, before oscillations commenced at 330 min and 340 min for bi-alkyne and mono alkyne substrate reactions, respectively. The onset of oscillation was marked

by subsequent autocatalytic decrease in pH. Each oscillatory cycle entailed autocatalytic HI formation and periods of HI consumption with palladium regeneration occurring during the H^+ consumption phase (Eq. 4.11 and 4.12). Oscillations were still ongoing when the experiments were stopped.

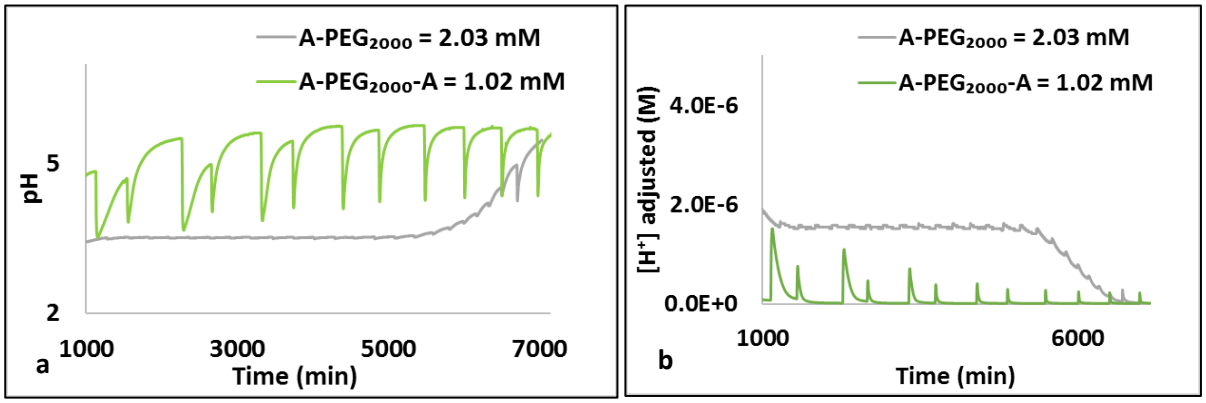

Figure 6.27. Selections of oscillations in the carbonylation reactions where [A-PEG$_{2000}$] ≈ 2 x [A-PEG$_{2000}$-A]. pH (a); [H^+] adjusted (b)

Excerpt of oscillations recorded from the carbonylation of mono and bi-alkyne substrates at [A-PEG$_{2000}$] ≈ 2 x [A-PEG$_{2000}$-A] is given in Figure 6.27(a-b). Very small pH amplitude oscillations were recorded with both substrates as oscillations commenced. The small oscillations transitioned to larger amplitude oscillations for bi-alkyne substrate reaction, while it remained as small amplitude oscillations for an extensive duration in the reaction with mono alkyne substrate (pH amplitude = 0.01 to 0.03pH units per oscillation). The presence of frequent smaller oscillations in reactions with mono alkyne substrate is consistent with earlier assumption made in Sub-section 6.3.3, wherein, the rate of the autocatalytic mono alkyne substrate conversion is assumed to proceed at a faster rate than reactions with bi-alkyne substrate.

6.3.3 Section Summary

Summaries of key features from oscillatory carbonylation at [PdI_2] = 22.7 μM and [KI] = 6 mM are given in Table 6.6 and Figures 6.28 to 6.30.

Table 6.6. Summary statistics of some features in the oscillatory carbonylation reactions at [PdI_2] = 22.7 μM and [KI] = 6 mM

Substrate name	[A-PEG$_{2000}$-A] (Bi-functional)	[A-PEG$_{2000}$]	[A-PEG$_{2000}$]
Substrate concentration (mM)	1.02	1.02	2.03
Autocatalytic ΔpH at the end of "slow H^+ formation" phase	3.00	1.22	1.76

Autocatalytic ΔH^+ adjusted at the end of "slow H^+ formation" phase (M)	1.91 x 10^{-6}	1.55 X 10^{-6}	3.89 X 10^{-6}

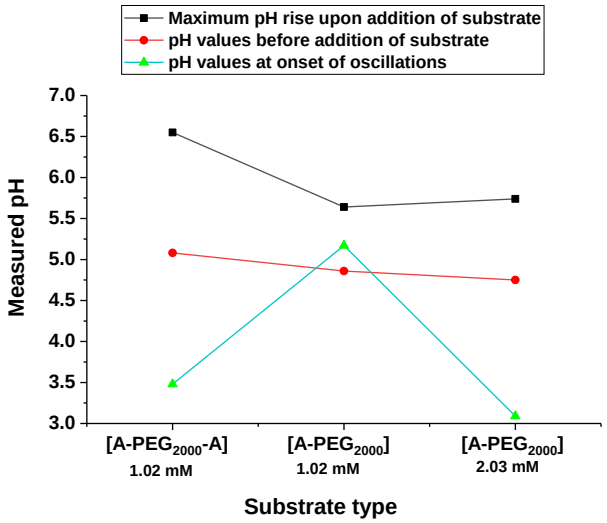

Figure 6.28. Graphical summary of pH values at different points of the carbonylation reaction. ([KI] = 6 mM and [PdI_2] = 22.7 μM)

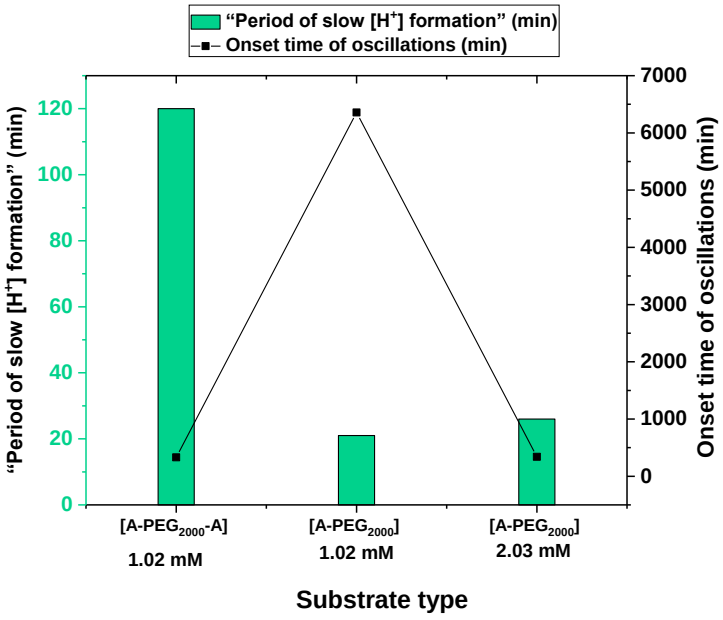

Figure 6.29. Changes in duration of slow H^+ formation and onset time of oscillation as a function of substrate type and substrate/alkyne concentration ([KI] = 6 mM and [PdI_2] = 22.7 μM)

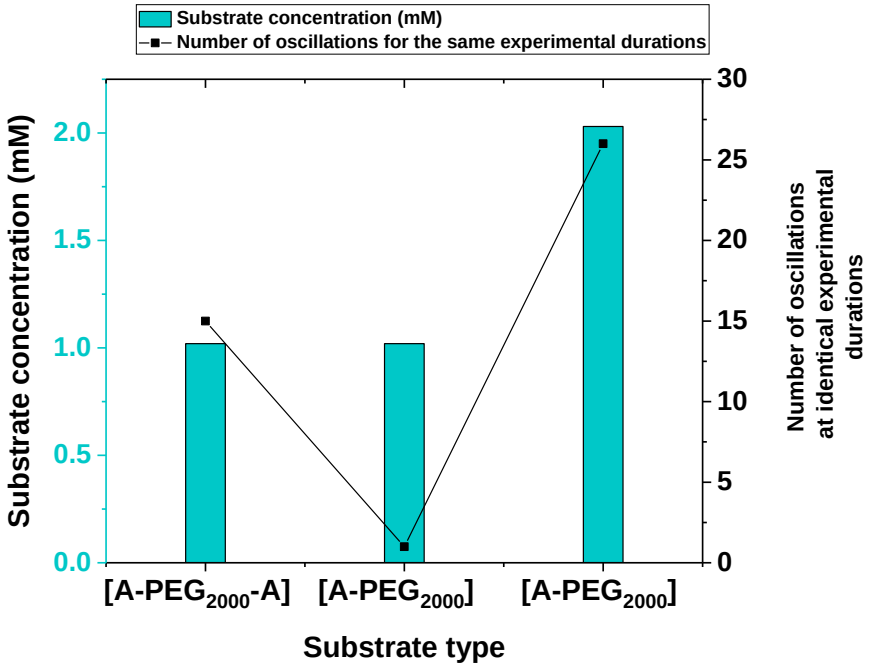

Figure 6.30. Number of oscillations recorded across studies in cases A and B as a function of substrate type and substrate/alkyne concentration ([KI] = 6 mM and [PdI_2] = 22.7 μM)

In conclusion,

1. Oscillations were recorded for all carbonylation reaction studies at [KI] = 6 mM and [PdI_2] = 22.7 μM
2. In reactions with equal mono and bi-alkyne substrate concentrations (1.02 mM but twice alkyne concentration present in bi-functional substrate), maximum pH rise on substrate addition was higher when bi-alkyne functionalised PEG was the reaction substrate, which is consistent with findings at same substrate concentration and higher PdI_2 concentration (29 μM, Section 6.2) (Case A).
3. At 1.02 mM bi-alkyne and 2.03 mM mono alkyne concentrations (equal alkyne concentration), pH rise on substrate addition was higher in the bi-alkyne reaction. This contrasts findings at [PdI_2] = 29 μM (Section 6.2.1) and is attributed to extended purging time (55 min) in mono alkyne reaction (is thought to have increased availability of H^+) (Case B).
4. Period of gradual H^+ formation prior to initial autocatalysis defined as period of "slow H^+ formation" was higher in bi-alkyne substrate reactions. It also increased from 115 min to 120 min on reducing PdI_2 concentrations from 29 to 22.7 μM in reactions with equal substrate concentrations (Case A).

5. In Case B, the duration of "slow H^+ formation" was lower in reaction with mono alkyne substrate, which contrast findings at higher PdI_2 concentration (29 μM; Section 6.2.3). The extended purging times in reaction with mono alkyne substrate is also suggested as reason for the disparity.
6. Extended purging time in reaction with equal alkyne and twice mono alkyne substrate concentration (Case B) appears to have reduced the duration of slow H^+ formation and, increased the $[H^+]$ formed from initial autocatalysis.
7. Initial $[H^+]$ from autocatalysis ($[PdI_2]$ = 22.7 μM) in reactions with twice alkyne concentration and equal substrate concentrations (Case A) was higher in reaction with bi-alkyne substrate and was lower in comparison to value at higher PdI_2 concentration (29 μM). This reduced concentration is attributed to lower catalyst concentration at 22.7 μM.
8. Onset time of oscillation was higher in reaction with bi-alkyne substrate for case A, while it was higher in reaction with mono alkyne substrate reaction for Case B. Both cases agree with findings in Section 6.2.1 and 6.2.3 respectively.
9. Number of oscillations decreased with decreasing PdI_2 concentration in Case A. The trade-off between number and size of oscillations postulated in Section 6.2.4 is supported by current study, since a larger number of smaller oscillations was recorded with mono alkyne substrate.

6.4 Influence of Number of Functional Groups on Polymeric Substrate at Constant Catalytic Concentration ($[PdI_2]$ = 17 μM and [KI] = 6 mM)

The catalyst concentration was further reduced, and the influence of alkyne functionality was assessed finally at $[PdI_2]$ = 17 μM and [KI] = 6 mM**.** Both scenarios, wherein, the alkyne concentration was twice (bi-alkyne functionalised substrate) though equal mono and bi-functional substrate concentrations were employed (Case A), and when the total alkyne concentration was held constant by employing twice the mono alkyne substrate concentration (Case B), were likewise investigated.

6.4.1 Case A: Reactions at Equal Mono Alkyne and Bi Alkyne Substrate Concentrations (Double Alkyne Concentration)

The effects of dual alkyne functionality were assessed by employing equal substrate concentrations of the mono and bi-alkyne substrates at constant catalytic concentration according to Table 6.7.

Table 6.7. Reactant concentrations employed in determining the influence of the number of alkyne groups at equal substrate concentrations. (V_{total} = 90 mL; stirring speed = 350 rpm; CO and air flow rates = 15 mL/min; temperature = 20±0.2°C).

[PdI_2] (μM)	[KI] (mM)	[A-PEG_{2000}-A] (mM)	[A-PEG_{2000}] (mM)
17	6.0	1.02	1.02

The reaction profiles in Figure 6.31(a-b) were obtained from the oxidative carbonylation of equal concentrations of mono-alkyne and bi-alkyne functionalised polyethylene glycols at constant palladium iodide and KI concentrations. Oscillations were recorded in both profiles at selected concentration. Reaction profile from bi-alkyne functionalised substrate presented with higher hydrogen ion concentration at later periods of the oscillatory phase on comparing both reactions, however, the [H^+] during the initial autocatalysis and onset of oscillations was higher in the reaction with mono alkyne substrate.

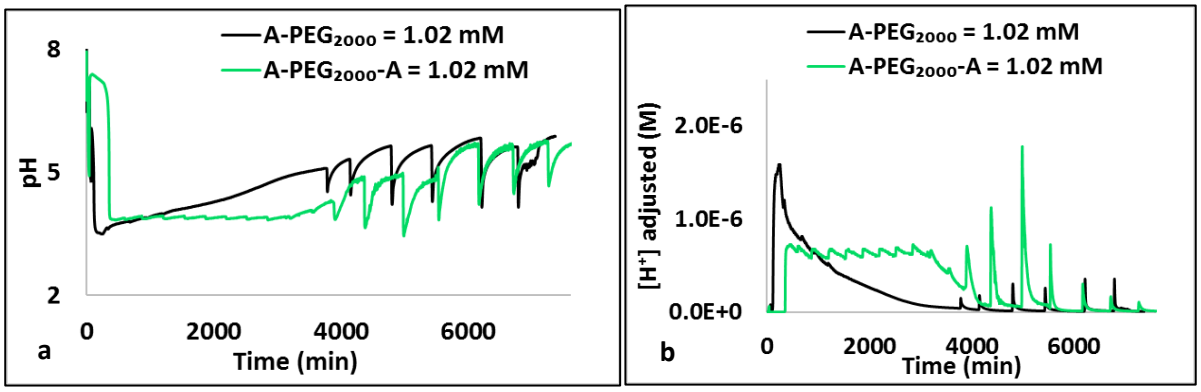

Figure 6.31. Reaction profiles from oscillatory carbonylation reactions at equal concentrations of mono alkyne and bi-alkyne functionalised polyethylene glycol substrates and constant catalytic concentration. (a) pH profiles (b) [H^+] adjusted profiles. (V_{total} = 90 mL; CO and air flow rates = 15 mL/min; [KI] = 6 mM; [PdI_2] = 17 μM)

The initial stages of the carbonylation reaction at equal substrate concentrations (twice the alkyne concentration) is give in Figure 6.32. The catalytic mixture was added to bulk methanol and allowed to equilibrate before the vessels were purged with CO and air. On purging (Figure 6.32 (arrow labelled "1"), the pH in both reactions decreased as the H^+ concentration arising from HI formed during solvent carbonylation increased. The pH drops in both reactions differed as purging continued. The differences in pH drop (increase in H^+) from purging is attributed to different water / moisture contents present, as this would affect Eq. 4.2 and 4.3 and thus, the concentration of HI formed.

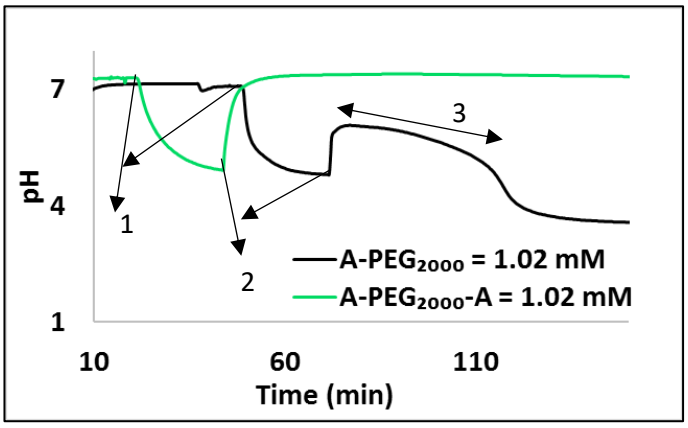

Figure 6.32. Initial features of reaction profiles obtained at equal concentrations of mono alkyne and bi-alkyne functionalised polyethylene glycol substrate and constant catalytic concentration. (1. purging with CO and air; 2. Substrate addition; 3. "Slow H^+ formation") (V_{total} = 90 mL; CO and air flow rates = 15 mL/min; [KI] = 6 mM; [PdI_2] = 17 μM)

Solutions of the substrates (dissolved in ≈ 3.5 mL of methanol) were added as the pH drop from purging began to equilibrate, causing a rise in pH values. The rise in pH on adding the substrate is indicated by the arrows, "2" in Figure 6.32. The maximum pH rise on substrate addition was higher in the reaction where bi-alkyne substrate was present (rose to 7.38 against 6.08 recorded for the mono-alkyne substrate). A period of gradual increase in [H^+] ("slow H^+" formation phase), exemplified by the double arrow "3" in Figure 6.32 succeeded substrate addition. This period of slow hydrogen ion formation was longer for reaction with bi-alkyne substrate; lasting for 322 min, while it lasted for 61 min in the reaction with mono alkyne PEG substrate. The durations of slow H^+ formation is much higher at this concentration than at [PdI_2] = 22.7 μM (120 min, bi-alkyne; 21 min, mono alkyne) regardless of using identical mono and bi-alkyne substrate concentrations (1.02 mM) in this study and the study in Section 6.3.1. Since catalyst concentration is reduced in this study, the longer durations are predictable as the rate of formation of HI is dependent on concentration of PdI_2. HI produced from solvent carbonylation and the initially slow substrate conversion reactions are assumed as source of protons, seen as the slowly falling pH in Figure 6.32 (double arrow "3").

As the concentration of HI slowly increases, a HI concentration which triggers the onset of the autocatalytic formation of HI is presumed to be reached. This assumption is supported by the rapid way the pH transitions from a period of slowly changing pH values in less acidic pH regions to very fast pH changes and arriving at a final value that is much more acidic. The autocatalytic substrate conversion reactions are proposed as reasons for the rapid change in pH. The autocatalytic decrease in pH (increased H^+ concentration) was followed by a short period of HI consumption before the onset of oscillations. Oscillations commenced at 330 min and 597 min in reactions with mono alkyne and bi-alkyne substrates, respectively. pH at onset of

oscillations was higher for the bi-alkyne functionalised substrate (3.9 pH units against 3.64 pH units for mono alkyne substrate). The higher pH at onset of oscillations in the reaction with bi-alkyne substrate suggests that less HI was formed in this reaction. Small amplitudes oscillations were recorded initially in mono and bi-alkyne reactions at equal substrate concentrations.

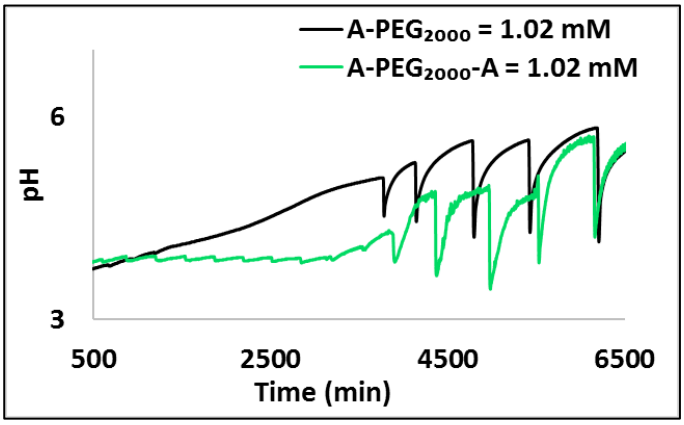

Figure 6.33. Oscillatory patterns at equal mono alkyne and bi-alkyne functionalised polyethylene glycol substrate concentrations and constant catalytic concentration

The small amplitude oscillations lasted till ≈ 4000 min from onset of both reactions, before the oscillations transitioned to larger amplitude simple oscillations. The transition from small oscillations to large oscillations is shown in Figure 6.33. Such transition from one type of oscillatory rhythm to another has been observed in other oscillating reactions and is discussed in detail in a subsequent section of this chapter. A total of 19 oscillations were recorded for the bi-alkyne substrate reaction while, 8 oscillations were obtained with the mono alkyne substrate for the same experimental duration. Oscillations were still ongoing when the reactions were stopped.

6.4.2 Case B: Mono Alkyne Substrate Concentration is Twice Bi-Alkyne Substrate Concentrations (Constant Alkyne Concentration)

The effects of number of functional groups per polymer chain at constant alkyne concentration and the influence of additional PEG backbone was studied by employing twice as much mono alkyne substrate concentration per bi-alkyne substrate concentration at the conditions presented in Table 6.8.

Table 6.8. Reactant concentrations employed in determining the influence of the number of alkyne groups at [A-PEG$_{2000}$] ≈ 2 x [A-PEG$_{2000}$-A]. (V_{total} = 90 mL; stirring speed = 350 rpm; CO and air flow rates = 15 mL/min; temperature = 20±0.2^{o}C)

[PdI_2] (μM)	[KI] (mM)	[A-PEG$_{2000}$-A] (mM)	[A-PEG$_{2000}$] (mM)
17	6.0	1.02	2.03

The reaction profiles in Figure 6.34(a-b) were acquired from reactions performed at the conditions in Table 6.8. pH profiles were acquired by automatically recording pH changes as the reaction progressed, while $[H^+]$ adjusted profiles were obtained by converting the pH profiles according to Eq. 4.1.

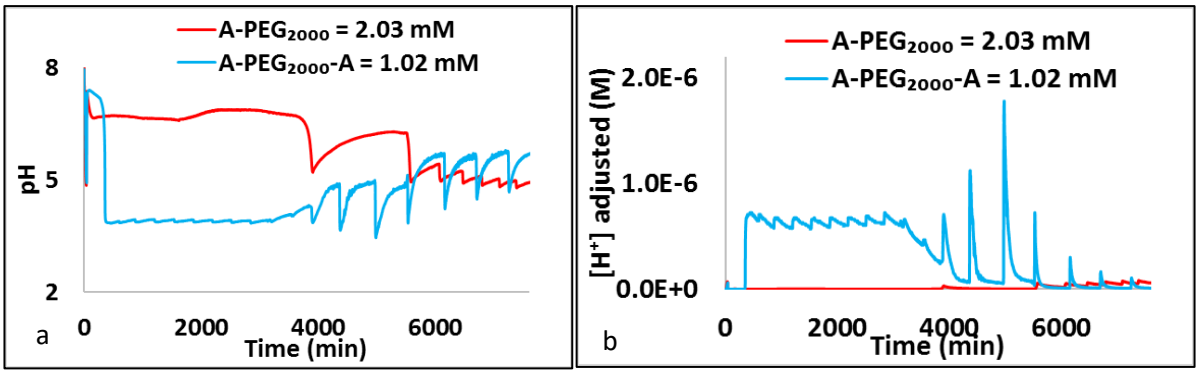

Figure 6.34. Reaction profiles from the oscillatory carbonylation reactions where mono alkyne substrate is twice the concentration of the bi-alkyne functionalised polyethylene glycol substrate ([A-PEG$_{2000}$] ≈ 2 x [A-PEG$_{2000}$-A]). (a) pH and (b) $[H^+]$ adjusted profiles. ([KI] = 6 mM; [PdI_2] = 17 μM; V_{total} = 90 mL; CO and air flow rates = 15 mL/min; temperature = 20±0.2^{o}C)

Oscillations were recorded in both substrates at constant catalytic concentration. $[H^+]$ adjusted values were higher in reaction with bi-alkyne substrate, despite both reactions having approximately equal concentrations of alkyne end groups. Oscillatory patterns were also different in both reactions. The oscillations in the reactions to which bi-alkyne substrate was added started off as small amplitude oscillations which eventually transitioned to large amplitude simple oscillations, while oscillations in the reaction with mono alkyne substrate started off with large amplitude oscillations that transitioned to small amplitude oscillations. Oscillations were still ongoing when both runs were stopped.

pH profiles illustrating changes in pH due to reactant addition are shown in Figure 6.35. The catalytic mixture was added to methanol and the solutions were purged with CO and air for 20 to 30 min leading to decrease in pH (increased $[H^+]$). The decrease in pH on purging the methanolic solution is proposed to arise from carbonylation of the solvent and agrees with previous findings in the oscillatory carbonylation of phenyl acetylene [8, 11, 30, 32, 103, 174]. The differences in pH drop on purging is similarly attributed to variations in quality of methanol and/or moisture present in gases and atmosphere (reactions were accomplished on different days).

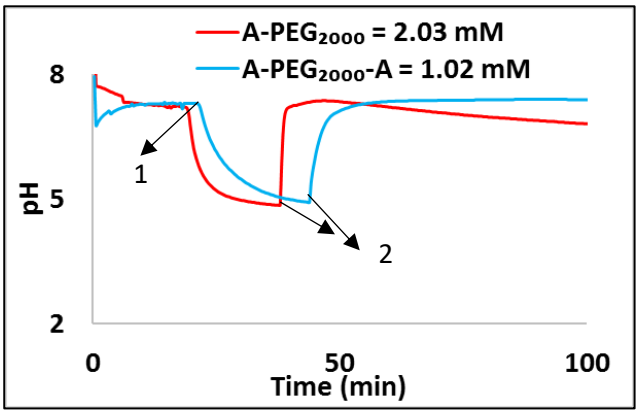

Figure 6.35. Initial profile features in the oscillatory carbonylation reactions where [A-PEG$_{2000}$] ≈ 2 x [A-PEG$_{2000}$-A]. (1. Reaction purging; 2. Substrate addition) ([KI] = 6 mM; [PdI_2] = 17 μM; V_{total} = 90 mL; CO and air flow rates = 15 mL/min; temperature = 20±0.2^{o}C)

The pH increased in both reactions as a result of reduced H^+ concentrations when methanolic solutions of mono and bi-alkyne substrates were added to the reactions. The points of substrate addition are indicated by the arrows, "2" in Figure 6.35. As discussed previously, methanol, substrate concentration / type and dilution are thought to play key roles in pH rises due to substrate addition.

The period of "slow H^+ formation" marked by gradual formation of [H^+] and the slowly decreasing pH followed substrate addition. During this phase, HI produced from Eq. 4.2 to 4.4, 4.6 and Eq. 5.1 and/or 5.3 are proposed as sources of hydrogen ions and the decrease in pH. The period of slow HI formation lasted 3716 min in reaction with mono alkyne substrate and 322 min for the reaction with bi-alkyne PEG substrate. A large difference in the duration of the slow H^+ formation phase is noted on comparing both substrates, although the alkyne group concentration was approximately equal. This period is also the longest recorded for slow HI formation across concentrations investigated in this chapter. The lower concentration of palladium iodide (17 μM) available for catalysis is presumed to limit the rate of HI formation and other reactions in the experimental run with mono-alkyne PEG as substrate. Whereas the bi-alkyne reaction had the same catalyst concentration, it appears that the presence of two alkyne end groups per chain enabled the formation of HI in the "slow phase". Thus, reducing the time spent in this phase. The next sharp pH drop shown in Figure 6.36 arose from the autocatalytic production of HI as the substrates were converted. The HI formed in the slow phase is proposed to reach inception points, which then trigger the autocatalytic substrate conversion and HI formation given in Eq. 4.6 and Eq. 5.1 and/or Eq.5.3.

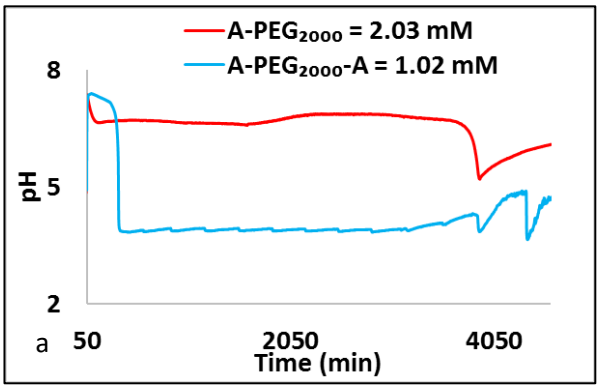

Figure 6.36. Initial autocatalysis and onset of oscillations in the carbonylation reactions where [A-PEG$_{2000}$] ≈ 2 x [A-PEG$_{2000}$-A]. ([KI] = 6 mM; [PdI_2] = 17 μM; V_{total} = 90 mL; CO and air flow rates = 15 mL/min; temperature = 20±0.2^{o}C)

Oscillations commenced immediately after the initial autocatalytic HI formation in both reactions, despite the duration required to reach the point of autocatalysis. Oscillations started at 3754 min for mono alkyne substrate and 597 min for the reaction with bi-alkyne substrate. pH at onset of oscillation was higher in the mono alkyne substrate reaction (5.37) than the bi-alkyne substrate (3.9) and is attributed to reduction in catalyst concentration and presence of dual alkyne end groups on the bi-functional substrate. Extract of oscillations during the carbonylation reaction is given in Figure 6.37.

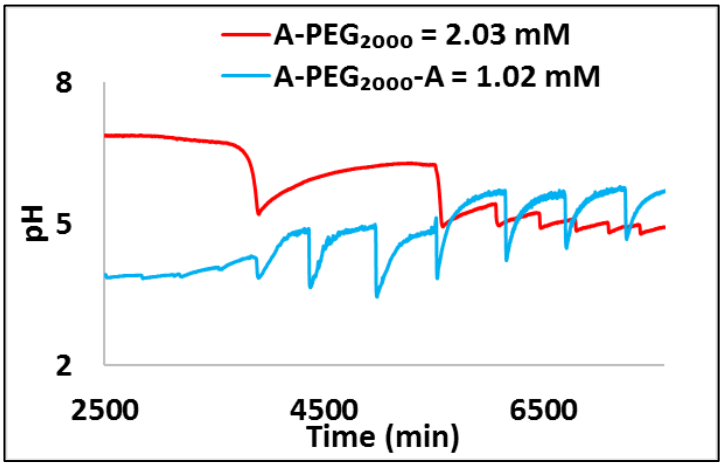

Figure 6.37. Oscillatory patterns in the oxidative carbonylation reactions where [A-PEG$_{2000}$] ≈ 2 x [A-PEG$_{2000}$-A]. ([KI] = 6 mM; [PdI_2] = 17 μM; V_{total} = 90 mL; CO and air flow rates = 15 mL/min; temperature = 20±0.2^{o}C)

6.4.3 Section Summary

Graphical and tabular summaries of key features of the reaction profiles discussed in Section 6.4 are given in Table 6.7 and Figures 6.38 to 6.40.

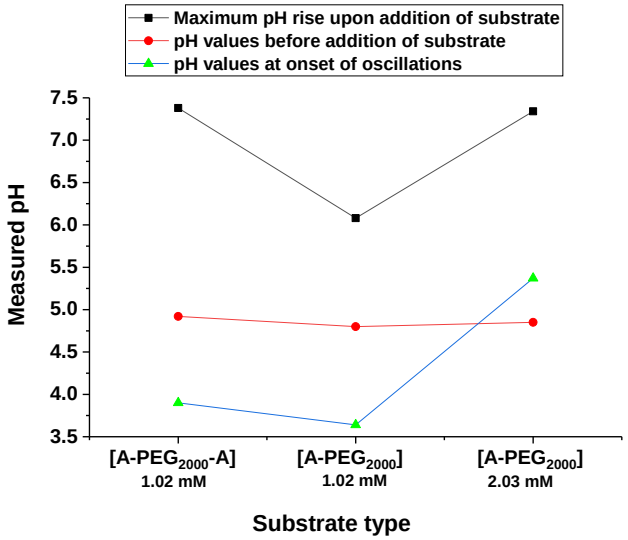

Figure 6.38. Graphical summary of pH values at different points of the carbonylation reaction. ([KI] = 6 mM and [PdI_2] = 17 μM)

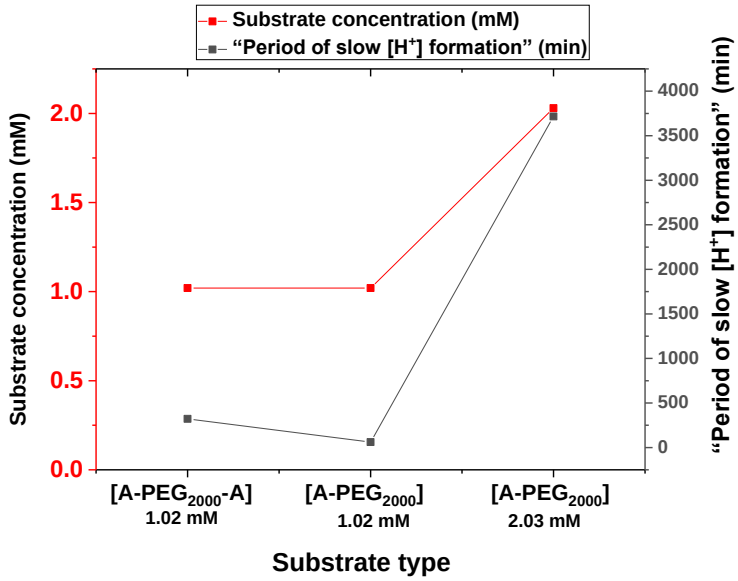

Figure 6.39. Changes in duration of slow H^+ formation as a function of substrate type and substrate/alkyne concentration ([KI] = 6 mM and [PdI_2] = 17 μM)

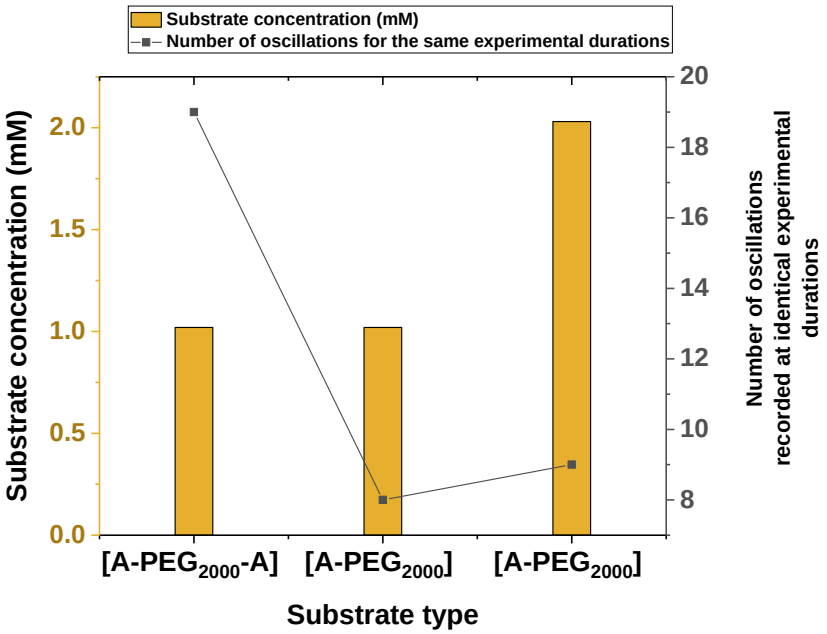

Figure 6.40. Number of oscillations recorded across studies in cases A and B as a function of substrate type and substrate/alkyne concentration ([KI] = 6 mM and [PdI_2] = 22.7 μM)

Table 6.9. Summary statistics of some features in the oscillatory carbonylation reactions at [PdI_2] = 17 μM and [KI] = 6 mM

	[A-PEG_{2000}-A] (Bi-functional)	[A-PEG_{2000}]	[A-PEG_{2000}]
Substrate concentration (mM)	1.02	1.02	2.03
Autocatalytic ΔpH at the end of "slow H^+ formation" phase	3.46	2.30	1.40
Autocatalytic ΔH^+ adjusted at the end of "slow H^+ formation" phase (M)	6.9×10^{-7}	1.54×10^{-6}	2.94×10^{-8}
Onset time of oscillations (min)	597	330	3960

The number of oscillations recorded for reaction with bi-alkyne functionalised polymer (1.02 mM) was considerably higher than oscillations at equivalent concentration of mono-alkyne substrate (1.02 mM) and was also higher when alkyne concentrations were kept constant (1.02 mM bi-alkyne and 2.03 mM, mono alkyne concentrations). Number of oscillations at 17 μM palladium iodide concentration was higher than oscillations recorded at 22.7 μM. Findings from studies in Sections 6.2, 6.3 and 6.4 which assessed the influence of number of functional groups per polymeric chain is summarised next.

Summary of studies in Sections 6.2, 6.3 and 6.4 at equal mono and bi-alkyne substrate concentration (the influence of doubling the alkyne concentration)

1. Maximum pH rises on adding substrates were consistently higher in reaction with bi-alkyne substrate irrespective of PdI_2 concentration (17 to 29 µM).
2. The duration of gradual increment in HI following substrate addition termed "slow H^+ formation" phase was longer in reactions with bi-alkyne substrate at all [PdI_2] investigated. This duration also increased as PdI_2 reduced from 29 to 17 µM.
3. Increase in H^+ from initial autocatalytic substrate conversion was greater in reaction with mono alkyne substrate at [PdI_2] = 17 µM, which contrasts the findings at [PdI_2] = 22.7 and 29 µM (higher for bi-alkyne reactions). This contrast is attributed to reduced catalyst concentration at 17 µM.
4. pH (lower H^+ value) and time at onset of oscillation was higher in reactions with bi-alkyne substrate at [PdI_2] = 17, while at [PdI_2] = 22.7 and 29 µM (higher catalyst concentration), pH and time at onset of oscillation was higher for mono alkyne substrate reactions.
5. Number of oscillations recorded was higher in reactions with bi-alkyne substrate at lower catalyst concentration (17 & 22.7 µM) for the same mono and bi-alkyne reaction durations. At higher catalyst concentration (29 µM), number of oscillations was higher for mono alkyne substrate.

Summary of studies in Sections 6.2, 6.3 and 6.4 where mono alkyne concentration is twice the bi-alkyne substrate concentration (effects of maintaining constant alkyne concentration)

1. Maximum pH rises on adding substrates was higher for bi-alkyne substrate reactions at 17 and 22.7 µM, while at 29 µM, pH rise was higher in the mono alkyne substrate. At reduced [PdI_2], less H^+ is formed on purging which may have promoted higher values for bi-alkyne substrate
2. The duration of "slow H^+ formation" was longer in reactions with mono alkyne substrate at 17 and 29 µM PdI_2 concentrations, but at [PdI_2] = 22.7 µM, the duration was longer in the reaction with bi-alkyne substrate.
3. Increase in H^+ from initial autocatalytic substrate conversion was greater in reaction with bi-alkyne substrate at [PdI_2] = 17 and 29 µM. At [PdI_2] = 22.7 µM, HI formed from initial autocatalysis was higher in mono alkyne substrate reaction (the reaction with mono alkyne substrate was purged for an extended period of time).

4. pH and time at onset of oscillation was higher in reactions with mono alkyne substrate at [PdI_2] = 17 and 29 µM. The pH at onset of oscillations when [PdI_2] = 22.7 µM was higher in bi-alkyne substrate reaction, but the onset time of oscillation longer in mono alkyne substrate. Consistent differences at 22.7 µM suggest the possibility of optimal catalyst vs substrate concentration.
5. Number of oscillations recorded was higher in reactions with bi-alkyne substrate at [PdI_2] = 17 µM, which contrast the higher number recorded for mono alkyne substrates at [PdI_2] = 22.7 and 29 µM.

6.5 Analysis of Experimentally Observed Complex Phenomena

In Chapters 4 and 5, and earlier sections of this chapter, oscillatory profiles from the carbonylation of alkyne functionalised polyethylene glycol were considered. In these chapters, certain features identified in the reaction profiles were briefly ascribed to the manifestation of some phenomena. These features include: -

a. Stable and lasting pH transitions from regions of higher acidity to lower acidity states and vice versa in non-oscillatory profiles
b. Stable and lasting pH transition during oscillations such that more than one oscillatory pH region is present in a single unperturbed profile. For example, it was possible to achieve lasting oscillations between pH 3 and 4 and then between pH 5 and 6 in a single run.
c. Mixed mode oscillations, intermittent oscillations [117] and a range of complex oscillations exhibiting varying degrees and combinations of several types of oscillations [6, 71, 98, 108-112, 114, 115, 184, 301-304].
d. Irregular aperiodic pH changes in oscillatory and non-oscillatory profiles occurring mostly at later stages of the oxidative carbonylation reactions.

The features in a-d above collectively represent most phenomena observed in experimental profiles. The aforementioned phenomena were reproducibly observed in the oxidative carbonylation of mono and bi-alkyne functionalised polyethylene glycols with palladium iodide as catalysts and KI as catalyst promoter. Usually, one phenomenon per profile was typical across the range of concentrations investigated. However, it was also possible to obtain reaction profiles showing combinations of the above-mentioned phenomena. Such pH transitions and variations in type of oscillations is known to occur in many oscillating chemical systems. These phenomena are not limited to chemical systems, as they have been be found in

biological systems and biochemical systems (neural, enzymatic etc.) [44, 47, 62, 97, 98, 119, 120, 296]; electrochemical systems [319-321]; surfaces [322-324] and in mathematics [325-328]. Earlier researchers in various fields where these phenomena were identified termed and defined the features after extensively investigating them. Based on the views and findings of earlier researchers, the features in a-d may be classified under several nonlinear phenomena proposed by these researchers. These phenomena include; multi-stability (bi-stability) [12, 14, 26, 89, 92, 94, 96, 296, 329], multi-rhythmicity [95, 96, 99, 116, 119, 120, 330, 331], several variations of mixed mode and complex oscillations [6, 71, 98, 108-112, 114, 115, 184, 301-304] and aperiodic (chaos) like irregularities [12, 14, 68, 109, 116, 119, 123, 195, 332]. Profiles with features described in "a" and "b" are classed as multi-stable and multi-rhythmic profiles based on the transitions and the absence of external perturbations. Profiles with features in "c" are as described in "c" and the oscillatory patterns present in these profiles are self-explanatory and profiles with features in "d" are classed aperiodic irregular profiles. The experimental profiles provided here are based on measurements from pH changes alone and are not backed or corroborated by additional investigative methods. This lack of corroboration may pose some questions on the sufficiency of characterising and classifying the features by changes in pH alone. As other methods were not used to support the classifications presented herein, this section serves as an introduction to the complexities of oscillatory carbonylation with polymeric substrates.

Nonetheless, extensive modelling and simulation studies of nonlinear systems support the existence of these phenomena and have successfully defined potential conditions for achieving them [12, 71, 89, 92, 111, 113, 174, 184, 186, 195, 198, 302, 303, 333-336]. These models usually assume flow/open chemical systems because they allow for systematic studies [92, 94, 105, 121, 122, 337]. Experimentally, it is also easier to study and obtain these phenomena in open systems since, the reaction dynamics can be forced to display these phenomena by applying external controls such as adjusting flowrates of selected species [17]. As such, phenomena originating from present experimental studies are typically associated with experiments in open chemical systems especially coupled CSTR oscillators [22, 92, 94-96, 99, 102, 121, 195] rather than semi-batch or batch reactors. It is possible to observe some of the above mentioned phenomena in experimental batch chemical systems [16, 32, 106, 108, 130, 314, 334] however, such studies are fewer in comparison to studies with open systems. Studies on the carbonylation system presented here were performed with semi-batch like reactors since the reacting solutions were continually purged with CO and air. Constant gas flow rates were maintained throughout each experiment and the same flow rate was used for all studies,

consequently, it is plausible to assume batch like behaviour for current studies. The range of phenomena observed experimentally are discussed in subsequent subsections.

6.5.1 Profiles Presenting with Features classed as Multi-Stability

Multi-stability specifically bi-stability is possibly the most common phenomena found in dynamic chemical systems. The identification of this phenomena plays a key role in the systematic design of chemical oscillators in open systems since, the possibility of oscillations exists where there is multi-stability [16, 92, 95-100]. A reacting system is said to show multi-stability when two or more stable dynamic states occur under a single set of "reacting conditions" [95, 100, 102, 292]. The stable dynamic states may consist of steady states (stationary or non-oscillatory state), period states, or a mixture of both, while, "reacting conditions" include reactant concentrations, temperature, pressure etc. Bi-stability in this sense is the existence of two stable states, and tri-stability [100] would be the existence of three stable states. An underlying fact in systems exhibiting multi-stability is the ability to remain stable for extended periods of time without external perturbation, as this proves that such a system is really bi-stable. Extensive research with coupled oscillators [22, 95, 96, 99-102, 290, 292, 338] have demonstrated that bi-stability in chemical oscillators is possible where autocatalytic reactions exist, especially in open systems. The manifestation of bi-stability in chemical systems indicate the possibility of oscillations hence, adjusting reacting conditions and autocatalytic specie concentrations with time could drive the reaction to limit cycles for oscillations to occur [92, 339]. Regulating the autocatalytic species concentration with time is achieved by introducing another reaction which would consume the autocatalytic species. In the present study, the system is assumed to be autocatalytic in HI, according to Eq. 4.6, 5.1, 5.3 and 5.4 for mono and bi-alkyne substrate conversion. Therefore, the conditions for bi-stability is present and can justify for the postulation for existence of bi-stable and tri-stable phenomena given in Figure 6.41.

Examples of bi-stability in the form of two stable steady states is shown in non-oscillatory experimental profiles in Figure 6.41. The arrows in Figure 6.41 indicate the points of transition from one stable steady state to another following the first autocatalytic drop in pH (double arrow). The reactant concentrations and reacting conditions were not altered throughout the experiment for both profiles in Figure 6.41, therefore, the transitions witnessed after 2000 min and 6000 min agree the condition for bi-stability.

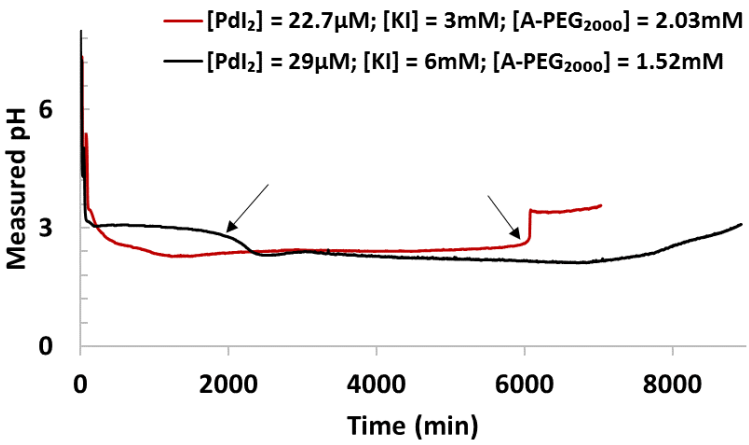

Figure 6.41. Potential bi-stability in profiles from the carbonylation of alkyne functionalised polyethylene glycols in non-oscillatory modes. (Arrows indicate transition to a different steady state)

Applying the same analogy, the non-oscillatory profile in Figure 6.42 shows tri-stability and in this instance, three stable steady states exist at the concentration investigated experimentally. The transition to the second steady state occurs before 4000 min, while transition to the third steady state occurs after 7500 min and the reaction remained in this state till experiment was terminated. As with experimental studies showing bi-stability, the study where tri-stability is thought to arise was not subject to external perturbations therefore the multi-stable phenomena is attributed to purely endogenous circumstances.

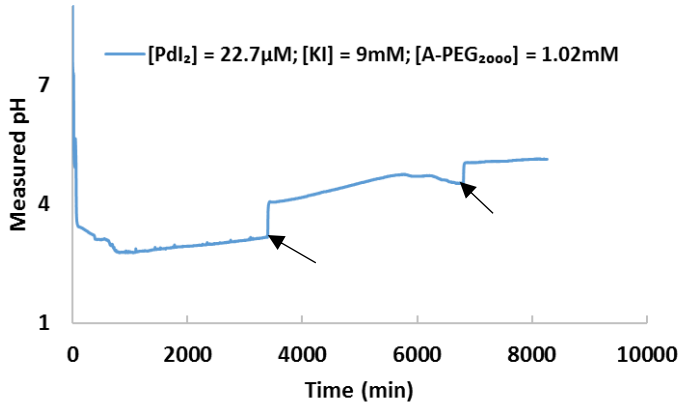

Figure 6.42. Non-oscillatory reaction profile showing tri-stability (Arrows indicate transition to a different steady state)

6.5.2 Profiles Presenting with Features classed as Multi-Rhythmicity

The existence of two or more stable oscillatory (periodic) regions in a dynamic system under the same set of reactant and reacting conditions is termed multi-rhythmicity [44, 93-95, 97, 98, 100, 116, 119, 120, 301, 330, 331]. Multi-rhythmicity may be likened to multi-stable systems, however, they are different because the dynamic stable states from which the multi-rhythmic

phenomena arise are stable periodic states, while the dynamic states for multi-stability are stable steady (stationary) states. The stable periodic/oscillatory states for multi-rhythmicity originate from multiple stable limit cycles, where each limit cycle possesses distinct intermediate species constraints for oscillations under one set of reactants and reacting conditions [93-100, 116, 119, 120, 330 331]. Autocatalytic reactions and feedbacks mechanisms are needed for multi-stable systems. Autocatalysis arises from substrate conversion wherein HI is formed auto-catalytically. The reactions for oxidation of HI and methyl iodide formation in excess KI (Eq. 4.8 and 4.9) are proposed to regulate the autocatalytic HI species, thus satisfying the conditions for oscillations and accounting for bi-rhythmicity in the profiles. Multi-rhythmicity in the form of bi-rhythmicity was reproducibly obtained at different reaction conditions from experimental studies on the oxidative carbonylation of alkyne functionalised polyethylene glycols.

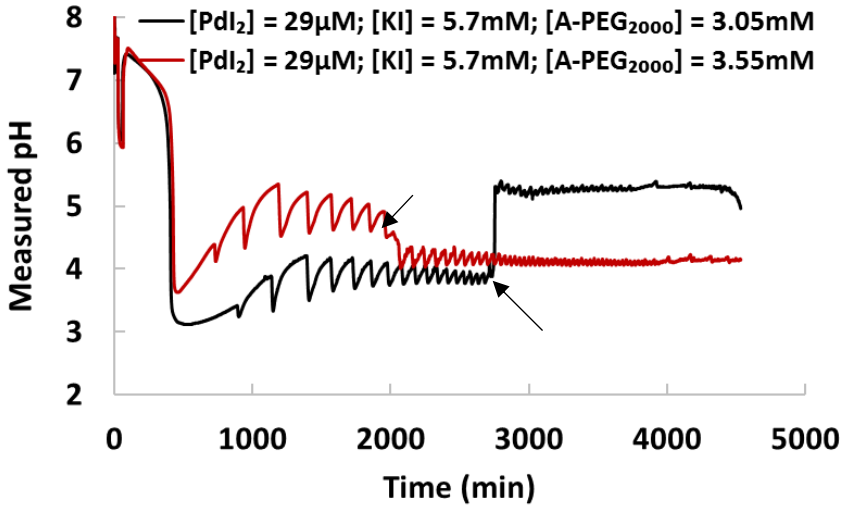

Figure 6.43. Bi-rhythmicity in oxidative carbonylation of alkyne functionalised polyethylene glycol (arrows indicate transition to second rhythm)

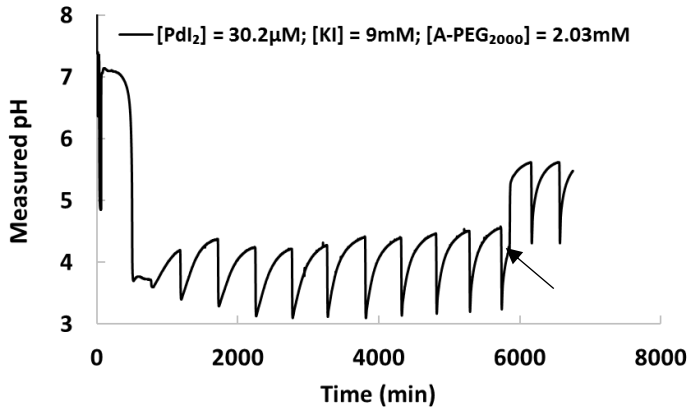

Figure 6.44. Presence of bi-rhythmicity in the carbonylation of alkyne functionalised polyethylene glycol (arrow indicates transition between steady states)

Example profiles classed under bi-rhythmicity are given in Figures 6.43 and 6.44. In a bi-rhythmic system, two stable periodic states (limit cycles) exist around different mean values. The transition from one rhythm to another is indicated by the arrows in both figures. The transitions between rhythmic states can occur both ways; either from regions of high pH values to lower pH values (Figure 6.43 -: [A-PEG_{2000}] = 3.55 mM, [KI] = 5.7 mM and [PdI_2] = 29 μM) or from regions of lower pH values to higher pH values (Figure 6.43 -: [A-PEG_{2000}] = 3.05 mM, [KI] = 5.7 mM and [PdI_2] = 29 μM and Figure 6.44).

Bi-rhythmicity is known to occur in many biological and biochemical systems [44, 97, 98, 116, 119, 120] and chemical systems [71, 93-96, 99-102, 292, 338]. Coupling of two oscillating reactions generates most bi-rhythmicity in open systems and has been extensively studied by Epstein and co-workers [71, 89, 93-96, 99-101, 290, 292, 338]. Previous studies in the carbonylation of phenyl acetylene with only methanol as solvent did not explicitly show bi-rhythmicity. When water-methanol solvent system was employed in oscillatory carbonylation of phenyl acetylene, possible bi-rhythmicity was identified in a semi-batch experiment where 95% methanol and 5% water was used as reaction solvent at much higher reaction conditions (phenyl acetylene concentration = 0.124 M; [PdI_2] = 2.64 mM; [KI] = 0.494 M; [NaOAc] = 3.05 mM; CO = 50 mL min^{-1} and air = 50 mL min^{-1}; 30^oC) [176]. Two stable oscillatory states were identified from their experimental results, suggesting the possibility of bi-rhythmicity [176]. This implies that the possibility of bi-rhythmic phenomena from experimental studies in the carbonylation of alkyne functionalised polyethylene glycol with a purely methanol solvent is new to oscillatory carbonylation reactions. An additional type of multi-rhythmicity in the form of tri-rhythmicity [98, 116] (3 oscillatory states at same reaction conditions) was possibly identified using the bi-alkyne functionalised substrate (A-PEG_{2000}-A) at 3.04 mM, KI at 5.7 mM and PdI_2 at 29 μM in semi-batch system and is given in Appendix A8.

6.5.3 Examples of Experimentally Observed Mixed Mode and Canard-like Oscillations

Some oscillatory profiles from experimental studies in the carbonylation of alkyne functionalised polyethylene glycols are classed as mixed mode oscillations (MMO) and Canard-like oscillations based on the type of oscillations recorded. In a broad context, mixed mode oscillations (MMO) occur in nonlinear systems when cycles of oscillations with different amplitudes are interspersed, forming complex oscillatory patterns [109-115, 122, 321, 340]. The oscillatory cycles usually start with small amplitude oscillations which gradually increase in size to much larger amplitude oscillations per cycle. In MMO, each amplitude in the oscillatory regime is believed to be created by a different mechanism and transitions between

amplitudes are governed by additional mechanisms, accounting for the variation in amplitudes [31, 109-115, 321, 340]. MMO from experimental studies in chemical systems were initially identified in B-Z [341] and peroxidase-oxidase systems [109, 112]. The reaction profiles in Figure 6.45(a-c) are examples of MMO and Canard-like oscillations recorded during experimental studies. A visual assessment of Figure 6.45(a-c) conveys a difference between the profiles in Figure 6.45a and Figure 6.45(b-c). The profile in Figure 6.45a does not exhibit the alternating amplitude size characteristic classic to mixed mode oscillations. The profiles in Figure 6.45a are proposed to exhibit a "Canard" like behaviour. Canards phenomena is a class of phenomenon wherein stable small amplitude oscillatory cycles transition to large amplitude relaxation oscillations [113, 114, 302-304].

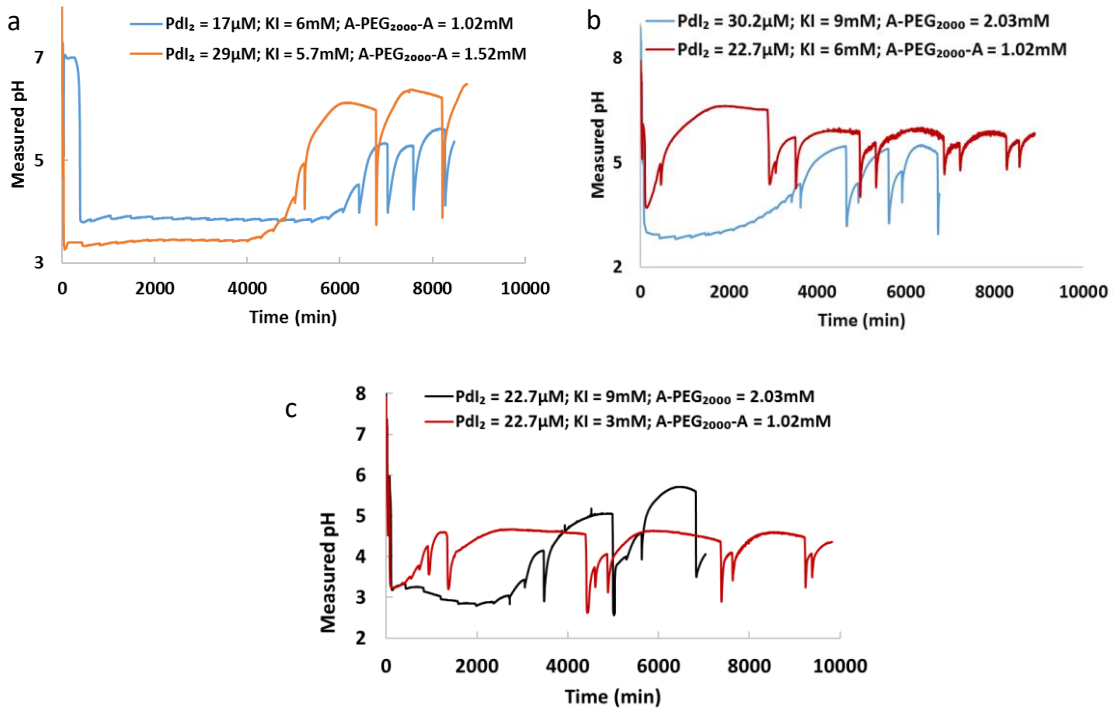

Figure 6.45. Mixed mode oscillations in the carbonylation of mono and bi-alkyne functionalised polyethylene glycols. (a. Canard like oscillations; b. two cycle mixed oscillations; c. three cycle mixed mode oscillations)

Some researchers describe this canard like behaviour as a region of transition [110, 113-115, 302-304], such that a slight shift in intermediate species drives the reactions to classic MMO (alternating between small and large amplitude oscillations). The profiles in Figures 6.45b ([A-PEG_{2000}] = 2.03 mM, [KI] = 9 mM and [PdI_2] = 30.2 µM) and 6.48c ([A-PEG_{2000}] = 2.03 mM, [KI] = 9 mM and [PdI_2] = 22.7 µM) wherein small amplitude oscillations precedes the transition to classic MMO agrees with the suggestion of the presence of canard like oscillations for the profiles in Figure 6.45a. Examples of classic MMO obtained from experimental studies are given in Figures 6.45 (b-c). The MMO in Figure 6.45b consist of 2 cycles (one small amplitude

and one big amplitude), while the MMO in Figure 6.45c consist mainly of 3 cycles (2 smaller amplitudes and one big amplitude). Initial experimental examples of MMO in pH oscillators were recorded in aqueous open systems [122, 195]. Examples of mixed mode oscillations in pH oscillating systems include the hydrogen peroxide-thiosulphate-sulphite flow system where MMO was observed on increasing the flowrate [122], the Cu^{2+}catalysed oxidation of thiosulfate-hydrogen peroxide-sulphuric acid system [110, 342] and hemin-hydrogen peroxide sulphite system [104]. Mixed mode oscillations in oscillatory carbonylation of terminal alkynes was discovered in reactions with phenyl acetylene as substrates [8, 9, 31, 32]. However, two different kinds of mixed mode oscillations; classic MMO and mixed mode "bursting" oscillations (MMbO) were identified with phenyl acetylene system. The "burst" component describes mixed mode oscillations where the alternation between small and large amplitude oscillations consists of much longer sets of small amplitude than large amplitude oscillations [8, 9, 32]. In bursting, non-oscillatory or very small amplitude oscillations exist between each group of alternating oscillations [116, 117, 296, 343]. MMbO was found in reactions with phenyl acetylene substrate at lower temperatures (0^oC and 10^oC) [8, 9, 32] when alternate catalyst ligands (palladium acetate, sodium chloride-palladium acetate and polymer bound palladium) [31] were used and, when the phenyl acetylene system was perturbed by adding HI [31]. The MMO observed from experimental studies with mono alkyne and bi-alkyne functionalised polyethylene glycol substrates did not display MMbO. The lack of MMbO in current studies can be attributed to difference in reaction conditions since a higher temperature (~ 20^oC) and a simple palladium iodide/KI ligand was employed from onset. Also, the absence of external perturbations such as the HI added to the phenyl acetylene study [31], may account for the lack of MMbO in present work.

The presence of different mechanisms for the same set of reaction conditions drive open systems to mixed mode oscillations and is also a causative factor for complex oscillations in general [95-100, 108, 109-115]. The proposition that different mechanisms drive these phenomena (specifically MMbO) was demonstrated experimentally when two different sources of palladium salts were employed in semi-batch oxidative carbonylation reactions of phenyl acetylene [31]. $Na_2PdAc_2Cl_2$ and $K_2PdAc_2I_2$ were suggested as catalytic species supporting the different mechanism generating the mixed mode oscillations (MMbO) [31]. On the other hand, similar MMbO were noted in other oxidative carbonylation experiments with phenyl acetylene substrate when only PdI_2 was introduced as catalyst [8, 9, 32]. This suggests that even without the introduction of other catalytic species, MMO are still possible.

In the current study, the initial assumption that, the additional alkyne end groups in the bi-functional substrate, was "exclusively" prompting MMO and complex oscillations is unlikely since, MMO and complex oscillations were also observed in reactions with mono-alkyne functionalised substrates. Thus, the observed contribution of polymeric substrates to presence or absence of mixed mode oscillations is proposed to be more of a function of the substrate concentration in the reaction than the type of substrate (number of functional groups) used. Based on this, the availability of other catalytic species as well is now suggested as another reason for the experimentally observed complexity of oscillation. For the experimental studies conducted, PdI_2/KI/methanol catalytic mixture was used. It is plausible that other species of palladium iodide are formed in the reaction, especially in the presence of excess KI, since it provides extra iodide ions. From the reaction network under consideration in this thesis, HPdI, IPdCOOH and $IPdCOOCH_3$ from Eq. 4.2, 4.3 and 4.4 are some Pd species formed during the reaction, which may serve as *in situ* catalytic species generating the different mechanisms, presenting as MMO and Canard-like oscillations.

These species from Eq. 4.2 to 4.4, in addition to other Pd species such as PdI_4^{2-} (forms on dissolution in KI); $CH_3COOPdI_3^{2-}$ [8]; Pd_2I_2 [38, 344]; $Pd_2X_2(CO(O))_2$ and $Pd_2(O)_2X_4$ [344] (where X = halide) generated *in situ* have been proposed as intermediate species in various oxidative carbonylation reactions with PdI_2 as starting catalyst. Consequently, it is feasible to achieve complex, MMO and Canard-like oscillations since the abovementioned intermediate palladium species provide different mechanisms within a specific reaction condition, thus, satisfying the criteria for occurrence of these phenomena.

6.5.4 Profiles Presenting with Features classed as Complex Oscillations

Compound / complex oscillations which are proposed to arise from interaction of distinct oscillatory cycles were identified in the oscillatory carbonylation of alkyne functionalised polyethylene glycol. Compound oscillations are commonly found in flow/open chemical systems. Since open systems allow for coupling of oscillating systems this creates the entrainment and arising complex oscillatory features. An example of such system is the chlorite-bromate-iodide-sulphuric acid coupled flow oscillator, where an intermediate flowrate value lying between oscillatory flowrates for two coupled oscillators was used to drive the system to merge into compound oscillations [17, 95].

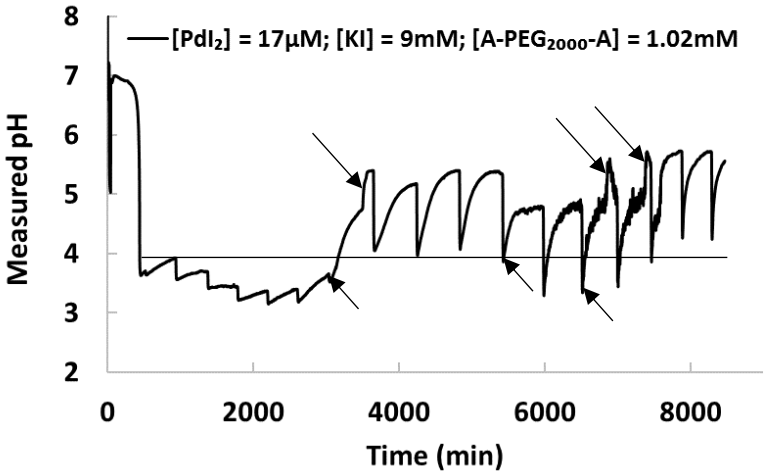

Figure 6.46. Complex oscillatory cycle in the carbonylation of alkyne functionalised polyethylene glycol. (Arrows above the horizontal line indicate compound oscillation; arrows below the horizontal line indicative of transition between compound and simple oscillations)

An example of a complex oscillatory profile obtained from present experimental study is given in Figure 6.46. The arrows above the horizontal line shows regions of visible entrainment or dominance of one cycle (marked by the complexity of new shape), while the arrows below the horizontal line shows the points of transition to/from compound oscillatory mode. Unlike coupled compound oscillators, intrinsic characteristics of the carbonylation system drive the compound phenomena witnessed, since no external factor such as additional methanol etc. occurred. As far as known, similar compound or entrained oscillations were not observed in small molecule [8-10, 31-33, 103, 173, 175] (phenyl acetylene, non-1-yne etc.) oscillatory carbonylation reactions. However, a resemblance of such compound oscillation was observed on reviewing the methylene glycol–sulphite–gluconolactone pH oscillator in a flow reactor [26]. These phenomena were also reproduced experimentally in the carbonylation of alkyne functionalised PEG.

6.5.5 Experimental Reaction Profiles with a Mixture of Phenomena

A mixture of phenomena described in sections sub-sections 6.6.1 to 6.6.4 were obtained in some reaction profiles following experimental studies. Figures 6.47 and 6.48 illustrate the variety of phenomena observed. In Figure 6.47, the reaction profile with bi-alkyne functionalised substrate (A-PEG_{2000}-A) at 1.02 mM ([KI] = 6 mM and [PdI_2] = 22.7 μM), displayed 2 cycle mixed mode oscillations from onset of oscillations till well into the reaction, before transitioning to simple oscillations with a semblance of compound oscillation around 8000 min after which the reaction was terminated. The second profile in Figure 6.47, with mono alkyne substrate ([A-PEG_{2000}] = 2.03 mM, [KI] = 6 mM and [PdI_2] = 22.7 μM) exhibited an opposite behaviour (mirrored oscillations). Oscillations commenced as simple limit cycle

oscillations before transitioning to mixed mode oscillations after 2000 min and continued as mixed mode oscillations till experiment was terminated.

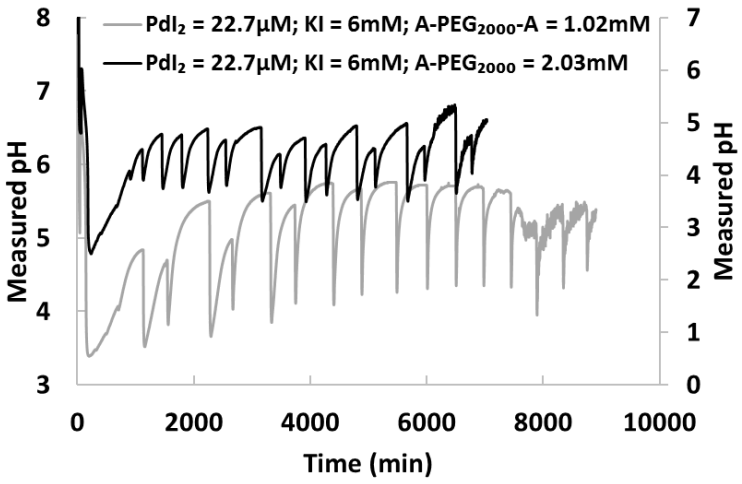

Figure 6.47. Transitions between mixed mode and simple relaxation oscillations in the carbonylation of mono and bi-alkyne functionalised polyethylene glycols

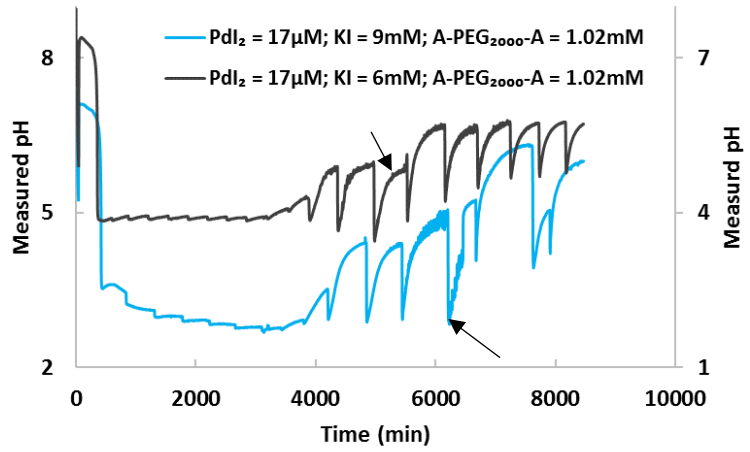

Figure 6.48. Bi-rhythm, Canard like phenomena and transition to mixed mode oscillations in the oxidative carbonylation of bi-alkyne functionalised polyethylene glycol (Arrows indicate transition to bi-rhythm and/or mixed mode oscillations)

The mirrored behaviour in Figure 6.47 becomes interesting in terms of reproducibility. If the alkyne end group concentrations are taken into consideration, then, both profiles in Figure 6.47 have roughly the same concentration of alkyne end groups although mono and bi-functional substrates were used (same concentration of catalytic mixture) yet, the oscillations occur in opposite fashions.

Figure 6.48 presents a different set of mixed phenomena profiles. Experimental studies for both profiles were conducted under identical substrate and catalyst conditions at different KI concentrations. Both profiles showed similar canard like patterns from onset of oscillation till

both transitioned to different oscillatory states (bi-rhythmicity). Transitions attributed to bi-rhythmicity arose first in sample with less KI (6 mM) and simple periodic oscillations were observed following the switch in oscillatory states (black legend line). For sample with higher KI value (9 mM), bi-rhythmic switch in oscillatory states caused the profile to switch from canard like phenomena to classic MMO. In Sub-section 6.6.3, canards were described as transitory region to MMO. This example at [KI] = 9 mM further supports the presence of canard like phenomena in oscillatory carbonylation of alkyne functionalised polymer substrates since an internal shift in intermediate species in the form of bi-rhythmicity caused a transition from Canards to classic MMO.

6.5.6 Additional Phenomena - Complex Spiked Oscillations with Intermittency and Mixed Mode Features, Spikes within Oscillatory Cycles and Irregularities

Other phenomena showing degrees of irregularity were observed from experimental studies in oscillatory and non-oscillatory modes. The complex profile given in Figure 6.49 is one of such studies. A combination of complex intermittent and mixed mode intermittent oscillations with spikes in pH (spiked MMO) were obtained from a semi-batch study with bi-alkyne functionalised polyethylene glycol substrate. "Intermittent oscillations" used here describes the oscillations at the beginning and end of Figure 6.49 because, each complex oscillation is separated by an aperiodic non-oscillatory region. Like mixed mode oscillations, intermittent oscillations and spikes in oscillations have been observed in batch and CSTR systems [44, 45, 49, 108, 114, 117, 118, 331]. Forced intermittent oscillation was noted after extra methanol was added to account for evaporative losses in oscillatory carbonylation of phenyl acetylene at 40^{o}C [10] and intermittent oscillations were also reported in batch and CSTR studies with Briggs-Rauscher oscillators perturbed with phenol [117]. In both studies, intermittent oscillations seemed dependent on system perturbations. However, this is not the case with Figure 6.49, as the reaction was not perturbed. The intermittency here is proposed to arise from the complex reaction mechanisms leading to variations in modes of HI formation. This is evidenced by the spiking pattern of the oscillations and transitions between intermittency and mixed mode as shown in Figure 6.49. Note that the pattern of oscillations in Figure 6.49 is completely different from any other oscillatory pattern witnessed in the course of this project as it appears to be the reverse of typical oscillation profiles obtained from carbonylation studies reported throughout this thesis.

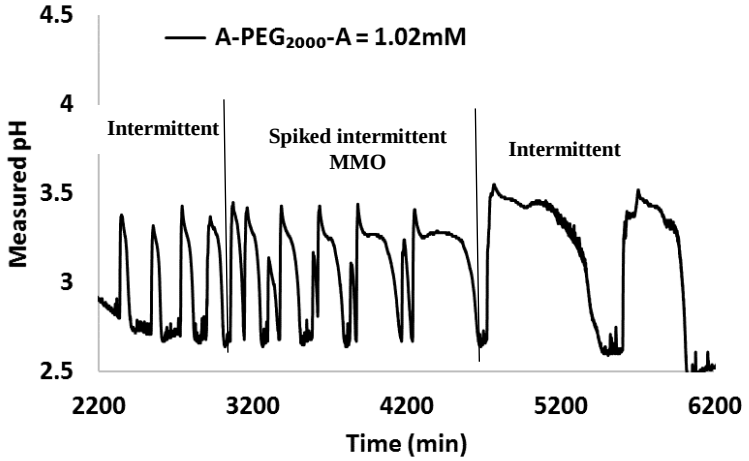

Figure 6.49. Intermittency and periodic spiking mixed mode oscillations in the carbonylation of bi-alkyne functionalised polyethylene glycol

Other form of oscillations with spikes were also recorded during the experimental studies. Figures 6.50 (a-b) show irregular spikes recorded during the oscillatory carbonylation of mono-alkyne functionalised polyethylene glycol. The irregularity of the spikes makes it difficult to attempt to assign this phenomenon to a class of phenomena in chemical systems. Some researchers may class these oscillations as "chaotic" [44, 68, 109, 110, 114, 116, 119, 121-123, 195, 301, 316] due to the irregular spikes. However, since it is possible to make out individual oscillations irrespective of the spikes on the peaks of each cycle, these oscillations are difficult to explain. They may arise from cumulating effects of some other complex modes of oscillations particular to this system. Deciphering such effects would require extensive modelling and experimental work beyond the scope of this thesis hence, it is recommended as a subject for future discourse. The last class of phenomenon covered here is the appearance of large spans of aperiodic irregular pH changes in carbonylation reactions exhibiting oscillatory and non-oscillatory modes. Examples of these features in oscillatory and non-oscillatory modes is given in Figure 6.51. The appearance of such aperiodic spans was more common in non-oscillatory carbonylation reactions than oscillatory reactions. In both oscillatory and non-oscillatory modes, such features occurred in later stages (after 3500 min) of the reactions across runs (including samples not shown).

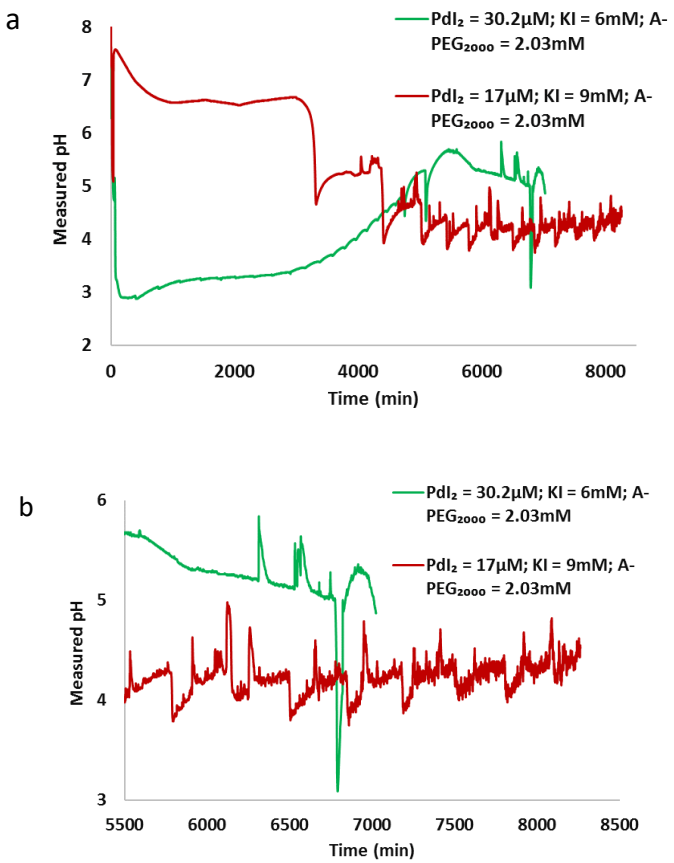

Figure 6.50. Irregular spikes in relaxation oscillations in the carbonylation of mono alkyne functionalised polyethylene glycol (complex oscillations); (a) full profiles; (b) expert from the full profiles)

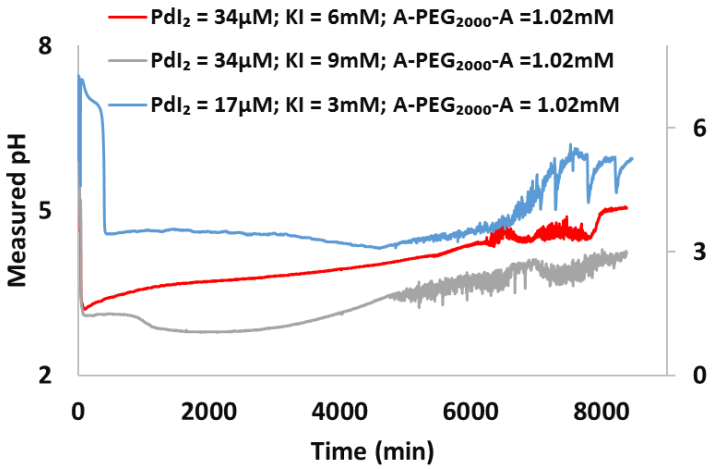

Figure 6.51. Chaos like phenomena in oscillatory and non-oscillatory carbonylation of alkyne functionalised polyethylene glycol

Analysis of spikes and aperiodic spans in pH profiles are not discussed mechanistically as information available in literature on such oscillatory carbonylation systems are limited. Also, these features would need to be corroborated with additional methods to support the findings described here.

6.5.7 Section Summary

A wide range of nonlinear dynamics phenomena were identified from the oxidative carbonylation of mono alkyne and bi-alkyne functionalised polyethylene glycols. The occurrence of complex phenomena such as mixed mode, Canard-like and complex oscillations support the possibility of more than one palladium specie catalysing the pathway for substrate conversion and formation of HI. Substrate concentration is an important consideration since complex phenomena is present in both mono functional and bi-functional substrates. The manifestation of several complex nonlinear phenomena from experimental studies in one chemical system is uncommon and may offer prospective applications. Profiles classed as multi-rhythmic profiles in this system may be useful in applications mimicking neuronal oscillators [330] since, bi-rhythmicity is important for maintaining the different modes of oscillations, which can be linked to the organisation and sequences of various biochemical processes (in response to environment) in neuronal oscillators. The complexities found here may be more applicable to studies centred on biological and biochemical processes than on physical systems. For physical systems, "mono-rhythmicity" or simple oscillations is of more practical importance, as the presence of other oscillatory complex oscillations, aperiodic spans and spikes may limit the efficiency of prospective applications and increase the vulnerability of physical applications incorporating this polymeric chemical oscillator. Ultimately, the ability to control and tune the system from simple to complex and mixed mode oscillations is essential.

6.6 Proposed reaction scheme for oxidative carbonylation of mono and bi-alkyne functionalised polyethylene glycols

Reactions, mechanisms, and pathways supporting observations recorded in pH profiles from the carbonylation of mono and bi-alkyne functionalised polyethylene glycols were discussed in Chapters 4 and 5 and earlier sections of this chapter. Most reactions and pathways suggested were adapted or taken from existing knowledge of carbonylation and oscillatory reactions. Several aspects of reactions with mono and bi-alkyne substrates including pH transitions during substrate addition, share similar reaction modes. Other features (e.g. amplitudes and periods of oscillations) of the reaction profiles suggest the existence of differences between both substrates. In this section, a comprehensive scheme accounting for changes in reaction kinetics during the oxidative carbonylation of mono and bi-alkyne functionalised PEG in oscillatory and non-oscillatory modes, is provided. This inclusive network is proposed based

on experimental evidence from studies in this thesis and are backed by accounts on palladium catalysed carbonylation reactions, oscillatory reactions with phenyl acetylene, the reaction network by Donlon and Novakovic [29] and complementing modelling studies [29, 345]. The proposed reaction scheme for mono alkyne and bi-alkyne functionalised polyethylene glycol polymeric substrates is given below.

$PdI_2 + CO + H_2O \rightarrow IPdH + HI + CO_2$	Eq. 4.2
$PdI_2 + CO + H_2O \rightarrow IPdCOOH + HI$	Eq. 4.3
$PdI_2 + CO + CH_3OH \leftrightarrow IPdCOOCH_3 + HI$	Eq. 4.4
$PdI_2 + CO + H_2O \rightarrow Pd + 2HI + CO_2$	Eq. 4.5
$A - PEG_{2000} + 2CO + 2CH_3OH + PdI_2 \xrightarrow{HI} Pd + P - PEG_{2000} + 2HI$	Eq. 4.6
A-PEG_{2000}-A $+ 2CO + 2CH_3OH + 2PdI_2 \xrightarrow{HI}$ Pd + 2HI + P-PEG_{2000}-P	Eq. 5.1
A-PEG_{2000}-A$+ 2CO + 2CH_3OH + PdI_2 \xrightarrow{HI}$ Pd + 2HI + A-PEG_{2000}-P	Eq. 5.3
A-PEG_{2000}-P $+ 2CO + 2CH_3OH + PdI_2 \xrightarrow{HI}$ Pd + 2HI + P-PEG_{2000}-P	Eq. 5.4
$HI \leftrightarrow H^+ + I^-$	Eq. 6.1
$\frac{1}{2}O_2 + 2HI \rightarrow I_2 + H_2O$	Eq. 4.8
$CH_3OH + HI \leftrightarrow CH_3I + H_2O$	Eq. 4.9
$I_2 + H_2O \leftrightarrow HOI + HI$	Eq. 4.10
$I_2 + Pd \rightarrow PdI_2$	Eq. 4.11
$I_2 + Pd \xrightarrow{PdI_2} PdI_2$	Eq. 4.12
$KI \leftrightarrow K^+ + I^-$	Eq. 6.2
$I^- + I_2 \leftrightarrow I_3^-$	Eq. 6.3
$I^- + I^- \rightarrow I_2$	Eq. 6.4
$Pd + I_3^- \rightarrow PdI_3^-$	Eq. 6.5
$PdI_2 + I^- \rightarrow PdI_3^-$	Eq. 6.6

Eq. 4.2 to 4.5 are proposed to account for the initial changes in the reaction. This occurs on purging the methanolic catalytic solutions with CO and air to form HI (observed as increased pH acidity). The reactions with water as reactants were included since residual fractions of water or moisture is thought to be present. The water is most likely from methanol (used as purchased and contains trace amounts of water), gases for purging (CO and air were not pre-

dried) and possibly, atmospheric exposure around probes (sealants had small gaps). The presence of water is also the most plausible explanation for differences in H^+ concentration from purging the reactions at constant catalytic concentrations. Eq. 4.6, Eq. 5.1, Eq. 5.3 and 5.4 are proposed for autocatalytic conversion of mono alkyne (Eq. 4.6) and bi-alkyne substrates (Eq. 5.1, Eq. 5.3 and 5.4). For the bi-alkyne PEG substrate, different variants of the autocatalytic substrate conversion reactions are proposed since the presence of two alkyne end groups per chain is hypothesised to change the reaction dynamics. In the proposed variants of the autocatalytic bi-alkyne substrate conversion, the terminal alkyne conversion proceeds either sequentially (tandem) (Eq. 5.3 and 5.4) or simultaneously (Eq. 5.1). Eq. 6.1 and 6.2. are proposed for incomplete dissociation of HI and KI in methanol. Incomplete dissociation is assumed since the solvent is non aqueous and may be further compounded by the presence of excess KI. Eq. 4.8 is proposed for HI oxidation and formation of iodine for catalyst regeneration. In some experimental reaction profiles, a second region of HI formation follows the initial autocatalysis (substrate conversion) instead of oxidation of HI. Eq. 4.9 and 4.10 account for the observed changes. The formation of water and presence of excess iodide ions (from KI) is suggested to promote Eq. 4.9 and 4.10. Eq. 4.11, 4.12, 6.5 and 6.6 are proposed for regeneration of palladium. Eq. 4.11, 6.5 and 6.6 account for non-autocatalytic regeneration while Eq. 4.12 accounts for autocatalytic Pd regeneration. Eq. 6.3 and 6.4 are proposed as alternate sources of iodine and triiodide for alternative palladium salts. Palladium triiodide complex is included in the scheme and KI is proposed to promote its formation. The triiodide salt of palladium may explain why the presence of higher concentrations of KI appeared to promote oscillations in studies in chapter 4 and 5. Also, the increased solubility of PdI_2 in the presence of excess KI supports the hypothesis for PdI_3^- complex formation. The autocatalytic substrate conversion reactions given in Eq. 4.6, 5.1 and 5.3 are assumed to consist of multiple intermediate steps. This assumption is made because the reaction presented in the above-mentioned equations are too complex to proceed in a single step. The assumption is also backed by unexpected incidences such as the rise in pH (decrease in H^+ concentration), instead of decreasing pH values on adding the substrates. If Eq. 4.6, 5.1 and 5.3 were simple or single step reactions, one would expect an increase in H^+ concentration (or constant pH values till autocatalysis initiates) on adding substrates due to the autocatalytic nature of these reactions. The rise in pH on substrate addition and the manifestations of periods of slow H^+ formation suggest that HI is consumed during and after substrate addition and this consumption occurs before the autocatalytic substrate conversion equations given in the comprehensive scheme

above. Nonetheless, reactions supporting this assumption (HI consumption on substrate addition) are not proposed, as further experimental evidence is required to support this theory.

Chapter 7. Conclusions and Recommendations for Future Work

7.1 Conclusions

Reaction mechanism elucidation in systems of complex reactions such as the oxidative carbonylation reaction studied here, is an arduous undertaking. The process of postulating and supporting viable reaction networks in such instances generally require in-depth systematic experimental investigations and perhaps, modelling/simulation studies. Since the application of polymeric substrates in oscillatory carbonylation reactions is new, only a communication with limited experimental data [29] and a few validated models based on reaction network postulated in the initial study [29, 345], are available. Due to this limitation, it became vital to devote this thesis to gathering experimental data for the purpose of understanding, improving, and supplying further experimental evidence for expanding and proposing reaction mechanisms for the polymeric oscillatory system. To achieve this, each reaction profile obtained from the experiments was systematically analysed in sections; right from the onset of the reaction till it was terminated. Extensive analysis of pH profiles obtained from experiments designed to assess oscillatory and non-oscillatory modes in the oxidative carbonylation of mono alkyne and bi-alkyne functionalised polyethylene glycols, was thus, successfully accomplished. For most reactions, oscillations were still ongoing when the experiment were terminated, which suggests that the rate of polymeric substrates conversions in oscillatory carbonylation mode was generally slow. This thesis offers broad ranges of experimental data recorded over long durations. This project also proposes likely reaction mechanisms/networks that account for pH profiles recorded and these studies are summarised in paragraphs throughout the rest of this section.

The functionalisation of polyethylene glycols with either one (mono) alkyne or two (bi-) alkyne groups at the hydroxyl terminal(s) of the polymer was successful as confirmed by the ^{1}H NMR spectra in Sub-section 3.2.1. Polymeric product separation and quantification on terminating the experiments was not assessed, however, the products obtained from the oscillatory carbonylation reaction were identified by associating known products from oscillatory carbonylation of phenyl acetylene [8, 30, 31, 173, 175, 177] to generate likely polymeric analogues. Afterwards, on analysing the peaks in the ^{1}H and ^{13}C NMR product spectra with the generated polymeric analogues, it was possible to confirm which products were most likely formed. Six polymeric product analogues (Figure 3.9) were identified as most likely based on the NMR spectra analysis. The certainty for polymeric products is supported by the absence of small molecules following GC-MS analysis in the original study [29].

In the original study by Donlon and Novakovic [29], oscillations were identified in the carbonylation of mono alkyne functionalised methoxy-polyethylene glycol at [PdI_2] = 40.5 µM, [A-PEG_{2000}] = 2.03 mM and [KI] = 2.28 mM when polymers of 2 kg/mole and 5 kg/mole molecular weight were used. The studies outlined in Chapter 4 extended the original work by investigating a wider range of substrate concentrations for the 2 kg/mole molecular weight mono alkyne functionalised methoxy-polyethylene glycol (A-PEG_{2000}). The mono alkyne substrate concentration investigated here ranged from 0.508 mM to 3.55 mM. The concentration of the catalytic mixture employed in the reactions with mono-alkyne substrates was similarly expanded to include PdI_2 concentrations ranging from 15.1 µM to 45.4 µM and KI from 3 mM to 9 mM. In addition to expanding these ranges and individually assessing the effects of mono alkyne substrate, PdI_2, and KI on the pH oscillations, other factors were also investigated. These factors comprised-: the effects of introducing additional methanol during the reaction; prolonging extra KI addition times from 0 hr to 24 and then 48 hr; influence of substrate concentration on gradual formation of H^+ following substrate addition and the manifestation of complex oscillations as a function of substrate concentration.

When different concentrations of the catalytic mixture (PdI_2/KI/CH_3OH) were assessed at the same substrate concentration (2.03 mM) employed in the original study [29], pH oscillations were reproduced. Oscillations were reproduced at reduced PdI_2 concentrations (15.1 µM to 37.8 µM) in comparison with the original study (40.5 µM) and is therefore noteworthy in terms of future applications. When the effects of individual components of the catalytic mixture were evaluated at identical substrate concentration (2.03 mM) used in the original study [29], increasing the concentration of KI facilitated an increase in the size of the oscillations with respect to amplitude and period changes per oscillatory cycle. Although oscillation sizes were larger at higher KI concentrations, the adjusted H^+ values from onset of purging (with CO and air) and the overall H^+ concentration during the reactions decreased as potassium iodide concentration increased. It seemed that iodide ions originating from dissociated KI may have a counteracting effect on H^+ formation, consumption and detection as reflected by the changes in pH during the reaction. This assumption is supported by the longer period per oscillatory cycle (suggestive of a decrease in rate of H^+ formation or consumption) seen at higher KI concentrations.

Increased concentrations of PdI_2 at constant KI and substrate concentration increased the apparent H^+ concentration formed (pH more acidic) during purging with CO and air. Increase in palladium iodide concentrations likewise led to decreasing periods of gradual H^+ formation termed "slow H^+ formation" in this thesis and the H^+ concentration from initial autocatalytic

substrate conversion was also greater when PdI_2 was high. The increase in H^+ concentration with increasing PdI_2 concentration agrees with previous findings in oscillatory carbonylation of phenyl acetylene [242]. It supports previously postulated mechanisms [3, 137, 156, 157, 172, 271, 318] with respect to the role of palladium in increasing the reaction rate in the carbonylation process. At higher PdI_2 concentrations, the interaction from excess iodide was also reduced. This supports the assumption that large excess of iodide ions (ratio) may limit reaction rates or the rate of dissociation of HI when PdI_2 is kept constant. The H^+ generated over the course of the reaction is believed to arise from methanol, residual water and autocatalytic substrate conversion, and generally increased as the catalyst concentration increases.

At constant catalytic concentration (KI and PdI_2), increased mono alkyne substrate concentrations increased the size of the pH oscillations (amplitudes and periods). As the ratios of PdI_2 to substrate concentration increased, the duration of the "slow H^+ formation" phase and degree of pH rise on adding substrate also increased. The most likely reason for these increments is a reduction in reaction rates since the concentration of PdI_2 available for substrate conversion decreases as the concentrations of mono alkyne substrate increases at constant PdI_2 concentration. This finding complements similar findings noted when the mono alkyne substrate was kept constant and catalytic concentration varied.

On studying the effects of introducing additional methanol during the reaction, it was found that introducing methanol changed the size and shapes of pH oscillations and generally led to increases in pH values. This agrees with findings in oscillatory carbonylation of phenyl acetylene [10, 32, 173-175] and is postulated to arise from dilution of $[H^+]$ present. Nonetheless residual water was proposed as an alternate cause in the study with phenyl acetylene. Since evaporation occurs in the absence of additional methanol, variations in concentrations of products, intermediates and reactants with time is proposed to ensue. Therefore, evaporation may be another important factor to consider in these reactions when reaction volume is not maintained constant by topping up methanol over the course of the reaction.

Delaying additional (extra) KI addition times at constant PdI_2 and mono alkyne substrate concentration shifted the reactions from oscillatory to non-oscillatory modes. By prolonging KI addition times from 0 hr to 24 hr and then 48 hr, it was found that onset of oscillations was delayed, or oscillations were absent. The absence of oscillation and/or smaller amplitude oscillations was also distinctive in this study when the concentration of the "extra" KI added at either 0, 24 or 48 hr was reduced at constant PdI_2 and mono alkyne concentration. These

findings concur with the proposition that KI promotes onset of oscillations and oscillation size (larger amplitudes and periods) even though it may dampen the overall rate of the reaction in terms of measurable H^+ concentration (higher pH values at high KI, hence reduced $[H^+]$).

Halving the mono alkyne substrate concentration (from 2.03 mM to 1.02 mM) at lower PdI_2 concentration (17 µM) was found to significantly reduce the duration of gradual formation of H^+ (defined as slow H^+ formation) following substrate addition by thousands of minutes (reductions in time > 2000 min). The study also found that reducing the mono alkyne substrate concentration by half generally decreased the manifestation of mixed mode oscillations. This finding suggests that the concentration of substrate present is a crucial factor in driving the reactions from simple oscillations to diversified complex oscillations. The increase in alkyne concentration present at higher polymeric substrate concentration may have encouraged the transition in oscillation types.

In Chapter 5, bi-alkyne functionalised PEG substrate was investigated. Oscillatory carbonylation studies employing bi-alkyne functionalised polyethylene glycol is novel. Unlike the mono functional counterpart, published experimental studies which may have served as starting point was unavailable, hence, the studies reported here are the first of its kind. The studies were designed to mirror the mono alkyne system, but, the ranges of substrate and catalytic concentrations employed are different from ranges investigated for the mono alkyne system. The effects of varying palladium iodide, KI and bi-alkyne substrate concentrations were explored individually and their impact on pH oscillations and reaction rates examined. Bi-alkyne functionalised polyethylene glycol substrate concentrations ranging from 0.254 mM to 3.04 mM, KI concentrations ranging from 3 mM to 9 mM and PdI_2 concentrations ranging from 17 µM to 60.4 µM were studied.

Oscillations were achieved for the range of substrate concentrations investigated at constant PdI_2 and KI concentrations. At higher ratios of the bi-alkyne substrate to palladium iodide concentration, the rise in pH upon substrate addition increased, and such dependency was also found with the mono alkyne version. Mixed mode oscillations and a range of oscillations with varying degrees of complexity were increasingly present in reactions with bi-alkyne substrate. Some pH profiles where bi-alkyne PEG was employed as substrate exhibited several types of oscillations over the course of the reaction (combinations of mixed mode, compound, complex and simple oscillations in a single pH profile). The study at constant catalytic concentration and increasing bi-alkyne substrate concentrations found the initial autocatalytic formation of H^+ due to substrate conversion to be dependent on the bi-alkyne to PdI_2 ratio. As the

concentration of bi-functional substrate increased at constant catalyst concentration, the initial autocatalytic H^+ increased until the 1.02 mM substrate concentration, after which, the initial H^+ started to decline as substrate concentration was further increased. This increase and subsequent decrease as concentration ratio increased further points to a possible existence of optimal and/or desirable substrate to PdI_2 concentration ratio for formation of H^+.

For studies at constant bi-alkyne substrate concentration, H^+ formed (identified by increased pH acidity) on purging the catalytic solution and during the initial autocatalytic substrate conversion increased with increasing PdI_2 concentration. On the other hand, duration spent in the phase defined as "slow H^+ formation" decreased as PdI_2 concentration increased. This agrees with findings with the mono alkyne substrate and further emphasises the role of PdI_2 in the carbonylation reactions.

Diverse range of oscillations including mixed mode oscillations were found to be common at lower PdI_2 concentrations than at higher PdI_2 concentrations. At higher PdI_2 concentrations, the concentration of catalyst available for substrate conversion is higher. Consequently, the absence of mixed mode oscillations at higher PdI_2 concentrations supports the outcomes from studies on halving the mono alkyne substrate concentration while keeping PdI_2 constant. It supports this outcome because, in both cases, increased availability of PdI_2 limited the formation of complex oscillations. These findings suggest that the formation of complex oscillations are equally driven by the reduction in rates of reactions which occur when PdI_2 for substrate conversion is less. This is very likely because slower rates (reactions in Section 6.6) may encourage other reaction pathways which favour oscillatory modes with other forms of Pd complex present. The studies at various PdI_2 concentration and constant bi-alkyne substrate concentration also found that oscillations were mostly absent at $[PdI_2]$ = 34 μM for the range of PdI_2 concentration assessed (17 μM to 60.4 μM) and that, smaller amplitude oscillations were observed when PdI_2 was further increased (60.4 μM). The transition from large oscillations at lower PdI_2 concentration to a near absence of oscillations (2 oscillations at [KI] = 9 mM and $[PdI_2]$ = 34 μM) and then, the presence of small oscillations at high $[PdI_2]$ (60.4 μM) portrays the ability of the system to switch between oscillatory and non-oscillatory modes when the concentration of reacting species fall outside the boundaries of oscillations.

Increasing KI concentration at constant catalyst and bi-alkyne substrate concentration promoted oscillations, though, it hindered the initial H^+ formed from autocatalytic substrate conversion. These outcomes are in line with findings when the mono alkyne substrate was employed at different KI concentrations and/or when extra KI addition time was varied.

The group of studies in Chapter 6 were designed to study the impact of moving from mono functional to bi-functional polymeric substrate. The studies assessed the influence of doubling the alkyne concentration by keeping the mono and bi-alkyne substrate concentrations constant and, the effects of maintaining the alkyne concentration constant by using twice as much mono alkyne substrate per bi-alkyne substrate concentration investigated.

The studies evaluating the influence of doubling the alkyne concentration by using equal amounts of mono alkyne and bi-alkyne substrates at constant PdI_2 and KI concentrations found that, pH rise immediately after substrate addition was consistently higher in reactions with bi-alkyne substrate and also, the duration termed "slow H^+ formation" was also longer with bi-alkyne substrates. As [PdI_2] was constant in both reactions, the longer duration observed in the bi-alkyne reaction is assumed to reflect the time required for conversion of two alkyne groups against one alkyne end in the mono functional substrate. The initial H^+ concentration from autocatalytic substrate conversion was higher in reaction with bi-alkyne substrates, as long as sufficient PdI_2 was present in the reaction. When PdI_2 was reduced (17 μM), the concentration of H^+ was more in mono alkyne substrate reaction. This once again points to the previously mentioned possibility of optimal substrate to catalyst conditions per catalyst concentration investigated. In addition, though the presence of two alkyne groups in the bi-alkyne substrate at equal mono and bi-alkyne substrate concentration clearly changed the reaction profiles in terms of, increased oscillation sizes, overall higher H^+ concentration and greater number of oscillations (at most [PdI_2] investigated), the concentration of PdI_2 present was crucial to observed differences.

The second study in Chapter 6 considered the influence of using twice the mono alkyne concentration per bi-alkyne substrate concentration studied, such that alkyne concentration was kept approximately constant. A common finding at all catalyst concentrations investigated for studies where the overall alkyne concentration was kept approximately constant irrespective of the substrate type used was the absence of substantial similarities between mono alkyne and bi-alkyne reaction profiles. The observed dissimilarity in both profiles at constant alkyne concentration is suggestive of differences in the reaction rates and routes for both substrates. Differences in pathways to substrate conversion for mono and bi-alkyne polymeric substrates, which appears to be a function of number of terminal alkynes per chain, has most likely prompted the dissimilarity. The only exception to this profile dissimilarity was the study at [PdI_2] = 22.7 μM, since the repeat for the mono alkyne substrate was quite similar to profile obtained for the bi-alkyne substrate reaction. At [PdI_2] = 22.7 μM, where the repeat run for the mono alkyne substrate (2.03 mM) reaction profile was similar to bi-alkyne substrate (1.02 mM)

reaction profile, analysis of both reaction profiles found that, largely, the mono alkyne substrate reaction proceeds at a faster than the bi-alkyne substrate reaction. The reason behind this is unclear at this point but, the outcome still points out the possibility of optimal substrate to catalyst ratio. Maximum rise in pH following substrate addition was found to be generally higher when bi-alkyne polymer served as the reaction substrate. However, the increased basicity of pH on bi-alkyne substrate addition did not generally lengthen the period of gradual H^+ formation (termed "slow H^+ formation"), which followed substrate addition. On average, longer durations of slow H^+ formation was observed for the mono alkyne substrate when the alkyne concentration was kept approximately constant for both substrates. This suggests that having two alkyne ends per chain may have prompted an increase in reaction rate at this point, hence reducing the time spent in this phase.

Irrespective of which substrate was employed, possible manifestations of a number of nonlinear phenomena were identified over the course of these experimental studies. Indication of pH transitions or offsets from regions or low to high pH and vice versa during oscillatory and non-oscillatory modes suggesting possible multi-stability and/or multi-rhythmicity were present at a range of concentration. Various forms of mixed mode oscillations, compound/complex oscillations, pH spikes in oscillatory and non-oscillatory modes, intermittent oscillations and undefined pH irregularities were found at various catalyst and substrate concentrations. Features such as, pH transitions from less acidic to more acidic values and vice versa during oscillations which created profiles with 2 or more oscillatory pH regions were typically detected with mono alkyne substrate reactions. Likewise, more complex features including pH spikes within oscillations, compound/complex oscillations and intermittency were observed when bi-alkyne substrate was employed. Some of these phenomena were identified in the oscillatory carbonylation of phenyl acetylene [30-32] and, based on experimental evidence from phenyl acetylene carbonylation [31], the presence of more than one catalytic specie in the reaction propagates the occurrence of mixed mode oscillations. Since palladium can form different coordination complexes [8, 38, 344] in carbonylation reactions, a similar theory was proposed for observations in this thesis for mixed mode and complex oscillations and non-oscillatory features present.

In the initial study by Donlon and Novakovic using the mono alkyne substrate [29], a reaction network was proposed for oscillatory behaviour reported, and the network was also validated via modelling/simulation study. The reaction network proposed by Donlon and Novakovic [29]

was further validated through a stoichiometric network analysis (SNA)[7] in a recent collaborative study [345], which confirmed that the reaction network proposed in 2014 [29] could adequately represent the experimental findings (oscillations in this case). Following considerations of pH reaction profiles for all studies carried out here using mono and bi-alkyne polymeric substrates, possible reaction networks were proposed. Expansion of this model to replace the autocatalytic steps with loops and future modelling studies are ongoing and will be based on experimental evidence generated in this thesis. The network proposed in Chapter 6, Section 6.6 are based on experimental evidence from studies in this thesis and are backed by accounts on palladium catalysed carbonylation reactions, oscillatory reactions with phenyl acetylene, the reaction network by Donlon and Novakovic [29] and supplementing modelling studies [29, 345]. The reaction network accounts for the initial changes in the reaction; right from purging the methanolic catalytic solutions with CO and air to adding reaction substrate and other profile features following substrate addition. Unlike the mono alkyne substrate, the bi-alkyne substrate conversion was proposed to proceed either sequentially (tandem) (Eq. 5.3 and 5.4) or simultaneously (Eq. 5.1) based on differing profile features and dissimilarity in oscillation sizes recorded.

The goals of this thesis were to introduce and/or broaden experimental basis of polymeric oscillating reactions and enhance understanding of the reaction mechanisms when polymeric substrates are employed in oscillatory carbonylation reactions. This was a challenging task due to the number of reactants employed, difficulty in deciphering potential intermediate species and the gas-liquid reaction albeit the gases were purged through the solutions. Nonetheless, reactions have been postulated based on the pH profiles from the experiments and, general observations made during the studies including colour changes and palladium precipitate formation. Generally, both functionalised polymers have been confirmed as viable substrates in oscillatory carbonylation reactions over a range of reactant and reacting conditions. Consequently, this work supports the possibility and feasibility of oscillatory carbonylation with a range of poly-functional polymeric substrates, which may well be a key step to achieving chemically driven autonomous motion in soft materials.

[7] SNA is a powerful method for systematic examination of the models of complex reaction systems, identification of underlying reaction pathways, and stability analysis of dynamic states without explicit knowledge of rate constants. The SNA studies the time evolution of the internal species for given concentrations of the external ones. It focuses on intermediate species.

7.2 Recommendations for Future work

Future work could include confirming the reaction networks proposed, especially the reaction network for bi-alkyne functionalised PEG substrate, since this an entirely new addition and no modelling study has been conducted on this system. The proposed autocatalytic mono and bi-alkyne substrate conversion equations could be investigated in-depth to decipher elementary reaction steps constituting the complex reactions given in the network in Section 6.6. Testing poly functional polymers in oscillatory carbonylation is also recommended, as this may serve as further proof for findings reported here. Polymers of larger molecular weights could also be tested with a view of application as autonomous pulsatile materials in mind. Larger molecular weight polymers may be more robust and could limit leakages or fragmentation. Other studies consisting of palladium with different ligands could also be studied. Perhaps, the mechanism behind such system could prove useful in dispelling or supporting the influence of potassium iodide in oscillatory carbonylation reactions reported here. It would also be useful in deciphering how KI or iodide ions influences the dissociation of HI in methanol. Product separation, monitoring and quantification was not a focus of this thesis as such is proposed for further studies. Possibly products from the carbonylation may be useful and if the reactions are optimised, it may find use in other fields. Extensive studies on the influence of evaporative losses on oscillatory carbonylation reaction could be conducted, although an average of 6 mL/day was lost from 90 mL batch (90 mL at time zero), operating at higher temperatures would mean higher losses and the implications of evaporation for reactions lasting several days should be considered in future decisions and studies with this system for the sake of potential applications. Several complex oscillations and complex non-oscillatory features were noted throughout the studies designed. Substantial research into reasons for the appearance of these complex features and, studies that could conclusively confirm the presence of some of these features including multi stability, multi-rhythmicity, compound oscillations and irregular pH fluctuations are suggested. These studies could include reassessing the concentrations presented in this thesis with some other method to corroborate the dramatic changes. Such methods could include redox electrode and turbidity measurements in addition to monitoring the pH of the reaction. Multiple sources of autocatalysis are suspected; as such, other forms of Pd which could proceed via autocatalysis during the carbonylation of alkyne functionalised PEG should be investigated. Further considerations may well be given to the influence of ionic strength in the methanolic reactions and the influence of H^+ activities on pH dip following catalytic mix addition. The attainment of an intrinsically determined concentration is proposed to determine the duration of gradual H^+ formation. This could be assessed via modelling studies

to ascertain the exactness of this assumption. These studies were conducted with the experimental setup given in Chapter 3 and the process of manually setting up and introducing reactants in the 6 parallel system meant that time lags were present at each stage of reactant addition throughout the studies presented here. Automation of sections of the setup including provision of robotic arms could eliminate lag and lead to improved precision in profiles obtained. The influence of the polymeric backbone on pH rise following substrate addition is recommended as a future investigation. During this work, certain instances of variations in pH rise at constant alkyne concentrations suggest that the polymeric backbone may have a contributory effect. Since this was not investigated and is only still an assumption, studies with ranges of PEG polymeric substrate variants could be assessed to support or refute this assumption. Finally, studies incorporating polymeric substrate and polymeric catalyst to produce fully polymeric systems are also recommended as this thesis could serve as basis for such studies.

Appendix A. Supplementary Profiles and Images from Reactions Employing Mono Alkyne and Bi-Alkyne Functionalised Polyethylene Glycol

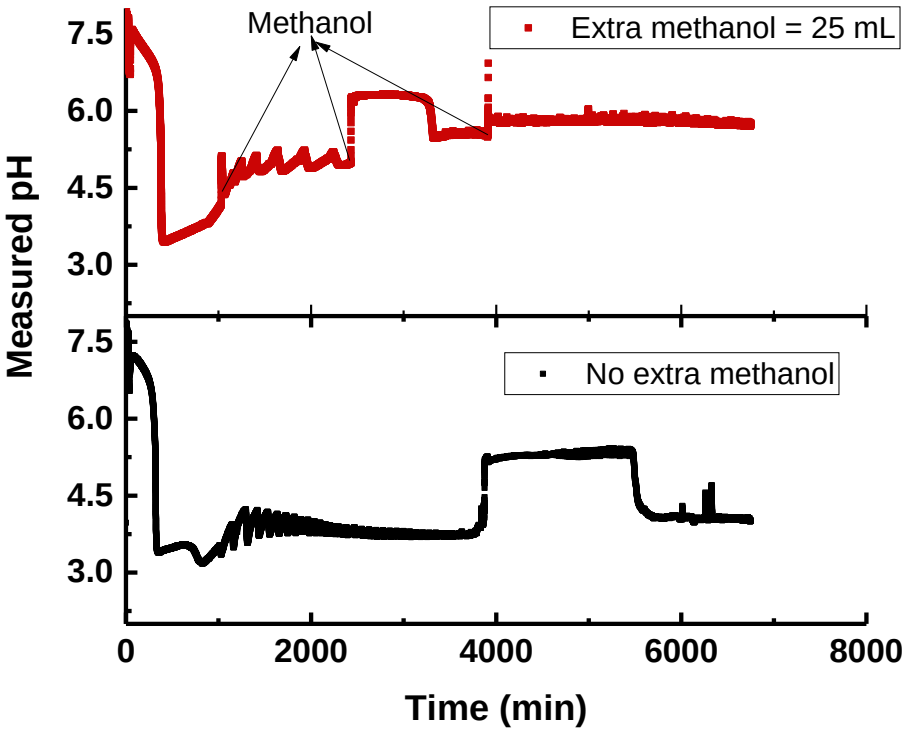

A1. Supplementary experimental runs, showing the effects of additional methanol during the reaction. Palladium iodide, KI and mono alkyne substrate were kept constant in both runs above

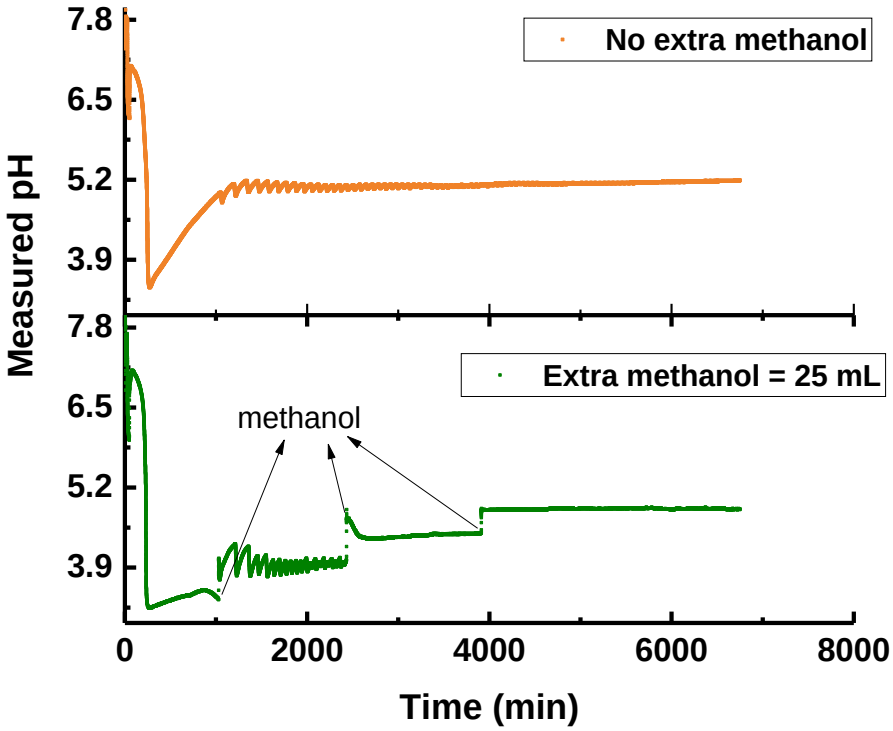

A2. Supplementary experimental runs, showing the effects of additional methanol during the reaction. Palladium iodide, KI and mono alkyne substrate were identical in both runs

A3. Palladium particles filtered off from an oscillatory carbonylation solution

A4. Differences in colour of reaction solutions at the end of an oscillatory run. The third solution from the left had the least amount of palladium from onset of the reaction and [KI] = 6 mM. The yellow colour of this solution suggests the presence of triiodide ions

A5. Black palladium particles present in carbonylated solutions on terminating an experimental run

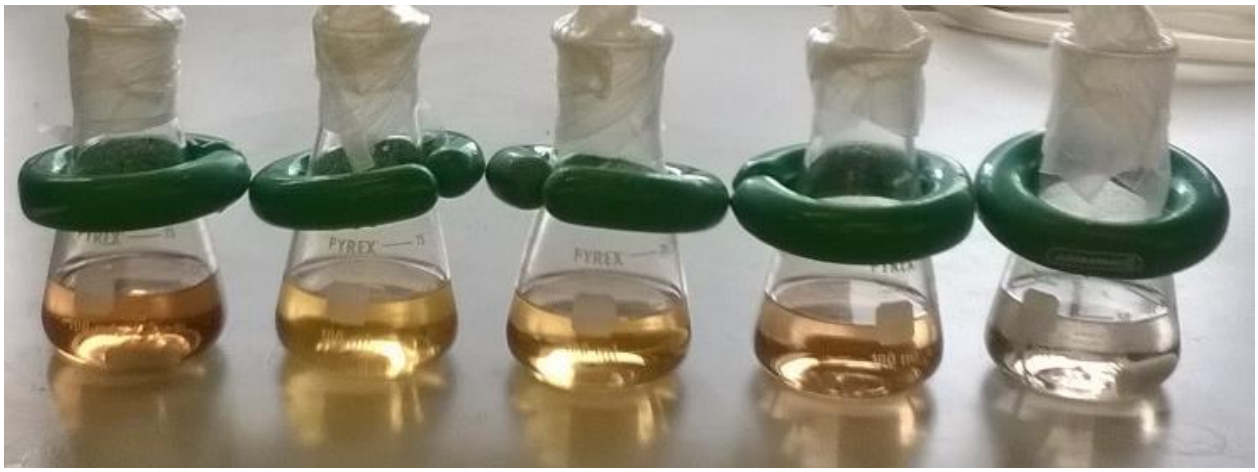

A6. Differences in colour of reaction solutions at the end of an oscillatory run. From the left, the first and 4th flasks contained the highest amount of palladium iodide and KI. The second and third flasks from the left had less palladium iodide and KI at 6 mM. The first flask from the right had the same amount of palladium iodide as flasks 2 and 3 from the left, but [KI] = 3 mM in this flask

A7. Range of concentrated raw product oils obtained after evaporating residual methanol at the end of an oscillatory reaction. First vial from the right had highest concentration of KI (9 mM) at constant palladium iodide and substrate concentration. The second and third vials from the left were obtained at the same PdI2 and substrate concentration but [KI] = 6 mM. The last vial from the left also contained the same concentration of PdI_2 and substrate and in this instance, [KI] = 3 mM

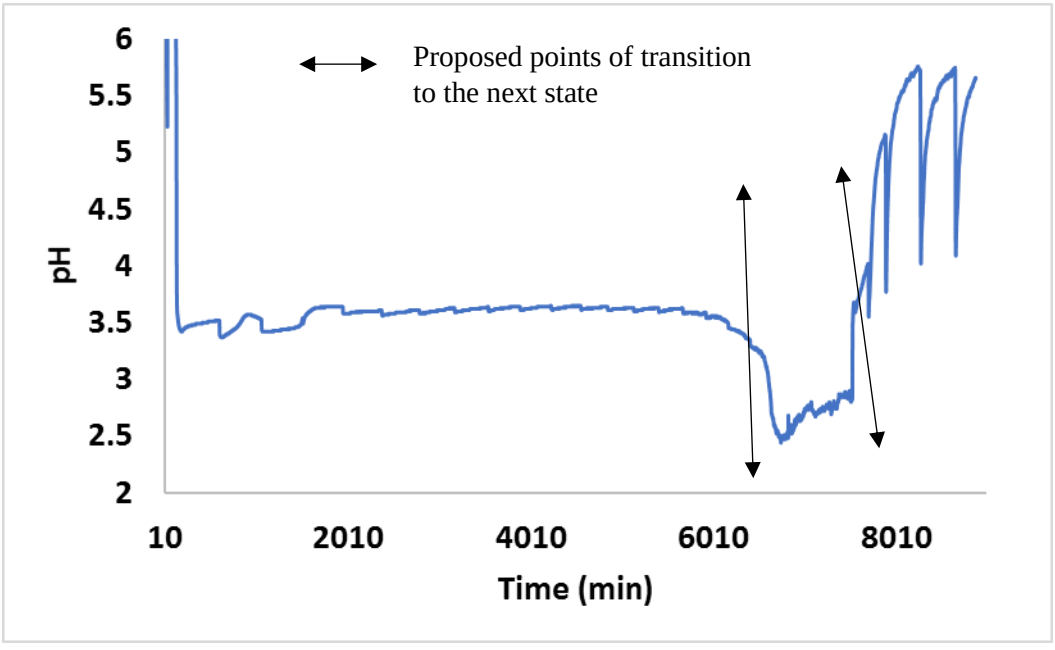

A8. Possible tri-rhythmicity in the oscillatory carbonylation of bi-alkyne functionalized Polyethylene glycol. [KI] = 5.7 mM and [A-PEG_{2000}-A] = 3.04 mM and [PdI_2] = 29 µM

References

1. Bertleff, W., *Carbonylation.* Ullmann's Encyclopedia of Industrial Chemistry, 2000.
2. Beller, M., *Catalytic carbonylation reactions*. Vol. 18. 2006: Springer.
3. Gabriele, B., G. Salerno, and M. Costa, *Oxidative carbonylations*, in *Catalytic carbonylation reactions*. 2006, Springer. p. 239-272.
4. Beller, M. and X.-F. Wu, *Transition metal catalyzed carbonylation reactions*. 2013: Springer.
5. Colquhoun, H., D. Thompson, and M.V. Twigg, *Carbonylation: direct synthesis of carbonyl compounds*. 2013: Springer Science & Business Media.
6. Gorodsky, S.N., *New type of oscillatory processes—oxidative carbonylation of alkynes in the homogeneous catalysis by Pd complexes. Phenylacetylene.* Reaction Kinetics, Mechanisms and Catalysis, 2018: p. 1-20.
7. Gorodsky, S.N., *Oxidative Carbonylation of 2-Propyn-1-ol and 2-Methyl-3-butyn-2-ol in an Oscillatory Mode.* Organic Chemistry International, 2012. **2012**: p. 6.
8. Parker, J. and K. Novakovic, *The Effect of Temperature on Selectivity in the Oscillatory Mode of the Phenylacetylene Oxidative Carbonylation Reaction.* ChemPhysChem, 2017. **18**(15): p. 1981-1986.
9. Novakovic, K., A. Mukherjee, M. Willis, A. Wright, and S. Scott, *The influence of reaction temperature on the oscillatory behaviour in the palladium-catalysed phenylacetylene oxidative carbonylation reaction.* Physical Chemistry Chemical Physics, 2009. **11**(40): p. 9044-9049.
10. Novakovic, K., C. Grosjean, S. Scott, A. Whiting, M. Willis, and A. Wright, *Achieving pH and Qr oscillations in a palladium-catalysed phenylacetylene oxidative carbonylation reaction using an automated reactor system.* Chemical physics letters, 2007. **435**(1): p. 142-147.
11. Malashkevich, A.V., L.G. Bruk, and O.N. Temkin, *New oscillating reaction in catalysis by metal complexes: a mechanism of alkyne oxidative carbonylation.* The Journal of Physical Chemistry A, 1997. **101**(51): p. 9825-9827.
12. Epstein, I.R. and J.A. Pojman, *An introduction to nonlinear chemical dynamics: oscillations, waves, patterns, and chaos*. 1998: Oxford University Press.
13. Sagués, F. and I.R. Epstein, *Nonlinear chemical dynamics.* Dalton transactions, 2003(7): p. 1201-1217.
14. Epstein, I.R. and K. Showalter, *Nonlinear chemical dynamics: oscillations, patterns, and chaos.* The Journal of Physical Chemistry, 1996. **100**(31): p. 13132-13147.
15. Pojman, J.A., D.C. Leard, and W. West, *Periodic polymerization of acrylonitrile in the cerium-catalyzed Belousov-Zhabotinskii reaction.* Journal of the American Chemical Society, 1992. **114**(21): p. 8298-8299.
16. Ruoff, P. and R.M. Noyes, *Chemical oscillations and instabilities. Part 61. Temporary bistability and unusual oscillatory behavior in a closed Belousov-Zhabotinskii reaction system.* The Journal of Physical Chemistry, 1985. **89**(8): p. 1339-1341.

17. Hudson, J.L., M. Hart, and D. Marinko, *An experimental study of multiple peak periodic and nonperiodic oscillations in the Belousov–Zhabotinskii reaction.* The Journal of Chemical Physics, 1979. **71**(4): p. 1601-1606.
18. Heilweil, E.J., M.J. Henchman, and I.R. Epstein, *Sequential oscillations in mixed-substrate Belousov-Zhabotinskii systems.* Journal of the American Chemical Society, 1979. **101**(13): p. 3698-3700.
19. Zhabotinsky, A.M., *Periodical oxidation of malonic acid in solution (a study of the Belousov reaction kinetics).* Biofizika, 1964. **9**: p. 306-311.
20. Yoshida, R., S. Onodera, T. Yamaguchi, and E. Kokufuta, *Aspects of the Belousov-Zhabotinsky reaction in polymer gels.* The Journal of Physical Chemistry A, 1999. **103**(43): p. 8573-8578.
21. Tyson, J.J., *What everyone should know about the Belousov-Zhabotinsky reaction*, in *Frontiers in mathematical biology*. 1994, Springer. p. 569-587.
22. Adamčíková, Ľ. and I. Schreiber, *Experimental study of coupled chemical oscillators of the Belousov-Zhabotinskii type.* Chemical Papers, 1990. **44**(4): p. 441-450.
23. Belousov, B.P., *A periodic reaction and its mechanism.* Ref. Radiats. Med., 1958.
24. Rabai, G., M. Orban, and I.R. Epstein, *Systematic design of chemical oscillators. 64. Design of pH-regulated oscillators.* Accounts of Chemical Research, 1990. **23**(8): p. 258-263.
25. Orbán, M., K. Kurin-Csörgei, and I.R. Epstein, *pH-Regulated Chemical Oscillators.* Accounts of Chemical Research, 2015. **48**(3): p. 593-601.
26. Kovacs, K., R.E. McIlwaine, S.K. Scott, and A.F. Taylor, *pH oscillations and bistability in the methylene glycol–sulfite–gluconolactone reaction.* Physical Chemistry Chemical Physics, 2007. **9**(28): p. 3711-3716.
27. Kovacs, K., R.E. McIlwaine, S.K. Scott, and A.F. Taylor, *An organic-based pH oscillator.* The Journal of Physical Chemistry A, 2007. **111**(4): p. 549-551.
28. Isakova, A. and K. Novakovic, *Oscillatory chemical reactions in the quest for rhythmic motion of smart materials.* European Polymer Journal, 2017. **95**(Supplement C): p. 430-439.
29. Donlon, L. and K. Novakovic, *Oscillatory carbonylation using alkyne-functionalised poly (ethylene glycol).* Chemical Communications, 2014. **50**(98): p. 15506-15508.
30. Donlon, L., J. Parker, and K. Novakovic, *Oscillatory carbonylation of phenylacetylene in the absence of externally supplied oxidant.* Reaction Kinetics, Mechanisms and Catalysis, 2014. **112**(1): p. 1-13.
31. Isakova, A., B.J. Murdoch, and K. Novakovic, *From small molecules to polymeric catalysts in the oscillatory carbonylation reaction: multiple effects of adding HI.* Physical Chemistry Chemical Physics, 2018. **20**(14): p. 9281-9288.
32. Parker, J. and K. Novakovic, *Autonomous reorganization of the oscillatory phase in the PdI2 catalyzed phenylacetylene carbonylation reaction.* Reaction Kinetics, Mechanisms and Catalysis, 2016. **118**(1): p. 73-85.

33. Gorodsky, S., *Concentration oscillations in the oxidative carbonylation of non-1-yne in the PdI 2-KI-CO-O 2-CH 3 OH and PdI 2-KI-CO-O 2-phenylacetylene-CH 3 OH systems.* Kinetics and Catalysis, 2012. **53**(4): p. 493-496.
34. Kim, Y.S., R. Tamate, A.M. Akimoto, and R. Yoshida, *Recent developments in self-oscillating polymeric systems as smart materials: from polymers to bulk hydrogels.* Materials Horizons, 2017. **4**(1): p. 38-54.
35. Novakovic, K., S. Matcham, and A. Scott, *Intelligent Hydrogels as Drug Delivery Systems*, in *Hydrogels*. 2018, Springer. p. 1-28.
36. Nwosu, C.J., G.A. Hurst, and K. Novakovic, *Genipin cross-linked chitosan-polyvinylpyrrolidone hydrogels: Influence of composition and postsynthesis treatment on pH responsive behaviour.* Advances in Materials Science and Engineering, 2015. **2015**.
37. Kanamala, M., W.R. Wilson, M. Yang, B.D. Palmer, and Z. Wu, *Mechanisms and biomaterials in pH-responsive tumour targeted drug delivery: a review.* Biomaterials, 2016. **85**: p. 152-167.
38. Gorodskii, S., E. Kalenova, L. Bruk, and O. Temkin, *Oxidative carbonylation of alkynes in self-oscillating mode. Effect of the nature of substrates on the dynamic behavior of reaction system.* Russian chemical bulletin, 2003. **52**(7): p. 1534-1543.
39. Anna, I. and N. Katarina, *Pulsatile release from a flat self-oscillating chitosan macrogel.* Journal of Materials Chemistry B, 2018. **6**(30): p. 5003-5010.
40. Strijbos, J. *Oscillations – Axon and Homeostase 13/7/2016*. exhibitions [online] 2016 [cited 2017 6/11/2017]; press]. Available from: http://nomegallery.com/exhibitions/oscillations/.
41. Hirniak, J., *Zur Frage der periodischen Reaktionen.* Zeitschrift für Physikalische Chemie, 1911. **75**(1): p. 675-680.
42. Lotka, A.J., *Analytical note on certain rhythmic relations in organic systems.* Proceedings of the National Academy of Sciences, 1920. **6**(7): p. 410-415.
43. Wulund, L. and A.B. Reddy, *A brief history of circadian time: The emergence of redox oscillations as a novel component of biological rhythms.* Perspectives in Science, 2015. **6**: p. 27-37.
44. Goldbeter, A., *Biochemical oscillations and cellular rhythms: the molecular bases of periodic and chaotic behaviour*. 1997: Cambridge university press.
45. Rapp, P., *Why are so many biological systems periodic?* Progress in neurobiology, 1987. **29**(3): p. 261-273.
46. Achoff, J., *A survey on biological rhythms.* Biological Rhythms, 1981. **4**: p. 3-10.
47. Chance, B., A.K. Ghosh, and E.K. Pye, *Biological and biochemical oscillators*. 2014: Academic Press.
48. Semenov, S.N., L.J. Kraft, A. Ainla, M. Zhao, M. Baghbanzadeh, V.E. Campbell, K. Kang, J.M. Fox, and G.M. Whitesides, *Autocatalytic, bistable, oscillatory networks of biologically relevant organic reactions.* Nature, 2016. **537**(7622): p. 656-660.

49. Szucs, A., P. Varona, A.R. Volkovskii, H.D. Abarbanel, M.I. Rabinovich, and A.I. Selverston, *Interacting biological and electronic neurons generate realistic oscillatory rhythms.* Neuroreport, 2000. **11**(3): p. 563-9.
50. Shitiri, E., A.V. Vasilakos, and H.-S. Cho, *Biological Oscillators in Nanonetworks—Opportunities and Challenges.* Sensors, 2018. **18**(5): p. 1544.
51. Hess, B. and A. Boiteux, *Oscillatory phenomena in biochemistry.* Annual review of biochemistry, 1971. **40**(1): p. 237-258.
52. Lotka, A.J., *Contribution to the theory of periodic reactions.* The Journal of Physical Chemistry, 1910. **14**(3): p. 271-274.
53. Lotka, A.J., *Undamped oscillations derived from the law of mass action.* Journal of the american chemical society, 1920. **42**(8): p. 1595-1599.
54. Lotka, A.J., *Elements of physical biology.* Science Progress in the Twentieth Century (1919-1933), 1926. **21**(82): p. 341-343.
55. Volterra, V., *Fluctuations in the abundance of a species considered mathematically.* Nature, 1926. **118**(2972): p. 558-560.
56. Chance, B., R.W. Estabrook, and A. Ghosh, *Damped sinusoidal oscillations of cytoplasmic reduced pyridine nucleotide in yeast cells.* Proceedings of the National Academy of Sciences, 1964. **51**(6): p. 1244-1251.
57. Duysens, L. and J. Amesz, *Fluorescence spectrophotometry of reduced phosphopyridine nucleotide in intact cells in the near-ultraviolet and visible region.* Biochimica et biophysica acta, 1957. **24**: p. 19-26.
58. Lardy, H. and S. Graven. *RELATION BETWEEN ALKALI CATIONS AND HYDROLYSIS OF ATP BY LIVER MITOCHONDRIA.* in *Federation Proceedings*. 1965. FEDERATION AMER SOC EXP BIOL 9650 ROCKVILLE PIKE, BETHESDA, MD 20814-3998.
59. Packer, L., J. Wrigglesworth, P. Fortes, and B. Pressman, *Expansion of the inner membrane compartment and its relation to mitochondrial volume and ion transport.* The Journal of cell biology, 1968. **39**(2): p. 382-391.
60. Hess, B., *The glycolytic oscillator.* Journal of Experimental Biology, 1979. **81**(1): p. 7-14.
61. Bánsági Jr, T.s. and A.F. Taylor, *Role of Differential Transport in an Oscillatory Enzyme Reaction.* The Journal of Physical Chemistry B, 2014. **118**(23): p. 6092-6097.
62. Goldbeter, A. and S.R. Caplan, *Oscillatory enzymes.* Annual review of biophysics and bioengineering, 1976. **5**(1): p. 449-476.
63. Novak, B. and J.J. Tyson, *Design principles of biochemical oscillators.* Nat Rev Mol Cell Biol, 2008. **9**(12): p. 981-991.
64. Nicolis, G. and J. Portnow, *Chemical oscillations.* Chemical Reviews, 1973. **73**(4): p. 365-384.
65. Fung, E., W.W. Wong, J.K. Suen, T. Bulter, S.-g. Lee, and J.C. Liao, *A synthetic gene-metabolic oscillator.* Nature, 2005. **435**(7038): p. 118-122.

66. Purcell, O., N.J. Savery, C.S. Grierson, and M. di Bernardo, *A comparative analysis of synthetic genetic oscillators.* Journal of the Royal Society Interface, 2010. **7**(52): p. 1503-1524.
67. Vilar, J.M., H.Y. Kueh, N. Barkai, and S. Leibler, *Mechanisms of noise-resistance in genetic oscillators.* Proceedings of the National Academy of Sciences, 2002. **99**(9): p. 5988-5992.
68. Lakshmanan, M. and S. Rajaseekar, *Nonlinear dynamics: integrability, chaos and patterns*. 2003: Springer Science & Business Media.
69. Sevcik, P., K. Kissimonova, and L.u. Adamcikova, *Oxygen production in the oscillatory Bray-Liebhafsky reaction.* Journal of Physical Chemistry A, 2000. **104**(17): p. 3958-3963.
70. Rábai, G., A. Kaminaga, and I. Hanazaki, *Mechanism of the Oscillatory Bromate Oxidation of Sulfite and Ferrocyanide in a CSTR.* The Journal of Physical Chemistry, 1996. **100**(40): p. 16441-16442.
71. Orban, M. and I.R. Epstein, *Systematic design of chemical oscillators. Part 13. Complex periodic and aperiodic oscillation in the chlorite-thiosulfate reaction.* The Journal of Physical Chemistry, 1982. **86**(20): p. 3907-3910.
72. Kurin-Csörgei, K., G. Nagy, and E. Körös, *Temperature-triggered chemical oscillators. A peculiar temperature effect in perturbed uncatalyzed bromate-driven reactions.* Chemical physics letters, 1997. **271**(1-3): p. 67-72.
73. Dutt, A. and S. Mueller, *Effect of stirring and temperature on the Belousov-Zhabotinskii reaction in a CSTR.* The Journal of Physical Chemistry, 1993. **97**(39): p. 10059-10063.
74. Nagypal, I. and I.R. Epstein, *Fluctuations and stirring rate effects in the chlorite-thiosulfate reaction.* The Journal of Physical Chemistry, 1986. **90**(23): p. 6285-6292.
75. Zhabotinsky, A.M., *A history of chemical oscillations and waves.* Chaos: An Interdisciplinary Journal of Nonlinear Science, 1991. **1**(4): p. 379-386.
76. Bray, W.C. and H.A. Liebhafsky, *Reactions involving hydrogen peroxide, iodine and iodate ion. I. Introduction.* Journal of the American Chemical Society, 1931. **53**(1): p. 38-44.
77. Sharma, K.R. and R.M. Noyes, *Oscillations in chemical systems. 13. A detailed molecular mechanism for the Bray-Liebhafsky reaction of iodate and hydrogen peroxide.* Journal of the American Chemical Society, 1976. **98**(15): p. 4345-4361.
78. Treindl, L. and R.M. Noyes, *A new explanation of the oscillations in the Bray-Liebhafsky reaction.* The Journal of Physical Chemistry, 1993. **97**(43): p. 11354-11362.
79. Valent, I., a. L'Ubica Adamčíková, and P. Ševčík, *Simulations of the iodine interphase transport effect on the oscillating Bray-Liebhafsky reaction.* The Journal of Physical Chemistry A, 1998. **102**(39): p. 7576-7579.
80. Kolar-Anić, L. and G. Schmitz, *Mechanism of the Bray–Liebhafsky reaction: effect of the oxidation of iodous acid by hydrogen peroxide.* Journal of the Chemical Society, Faraday Transactions, 1992. **88**(16): p. 2343-2349.

81. Liebhafsky, H.A., W.C. McGavock, R.J. Reyes, G.M. Roe, and L.S. Wu, *Reactions involving hydrogen peroxide, iodine, and iodate ion. 6. Oxidation of iodine by hydrogen peroxide at 50. degree. C.* Journal of the American Chemical Society, 1978. **100**(1): p. 87-91.
82. Prigogine, I., *Thermodynamics of irreversible processes*. Vol. 404. 1955: Thomas.
83. Noyes, R.M., R. Field, and E. Koros, *Oscillations in chemical systems. I. Detailed mechanism in a system showing temporal oscillations.* Journal of the American Chemical Society, 1972. **94**(4): p. 1394-1395.
84. Vanag, V.K., L. Yang, M. Dolnik, A.M. Zhabotinsky, and I.R. Epstein, *Oscillatory cluster patterns in a homogeneous chemical system with global feedback.* Nature, 2000. **406**(6794): p. 389-391.
85. Yoshida, R., T. Sakai, Y. Hara, S. Maeda, S. Hashimoto, D. Suzuki, and Y. Murase, *Self-oscillating gel as novel biomimetic materials.* Journal of Controlled Release, 2009. **140**(3): p. 186-193.
86. Ludlow, R.F. and S. Otto, *Systems chemistry.* Chemical Society Reviews, 2008. **37**(1): p. 101-108.
87. Field, R.J., E. Koros, and R.M. Noyes, *Oscillations in chemical systems. II. Thorough analysis of temporal oscillation in the bromate-cerium-malonic acid system.* Journal of the American Chemical Society, 1972. **94**(25): p. 8649-8664.
88. Briggs, T.S. and W.C. Rauscher, *An oscillating iodine clock.* J. Chem. Educ, 1973. **50**(7): p. 496.
89. De Kepper, P. and I.R. Epstein, *Mechanistic study of oscillations and bistability in the Briggs-Rauscher reaction.* Journal of the American Chemical Society, 1982. **104**(1): p. 49-55.
90. Gurel, O. and D. Gurel, *Types of oscillations in chemical reactions*, in *Oscillations in Chemical Reactions*. 1983, Springer. p. 1-73.
91. Noyes, R.M., *Mechanisms of some chemical oscillators.* Journal of Physical Chemistry, 1990. **94**(11): p. 4404-4412.
92. Boissonade, J. and P. De Kepper, *Transitions from bistability to limit cycle oscillations. Theoretical analysis and experimental evidence in an open chemical system.* The Journal of Physical Chemistry, 1980. **84**(5): p. 501-506.
93. De Kepper, P., I.R. Epstein, and K. Kustin, *A systematically designed homogeneous oscillating reaction: the arsenite-iodate-chlorite system.* Journal of the American Chemical Society, 1981. **103**(8): p. 2133-2134.
94. De Kepper, P., I.R. Epstein, and K. Kustin, *Bistability in the oxidation of arsenite by iodate in a stirred flow reactor.* Journal of the American Chemical Society, 1981. **103**(20): p. 6121-6127.
95. Alamgir, M. and I.R. Epstein, *Systematic design of chemical oscillators. 17. Birhythmicity and compound oscillation in coupled chemical oscillators: chlorite-bromate-iodide system.* Journal of the American Chemical Society, 1983. **105**(8): p. 2500-2502.

96. Alamgir, M. and I.R. Epstein, *Systematic design of chemical oscillators. Part 19. Experimental study of complex dynamical behavior in coupled chemical oscillators.* The Journal of Physical Chemistry, 1984. **88**(13): p. 2848-2851.

97. Decroly, O. and A. Goldbeter, *Multiple periodic regimes and final state sensitivity in a biochemical system.* Physics Letters A, 1984. **105**(4-5): p. 259-262.

98. Goldbeter, A., O. Decroly, Y.-X. Li, J.L. Martiel, and F. Moran, *Finding complex oscillatory phenomena in biochemical systems An empirical approach.* Biophysical chemistry, 1988. **29**(1-2): p. 211-217.

99. Maselko, J. and I.R. Epstein, *Systematic design of chemical oscillators. Part 22. Dynamical behavior of coupled chemical oscillators: chlorite-thiosulfate-iodide-iodine.* The Journal of Physical Chemistry, 1984. **88**(22): p. 5305-5308.

100. Orban, M., C. Dateo, P. De Kepper, and I.R. Epstein, *Systematic design of chemical oscillators. 11. Chlorite oscillators: new experimental examples, tristability, and preliminary classification.* Journal of the American Chemical Society, 1982. **104**(22): p. 5911-5918.

101. Edblom, E.C., M. Orban, and I.R. Epstein, *A new iodate oscillator: the Landolt reaction with ferrocyanide in a CSTR.* Journal of the American Chemical Society, 1986. **108**(11): p. 2826-2830.

102. Gaudioso, J. and S. Sattar, *New Experimental Studies and Simulations of the Bromate-Chlorite-Iodide Coupled Oscillator.* The Journal of Physical Chemistry, 1995. **99**(40): p. 14749-14751.

103. Gorodskii, S., A. Zakharov, A. Kulik, L. Bruk, and O. Temkin, *Oxidative carbonylation of alkynes in an oscillation mode: I. Concentration limits for oscillations in the course of phenylacetylene carbonylation and possible mechanisms of the process.* Kinetics and catalysis, 2001. **42**(2): p. 251-263.

104. Hauser, M.J.B., A. Strich, R. Bakos, Z. Nagy-Ungvarai, and S.C. Müller, *pH oscillations in the hemin–hydrogen peroxide–sulfite reaction.* Faraday discussions, 2002. **120**: p. 229-236.

105. Hocker, C.G., I.R. Epstein, K. Kustin, and K. Tornheim, *Glycolytic pH oscillations in a flow reactor.* Biophysical chemistry, 1994. **51**(1): p. 21-35.

106. Poros, E., K. Kurin-Csörgei, I. Szalai, G. Rábai, and M. Orbán, *pH-oscillations in the bromate–sulfite reaction in semibatch and in gel-fed batch reactors.* Chaos: An Interdisciplinary Journal of Nonlinear Science, 2015. **25**(6): p. 064602.

107. Gao, Q. and J. Wang, *pH oscillations and complex reaction dynamics in the non-buffered chlorite–thiourea reaction.* Chemical physics letters, 2004. **391**(4-6): p. 349-353.

108. Strizhak, P.E. and A.L. Kawczynski, *Complex transient oscillations in the belousov-zhabotinskii reaction in a batch reactor.* The Journal of Physical Chemistry, 1995. **99**(27): p. 10830-10833.

109. Aguda, B.D., R. Larter, and B.L. Clarke, *Dynamic elements of mixed-mode oscillations and chaos in a peroxidase–oxidase model network.* The Journal of Chemical Physics, 1989. **90**(8): p. 4168-4175.

110. Bakeš, D., L. Schreiberová, I. Schreiber, and M.J.B. Hauser, *Mixed-mode oscillations in a homogeneous p H-oscillatory chemical reaction system.* Chaos: An Interdisciplinary Journal of Nonlinear Science, 2008. **18**(1): p. 015102.

111. Brøns, M., T.J. Kaper, and H.G. Rotstein, *Introduction to focus issue: mixed mode oscillations: experiment, computation, and analysis*. 2008, AIP.

112. Hauck, T. and F.W. Schneider, *Mixed-mode and quasiperiodic oscillations in the peroxidase-oxidase reaction.* The Journal of Physical Chemistry, 1993. **97**(2): p. 391-397.

113. Jalics, J., M. Krupa, and H.G. Rotstein, *Mixed-mode oscillations in a three time-scale system of ODEs motivated by a neuronal model.* Dynamical Systems, 2010. **25**(4): p. 445-482.

114. Krupa, M., N. Popović, N. Kopell, and H.G. Rotstein, *Mixed-mode oscillations in a three time-scale model for the dopaminergic neuron.* Chaos: An Interdisciplinary Journal of Nonlinear Science, 2008. **18**(1): p. 015106.

115. Petrov, V., S.K. Scott, and K. Showalter, *Mixed-mode oscillations in chemical systems.* The Journal of chemical physics, 1992. **97**(9): p. 6191-6198.

116. Haberichter, T., M. Marhl, and R. Heinrich, *Birhythmicity, trirhythmicity and chaos in bursting calcium oscillations.* Biophysical Chemistry, 2001. **90**(1): p. 17-30.

117. Čupić, Ž.D., L.Z. Kolar-Anić, S.R. Anić, S.R. Maćešić, J.P. Maksimović, M.S. Pavlović, M.C. Milenković, I.N.M. Bubanja, E. Greco, and S.D. Furrow, *Regularity of Intermittent Bursts in Briggs Rauscher Oscillating Systems with Phenol.* Helvetica Chimica Acta, 2014. **97**(3): p. 321-333.

118. Wang, D., S. Grillner, and P. Wallen, *Endogenous release of 5-HT modulates the plateau phase of NMDA-induced membrane potential oscillations in lamprey spinal neurons.* Journal of neurophysiology, 2014. **112**(1): p. 30-38.

119. Decroly, O. and A. Goldbeter, *Birhythmicity, chaos, and other patterns of temporal self-organization in a multiply regulated biochemical system.* Proceedings of the National Academy of Sciences, 1982. **79**(22): p. 6917-6921.

120. Moran, F. and A. Goldbeter, *Onset of birhythmicity in a regulated biochemical system.* Biophysical chemistry, 1984. **20**(1-2): p. 149-156.

121. Ivanović, A., Ž. Čupić, M. Janković, L.Z. Kolar-Anić, and S. Anić, *The chaotic sequences in the Bray–Liebhafsky reaction in an open reactor*. Physical Chemistry Chemical Physics, 2008. **10**(38): p. 5848-5858.

122. Rábai, G. and I. Hanazaki, *Chaotic pH Oscillations in the Hydrogen Peroxide− Thiosulfate− Sulfite Flow System.* The Journal of Physical Chemistry A, 1999. **103**(36): p. 7268-7273.

123. Strizhak, P. and M. Menzinger, *Nonlinear dynamics of the BZ reaction: A simple experiment that illustrates limit cycles, chaos, bifurcations, and noise*. Journal of chemical education, 1996. **73**(9): p. 868.

124. Orban, M. and I.R. Epstein, *Systematic design of chemical oscillators. 39. Chemical oscillators in group VIA: the copper (II)-catalyzed reaction between hydrogen peroxide and thiosulfate ion.* Journal of the American Chemical Society, 1987. **109**(1): p. 101-106.

125. Koper, M.T., E.A. Meulenkamp, and D. Vanmaekelbergh, *Oscillatory behavior of the hydrogen peroxide reduction at gallium arsenide semiconductor electrodes.* The Journal of Physical Chemistry, 1993. **97**(28): p. 7337-7341.

126. Pešek, O., V. Kofrankova, L. Schreiberová, and I. Schreiber, *Response Dynamics to Pulsed Perturbations of the Hydrogen Peroxide− Thiosulfate− Cu2+ Reaction.* The Journal of Physical Chemistry A, 2008. **112**(5): p. 826-832.

127. Shen, J., S. Pullela, M. Marquez, and Z. Cheng, *Ternary Phase Diagram for the Belousov− Zhabotinsky Reaction-Induced Mechanical Oscillation of Intelligent PNIPAM Colloids.* The Journal of Physical Chemistry A, 2007. **111**(48): p. 12081-12085.

128. Edblom, E.C., Y. Luo, M. Orban, K. Kustin, and I.R. Epstein, *Systematic design of chemical oscillators. 45. Kinetics and mechanism of the oscillatory bromate-sulfite-ferrocyanide reaction.* The Journal of Physical Chemistry, 1989. **93**(7): p. 2722-2727.

129. Kurin-Csörgei, K., I.R. Epstein, and M. Orbán, *Systematic design of chemical oscillators using complexation and precipitation equilibria.* Nature, 2005. **433**(7022): p. 139-142.

130. Poros, E., V. Horváth, K. Kurin-Csörgei, I.R. Epstein, and M. Orbán, *Generation of pH-oscillations in closed chemical systems: method and applications.* Journal of the American Chemical Society, 2011. **133**(18): p. 7174-7179.

131. Beller, M., H. Fischer, K. Kühlein, C.-P. Reisinger, and W. Herrmann, *First palladium-catalyzed Heck reactions with efficient colloidal catalyst systems.* Journal of organometallic chemistry, 1996. **520**(1-2): p. 257-259.

132. Adams, G.E. and E.J. Hart, *Radiolysis and Photolysis of Aqueous Formic Acid. Carbon Monoxide Formation.* Journal of the American Chemical Society, 1962. **84**(21): p. 3994-3999.

133. Peng, C., *Quantitative GC determination of carbon monoxide by calibration via the production of CO from formic acid.* Chromatographia, 1990. **29**(7-8): p. 347-350.

134. Shi, Y.L., Y.C. Gao, Q.Z. Shi, D.L. Kershner, and F. Basolo, *Oxygen atom transfer reactions to metal carbonyls. Kinetics and mechanism of carbon monoxide substitution reactions of M (CO) 6 (M= chromium, molybdenum, tungsten) in the presence of trimethylamine oxide.* Organometallics, 1987. **6**(7): p. 1528-1531.

135. Zobi, F., *CO and CO-releasing molecules in medicinal chemistry.* Future, 2013. **5**(2): p. 175-188.

136. Bird, C., *Synthesis of Organic Compounds by Direct Carbonylation Reactions Using Metal Carbonyls.* Chemical Reviews, 1962. **62**(4): p. 283-302.

137. Gabriele, B., G. Salerno, M. Costa, and G.P. Chiusoli, *A new regioselective synthesis of 3-substituted furan-2 (5H)-ones by palladium-catalysed reductive carbonylation of alk-1-ynes.* Tetrahedron letters, 1999. **40**(5): p. 989-990.

138. Kiss, G., *Palladium-catalyzed reppe carbonylation.* Chemical reviews, 2001. **101**(11): p. 3435-3456.

139. Doherty, S., J. Knight, T. Backhouse, E. Abood, H. Alshaikh, I.J.S. Fairlamb, R. Bourne, T. Chamberlain, and R. Stones, *Highly efficient aqueous phase chemoselective hydrogenation of α, β-unsaturated aldehydes catalysed by phosphine-decorated polymer immobilized IL-stabilized PdNPs.* Green Chemistry, 2017. **19**(7): p. 1635-1641.

140. Doherty, S., J.G. Knight, R.K. Rath, W. Clegg, R.W. Harrington, C.R. Newman, R. Campbell, and H. Amin, *Ruthenium complexes of six-electron-donor NUPHOS-type diphosphines: Highly selective catalysts for the hydrocarboxylation of terminal alkynes.* Organometallics, 2005. **24**(11): p. 2633-2644.

141. Zhao, L., B. Pudasaini, A. Genest, J.D. Nobbs, C.H. Low, L.P. Stubbs, M. van Meurs, and N. Rösch, *Palladium-Catalyzed Hydroxycarbonylation of Pentenoic Acids. Computational and Experimental Studies on the Catalytic Selectivity.* ACS Catalysis, 2017. **7**: p. 7070-7080.

142. Doherty, S., J.G. Knight, and M. Betham, *The first insoluble polymer-bound palladium complexes of 2-pyridyldiphenylphosphine: highly efficient catalysts for the alkoxycarbonylation of terminal alkynes.* Chemical Communications, 2006(1): p. 88-90.

143. Dong, K., X. Fang, S. Gülak, R. Franke, A. Spannenberg, H. Neumann, R. Jackstell, and M. Beller, *Highly active and efficient catalysts for alkoxycarbonylation of alkenes.* Nature communications, 2017. **8**.

144. Marshall, J.A. and M.A. Wolf, *Amination, aminocarbonylation, and alkoxycarbonylation of allenic/propargylic Pd intermediates derived from nonracemic propargylic mesylates: synthesis of nonracemic propargyl amines, allenic amides, and butenolides.* The Journal of Organic Chemistry, 1996. **61**(10): p. 3238-3239.

145. Peng, J.-B., X. Qi, and X.-F. Wu, *Recent Achievements in Carbonylation Reactions: A Personal Account.* Synlett, 2017. **28**(02): p. 175-194.

146. Schnyder, A., M. Beller, G. Mehltretter, T. Nsenda, M. Studer, and A.F. Indolese, *Synthesis of primary aromatic amides by aminocarbonylation of aryl halides using formamide as an ammonia synthon.* The Journal of organic chemistry, 2001. **66**(12): p. 4311-4315.

147. Cenini, S. and F. Ragaini, *Catalytic reductive carbonylation of organic nitro compounds*. Vol. 20. 2013: Springer Science & Business Media.

148. Gabriele, B., G. Salerno, M. Costa, and G.P. Chiusoli, *Combined oxidative and reductive carbonylation of terminal alkynes with palladium iodide-thiourea catalysts.* Journal of organometallic chemistry, 1995. **503**(1): p. 21-28.

149. Beller, M., B. Cornils, C.D. Frohning, and C.W. Kohlpaintner, *Progress in hydroformylation and carbonylation.* Journal of Molecular Catalysis A: Chemical, 1995. **104**(1): p. 17-85.

150. Ji, F., X. Li, W. Wu, and H. Jiang, *Palladium-Catalyzed Oxidative Carbonylation for the Synthesis of Polycyclic Aromatic Hydrocarbons (PAHs).* The Journal of organic chemistry, 2014. **79**(22): p. 11246-11253.

151. King, S., *Reaction mechanism of oxidative carbonylation of methanol to dimethyl carbonate in Cu–Y zeolite.* Journal of Catalysis, 1996. **161**(2): p. 530-538.
152. Li, W., C. Liu, H. Zhang, K. Ye, G. Zhang, W. Zhang, Z. Duan, S. You, and A. Lei, *Palladium-Catalyzed Oxidative Carbonylation of N-Allylamines for the Synthesis of β-Lactams.* Angewandte Chemie International Edition, 2014. **53**(9): p. 2443-2446.
153. Liu, Q., H. Zhang, and A. Lei, *Oxidative Carbonylation Reactions: Organometallic Compounds (R□ M) or Hydrocarbons (R□ H) as Nucleophiles.* Angewandte Chemie International Edition, 2011. **50**(46): p. 10788-10799.
154. Temkin, O.N. and L.G. Bruk, *Oxidative carbonylation–homogeneous.* Encyclopedia of catalysis, 2003.
155. Wu, X.F., H. Neumann, and M. Beller, *Palladium-Catalyzed Oxidative Carbonylation Reactions.* ChemSusChem, 2013. **6**(2): p. 229-241.
156. Gabriele, B., R. Mancuso, and G. Salerno, *Oxidative carbonylation as a powerful tool for the direct synthesis of carbonylated heterocycles.* European Journal of Organic Chemistry, 2012. **2012**(35): p. 6825-6839.
157. Gabriele, B., G. Salerno, R. Mancuso, and M. Costa, *Efficient synthesis of ureas by direct palladium-catalyzed oxidative carbonylation of amines.* The Journal of organic chemistry, 2004. **69**(14): p. 4741-4750.
158. Gadge, S.T. and B.M. Bhanage, *Recent developments in palladium catalysed carbonylation reactions.* RSC Advances, 2014. **4**(20): p. 10367-10389.
159. Tsuji, J., *25 years in the organic chemistry of palladium.* Journal of organometallic chemistry, 1986. **300**(1-2): p. 281-305.
160. Tsuji, J., *Palladium reagents and catalysts: new perspectives for the 21st century*. 2006: John Wiley & Sons.
161. Smidt, J. and W. Hafner, *Eine Reaktion von Palladiumchlorid mit Allylalkohol.* Angewandte Chemie, 1959. **71**(8): p. 284-284.
162. Tsuji, J., J. Kiji, S. Imamura, and M. Morikawa, *Organic Syntheses by Means of Noble Metal Compounds. VIII. 1 Catalytic Carbonylation of Allylic Compounds with Palladium Chloride.* Journal of the American Chemical Society, 1964. **86**(20): p. 4350-4353.
163. Tsuji, J., *Carbon-carbon bond formation via palladium complexes.* Accounts of Chemical Research, 1969. **2**(5): p. 144-152.
164. Tsuji, J. and T. Nogi, *Organic Syntheses by Means of Noble Metal Compounds. XXII. 1 Palladium-Catalyzed Carbonylation of Diphenylacetylene.* Journal of the American Chemical Society, 1966. **88**(6): p. 1289-1292.
165. Chinchilla, R. and C. Najera, *Chemicals from alkynes with palladium catalysts.* Chemical reviews, 2013. **114**(3): p. 1783-1826.
166. Deng, Y., A.K.Å. Persson, and J.-E. Bäckvall, *Palladium-Catalyzed Oxidative Carbocyclizations.* Chemistry – A European Journal, 2012. **18**(37): p. 11498-11523.

167. Drent, E., P. Arnoldy, and P. Budzelaar, *Efficient palladium catalysts for the carbonylation of alkynes.* Journal of organometallic chemistry, 1993. **455**(1-2): p. 247-253.
168. Fang, W., H. Zhu, Q. Deng, S. Liu, X. Liu, Y. Shen, and T. Tu, *Design and Development of Ligands for Palladium-Catalyzed Carbonylation Reactions.* Synthesis, 2014. **46**(13): p. 1689-1708.
169. Quintero-Duque, S., K.M. Dyballa, and I. Fleischer, *Metal-catalyzed carbonylation of alkynes: key aspects and recent development.* Tetrahedron Letters, 2015. **56**(21): p. 2634-2650.
170. Brennführer, A., H. Neumann, and M. Beller, *Palladium-Catalyzed Carbonylation Reactions of Alkenes and Alkynes.* ChemCatChem, 2009. **1**(1): p. 28-41.
171. Tsuji, J., Y. Mori, and M. Hara, *Organic syntheses by means of noble metal compounds-XLVIII: Carbonylation of butadiene catalyzed by palladium-phosphine complexes.* Tetrahedron, 1972. **28**(14): p. 3721-3725.
172. Gabriele, B., G. Salerno, and M. Costa, *PdI2-Catalyzed Synthesis of Heterocycles.* Synlett, 2004. **2004**(14): p. 2468-2483.
173. Novakovic, K., C. Grosjean, S.K. Scott, A. Whiting, M.J. Willis, and A.R. Wright, *The influence of oscillations on product selectivity during the palladium-catalysed phenylacetylene oxidative carbonylation reaction.* Physical Chemistry Chemical Physics, 2008. **10**(5): p. 749-753.
174. Novakovic, K. and J. Parker, *Catalyst Initiation in the Oscillatory Carbonylation Reaction.* International Journal of Chemical Engineering, 2011. **2011**: p. 11.
175. Parker, J. and K. Novakovic, *Influence of water and the reactant addition sequence on palladium (II) iodide-catalyzed phenylacetylene carbonylation.* Industrial & Engineering Chemistry Research, 2013. **52**(7): p. 2520-2527.
176. Parker, J. and K. Novakovic, *The effect of using a methanol–water solvent mixture on pH oscillations in the palladium-catalyzed phenylacetylene oxidative carbonylation reaction.* Reaction Kinetics, Mechanisms and Catalysis, 2018. **123:**: p. 113–124.
177. Grosjean, C., K. Novakovic, S.K. Scott, A. Whiting, M.J. Willis, and A.R. Wright, *Product identification and distribution from the oscillatory versus non-oscillatory palladium (II) iodide-catalysed oxidative carbonylation of phenylacetylene.* Journal of Molecular Catalysis A: Chemical, 2008. **284**(1): p. 33-39.
178. Quaranta, M., M. Murkovic, and I. Klimant, *A new method to measure oxygen solubility in organic solvents through optical oxygen sensing.* Analyst, 2013. **138**(21): p. 6243-6245.
179. Tonner, S.P., M.S. Wainwright, D.L. Trimm, and N.W. Cant, *Solubility of carbon monoxide in alcohols.* Journal of Chemical and Engineering Data, 1983. **28**(1): p. 59-61.
180. Field, R.J. and F. Schneider, *Oscillating chemical reactions and nonlinear dynamics.* J. Chem. Educ, 1989. **66**(3): p. 195.
181. Gillespie, D.T., *Stochastic Simulation of Chemical Kinetics.* Annual Review of Physical Chemistry, 2007. **58**(1): p. 35-55.

182. Wiechert, W., *Modeling and simulation: tools for metabolic engineering.* Journal of Biotechnology, 2002. **94**(1): p. 37-63.
183. Higham, D.J., *Modeling and Simulating Chemical Reactions.* SIAM Review, 2008. **50**(2): p. 347-368.
184. Schuster, S., M. Marhl, and T. Höfer, *Modelling of simple and complex calcium oscillations.* European Journal of Biochemistry, 2002. **269**(5): p. 1333-1355.
185. Kolar-Anić, L., Ž. Čupić, G. Schmitz, and S. Anić, *Improvement of the stoichiometric network analysis for determination of instability conditions of complex nonlinear reaction systems.* Chemical engineering science, 2010. **65**(12): p. 3718-3728.
186. Lozano-Parada, J.H., H. Burnham, and F. Machuca Martinez, *Pedagogical Approach to the Modeling and Simulation of Oscillating Chemical Systems with Modern Software: The Brusselator Model.* Journal of Chemical Education, 2018. **95**(5): p. 758-766.
187. Yashin, V.V. and A.C. Balazs, *Pattern formation and shape changes in self-oscillating polymer gels.* Science, 2006. **314**(5800): p. 798-801.
188. Kapral, R. and K. Showalter, *Chemical waves and patterns*. Vol. 10. 2012: Springer Science & Business Media.
189. Yang, L., M. Dolnik, A.M. Zhabotinsky, and I.R. Epstein, *Pattern formation arising from interactions between Turing and wave instabilities.* The Journal of chemical physics, 2002. **117**(15): p. 7259-7265.
190. Kolar-Anić, L., Ž. Čupić, S. Anić, and G. Schmitz, *Pseudo-steady states in the model of theBray–Liebhafsky oscillatory reaction.* Journal of the Chemical Society, Faraday Transactions, 1997. **93**(12): p. 2147-2152.
191. Maćešić, S., Ž. Čupić, and L. Kolar-Anić, *Bifurcation analysis of the reduced model of the Bray–Liebhafsky reaction.* Reaction Kinetics, Mechanisms and Catalysis, 2016. **118**(1): p. 39-55.
192. Stanković, B., Ž. Čupić, S. Maćešić, N. Pejić, and L. Kolar-Anić, *Complex bifurcations in the oscillatory reaction model.* Chaos, Solitons & Fractals, 2016. **87**: p. 84-91.
193. Edelson, D., *Sensitivity analysis of proposed mechanisms for the Briggs-Rauscher oscillating reaction.* The Journal of Physical Chemistry, 1983. **87**(7): p. 1204-1208.
194. Furrow, S.D. and R.M. Noyes, *The oscillatory Briggs-Rauscher reaction. 1. Examination of subsystems.* Journal of the American Chemical Society, 1982. **104**(1): p. 38-42.
195. Râbai, G., *Modeling and designing of pH-controlled bistability, oscillations, and chaos in a continuous-flow stirred tank reactor.* 1998.
196. Szántó, T.G. and G. Rábai, *pH Oscillations in the BrO3-− SO32-/HSO3-Reaction in a CSTR.* The Journal of Physical Chemistry A, 2005. **109**(24): p. 5398-5402.
197. Yuan, L., T. Yang, Y. Liu, Y. Hu, Y. Zhao, J. Zheng, and Q. Gao, *pH oscillations and mechanistic analysis in the hydrogen peroxide–sulfite–thiourea reaction system.* The Journal of Physical Chemistry A, 2014. **118**(15): p. 2702-2708.

198. Bruk, L., S. Gorodskii, A. Zeigarnik, R. Valdés-Peréz, and O. Temkin, *Mechanism of oxidative carbonylation of phenylacetylene and methylacetylene. Generation and experimental discrimination of hypotheses.* Russian chemical bulletin, 1999. **48**(5): p. 873-880.

199. Jimenez-Prieto, R., M. Silva, and D. Perez-Bendito, *Analyte pulse perturbation technique: a tool for analytical determinations in far-from-equilibrium dynamic systems.* Analytical Chemistry, 1995. **67**(4): p. 729-734.

200. Tikhonova, L., L. Zakrevskaya, and K. Yatsimirskij, *Catalytic method of ruthenium determination based on oscillating chemical reaction.* Zhurnal Analiticheskoj Khimii, 1978. **33**(10): p. 1991-1994.

201. Pojman, J.A. and Q. Tran-Cong-Miyata, *Nonlinear Dynamics in Polymeric Systems*. ACS Symposium Series. Vol. 869. 2003: American Chemical Society. 380.

202. Dhanarajan, A.P., G.P. Misra, and R.A. Siegel, *Autonomous Chemomechanical Oscillations in a Hydrogel/Enzyme System Driven by Glucose.* The Journal of Physical Chemistry A, 2002. **106**(38): p. 8835-8838.

203. Leroux, J.-C. and R.A. Siegel, *Autonomous gel/enzyme oscillator fueled by glucose: Preliminary evidence for oscillations.* Chaos: An Interdisciplinary Journal of Nonlinear Science, 1999. **9**(2): p. 267-275.

204. Gang, H., B. Christopher, P.J. A., and T.A. F., *Time-lapse thiol-acrylate polymerization using a pH clock reaction.* Journal of Polymer Science Part A: Polymer Chemistry, 2010. **48**(13): p. 2955-2959.

205. Taylor, A.F., M.R. Tinsley, F. Wang, Z. Huang, and K. Showalter, *Dynamical Quorum Sensing and Synchronization in Large Populations of Chemical Oscillators.* Science, 2009. **323**(5914): p. 614-617.

206. Jimenez-Prieto, R., M. Silva, and D. Perez-Bendito, *Critical Review. Approaching the use of oscillating reactions for analytical monitoring.* Analyst, 1998. **123**(2): p. 1R-8R.

207. Jimenez-Prieto, R., M. Silva, and D. Perez-Bendito, *Application of Oscillating Reaction-based Determinations to the Analysis of Real Samples.* Analyst, 1997. **122**(3): p. 287-292.

208. Ren, J., X. Zhang, J. Gao, and W. Yang, *The application of oscillating chemical reactions to analytical determinations*, in *Open Chemistry*. 2013. p. 1023.

209. Cervellati, R., K. Höner, S.D. Furrow, F. Mazzanti, and S. Costa, *An Experimental and Mechanistic Investigation of the Complexities Arising During Inhibition of the Briggs□Rauscher Reaction by Antioxidants.* Helvetica Chimica Acta, 2004. **87**(1): p. 133-155.

210. Miyakawa, K., F. Sakamoto, R. Yoshida, E. Kokufuta, and T. Yamaguchi, *Chemical waves in self-oscillating gels.* Physical Review E, 2000. **62**(1): p. 793-798.

211. Hara, Y., Y. Yamaguchi, and H. Mayama, *Switching the BZ Reaction with a Strong-Acid-Free Gel.* The Journal of Physical Chemistry B, 2014. **118**(2): p. 634-638.

212. Masuda, T., M. Hidaka, Y. Murase, A.M. Akimoto, K. Nagase, T. Okano, and R. Yoshida, *Self-Oscillating Polymer Brushes.* Angewandte Chemie International Edition, 2013. **52**(29): p. 7468-7471.
213. Yoshida, R. and T. Ueki, *Evolution of self-oscillating polymer gels as autonomous polymer systems.* NPG Asia Materials, 2014. **6**(6): p. e107.
214. Shiraki, Y. and R. Yoshida, *Autonomous Intestine-Like Motion of Tubular Self-Oscillating Gel.* Angewandte Chemie International Edition, 2012. **51**(25): p. 6112-6116.
215. Maeda, S., Y. Hara, R. Yoshida, and S. Hashimoto, *Peristaltic motion of polymer gels.* Angewandte Chemie, 2008. **120**(35): p. 6792-6795.
216. Masuda, T., N. Shimada, T. Sasaki, A. Maruyama, A.M. Akimoto, and R. Yoshida, *Design of a Tunable Self‐Oscillating Polymer with Ureido and Ru(bpy)3 Moieties.* Angewandte Chemie International Edition, 2017. **56**(32): p. 9459-9462.
217. Tamate, R., T. Ueki, M. Shibayama, and R. Yoshida, *Effect of substrate concentrations on the aggregation behavior and dynamic oscillatory properties of self-oscillating block copolymers.* Physical Chemistry Chemical Physics, 2017. **19**(31): p. 20627-20634.
218. Yoshida, R., *Self-Oscillating Gels Driven by the Belousov–Zhabotinsky Reaction as Novel Smart Materials.* Advanced Materials, 2010. **22**(31): p. 3463-3483.
219. Yoshida, R., *Development of self-oscillating polymers and gels with autonomous function.* Polymer Journal, 2010. **42**: p. 777.
220. Uddin, W., G. Hu, L. Hu, Y. Hu, Z. Fang, R. Ullah, X. Sun, Y. Zhang, and J. Song, *Identification of two aromatic isomers between 2- and 3-hydroxy benzoic acid by using a Briggs-Rauscher oscillator.* Journal of Electroanalytical Chemistry, 2017. **803**(Supplement C): p. 135-140.
221. Zhang, Y., G. Hu, L. Hu, and J. Song, *Identification of Two Aliphatic Position Isomers between α-and β-Ketoglutaric Acid by Using a Briggs–Rauscher Oscillating System.* Analytical chemistry, 2015. **87**(19): p. 10040-10046.
222. Yatsimirskii, K. and L. Tikhonova, *Catalytic kinetic methods for the determination of platinum metals.* Talanta, 1987. **34**(1): p. 69-75.
223. Pejić, N.D., S.M. Blagojević, S.R. Anić, V.B. Vukojević, M.D. Mijatović, J.S. Ćirić, Z.S. Marković, S.D. Marković, and L.Z. Kolar-Anić, *Kinetic determination of morphine by means of Bray–Liebhafsky oscillatory reaction system using analyte pulse perturbation technique.* Analytica Chimica Acta, 2007. **582**(2): p. 367-374.
224. Milos, M. and D. Makota, *Investigation of antioxidant synergisms and antagonisms among thymol, carvacrol, thymoquinone and p-cymene in a model system using the Briggs–Rauscher oscillating reaction.* Food Chemistry, 2012. **131**(1): p. 296-299.
225. Gao, J., H. Yang, X. Liu, J. Ren, Q. Li, and J. Kang, *Determination of glutamic acid by an oscillating chemical reaction using the analyte pulse perturbation technique.* Talanta, 2002. **57**(1): p. 105-114.

226. Gao, J., H. Dai, W. Yang, H. Chen, D. Lv, J. Ren, and L. Wang, *Determination of furfural in an oscillating chemical reaction using an analyte pulse perturbation technique.* Analytical and Bioanalytical Chemistry, 2006. **384**(6): p. 1438-1443.

227. Cervellati, R., C. Renzulli, M.C. Guerra, and E. Speroni, *Evaluation of Antioxidant Activity of Some Natural Polyphenolic Compounds Using the Briggs−Rauscher Reaction Method.* Journal of Agricultural and Food Chemistry, 2002. **50**(26): p. 7504-7509.

228. Höfle, G., W. Steglich, and H. Vorbrüggen, *4-Dialkylaminopyridines as Highly Active Acylation Catalysts.[New synthetic method (25)]*. Angewandte Chemie International Edition in English, 1978. **17**(8): p. 569-583.

229. Neises, B. and W. Steglich, *Simple method for the esterification of carboxylic acids.* Angewandte Chemie International Edition in English, 1978. **17**(7): p. 522-524.

230. Neises, B. and W. Steglich, *Esterification of carboxylic acids with dicyclohexylcarbodiimide/4-dimethylaminopyridine: tert-butyl ethyl fumarate.* Organic Syntheses, 1985: p. 183-183.

231. Zalipsky, S., *Functionalized poly (ethylene glycols) for preparation of biologically relevant conjugates.* Bioconjugate chemistry, 1995. **6**(2): p. 150-165.

232. Harris, J.M., *Laboratory synthesis of polyethylene glycol derivatives.* Journal of Macromolecular Science-Reviews in Macromolecular Chemistry and Physics, 1985. **25**(3): p. 325-373.

233. Williams, D.H. and I. Fleming, *Spectroscopic methods in organic chemistry*. 1995.

234. Sanders, J.K.M. and B.K. Hunter, *Modern NMR spectroscopy: a guide for chemists*. 1988, United States: Oxford University Press.

235. Günther, H., *NMR spectroscopy: basic principles, concepts and applications in chemistry*. 2013: John Wiley & Sons.

236. Stothers, J., *Carbon-13 NMR Spectroscopy: Organic Chemistry, A Series of Monographs*. Vol. 24. 2012: Elsevier.

237. Jackman, L.M. and S. Sternhell, *Application of Nuclear Magnetic Resonance Spectroscopy in Organic Chemistry: International Series in Organic Chemistry*. 2013: Elsevier.

238. Opsteen, J.A. and J.C. van Hest, *Modular synthesis of block copolymers via cycloaddition of terminal azide and alkyne functionalized polymers.* Chemical Communications, 2005(1): p. 57-59.

239. Janz, G.J. and H. Taniguchi, *The Silver-Silver Halide Electrodes. Preparation, Stability, and Standard Potentials in Aqueous and non-Aqueous Media.* Chemical Reviews, 1953. **53**(3): p. 397-437.

240. Karlberg, B. and G. Johansson, *Alkaline errors of glass electrodes in non-aqueous solvents.* Talanta, 1969. **16**(12): p. 1545-1551.

241. Wilman, H., *The structure and orientation of silver halides.* Proceedings of the Physical Society, 1940. **52**(3): p. 323.

242. Parker, J., *A study of the phenylacetylene oxidative carbonylation reaction in oscillatory and non-oscillatory modes.* 2016.
243. Mukherjee, A., *Analysis and control of oscillations and chaos in reactions*. 2009, Newcastle University.
244. Jameson, C.J., *UNDERSTANDING NMR CHEMICAL SHIFTS.* Annual Review of Physical Chemistry, 1996. **47**(1): p. 135-169.
245. Liu, K.-J., *Nuclear magnetic resonance studies of polymer solutions. V. Cooperative effects in the ion-dipole interaction between potassium iodide and poly (ethlene oxide).* Macromolecules, 1968. **1**(4): p. 308-311.
246. Alper, H., N. Hamel, J.B. Woell, and D.J.H. Smith, *Iodide ion promotion of benzyl chloride-borate ester carbonylation reactions.* Tetrahedron letters, 1985. **26**(19): p. 2273-2274.
247. Beamish, F.E. and J. Dale, *Determination of palladium by means of potassium iodide*. Industrial & Engineering Chemistry Analytical Edition, 1938. **10**(12): p. 697-698.
248. Braca, G., L. Paladini, G. Sbrana, G. Valentini, G. Andrich, and G. Gregorio, *Carbonylation and homologation of dimethyl ether in the presence of ruthenium catalysts.* Industrial & Engineering Chemistry Product Research and Development, 1981. **20**(1): p. 115-122.
249. Khumtaveeporn, K. and H. Alper, *Sequential Ring Expansion and Ketene Elimination Reactions in the Novel Rhodium (I)-Catalyzed Carbonylation of Thiazolidines.* Journal of the American Chemical Society, 1994. **116**(13): p. 5662-5666.
250. Pri-Bar, I. and H. Alper, *Oxidative coupling of amines and carbon monoxide catalyzed by palladium complexes. Mono-and double carbonylation reactions promoted by iodine compounds.* Canadian Journal of Chemistry, 1990. **68**(9): p. 1544-1547.
251. Steinmetz, G.R. and M. Rule, *Carbonylation process for the production of aromatic*. 1989, Google Patents.
252. Dombek, B.D., *Novel catalytic system for homogeneous hydrogenation of carbon monoxide: ruthenium complexes in the presence of iodide promoters.* Journal of the American Chemical Society, 1981. **103**(21): p. 6508-6510.
253. Feldman, I., *Use and abuse of pH measurements.* Analytical Chemistry, 1956. **28**(12): p. 1859-1866.
254. Rived, F., I. Canals, E. Bosch, and M. Rosés, *Acidity in methanol–water.* Analytica chimica acta, 2001. **439**(2): p. 315-333.
255. Mussini, T., A. Covington, F. Dal Pozzo, P. Longhi, S. Rondinini, and Z.-Y. Zou, *Determination of standard pH values for potassium hydrogen phthalate reference buffer solutions in 10, 20, 50, 64 and 84.2 wt per cent methanol/water mixed solvents at temperatures from 283.15 to 313.15 K.* Electrochimica acta, 1983. **28**(11): p. 1593-1598.
256. Rosés, M., *Determination of the pH of binary mobile phases for reversed-phase liquid chromatography.* Journal of Chromatography A, 2004. **1037**(1-2): p. 283-298.

257. Castells, C.B., C. Rafols, M. Roses, and E. Bosch, *Effect of temperature on pH measurements and acid–base equilibria in methanol–water mixtures.* Journal of Chromatography A, 2003. **1002**(1-2): p. 41-53.

258. Porras, S.P. and E. Kenndler, *Capillary zone electrophoresis in non-aqueous solutions: pH of the background electrolyte.* Journal of Chromatography A, 2004. **1037**(1-2): p. 455-465.

259. De Ligny, C., P. Luykx, M. Rehbach, and A. Wieneke, *The pH of some standard solutions in methanol and methanol-water mixtures at 25° I. Theoretical Part.* Recueil des Travaux Chimiques des Pays-Bas, 1960. **79**(7): p. 699-712.

260. Amatore, C., B. Godin, A. Jutand, and F. Lemaitre, *Rate and mechanism of the reaction of alkenes with aryl palladium complexes ligated by a bidentate P, P ligand in Heck reactions.* Chemistry-A European Journal, 2007. **13**(7): p. 2002-2011.

261. Bauer, J., V. Tomišić, and P.B.A. Vrkljan, *The effect of temperature and ionic strength on the oxidation of iodide by iron (III): a clock reaction kinetic study.* Journal of chemical education, 2012. **89**(4): p. 540-544.

262. Critchfield, F.E. and J.B. Johnson, *Effect of neutral salts on pH of acid solutions.* Analytical Chemistry, 1959. **31**(4): p. 570-572.

263. Harris, T.K., V.L. Davidson, L. Chen, F.S. Mathews, and Z.-X. Xia, *Ionic strength dependence of the reaction between methanol dehydrogenase and cytochrome c-551i: evidence of conformationally coupled electron transfer.* Biochemistry, 1994. **33**(42): p. 12600-12608.

264. Henry, P.M., *Kinetics of the oxidation of ethylene by aqueous palladium (II) chloride.* Journal of the American Chemical Society, 1964. **86**(16): p. 3246-3250.

265. Robinson, H.W., *The influence of neutral salts on the pH of phosphate buffer mixtures.* Journal of Biological Chemistry, 1929. **82**(3): p. 775-802.

266. Smetana, A.J. and A.I. Popov, *On the influence of ionic strength on the equilibrium constant of an ion-molecule reaction.* The Journal of Chemical Thermodynamics, 1979. **11**(12): p. 1145-1149.

267. Brandariz, I., T. Vilariño, P. Alonso, R. Herrero, S. Fiol, and M.E.S. de Vicente, *Effect of ionic strength on the formal potential of the glass electrode in various saline media.* Talanta, 1998. **46**(6): p. 1469-1477.

268. Solomon, T., *The Definition and Unit of Ionic Strength.* Journal of Chemical Education, 2001. **78**(12): p. 1691.

269. Chiusoli, G., M. Costa, L. Cucchia, B. Gabriele, G. Salerno, and L. Veltri, *Carbon dioxide effect on palladium-catalyzed sequential reactions with carbon monoxide, acetylenic compounds and water.* Journal of Molecular Catalysis A: Chemical, 2003. **204**: p. 133-142.

270. Gabriele, B., L. Veltri, G. Salerno, M. Costa, and G.P. Chiusoli, *Synthesis of Maleic Anhydrides and Maleic Acids by Pd-Catalyzed Oxidative Dicarbonylation of Alk-1-ynes.* European Journal of Organic Chemistry, 2003. **2003**(9): p. 1722-1728.

271. Gabriele, B., G. Salerno, M. Costa, and G.P. Chiusoli, *Recent developments in the synthesis of heterocyclic derivatives by PdI2-catalyzed oxidative carbonylation reactions.* Journal of organometallic chemistry, 2003. **687**(2): p. 219-228.
272. Elding, L.I. and L.-F. Olsson, *Stabilities, solubility, and kinetics and mechanism for formation and hydrolysis of some palladium (II) and platinum (II) iodo complexes in aqueous solution.* Inorganica chimica acta, 1986. **117**(1): p. 9-16.
273. Shmidt, A.F., V.V. Smirnov, O.V. Starikova, and A.V. Elaev, *The effect of the coupling of the formation and regeneration of catalytically active complexes with the main catalytic cycle in the Heck reaction.* Kinetics and catalysis, 2001. **42**(2): p. 199-204.
274. Tonde, S.S., A.A. Kelkar, M.M. Bhadbhade, and R.V. Chaudhari, *Isolation and characterization of an iodide bridged dimeric palladium complex in carbonylation of methanol.* Journal of organometallic chemistry, 2005. **690**(6): p. 1677-1681.
275. Bruk, L., O. Temkin, A. Abdullaeva, E. Timashova, E.Y. Bukina, K.Y. Odintsov, and I. Oshanina, *Coupled processes in carbon monoxide oxidation: Kinetics and mechanism of CO oxidation by oxygen in PdX2-organic solvent-water systems.* Kinetics and Catalysis, 2010. **51**(5): p. 678-690.
276. Pasut, G. and F.M. Veronese, *State of the art in PEGylation: The great versatility achieved after forty years of research.* Journal of Controlled Release, 2012. **161**(2): p. 461-472.
277. Kao, M.J., D.C. Tien, C.S. Jwo, and T.T. Tsung, *The study of hydrophilic characteristics of ethylene glycol.* Journal of Physics: Conference Series, 2005. **13**(1): p. 442.
278. Flanagin, L.W., C.L. McAdams, W.D. Hinsberg, I.C. Sanchez, and C.G. Willson, *Mechanism of phenolic polymer dissolution: importance of acid− base equilibria.* Macromolecules, 1999. **32**(16): p. 5337-5343.
279. Miller-Chou, B.A. and J.L. Koenig, *A review of polymer dissolution.* Progress in Polymer Science, 2003. **28**(8): p. 1223-1270.
280. Perrin, D.D., *Ionisation constants of inorganic acids and bases in aqueous solution*. 2016: Elsevier.
281. Perrin, D.D., B. Dempsey, and E.P. Serjeant, *pKa prediction for organic acids and bases*. Vol. 1. 1981: Springer.
282. Woolley, E.M., J. Tomkins, and L.G. Hepler, *Ionization constants for very weak organic acids in aqueous solution and apparent ionization constants for water in aqueous organic mixtures.* Journal of Solution Chemistry, 1972. **1**(4): p. 341-351.
283. Hepler, L.G., E.M. Woolley, and D.G. Hurkot, *Ionization constants for water in aqueous organic mixtures.* The Journal of Physical Chemistry, 1970. **74**(22): p. 3908-3913.
284. Houston, P.L., *Chemical kinetics and reaction dynamics*. 2012: Courier Corporation.
285. Levine, R.D., *Molecular reaction dynamics*. 2009: Cambridge University Press.
286. Steinfeld, J.I., J.S. Francisco, and W.L. Hase, *Chemical kinetics and dynamics*. Vol. 3. 1989: Prentice Hall Englewood Cliffs (New Jersey).

287. Stone, H. and H. SHECHTER, *A new method for the preparation of organic iodides.* The Journal of Organic Chemistry, 1950. **15**(3): p. 491-495.
288. Yang, J., A. Haynes, and P.M. Maitlis, *The carbonylation of methyl iodide and methanol to methyl acetate catalysed by palladium and platinum iodides.* Chemical Communications, 1999(2): p. 179-180.
289. Patil, R.P., A.A. Kelkar, and R.V. Chaudhari, *Carbonylation of ethanol using homogeneous Ir complex catalyst: effect of ligands and reaction conditions.* Journal of molecular catalysis, 1988. **47**(1): p. 87-97.
290. Edblom, E.C., L. Gyorgyi, M. Orban, and I.R. Epstein, *Systematic design of chemical oscillators. 40. A mechanism for dynamical behavior in the Landolt reaction with ferrocyanide.* Journal of the American Chemical Society, 1987. **109**(16): p. 4876-4880.
291. Allen, T. and R. Keefer, *The formation of hypoiodous acid and hydrated iodine cation by the hydrolysis of iodine.* Journal of the American Chemical Society, 1955. **77**(11): p. 2957-2960.
292. Citri, O. and I.R. Epstein, *Systematic design of chemical oscillators. 42. Dynamic behavior in the chlorite-iodide reaction: a simplified mechanism.* Journal of Physical Chemistry, 1987. **91**(23): p. 6034-6040.
293. Jeffery, T., *Heck-type reactions in water.* Tetrahedron letters, 1994. **35**(19): p. 3051-3054.
294. Jeffery, T., *On the efficiency of tetraalkylammonium salts in Heck type reactions.* Tetrahedron, 1996. **52**(30): p. 10113-10130.
295. Bánsági, T. and A.F. Taylor, *Ester hydrolysis: Conditions for acid autocatalysis and a kinetic switch.* Tetrahedron, 2017. **73**(33): p. 5018-5022.
296. Bronnikova, T.V., W.M. Schaffer, and L.F. Olsen, *Nonlinear Dynamics of the Peroxidase− Oxidase Reaction: I. Bistability and Bursting Oscillations at Low Enzyme Concentrations.* The Journal of Physical Chemistry B, 2001. **105**(1): p. 310-321.
297. Avdeef, A., J.E.A. Comer, and S.J. Thomson, *pH-Metric log P. 3. Glass electrode calibration in methanol-water, applied to pKa determination of water-insoluble substances.* Analytical Chemistry, 1993. **65**(1): p. 42-49.
298. Noszticzius, Z., E. Noszticzius, and Z.A. Schelly, *Use of ion-selective electrodes for monitoring oscillating reactions. 1. Potential response of the silver halide membrane electrodes to hypohalous acids.* Journal of the American Chemical Society, 1982. **104**(23): p. 6194-6199.
299. Bates, R.G., M. Paabo, and R.A. Robinson, *INTERPRETATION OF pH MEASUREMENTS IN ALCOHOL—WATER SOLVENTS1.* The Journal of Physical Chemistry, 1963. **67**(9): p. 1833-1838.
300. Dempsey, C.E., *pH dependence of hydrogen exchange from backbone peptide amides of melittin in methanol.* Biochemistry, 1988. **27**(18): p. 6893-6901.
301. Goldbeter, A., D. Gonze, G. Houart, J.-C. Leloup, J. Halloy, and G. Dupont, *From simple to complex oscillatory behavior in metabolic and genetic control networks.* Chaos: An Interdisciplinary Journal of Nonlinear Science, 2001. **11**(1): p. 247-260.

302. Brøns, M. and K. Bar-Eli, *Canard explosion and excitation in a model of the Belousov-Zhabotinskii reaction.* The Journal of Physical Chemistry, 1991. **95**(22): p. 8706-8713.
303. Krupa, M. and P. Szmolyan, *Relaxation oscillation and canard explosion.* Journal of Differential Equations, 2001. **174(**2): p. 312-368.
304. Peng, B., V. Gáspár, and K. Showalter, *False bifurcations in chemical systems: canards.* Phil. Trans. R. Soc. Lond. A, 1991. **337**(1646): p. 275-289.
305. Sastre de Vicente, M.E., *The Concept of Ionic Strength Eighty Years after Its Introduction in Chemistry*. Journal of Chemical Education, 2004. **81**(5): p. 750.
306. Wolfenden, J.H., *A note on the kinetic salt effects.* Journal of Chemical Education, 1952. **29**(4): p. 167.
307. Bronsted, J.N. and C.E. Teeter, *On Kinetic Salt Effect*. The Journal of Physical Chemistry, 1923. **28**(6): p. 579-587.
308. Indelli, A. and R.D. Santis, *Kinetic Salt Effects on the Aquation Reaction of the Azidopentaaquochromium (III) Ion and Predictions of the Mayer Theory*. The Journal of Chemical Physics, 1971. **55**(10): p. 4811-4816.
309. Barthel, J.M., H. Krienke, and W. Kunz, *Physical chemistry of electrolyte solutions: modern aspects*. Vol. 5. 1998: Springer Science & Business Media.
310. Asperger, S., *Chemical kinetics and inorganic reaction mechanisms*. 2011: Springer Science & Business Media.
311. French, C.C., *The Effect of Neutral Salts on Certain Catalytic Decompositions.* The Journal of Physical Chemistry, 1928. **32**(3): p. 401-414.
312. Gaspar, V. and P. Galambosi, *Bifurcation diagram of the oscillatory Belousov-Zhabotinskii system of oxalic acid in a continuous flow stirred tank reactor. Further possible evidence of saddle node infinite period bifurcation behavior of the system.* The Journal of Physical Chemistry, 1986. **90**(10): p. 2222-2226.
313. Dombek, B., *Synergistic behavior of homogeneous ruthenium-rhodium catalysts for hydrogenation of carbon monoxide.* Organometallics, 1985. **4**(10): p. 1707-1712.
314. Kordylewski, W., S.K. Scott, and A.S. Tomlin, *Development of oscillations in closed systems.* Journal of the Chemical Society, Faraday Transactions, 1990. **86**(20): p. 3365-3371.
315. Hald, B.O. and P.G. Sørensen, *Modeling Diauxic Glycolytic Oscillations in Yeast.* Biophysical Journal, 2010. **99**(10): p. 3191-3199.
316. Nielsen, K., P.G. Sørensen, F. Hynne, and H.G. Busse, *Sustained oscillations in glycolysis: an experimental and theoretical study of chaotic and complex periodic behavior and of quenching of simple oscillations.* Biophysical Chemistry, 1998. **72**(1): p. 49-62.
317. Gabriele, B., G. Salerno, P. Plastina, M. Costa, and A. Crispini, *Expedient Synthesis of 4-Dialkylamino-5H-furan-2-ones by One-Pot Sequential Pd-Catalyzed Oxidative Carbonylation of 2-Yn-1-ols–Conjugate Addition-Lactonization.* Advanced Synthesis & Catalysis, 2004. **346**(2-3): p. 351-358.

318. Gabriele, B., G. Salerno, M. Costa, and G.P. Chiusoli, *Palladium-catalysed formation of maleic anhydrides from CO, CO 2 and alk-1-ynes.* Chemical Communications, 1999(15): p. 1381-1382.
319. Degn, H., *Theory of electrochemical oscillations.* Transactions of the Faraday Society, 1968. **64**(0): p. 1348-1358.
320. Hudson, J.L. and T.T. Tsotsis, *Electrochemical reaction dynamics: a review.* Chemical Engineering Science, 1994. **49**(10): p. 1493-1572.
321. Koper, M.T.M. and P. Gaspard, *The modeling of mixed-mode and chaotic oscillations in electrochemical systems.* The Journal of Chemical Physics, 1992. **96**(10): p. 7797-7813.
322. Eiswirth, M. and G. Ertl, *Kinetic oscillations in the catalytic CO oxidation on a Pt (110) surface.* Surface Science, 1986. **177**(1): p. 90-100.
323. Imbihl, R., M. Cox, and G. Ertl, *Kinetic oscillations in the catalytic CO oxidation on Pt (100): experiments.* The Journal of chemical physics, 1986. **84**(6): p. 3519-3534.
324. Imbihl, R. and G. Ertl, *Oscillatory kinetics in heterogeneous catalysis.* Chemical Reviews, 1995. **95**(3): p. 697-733.
325. Van der Pol, B., *LXXXVIII. On "relaxation-oscillations".* The London, Edinburgh, and Dublin Philosophical Magazine and Journal of Science, 1926. **2**(11): p. 978-992.
326. Guckenheimer, J. and P. Holmes, *Nonlinear oscillations, dynamical systems, and bifurcations of vector fields*. Vol. 42. 2013: Springer Science & Business Media.
327. Bohner, M. and S.H. Saker, *Oscillation of second order nonlinear dynamic equations on time scales.* The Rocky Mountain Journal of Mathematics, 2004: p. 1239-1254.
328. Strogatz, S.H., *Nonlinear dynamics and chaos: with applications to physics, biology, chemistry, and engineering*. 2018: CRC Press.
329. Guidi, G.M., M.-F. Carlier, and A. Goldbeter, *Bistability in the isocitrate dehydrogenase reaction: an experimentally based theoretical study.* Biophysical journal, 1998. **74**(3): p. 1229-1240.
330. Biswas, D., T. Banerjee, and J. Kurths, *Control of birhythmicity through conjugate self-feedback: Theory and experiment.* Physical Review E, 2016. **94**(4): p. 042226.
331. Goldbeter, A. and J.-L. Martiel, *Birhythmicity in a model for the cyclic AMP signalling system of the slime mold Dictyostelium discoideum.* FEBS letters, 1985. **191**(1): p. 149-153.
332. Lakshmanan, M. and S. Rajaseekar, *Nonlinear dynamics: integrability, chaos and patterns*. 2012: Springer Science & Business Media.
333. Borghans, J.M., G. Dupont, and A. Goldbeter, *Complex intracellular calcium oscillations A theoretical exploration of possible mechanisms.* Biophysical chemistry, 1997. **66**(1): p. 25-41.
334. Johnson, B.R., S.K. Scott, and B.W. Thompson, *Modelling complex transient oscillations for the BZ reaction in a batch reactor.* Chaos: An Interdisciplinary Journal of Nonlinear Science, 1997. **7**(2): p. 350-358.

335. Samoilov, M., S. Plyasunov, and A.P. Arkin, *Stochastic amplification and signaling in enzymatic futile cycles through noise-induced bistability with oscillations.* Proceedings of the National Academy of Sciences, 2005. **102**(7): p. 2310-2315.
336. Yashin, V.V. and A.C. Balazs, *Theoretical and computational modeling of self-oscillating polymer gels.* The Journal of Chemical Physics, 2007. **126**(12): p. 124707.
337. Epstein, I.R., *The role of flow systems in far-from-equilibrium dynamics*. 1989, ACS Publications.
338. Hocker, C.G. and I.R. Epstein, *Analysis of a four-variable model of coupled chemical oscillators.* The Journal of Chemical Physics, 1989. **90**(6): p. 3071-3080.
339. Epstein, I.R., K. Kustin, P. De Kepper, and M. Orbán, *Oscillating chemical reactions.* Scientific American, 1983. **248**(3): p. 112-123.
340. Kovacs, K., M. Leda, V.K. Vanag, and I.R. Epstein, *Small-Amplitude and Mixed-Mode pH Oscillations in the Bromate−Sulfite−Ferrocyanide−Aluminum(III) System.* The Journal of Physical Chemistry A, 2009. **113**(1): p. 146-156.
341. Schmitz, R., K. Graziani, and J.L. Hudson, *Experimental evidence of chaotic states in the Belousov–Zhabotinskii reaction.* The Journal of Chemical Physics, 1977. **67**(7): p. 3040-3044.
342. Orbán, M. and I.R. Epstein, *Chemical oscillators in group VIA: The Cu (II)-catalyzed reaction between thiosulfate and peroxodisulfate ions.* Journal of the American Chemical Society, 1989. **111**(8): p. 2891-2896.
343. Schaffer, W.M., T.V. Bronnikova, and L.F. Olsen, *Nonlinear Dynamics of the Peroxidase−Oxidase Reaction. II. Compatibility of an Extended Model with Previously Reported Model-Data Correspondences.* The Journal of Physical Chemistry B, 2001. **105**(22): p. 5331-5340.
344. Temkin, O. and L. Bruk, *Palladium (II, I, 0) complexes in catalytic reactions of oxidative carbonylation.* Kinetics and catalysis, 2003. **44**(5): p. 601-617.
345. Čupić, Ž., S. Maćešić, K. Novakovic, S. Anić, and L. Kolar-Anić, *Stoichiometric network analysis of a reaction system with conservation constraints.* Chaos: An Interdisciplinary Journal of Nonlinear Science, 2018. **28**(8): p. 083114.